A Regional Study of the Toro and Imburu Formation Aquifers in the Papuan Basin, Papua New Guinea

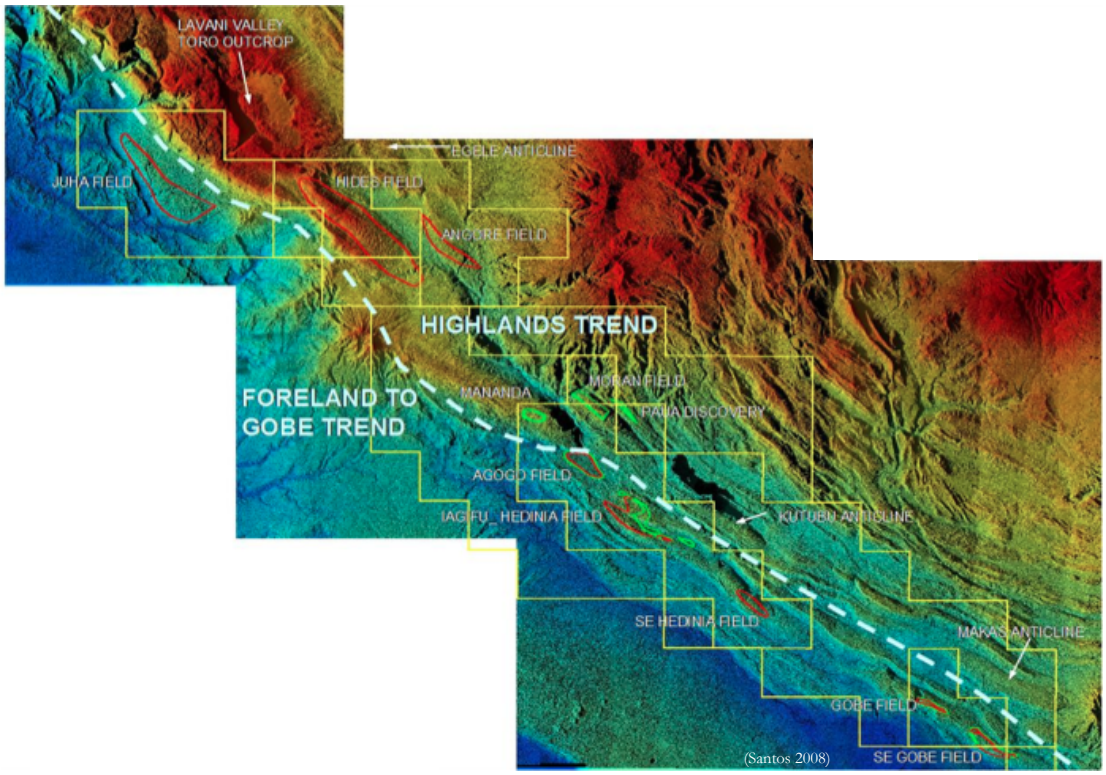

Blair Hopwood, BSc (Geology) - University of Adelaide

This thesis is submitted in partial fulfilment of the requirements for the
Honours Degree of Bachelor of Science (Petroleum Geology and Geophysics)

Australian School of Petroleum
University of Adelaide

November 2013

Abstract

This study represents a regional review of the Toro and Imburu Formation aquifers in the fold belt and foreland regions of the Papuan Basin, Papua New Guinea (PNG). This study extends previous Toro aquifer studies in the Papuan Basin (Eisenberg 1993; Eisenberg et al., 1994; Kotaka 1996). A comprehensive data set was assembled containing all currently available well formation fluid pressure, salinity and temperature data. These data were used to calculate hydraulic potential (Hw) values, which were subsequently used to generate a regional potentiometric map for the Toro Sandstone reservoir and semi-regional maps for the Digimu, Hedinia and Iagifu Sandstone reservoirs of the Imburu Formation.

The Toro potentiometric surface map generated in this study is consistent with an extensive hydrodynamic Toro aquifer system existing in the Papuan Basin Fold Belt. The Toro aquifer likely flows northwest to southeast parallel to the fold belt, from the Lavani Valley Toro outcrop (likely recharge region) in the Highlands, through to the Kutubu Complex, potentially via Hides, (possibly Angore) and the Mananda/South East Mananda Fields. The evidence for Toro aquifer hydrodynamic flow is strongest through the Kutubu Complex of fields, with water flow, entering via Agogo and exiting the fold belt, at the southern end of the Usano Field into the foreland of the basin. However, it should be noted that gas water contacts (GWCs) for Hides and Angore Fields are not yet available. These have been estimated in this study from Hides and Angore gas pressure gradient intersections with water pressure gradients identified from nearby wells (Lavani-1 and Egele-1). Therefore it is not currently possible to unequivocally identify a connected Toro aquifer system between Lavani Valley, (possibly Angore) and Hides. Nevertheless, the Lavani Valley-Hides-Mananda/South East Mananda system (LV-H-M/SEM) represents the most likely flow path for a Toro hydrodynamic aquifer model in the fold belt. Evidence for hydrodynamic Toro aquifer flow was identified in the opposite direction, in a southeast to northwest direction, in the South East Hedinia Field. Significant compartmentalisation of the Toro reservoir was identified in several Hinterland Fields and anticline structures (Egele, Angore, Moran, and Paua Fields along with the Kutubu and Makas Anticlines) and in the southeast region of the central fold belt (Gobe/South East Gobe Fields).

Likely Toro aquifer flow exit points from fold belt into foreland were identified at the southern end of Usano at Iorogabaui-1 and at southern end of South East Mananada Field at Libano-1 involving the Bosavi Lineament. Possible northwest to southeast Toro aquifer flow was identified in the foreland region of the basin from the Stanley Field in the northwest to the sea in the southeast. The Komewu and Darai Fault systems appear to operate as barriers to northeast to southwest Toro aquifer flow in the foreland.

Considerably less data were obtained in this study for the Digimu, Hedinia, Iagifu Sandstone reservoir aquifers compared to the Toro reservoir unit. However, key findings include; (1) for the Digimu Sandstone, hydrostatic and compartmentalised aquifer behaviour in the Agogo, Hedinia/Iagifu and Moran Fields, (2) for the Hedinia Sandstone, hydrodynamic aquifer behavior in the Hedinia/Iagifu and South East Hedinia Fields and (3) for the Iagifu Sandstone, hydrodynamic aquifer behavior in the Hedinia/Iagifu Fields, a significant Hw step between the Agogo and Hedinia/Iagifu Fields (not seen with any of the other reservoir sandstones) and a compartmentalised aquifer in the Gobe/South East Gobe Fields (where it acts as the main hydrocarbon reservoir).

The updated regional data and potentiometric maps generated in this study will assist sub-regional and field scale modelling of the Toro and Imburu Formation aquifers, future hydrodynamic trapping studies and provide increased confidence for hydrocarbon reserve determination in the Papuan Basin Fields.

Acknowledgements

I would like to thank Mike Starcher at Santos for his guidance on all aspects of the project and for giving me the opportunity to undertake this study. Many thanks for critically reviewing a draft version of my thesis. I am extremely grateful to Sharon Langston at Santos for her patience and help with the project, particularly with hydrogeology, Petrosys potentiometric mapping and reviewing a draft of my thesis. I would like to thank Mark Bunch for his supervision of the project at the ASP and providing feedback on a draft of my thesis. Thank you to Trish Moorfield for her help tracking down well completion reports and Darren Graetz for his help with Petrosys software during my stay at Santos. Thank you to everyone in the 2013 ASP class for making it an enjoyable year. Finally, a big thank you to Louise, Callie and Jess for their support and understanding throughout the year.

Table of Contents

Chapter 1: Introduction

1.1 Study Rationale/Significance

The fold belt and foreland of the Papuan Basin in Papua New Guinea (PNG) contain appreciable oil and gas reserves (Bradey et al., 2008; Berryman and Braisted, 2010; Ahmed et al., 2012) (Figures 1.1 and 1.2). The significant topographical relief of the Papuan Fold Belt (up to 3500m) and the high levels of rainfall experienced by the region (up to 8m/year) suggest that regional flow of water is likely to have an impact on the distribution and management of the hydrocarbons within the important reservoirs of the fold belt and foreland of the Papuan Basin (Cockroft et al., 1987).

There is presently evidence for a hydrodynamic aquifer system operating in the Kutubu Complex of fields (Agogo, Hedinia/Iagifu and Usano) in the central fold belt region (Figures 1.2 and 2.1b), resulting in a tilted oil-water contact (OWC) (Eisenberg, 1993; Eisenberg et al., 1994). However, there is still a limited understanding of the wider regional controls on water movement and the impact on hydrocarbon distribution within the important reservoirs in many of the fields in the Papuan Basin.

Aquifer continuity is significantly influenced by faulting and compartmentalisation of the reservoir units in the Papuan Fold Belt (Hennig et al., 2002; Williams and Lund, 2006, Bradey et al., 2008). However, because of the difficulty in obtaining good quality seismic data in the fold belt terrain, (as a result of a blanket of thick overlying refractory karsified limestone and steeply dipping structures), the level of compartmentalisation is highly uncertain (Eisenberg et al., 1994; Bradey et al., 2008).

The limited understanding of potentially more widespread hydrodynamic aquifer behaviour and poorly imaged faulting, makes it difficult to accurately assess hydrocarbon reserves, ie: compartmentalised with different hydrocarbon water contacts, or a tilted contact across the field. The position of the OWC or gas-water contact (GWC) in a field is one of the most important factors in determining reserves (Dennis et al., 2000; Cockroft et al., 1987).

This project aimed to provide up-to-date regional information about the behaviour of the aquifers in the important Toro Sandstone and Imburu Formation (Digimu, Hedinia and Iagifu Sandstone) reservoirs in the Papuan Basin. This will potentially enable the identification of additional hydrodynamically trapped hydrocarbon reserves in the Papuan Fold Belt and facilitate improved resource assessment in the basin. This is particularly important at present as PNG continues to develop its hydrocarbon resources and experiences renewed exploration efforts.

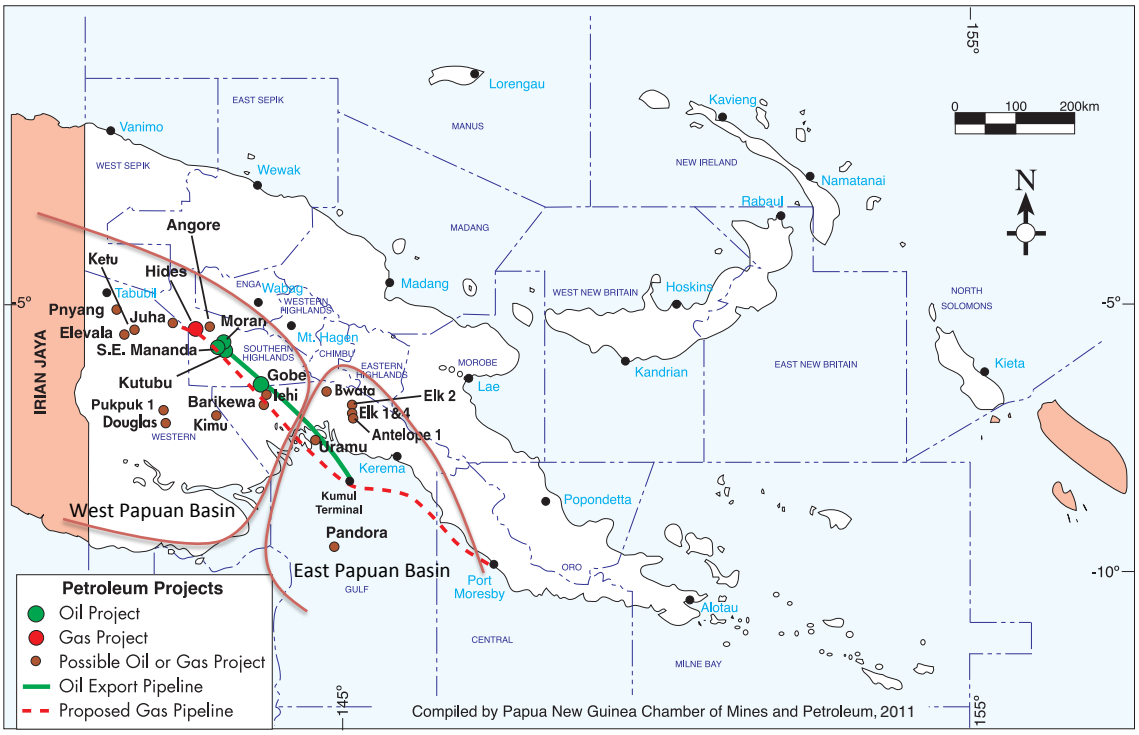

Figure 1.1: PNG Papuan Basin Oil and Gas Fields
Major fields include: Kutubu (~2.0 Tcf gas/300MMbbl oil), Hides (8.0 Tcf gas) and Elk-Antelope (8.0 Tcf gas /160MMbbl oil) (modified from PNG CMP, 2012).

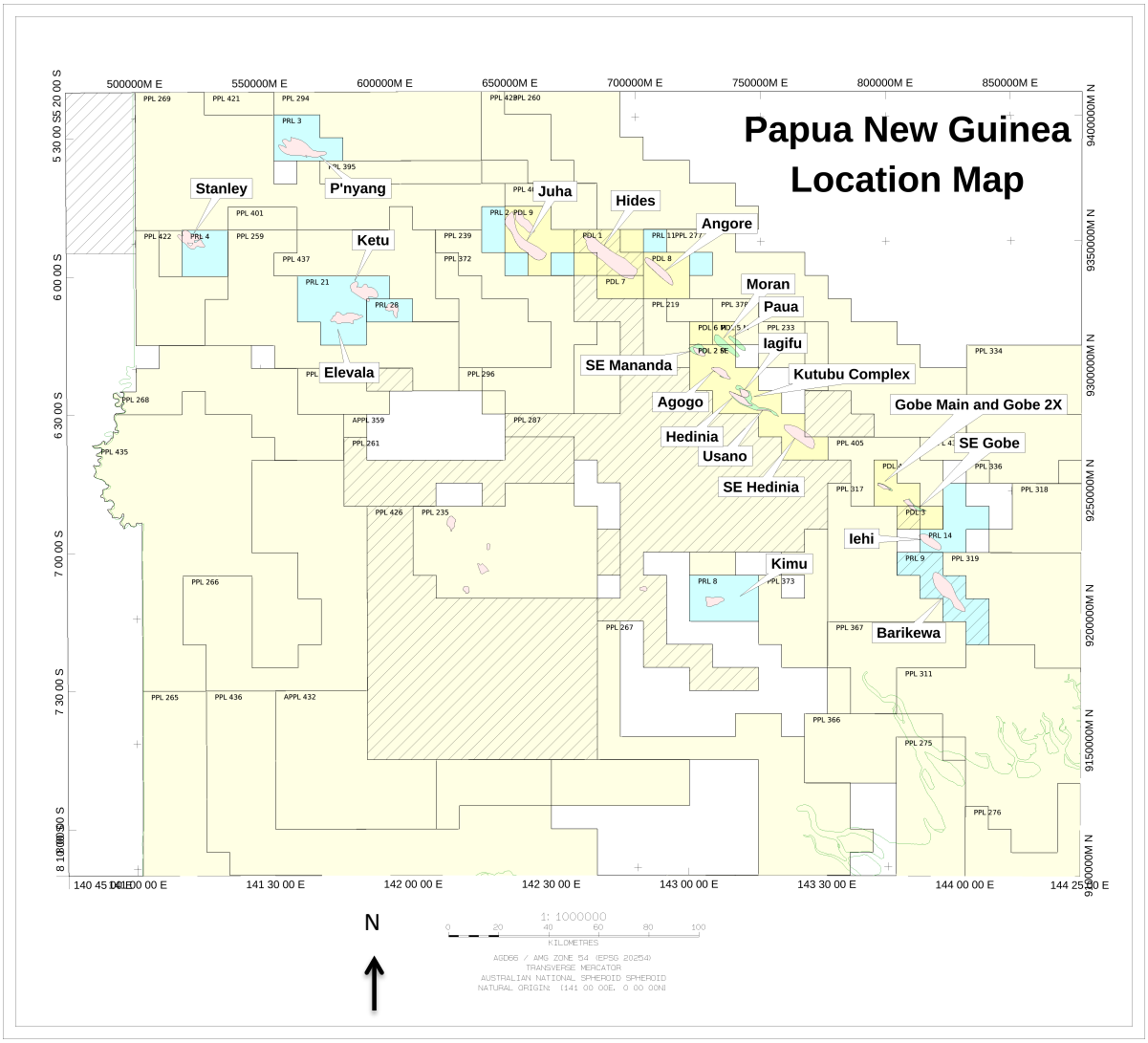

Figure 1.2: PNG Papuan Basin Location Map

Major gas and oil fields are labelled (gas fields - pink. Oil fields - green). Permit areas held by different companies (colour coded) also shown. (Santos, 2013)

1.2 Study Scope/Limitations

Previous aquifer studies have been carried out in the Papuan Basin, which include work by Eisenberg (1993), Eisenberg et al., (1994) and Kotaka (1996). This study represents an update of the regional analysis done by Kotaka (1996) and re-examination of some of the observations reported by Eisenberg (1993) and Eisenberg et al., (1994). It was beyond the scope and time frame of this project to model the data obtained at field-scale level in the same way as that presented by Eisenberg (1993).

The first stage of this study comprised the assembly of a newly updated comprehensive regional Papuan Basin data set containing the available well formation pressure, salinity and temperature data for the Toro and Imburu Formations. The second stage used these data to generate hydraulic potential (Hw) values, which have been used to constrain and generate preliminary potentiometric surface maps for the Toro and Imburu Formations (see Section 4.5). Previous studies have generated Hw values using a single assumed water pressure gradient value (0.435 psi/ft) for the fold belt and foreland regions of the Papuan Basin (Eisenberg, 1993; Eisenberg et al., 1994; Kotaka 1996). This study compared Hw values generated by three methods; (1) the original method using the assumed water pressure gradient value, (2) an approach using calculated water pressure gradients from each well/compartment, and (3) a method, also using the assumed water pressure gradient value, but in conjunction with salinity and temperature data, to further refine Hw values generated.

The primary focus of this study was to generate a regional potentiometric surface map for the Toro Sandstone reservoir, as it is the most important reservoir in the existing fields of the fold belt of the Papuan Basin (Bradey et al., 2008). However, limitations on the achievable detail of the Toro potentiometric map existed, as only a modest number of reliable Toro water pressure data points were available for the fold belt region, and very few data points were available for the foreland region. Even fewer data points were available for the Imburu Formation reservoir units (Digimu, Hedinia and Iagifu Sandstones). Therefore, these represented secondary objectives for this study, as it was only possible to generate coarse, semi-regional maps for these reservoir units.

Other limitations on the extent of potentiometric surface mapping possible for this study existed and included; (1) the lack of critical data points to identify gas/oil-water contacts in the Toro reservoir in several fields (eg. proposed wells in the Hides and Angore Fields are still to be drilled to obtain these data). (2) Limitations on the structural control of reservoir compartmentalisation for the aquifers in the fold belt, as a consequence of relatively poor seismic data. (ie. identifying the presence or absence of faults, the level of fault displacement and whether the fault is sealing or leaking. (3) A relatively coarse outcrop geology map of the Papuan Basin made it difficult to

unambiguously identify, for instance, Toro Sandstone outcrop, (ie. possible recharge areas for the aquifer other than the main areas previously identified at the Muller Anticline and Lavani Valley) (D'Addario et al., 1976; Hill et al., 1993).

It was outside the scope of this study to incorporate porosity and permeability data for the sandstone reservoirs and to identify and assess other lithological controls on aquifer behaviour. However, they likely play an important role in influencing aquifer behaviour within and between the fields in the Papuan Basin. In addition it was beyond the time frame available for this project to examine in detail formation water chemistry data. Such data would have been extremely helpful as a natural tracer for investigating aquifer behaviour across the fields, potential cross-compartmental connections and recharge regions (Glynn and Plummer, 2005; Underschultz et al., 2005; Abdou et al., 2011).

However, not withstanding these limitations, it is envisioned that the pressure-depth plot analysis and potentiometric maps generated in this study will provide additional information on aquifer behaviour in the Papuan Basin, particularly the Toro reservoir in the fold belt, and will permit updated aquifer flow models to be generated for some of the important fields in the Papuan Basin Fold Belt.

1.3 Study Aims

This study aimed to:
(1) Generate a comprehensive data set of up-to-date fluid pressure, salinity and temperature data, that will allow Hw values to be generated for all of the wells in the Papuan Basin for the Toro and Imburu Formation reservoirs.

(2) Generate up-to-date potentiometric surface maps within the fold belt and foreland regions of the Papuan Basin for the key reservoir intervals, the Toro Sandstone and the Imburu Formation (Digimu, Hedinia and Iagifu Sandstone units), by integrating the Hw data, regional topography, regional surface geology and major structural features recognized in the region that may serve as barriers to aquifer connectivity.

(3) Propose a qualitative Toro aquifer model incorporating key aspects of Toro reservoir hydrodynamic flow patterns identified from the potentiometric surface maps.

Chapter 2: Regional Geology

2.1 Basin Setting

The Papuan Basin is a member of a group of basins extending along the north-northwest margin of Australia, which make up the Westralian Superbasin (Bradshaw, 1993) (Figure 2.1a). The basin is located on the island of New Guinea within the Southern Highlands and Western Provinces of PNG, extending northwest just into West Papua and southeast offshore into the Gulf of Papua (Figures 1.1, 2.1a, 2.1b). The basin has been subdivided into western and eastern basin sections (Home et al., 1990; McConachie et al., 2000; Buchanan and Warburton, 1996; Ahmed et al., 2012) (Figures 1.1, 2.1b). This study has concentrated on the western section of the Papuan Basin within PNG, excluding the extended contiguous part of the basin in West Papua, which has alternatively been called the Akimeugah Basin (McConachie et al., 2000; Hill et al., 2004) (Figure 2.1a). The areal extent of the Toro Sandstone reservoir, which is the primary focus of this study, roughly defines the extent of the western section of the Papuan Basin (see section 2.4).

The western section of the Papuan Basin includes the Papuan Fold Belt region and the heterogeneous low-lying foreland region (Figure 2.1b). The Papuan Fold Belt, a northwest-southeast trending mountain range up to 3500m elevation, has been generated by oblique convergence, since the Late Miocene/Pliocene, of the Australian Plate, with the Pacific Plate and intervening microplates (Hill, 1991; Eisenberg, 1993; Hill et al., 2008; Craig and Warvakai, 2009) (Figure 2.2a). The foreland region represents the relatively undeformed and still developing foreland basin that includes the Fly Platform, Darai Plateau (Hulse and Harris, 2000), Omati and Turama Troughs, and Fly/Strickland Depocentre (Figure 2.1b).

The fold belt and foreland regions of the Papuan Basin combine with the Central Orogenic Belt (metamorphic and granitic basement), and a zone of sutured oceanic crust and island arcs (that New Guinea collided with earlier in the Eocene) to make up the four main tectonic provinces of PNG (Hill, 1991; Van Ufford and Cloos, 2005; Hill et al., 2008; Craig and Warvakai, 2009) (Figure 2.2b).

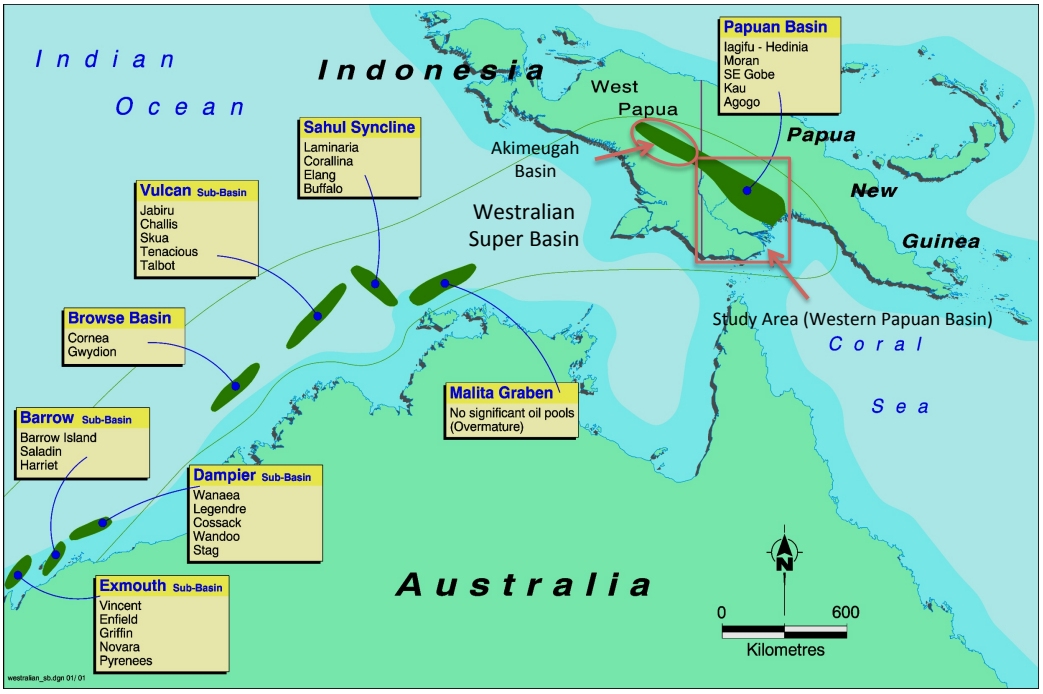

Figure 2.1a: Papuan Basin, Part of the Larger Westralian Super Basin

Location of the Papuan Basin is shown within the larger Westralian Superbasin. Study area shown as western section of the Papuan Basin. Continuation of Papuan Basin into West Papua called the Akimeugah Basin (modified from Buick et al., 2009).

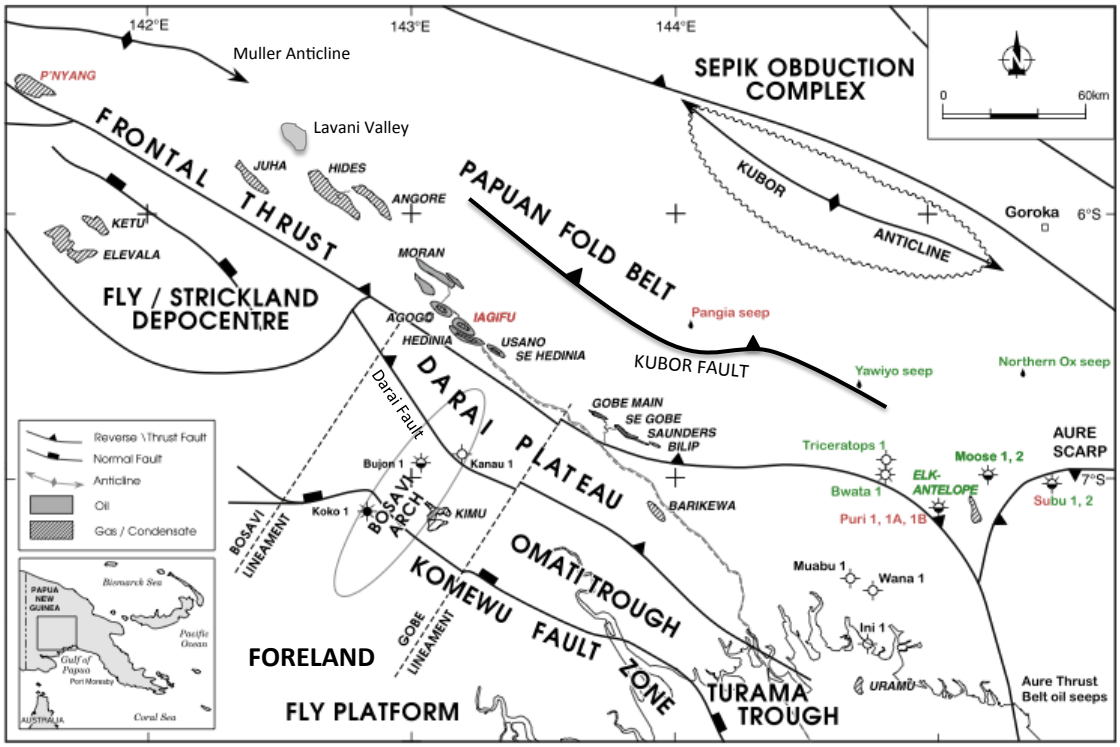

Figure 2.1b: Papuan Basin Structural Elements

Location map, structural elements and oil and gas fields of the Papuan Basin. The Papuan Basin is arbitrarily divided into western and eastern sections at a longitude of approximately 144° East (modified from Ahmed et al., 2012).

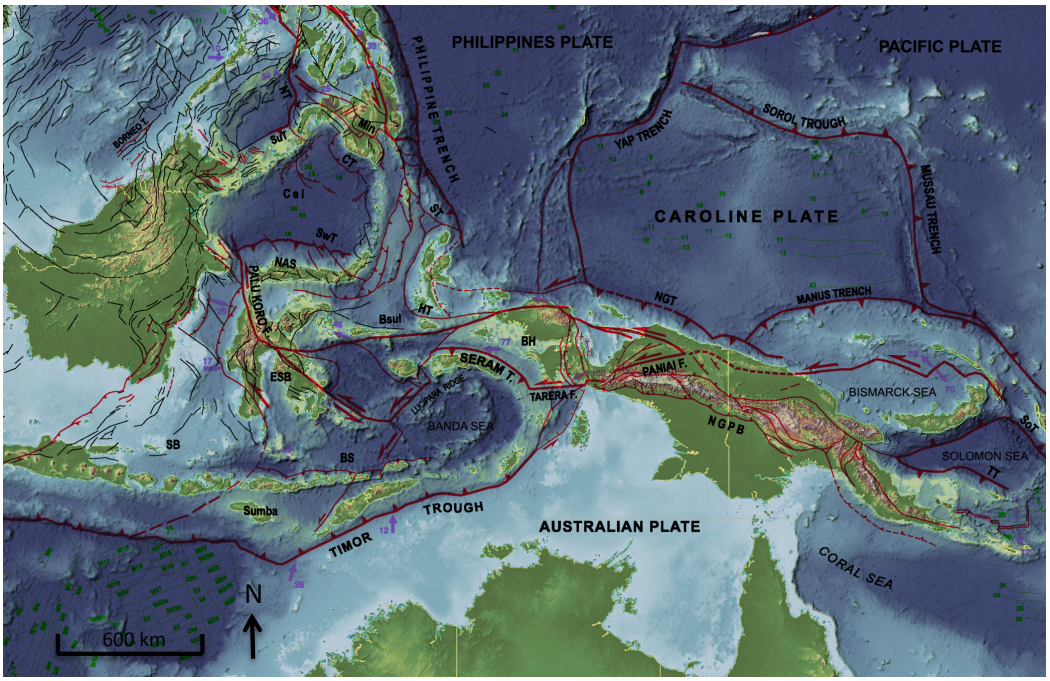

Figure 2.2a: Location of New Guinea on Australian Plate

Image shows relationship of Australian plate (with New Guinea and Australia) to the Pacific and smaller Philippines and Caroline Plates to the north (Santos, 2008).

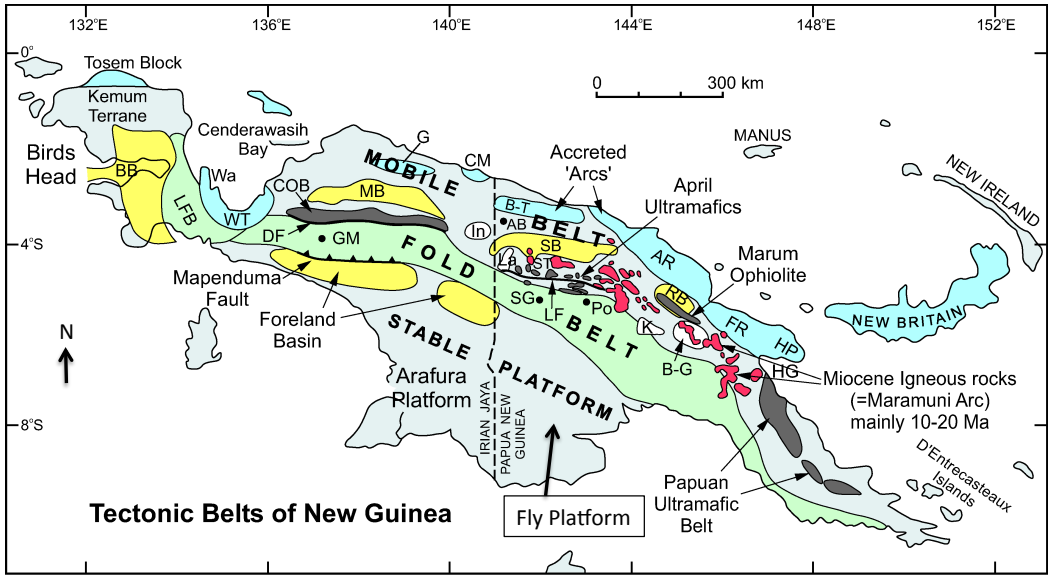

Figure 2.2b: Tectonic Provinces of New Guinea

New Guinea map showing simplified tectonic belts and the principal tectonic features. Four main tectonic provinces; Fly platform, Papuan Basin Fold Belt, Central Orogenic Belt/Mobile Belt and zone of sutured oceanic crust and accreted Island arcs (AB Amanab Block; AR Adelbert Ranges; BB Bintuni Basin; BG Bena Bena – Goroka Terrane; B-T Bewani-Torricelli Mountains; CM Cyclops Mountains; COB Central Ophiolite Belt; DF Derewo Fault; FR Finisterre Ranges; G Gauttier Terrane; GM Grasberg Mine; HG Huon Gulf; HP Huon Peninsula; In Indenburg Inlier; K Kubor Range; La Landslip Ranges; LF Lagaip Fault; MB Meervlakte Basin; Po Porgera Intrusive Complex and mine; RB Ramu Basin; SB Sepik Basin; SG Strickland Gorge; ST Sepik Terrane; Wa Wandaman Peninsula; WT Weyland Terrane) (Hill et al., 2008).

2.2 Tectonic-Stratigraphic Evolution

A schematic tectonic model for the evolution of the Papuan Basin and subsequent development of the fold belt and foreland regions is shown in Figure 2.3 (Hill et al., 2004). The Papuan Basin contains Mesozoic post-rift/continental shelf marine sequences and Cenozoic foreland basin sequences deposited on Paleozoic and Triassic granitic and metamorphic basement of the continental crust of the Australian Plate (Hill, 1991; Eisenberg, 1993).

The basin initially developed by rifting of the Australian continental margin in Triassic to Early Jurassic times in response to the break-up of Gondwana (Craig and Warvakai, 2009; Ahmed et al., 2012). Progressive sediment deposition from the Early Jurassic (syn-rift) through to the Early Cretaceous (post-rift/continental shelf) has then generated the source, reservoir, and sealing facies of the main petroleum system operating in the Papuan Basin (Hill et al., 2000) (Figures 2.4, 2.5a). The Toro and Imburu Formation Sandstones represent the main reservoir units in this petroleum system (Hill et al., 2000) (Figures 2.5a-b). The Mesozoic rift succession of sediments within the Papuan Basin are correlatable to that seen in other basins on the northwestern Australian continental margin as part of the larger Westralian Superbasin (Ahmed et al., 2012). During the Mesozoic, post-rift/continental shelf margins developed after the progressive breakup of Eastern Gondwana along the northern and then down the western flank of the Australian Plate margin (Struckmeyer et al., 1990; Home et al., 1990).

Within the Jurassic sediment sequence in the Papuan Basin, the most likely source rocks are the early-rift Magobu Formation coal measures and the later syn-rift fine marine shelf clastic sediments, such as the Lower Jurassic marine shales of the Barikewa and Koi-lang Formations (deposited during inundation of the continent margin) as well as the Middle Jurassic marine shales of the Imburu Formation (Hill et al., 2000; Hill et al., 2008; Ahmed et al., 2012).

The regressive fluvio-deltaic to marginal marine Lower Cretaceous Toro sandstone represents the major reservoir. The Upper Jurassic to Lower Cretaceous Digimu, Hedinia and Iagifu Sandstone members of the Imburu Formation also represent important reservoir units. During the Late Jurassic to Early Cretaceous, regional subsidence allowed deposition of the Iagifu, Hedinia, Digimu and Toro reservoir sands in shallow marine, shoreline to estuarine environments in a continental shelf margin setting, with continued deposition of Imburu Formation shale further offshore to the east and northeast of the palaeo-shoreline (Figures 2.6a-b) (Hennig et al., 2002; Bradey et al., 2008). These sediments were primarily sourced from the Australian craton from the southwest (Bradey et al., 2008).

Increasing marine transgression in the Early Cretaceous led again to the deposition of fine clastic sediments, muds and silts. These have formed the shales of the 1000m thick Ieru Formation,

which acts as the regional seal over much of the basin (Craig and Warvakai, 2009; Ahmed et al., 2012; Eisenberg, 1993) (Figure 2.5a). The Ieru Shale may also act as a possible source rock (Hill et al., 2008).

New Guinea was then uplifted during the Late Cretaceous to Paleocene, as a result of rifting in the Coral Sea to the southeast (Hill, 1991). This resulted in erosion and removal of Upper Cretaceous sediments in the fold belt and Fly Platform area of the basin and removal of Upper Jurassic to Upper Cretaceous sediments in the eastern part of the basin (Struckmeyer, 1990). Restricted deposition in the northern part of the basin occurred during the Paleocene, however more extensive deposition did not resume until late Eocene/Early Oligocene flooding, which allowed widespread formation of shallow marine carbonates, which have formed the Darai Limestone (Figure 2.5a). The Darai Limestone is a thick (1000-1500m) and regionally extensive limestone unit covering significant areas of the foreland and fold belt regions, and where exposed at the surface, is heavily karstified (Eisenberg, 1993; Hill et al., 2008). It also provides a major reservoir interval in the eastern part of the Papuan Basin (Struckmeyer, 1990).

Carbonate deposition was eventually halted by onset of compression in the Late Miocene, with the conversion of the Papuan Basin from a continental shelf margin to a foreland basin setting caused by the collision of the Australian continental lithosphere with the Pacific Plate, and the resulting influx of Orubadi Formation sediment from the growing fold belt (Hill et al., 2008). These Orubadi Formation sediments, deposited up to a thickness of 500m over the Darai Limestone, include inter-bedded terrestrial sandstones and siltstones of the Era Beds, as well as marine shales and volcaniclastics sediments (Berryman and Braistead, 2010) (Figure 2.5a). Quaternary alluvium, and volcanics associated with the active volcanoes in the region sit unconformably above the Era Beds of the Orubadi Formation (Eisenberg, 1993).

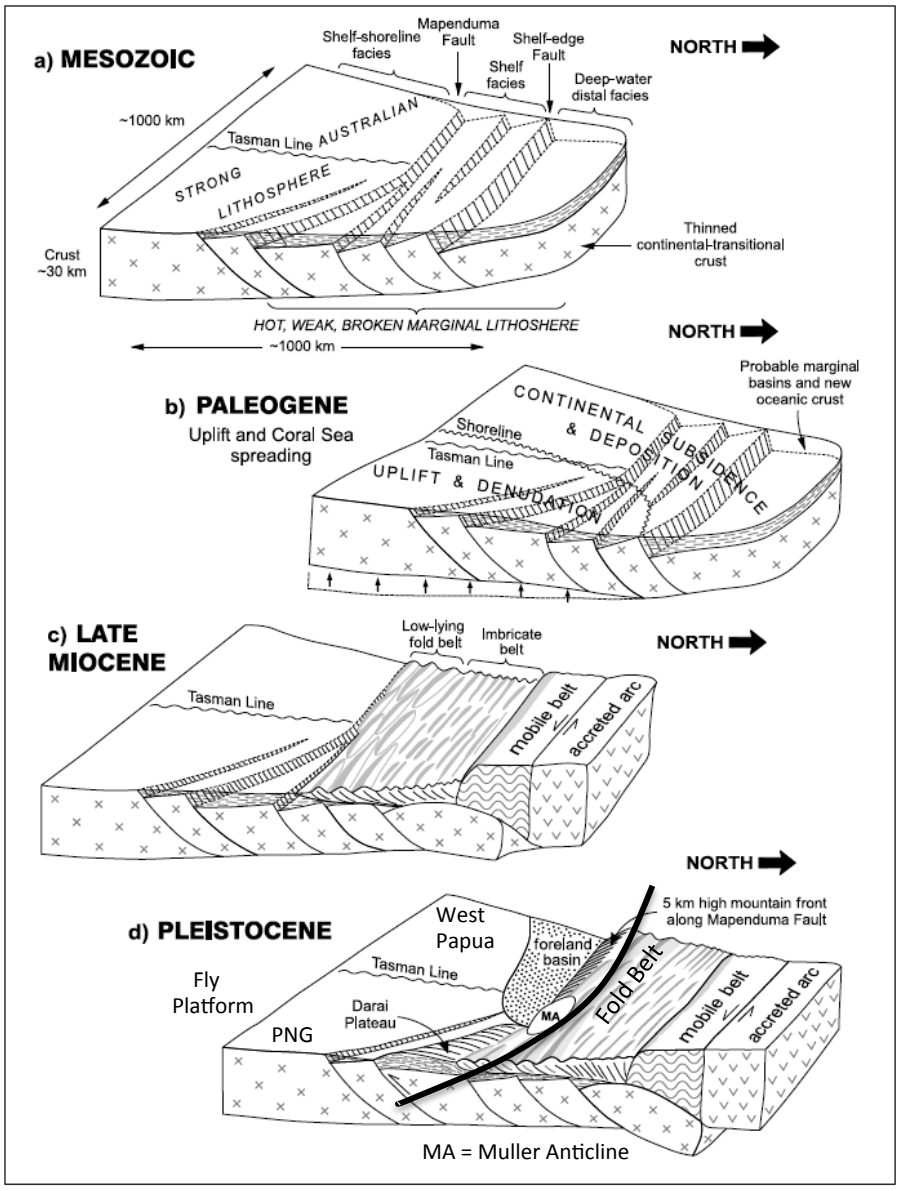

Figure 2.3: Schematic Tectonic Model for the Evolution of the New Guinea Fold Belt
(a) Jurassic-Cretaceous rifting and sedimentation along the northern margin of the Australian Plate. Imburu Formation and Toro reservoir sandstones were deposited on the shelf, with source rocks in the basin facies. (b) Late Cretaceous-Paleocene uplift and denudation of the area adjacent to rifting in the Coral Sea. (c) Early Miocene arc-continent collision generated a low-lying fold belt throughout New Guinea beginning in the late Miocene. (d) In the Pliocene-Pleistocene, the fold belt first built up in West Papua as the mobile belt and accreted terranes collided with the Australian Plate. The resulting mountains have generated an adjacent foreland basin. However, because of slightly oblique convergence, in PNG, the fold belt is lower lying and has not yet built up to the same heights as that in West Papua as it has not yet impinged on the Australian Craton to the same extent. In the Papuan Basin there has been minor inversion of basement faults, but a well-developed foreland basin is still being generated (modified from Hill et al., 2004).

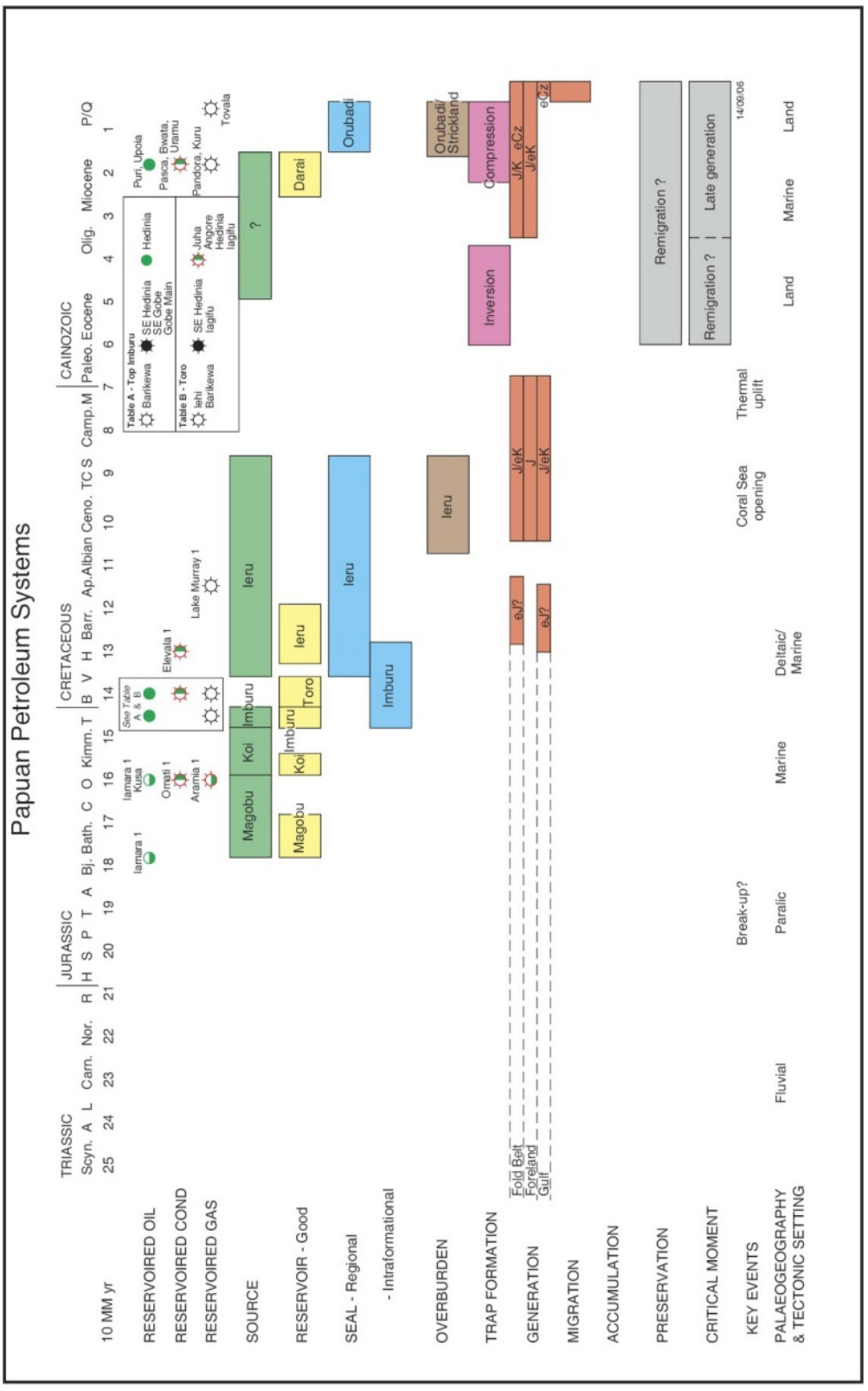

Figure 2.4: Papuan Basin Petroleum Systems
Schematic diagram depicting Papuan Basin petroleum systems (Santos, 2008).

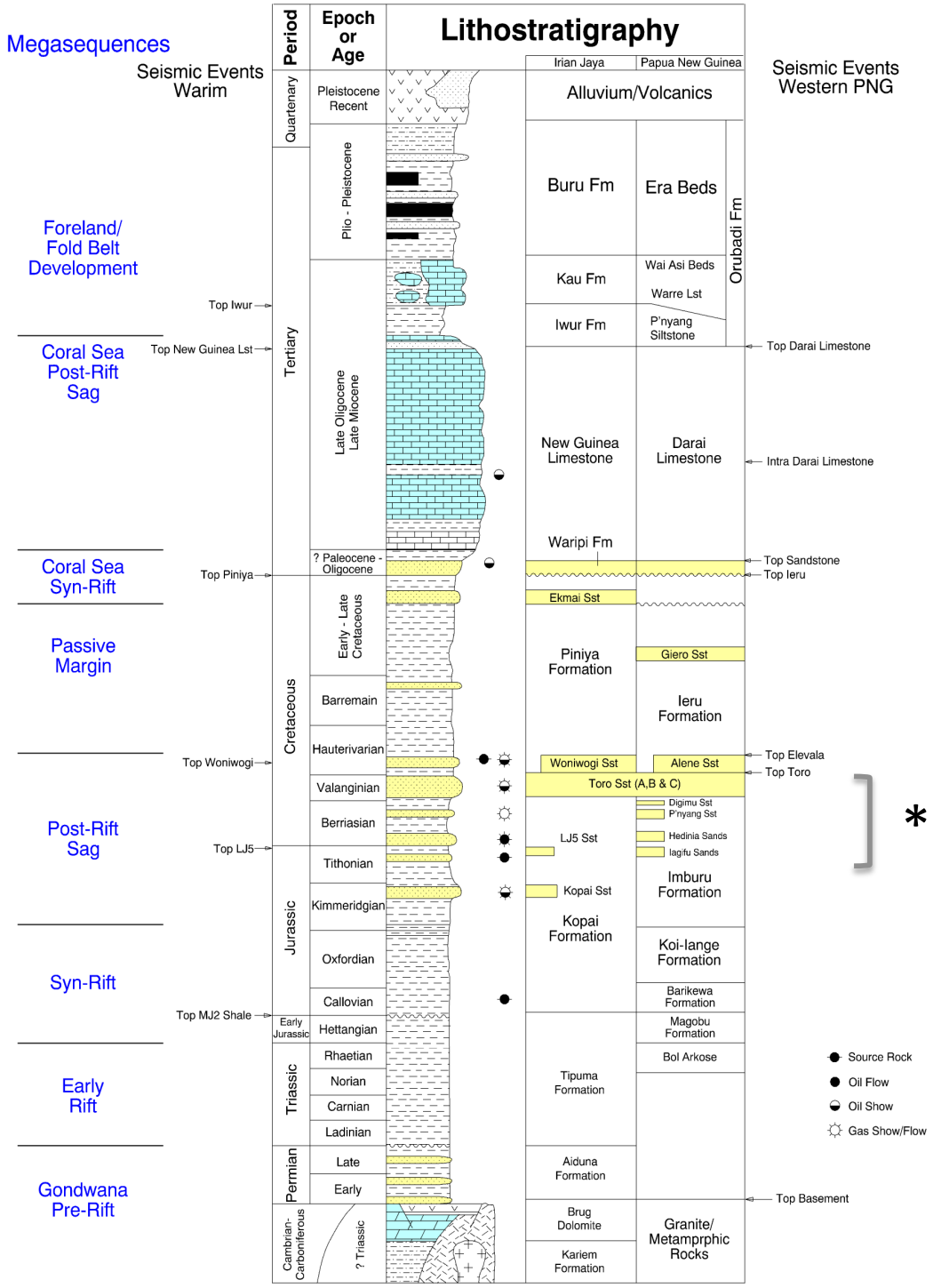

Figure 2.5a: Lithostratigraphic Chart of Papuan Basin

Lithostratigraphic chart of Papuan Basin showing major tectonic phases (Buick et al., 2009). (Asterisk denotes bracketed section of lithostrigraphic chart that is expanded and shown in increased detail in Figure 2.5b)

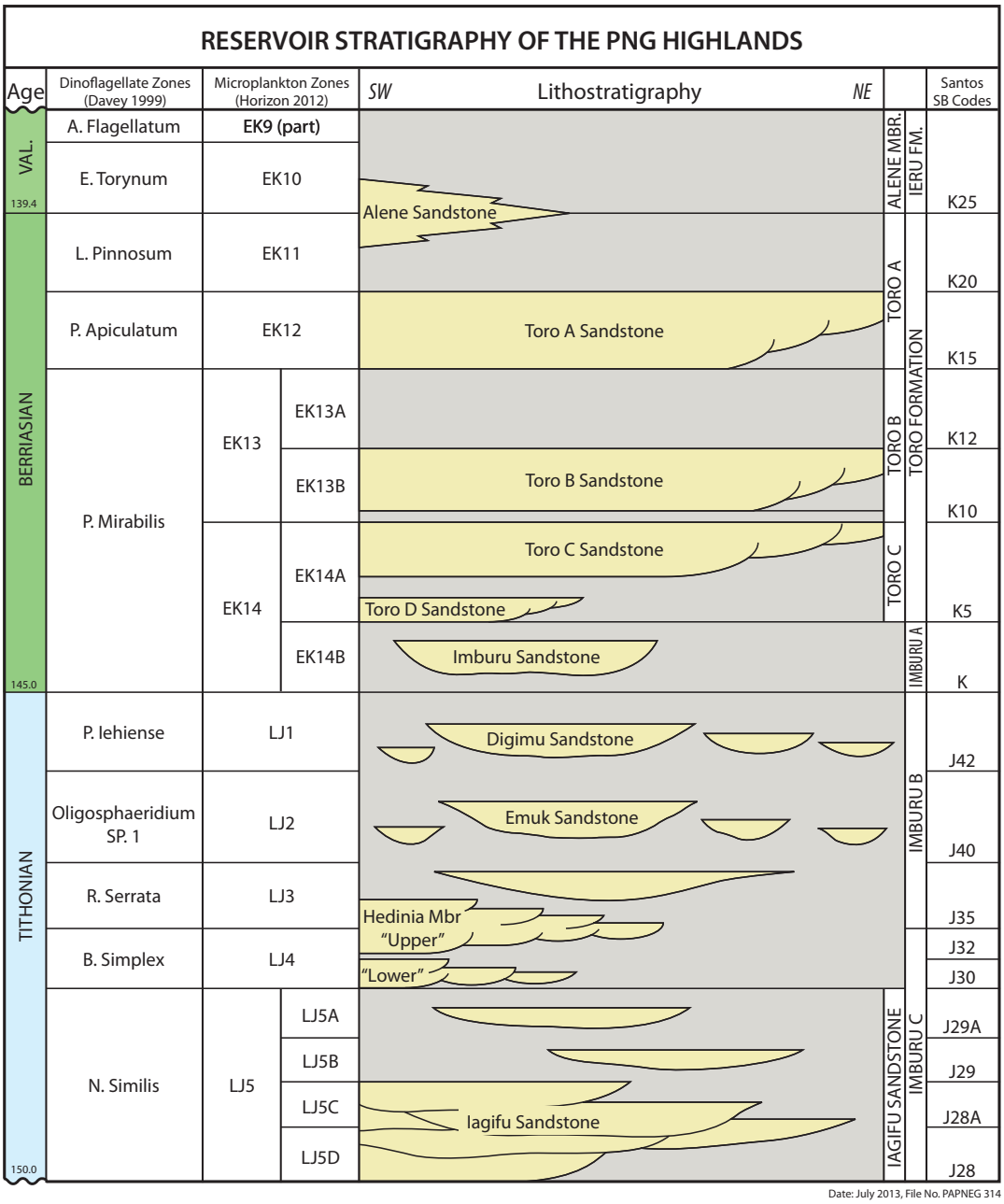

Figure 2.5b: Lithostratigraphic Chart of Papuan Basin

Expanded section of lithostratigraphic chart shown in Figure 2.5a marked by asterisk. Represents a more detailed/modified lithostratigraphic chart section showing important reservoirs of fold belt and foreland regions of Papuan Basin (Santos, 2013). Note there has been an update with this Santos stratigraphic designation of reservoir sand units compared to the earlier stratigraphic column shown in Figure 2.5a.

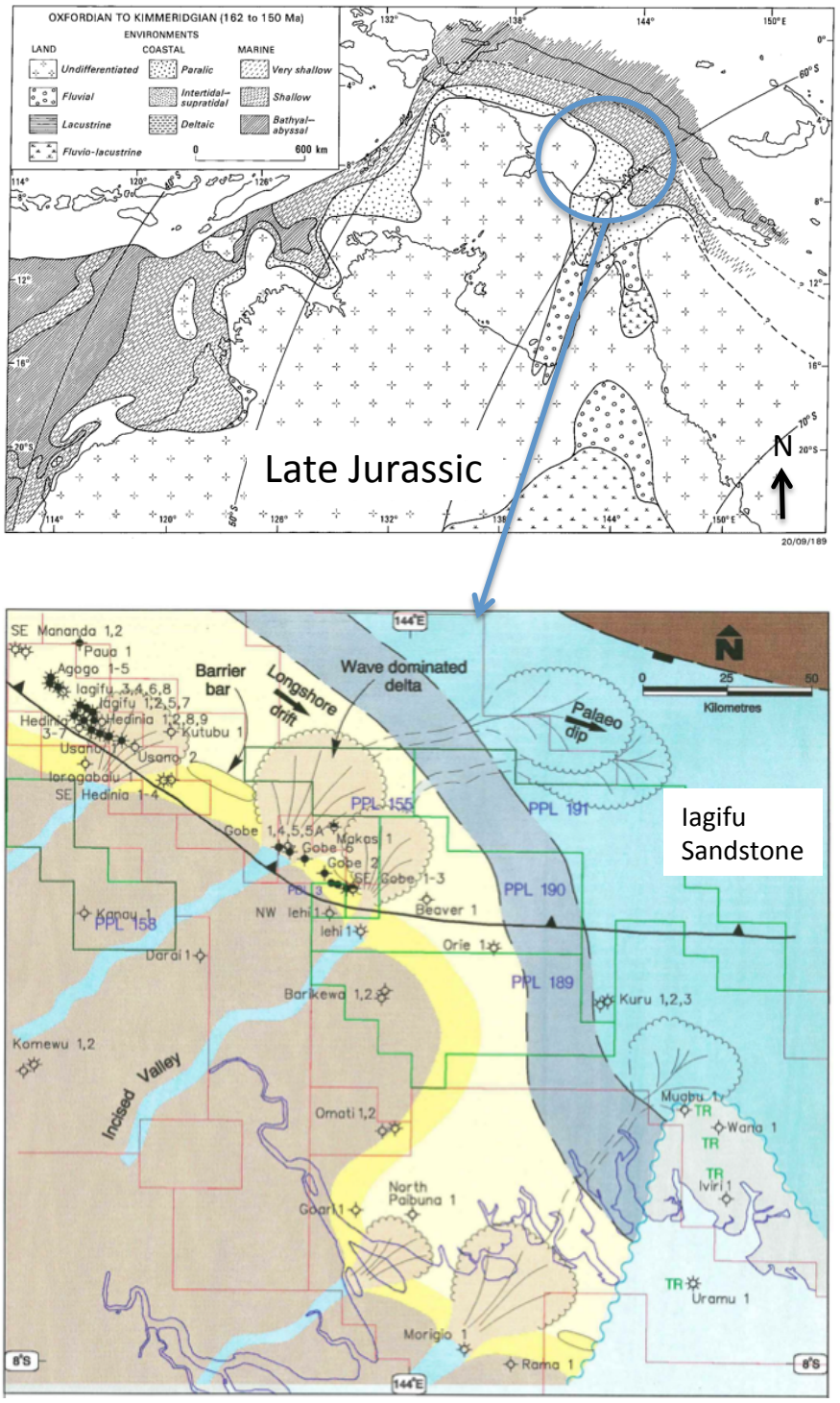

Figure 2.6a: Palaeo-Geography of Papuan Basin Region During Iagifu Sandstone Deposition

Top panel - Late Jurassic depositional environment off the northern margin of the Australian Craton, shown relative to current Australian continent and PNG landform structures. Bottom panel - Depicts palaeo-geographical model of Iagifu Sandstone deposition, showing location of shoreline during late Jurassic (located in southeastern portion of fold belt in Papuan Basin) relative to current PNG landform structure. Light brown - coastal plain, dark yellow - estuarine/shoreface, light yellow - inner shelf, and blue - deeper water/continental slope. (Struckmeyer, 1990; Santos, 2008)

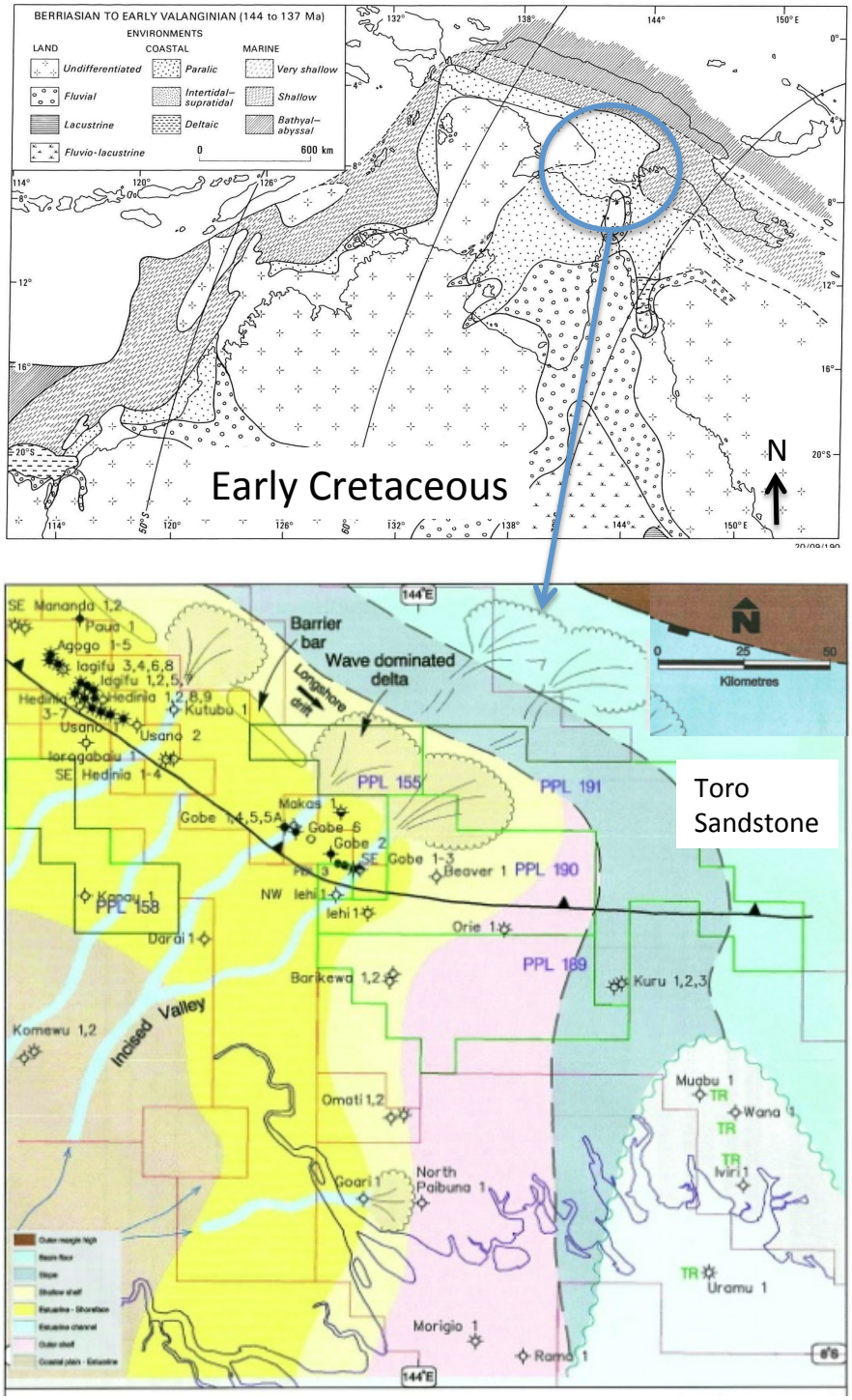

Figure 2.6b: Palaeo-Geography of Papuan Basin Region During Toro Sandstone Deposition

Top panel - Early Cretaceous depositional environment off the northern margin of the Australian Craton, shown relative to current Australian continent and PNG landform structures. Bottom panel - Depicts palaeo-geographical model of Toro Sandstone deposition, showing location of shoreline during early Cretaceous relative to current PNG landform structure. Light brown - coastal plain, dark yellow - estuarine/shoreface, light yellow - inner shelf, pink - outer shelf, and blue - deeper water/continental slope. (Struckmeyer, 1990; Santos, 2008)

2.3 Structural Setting

On-going arc-continent collision of the Australian Plate with the Pacific Plate, commencing in the Late Miocene to Pliocene, has caused the inversion of the Papuan Basin sedimentary deposits (Mesozoic post-rift/continental shelf margin marine sequences and Cenozoic foreland basin sequences) and has resulted in the development of the Papuan Fold Belt (Hill, 1991; Hill et al., 2004). Southwest verging fault propagation folds and northwest to southeast trending thrust faults, evident at the surface, characterise the Papuan Fold Belt (Hill, 1991) (Figure 2.7).

The fault-propagation folds generated along the leading edge of the Papuan Fold Belt form the major anticlinal trapping structures involving the Early Cretaceous Toro and Upper Jurassic Imburu Formation reservoir sandstones (Hill, 1991; Eisenberg, et al., 1994; Craig and Warvakai, 2009). Other potential trapping structures within the Papuan Fold Belt involve ramp anticlines, duplexes and sub-thrust anticlinal structures that are related to reactivated extensional structures that began as rollover anticlines present in the footwall (Hill, 1991; Buchanan and Warburton, 1996; Cole et al., 2000).

The surface geology and topography give an indication of the structure in the fold belt at depth. However, due the common occurrence of complex thrust detachments within the Ieru Formation shale layers, the depth structure at reservoir level is often offset from the surface geology (Hill et al., 2004). A series of cross sections along the fold belt (two of which also include foreland Papuan Basin regions) are shown in Figures 2.8 and 2.9a-e.

Sinuous anticlines characterise the southeastern portion of the fold belt in the Gobe and South East Gobe Fields up through the central fold belt to the Kutubu Complex of fields (Agogo-Hedinia/Iagifu-Usano) (see Figures 2.7 and 2.8). Whereas, in the northwest more extensive and broader anticlinal structures incorporating basement-involved faults predominate. The sinuous nature of the anticlines in the southeast of the fold belt, suggest the presence of en-echelon faults running along the fold belt, which may affect reservoir continuity. The en-echelon faulting in the fold belt is indicative of strike-slip tectonic stresses in operation, consistent with the oblique convergence generating the fold belt.

Cross cutting lineaments have been mapped from surface topography, aeromagnetic data, satellite imagery, and alignment of extrusive volcanics (Hill, 1991; Hill et al., 2000; Hill et al., 2008). These faults are not definitively identified at the surface, and are inferred due to significant changes in structural styles, topographic variations, and basement uplift. These features are most likely related to pre-existing basement faults (Figure 2.7). The most prominent of these features is the Bosavi Lineament, which appears to separate the Agogo and South East Mananda Fields and significantly fault the Moran Field (Figure 2.10). This northeast trending

transfer zone marks an abrupt change in fold style, with the basement-involved anticlines, such as the Muller Anticline to the northwest and shallower sinuous anticlines to the southeast (Hill et al., 2000; Hill et al., 2008). Cross cutting faults have also been observed to define the limits and separate Usano and Gobe Fields, and potentially provide barriers to the regional Toro and Imburu Formation aquifers or open aquifer flow to the foreland (Hill et al., 2000). There are also major shear zones/faults generated during previous tectonic extension and wrenching of the region that cut across the fold belt (Hill et al., 2000; Buick et al., 2009).

An important tectonic element controlling the fold belt development is the regional shelf edge (Hill et al., 2000). This is interpreted to be underlain by a crustal scale extensional fault that controlled the position of the shelf margin and hence the transition between Mesozoic and Tertiary basin depositional sequences (Figure 2.9a).

It is believed that the basement structures have influenced the deformation during compression by reactivation of normal faults, and varying levels of thrusting against different ramp geometries, for instance generating the thin-skinned deformation in the southeast of the fold belt compared to deeper deformation structures in the northwest (Buchanan and Warburton 1996; Hill et al., 2000; Hill et al., 2008). In addition, oblique convergence has caused the northwest of the fold belt in PNG to undergo considerably more deformation than the southeast, producing a developing foreland basin that is absent in the southeast of the basin (Figure 2.3) (Hill et al., 2004).

Within the foreland region of the Papuan Basin there are several major normal fault systems, which trend northwest to southeast and define the boundaries of several of the features in the foreland (Darai Plateau, Omati and Turama Troughs, Fly Platform and the Fly/Strickland Depocentre to the northwest) (Figure 2.1b). These include the Komewu and Darai Fault zones that have been generated from earlier extensional events that were involved in initiation of the Papuan Basin in the late Triassic/Early Jurassic (Figure 2.1b). These fault systems have undergone reactivation to varying extents within the foreland with the compression of the fold belt to the northeast (McConachie et al., 2000).

In most cases, seismic data is of poor quality throughout the fold belt, and has not been used as the sole basis for mapping. Field mapping has been achieved by utilising a variety of data and methods [ie. combination of surface geology, synthetic aperture radar (SAR), topography, aeromagnetic data, strontium isotope data, palynology, dipmeter data, and 2D balanced cross sections (Cole et al., 2000)]. However, seismic data has improved sufficiently in the last 10 years with advances in both acquisition and processing to begin to delineate hanging wall structures in the fold belt and prove a useful guide to final structural interpretation (Cole et al., 2000; Hill et

al., 2004; Bradey et al., 2008; Goffey et al., 2010). Backlimb and near crestal positions of structures in the fold belt are now adequately imaged, but steeply dipping to near vertical forelimb and footwall geometries are still proving difficult to image (Kveton et al., 1998; Johnstone and Emmett, 2000). Because of a lack of good quality seismic data, reservoir pressure data becomes very important for indicating the presence or lack of reservoir continuity. When combined with surface geology and subsurface well control, particularly dipmeter data, pressure data provide important information for working out the complex fold and thrust belt structures (Eisenberg, 1993).

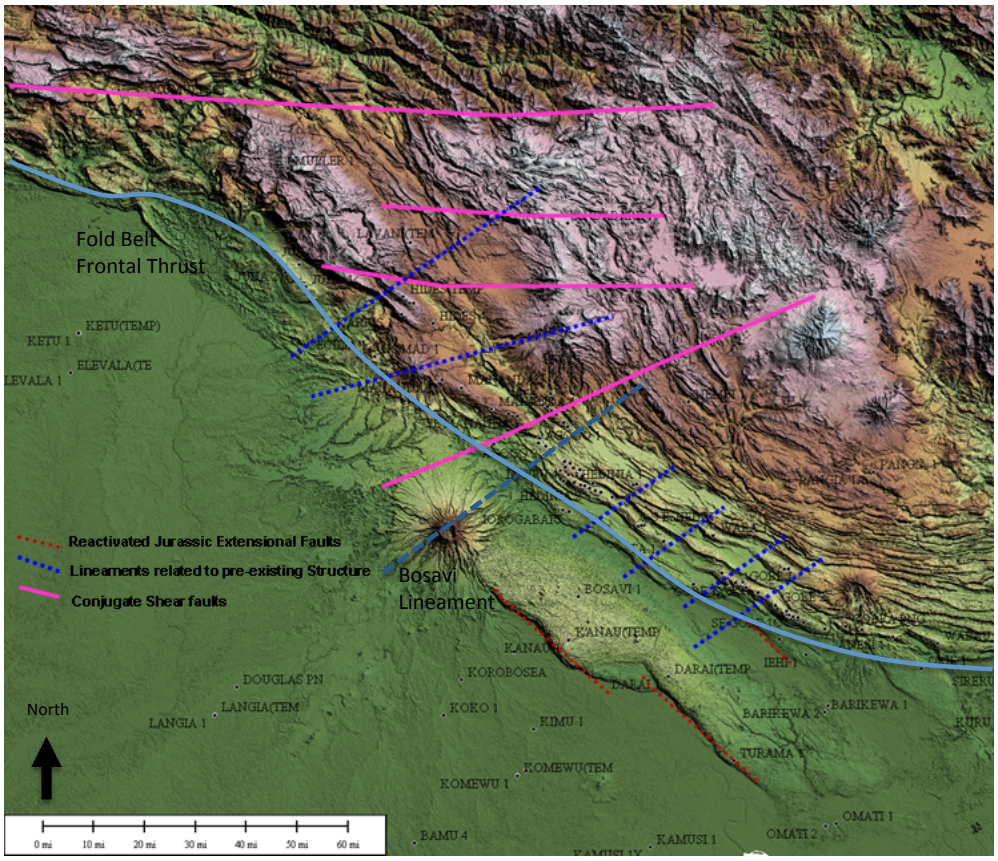

Figure 2.7: Papuan Basin Structural Elements Interpreted from Surface Image Data
Satellite image of Papuan Basin showing central fold belt region and adjacent northeast region of foreland. Note the presence of sinuous anticlines south of the Bosavi Lineament in southeast region of fold belt. While, in the northwest of the fold belt, north of the Bosavi Lineament extensive and broader anticline structures are present (Buick et al., 2009).

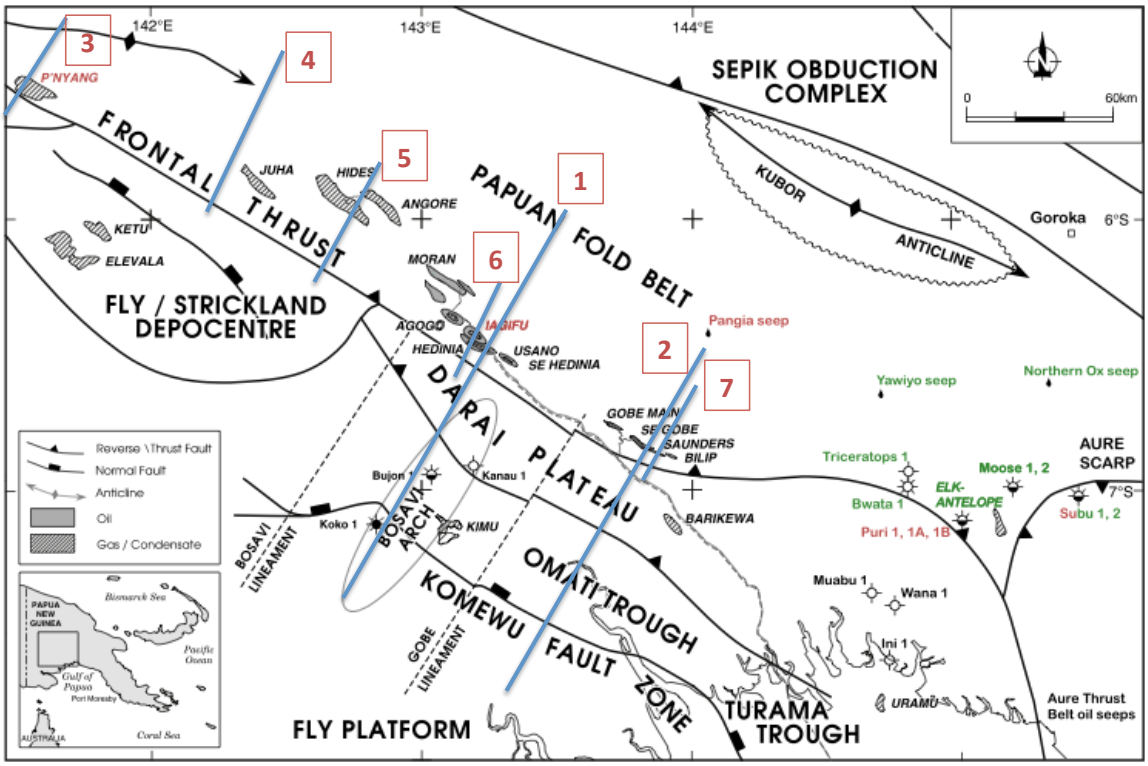

Figure 2.8: Papuan Basin Cross Section Lines

Cross section lines 1-7 presented in Figures 2.9a-c. (modified from Ahmed et al., 2012)

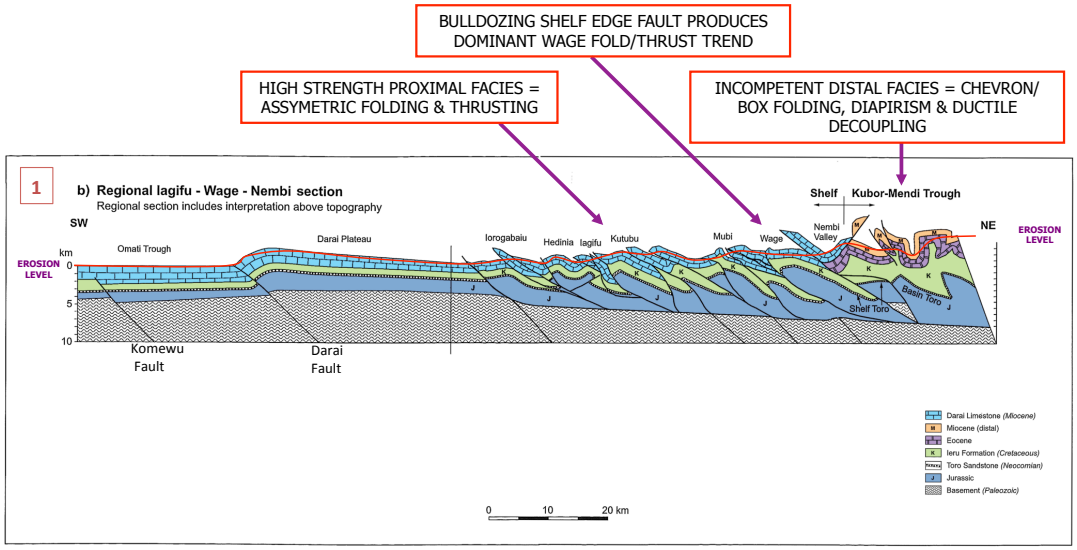

Figure 2.9a: Papuan Basin Cross Section Line 1

Cross section location presented in Figure 2.8. (Santos, 2008, modified from Hill et al., 2004)

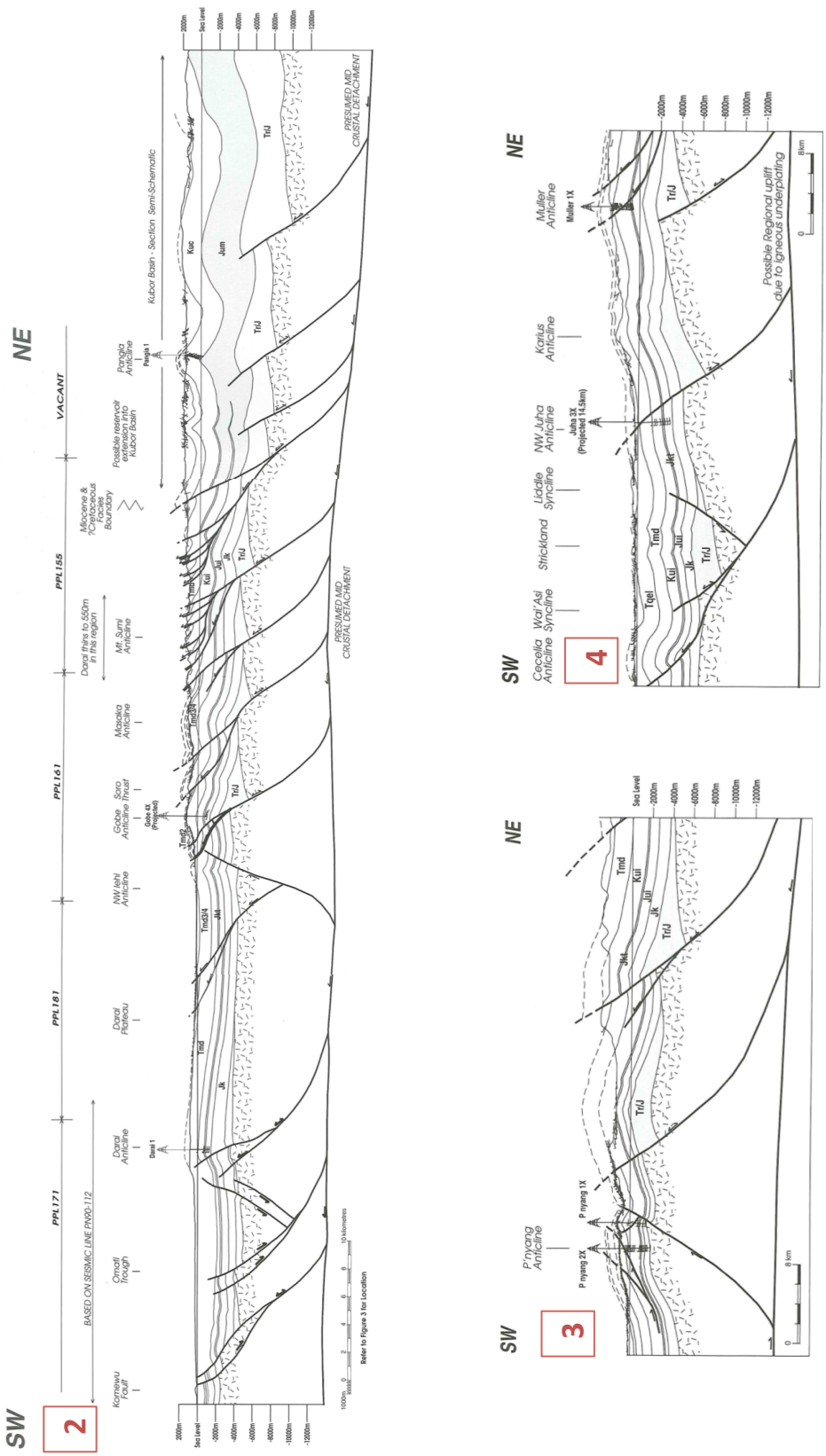

Figure 2.9b: Papuan Basin Cross Section Lines 2-4
Cross section locations presented in Figure 2.8. (Buchanan and Warburton, 1996)

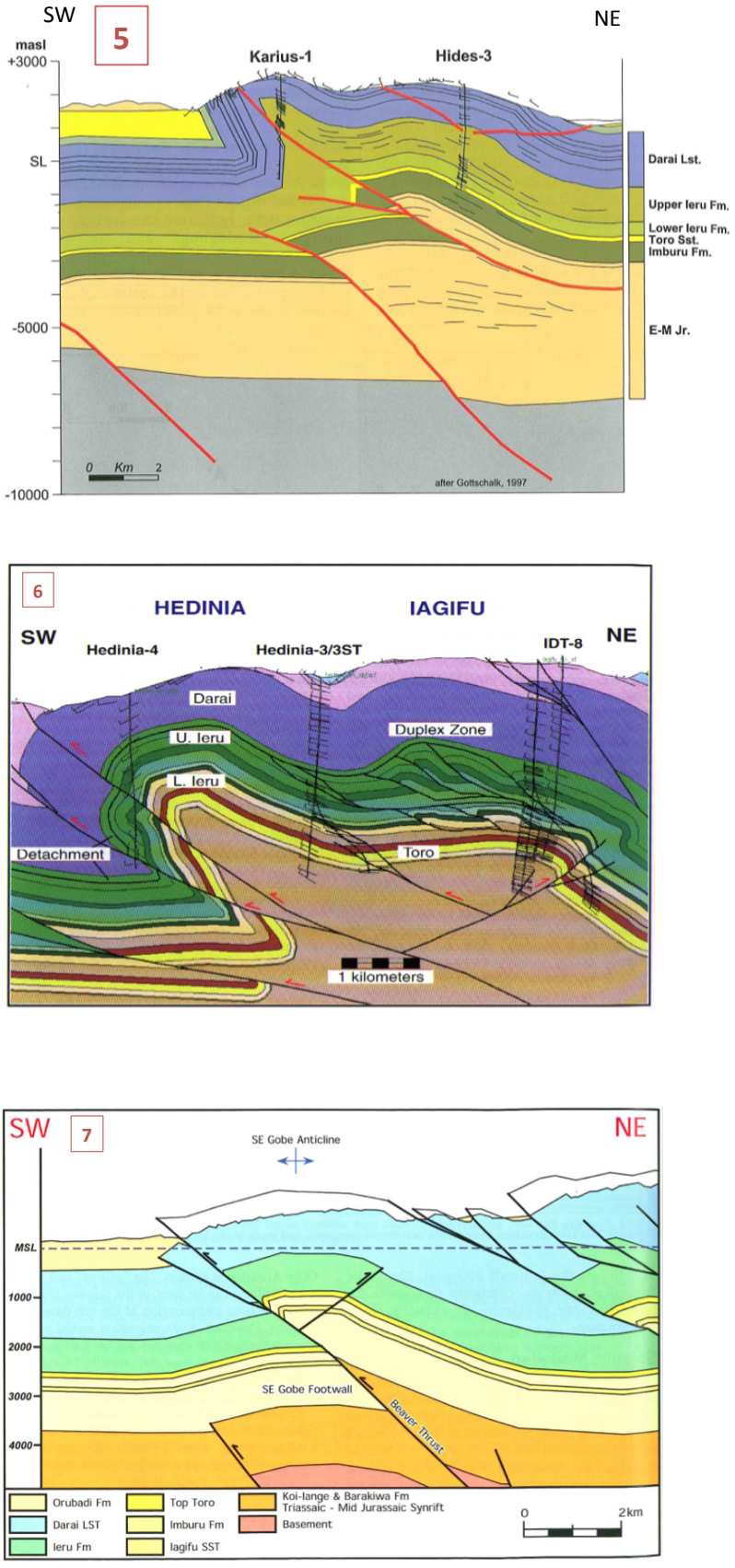

Figure 2.9c: Papuan Basin Cross Section Lines 5-7

Cross section locations presented in Figure 2.8. (Panels 5 and 6 - Santos, 2008; Panel 7 - Johnstone and Emmett, 2000)

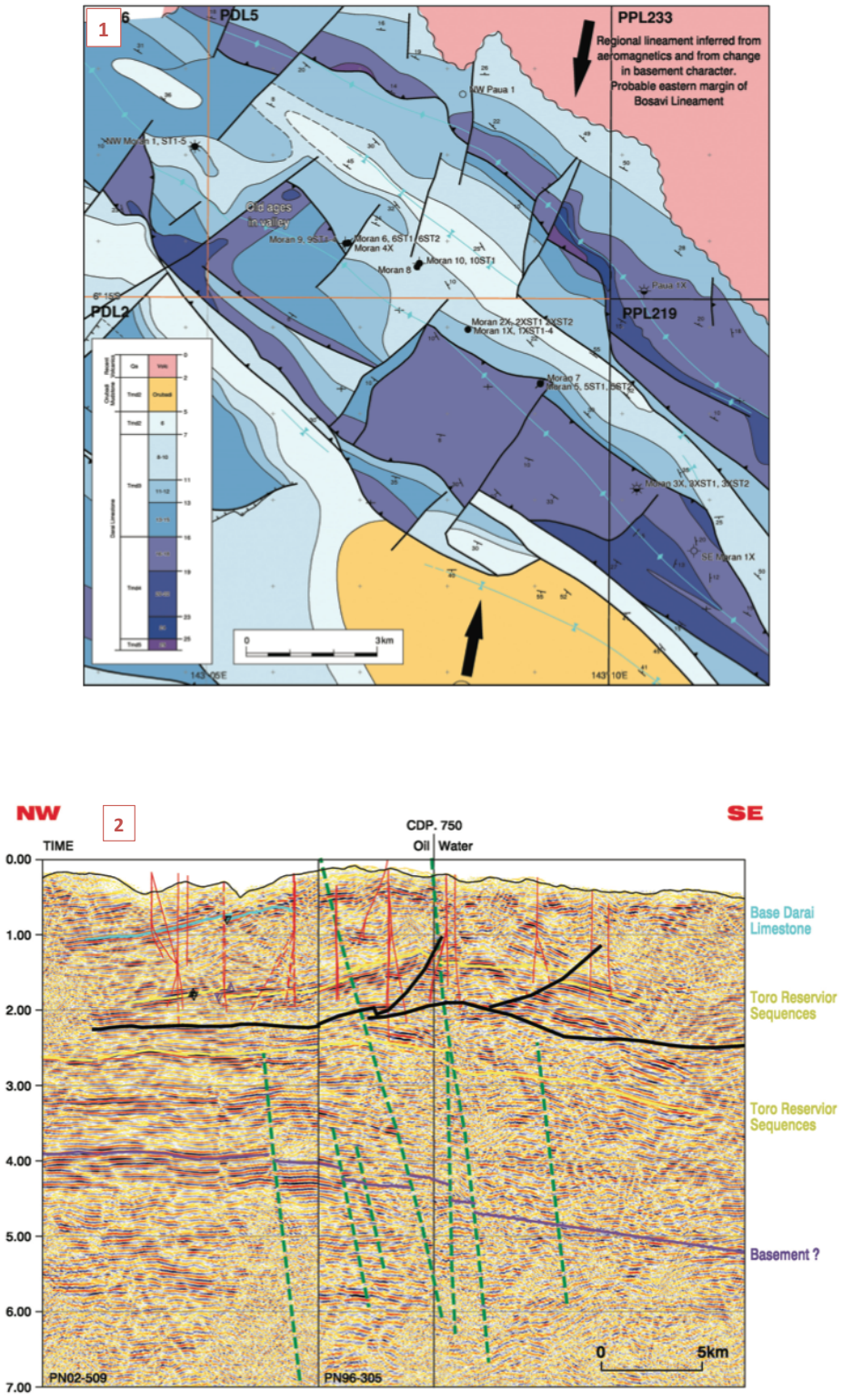

Figure 2.10: Faulting in the Moran Field

Panel 1 - Moran faults at surface determined by Sr isotope mapping data. Panel 2 - Moran Field seismic strike line, showing basement faulting (Bosavi Lineament) influencing the faulting and structure of overlying Toro reservoir (Hill et al., 2008).

2.4 Key Reservoir Units

The properties and distributions of the Toro Sandstone and Imburu Formation (Digimu, Hedinia and Iagifu Sandstone units) in the Papuan Basin are described in this section. The main reservoir interval in the Papuan Basin Fold Belt is the Lower Cretaceous Toro Sandstone, which has excellent lateral continuity (and is typically ~100m thick gross interval) along the length of the fold belt. This is because the reservoir sands were deposited in an extensive shoreline aligned roughly parallel to the present day fold belt. The Toro Sandstone was predominantly deposited in a near-shore high-energy environment with reworking by waves (Varney and Brayshaw, 1993; Madu, 1996; Hirst and Price, 1996). Toro reservoir distribution and thickness are shown in Figure 2.11. A regional gamma-ray log correlation of the Toro Sandstone is shown in Figure 2.12 across the Agogo-Hedinia/Iagifu Fields, which demonstrates good lateral continuity (Bradey et al., 2008).

Toro reservoir quality is laterally consistent along the fold belt (palaeo-shoreline) northwest to southeast but displays reduced quality moving west to southwest from the main palaeo-shoreline depositional setting. This is seen in the example where even though the Toro gross reservoir interval maintains a stratigraphic thickness ~100m, it shows a trend of decreasing net/gross from 70% at Mananda in the southeast to Hides (44-62%) to 21% at Juha in the west (Johnstone and Emmett, 2000).

The Toro Sandstone is divided into three coarsening up units, A, B and C, that are separated by thin silty layers (Eisenberg et al., 1994) in the Hedini/Iagifu Fields. The basal unit, Toro C, is made up of lower shore face silty sandstones, which are inter-bedded with clean sands deposited in high-energy near shore to estuarine depositional environments. However, in the Hides Field, Toro C is interpreted to be of entirely estuarine depositional origin. The overlying Toro B is a transgressive, predominantly shale prone interval, often further divided into Upper and Lower Toro B. The Lower Toro B consists of offshore mudstone with locally integrated middle to lower shore face sandstones. The Upper Toro B is predominantly shale. The Toro A is generally the best quality of the Toro sands. This unit comprises clean progradational sandstone with upward coarsening profiles typical of a shoreline dominated depositional system (Varney and Brayshaw, 1993; Madu, 1996; and Hirst and Price, 1996).

The Toro A, B, and C units have been found to behave as separate reservoirs in the region between the Hedinia and Iagifu Anticlines in the Kutubu Complex (Eisenberg, 1993). However, pressure data suggests the reservoirs act as a single unit in some fields where they are mapped (eg. at Hides Field - Johnstone and Emmett, 2000). This interconnectivity has been interpreted to

be due to conductive intra-field faulting, abutting different sand packages across a fault. It is unlikely that in many wells (eg. Hides Field) there is vertical communication through the intervening marine shale units without faulting (Langston, 2013).

Toro porosity in the Kutubu Complex of fields (Agogo-Hednia/Iagifu-Usano) is between 12-15% and permeability ranges up to 2 darcies, but in general is several hundred millidarcies (Daniels, 1993). In the Hides Field, Toro porosity is slightly reduced over all (7-10%) with permeabilities of up to 800 millidarcies (Johnstone and Emmett, 2000). The majority of the Toro at Juha and Angore Fields has 5-6% porosity at under 10 millidarcies permeability but with some intervals up to 9% porosity and 200 millidarcies permeability (Starcher, 2013).

The Digimu Sandstone member of the Upper Jurassic Imburu Formation is a 25m thick marine sandstone very similar to the Toro Sandstone (Eisenberg et al., 1994). It has a similar depositional setting to the Toro Sandstone, however was less extensive. Facies variations occur within this unit from offshore to shoreface, so reservoir quality and thickness vary (Madu, 1996). The Digimu Sandstone reservoir unit is important in the Moran Field where it hosts the majority of the hydrocarbons. Digimu reservoir distribution and thickness are shown in Figure 2.13.

The Hedinia Sandstone is the least important reservoir of the four reservoirs, as the unit does not contain significant volumes of hydrocarbon in the existing fields. It has a similar shoreface depositional setting to the Toro and Digimu Sandstones. Like the Toro, the Hedinia Sandstone also consists of three sandstone units separated by shalier layers (Madu, 1996). Hedinia reservoir distribution and thickness are shown in Figure 2.14. It varies in thickness up to 40m, but averages ~20m thickness along the fold belt region between Mananda and Gobe (Madu, 1996).

The Iagifu Sandstone forms the main reservoir for the Gobe Field where hydrocarbons are actually absent from the Toro and Digimu units. Iagifu reservoir distribution and thickness are shown in Figure 2.15. The Iagifu Sandstone is more laterally variable than the other three sandstones (suggesting a delta front depositional system - see Figure 2.6), with four main areas or lobes of Iagifu Sandstone deposition mapped in the fold belt region (Iagifu, South East Hedinia - Ta-1X, Gobe and South East Gobe lobes) (Madu et al., 1996). [Iagifu thickness at Iagifu lobe ~10m, South East Hedinia - Ta-1X lobe up to 90m, Gobe lobe average thickness ~100m and South East Gobe lobe average thickness ~50m (Madu, 1996)]. There are significant shaley sections laterally between the four lobes of thickest Iagifu Sandstone deposition. This suggests significant potential for lithological compartmentalisation of the Iagifu reservoir. In general the porosity in these four reservoir units ranges from ~5 to 15%, and permeability is typically in the range of 1 millidarcy up to ~1 darcy (Buick et al., 2009).

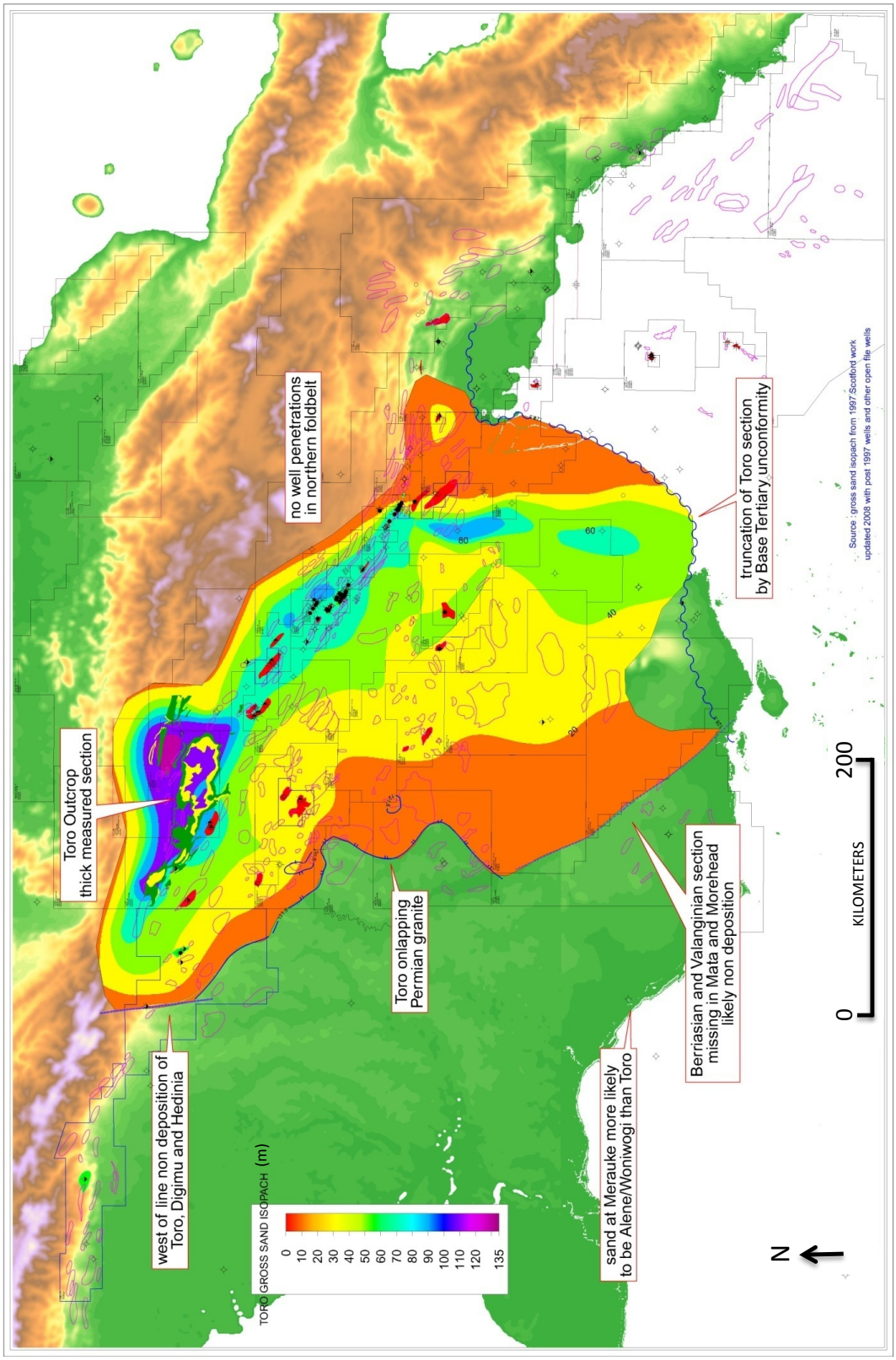

Figure 2.11: Toro Sandstone Distribution and Thickness in the Papuan Basin
(Santos, 2008)

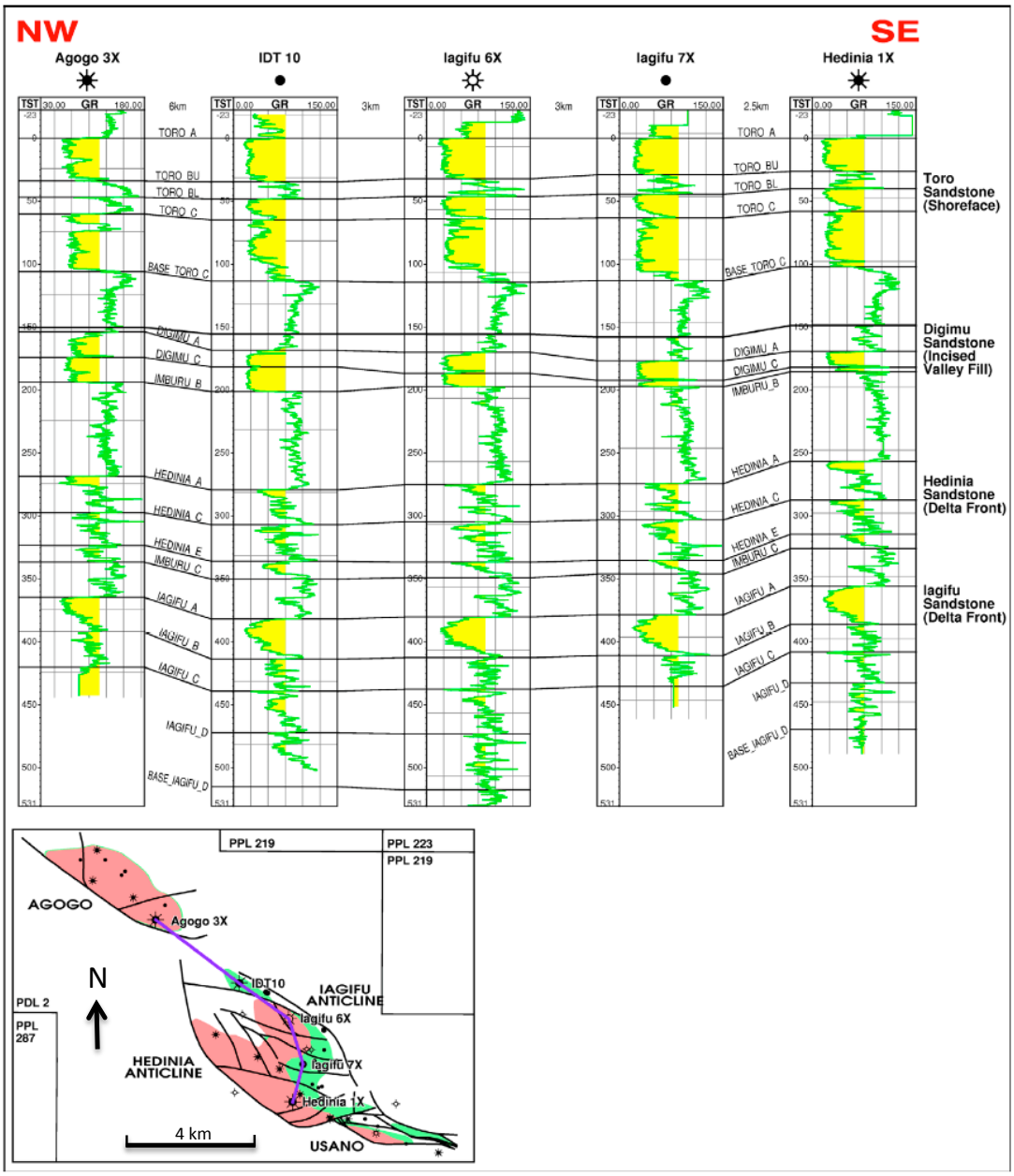

Figure 2.12: Gamma-ray Log Correlation of Toro and Imburu Formation Sandstones Across the Kutubu Complex Fields

Top panel – Gamma-ray log correlation of Toro and Imburu Formation sandstones. Bottom panel - map of Kutubu Complex. Purple line represents orientation of correlated top panel. Pink - gas. Green - oil (Bradey et al., 2008)

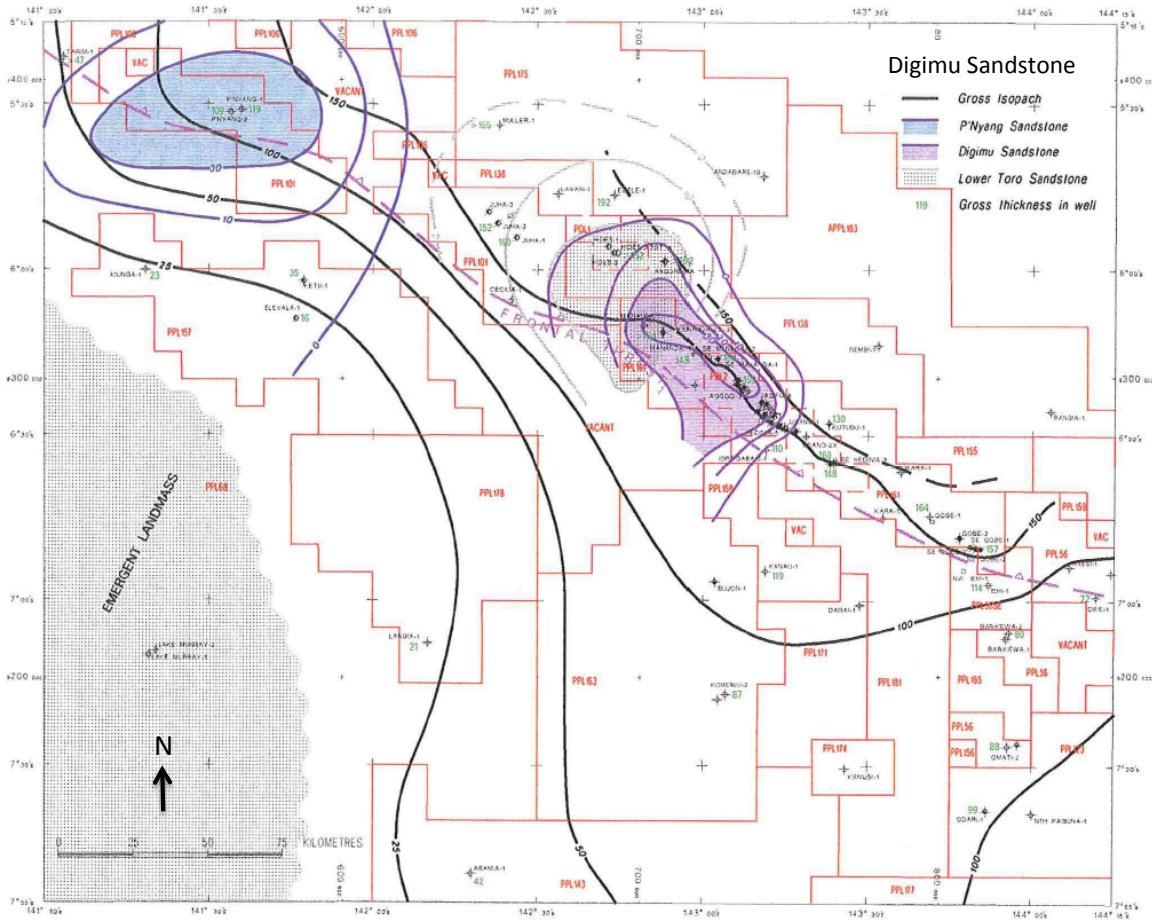

Figure 2.13: Digimu Sandstone Distribution and Thickness in the Papuan Basin
Distribution and thickness of Digimu Sandstone shown in light purple shading and purple contour lines (contour range 0-30m and contour interval 10m). Digimu Sandstone distribution centred over Agogo Field in Papuan Fold Belt. (Hirst and Price, 1996)

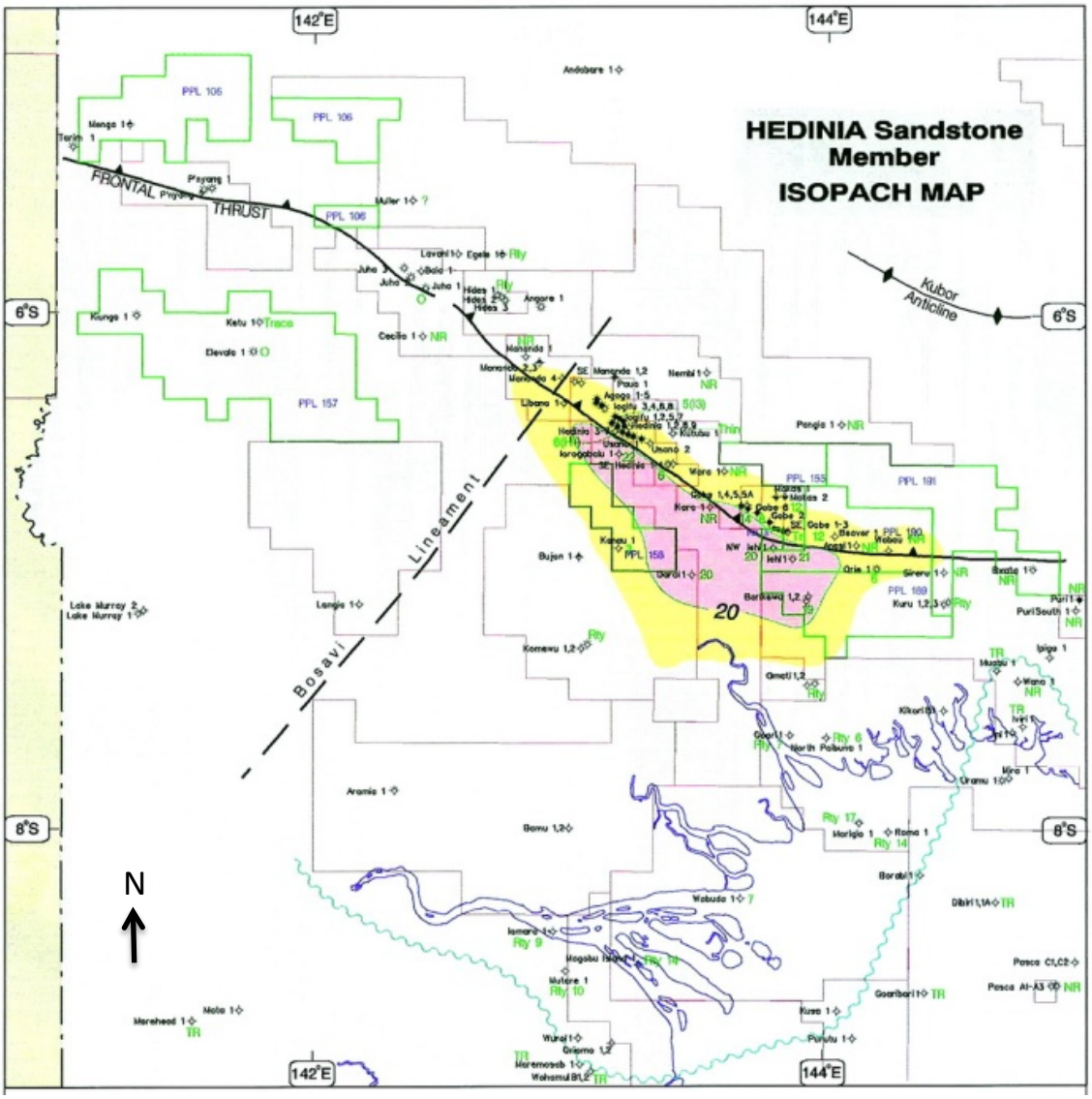

Figure 2.14: Hedinia Sandstone Distribution and Thickness in the Papuan Basin
Hedinia Sandstone shown in yellow and pink shading (contour range 0-20m and contour interval 10m) (Santos, 2008)

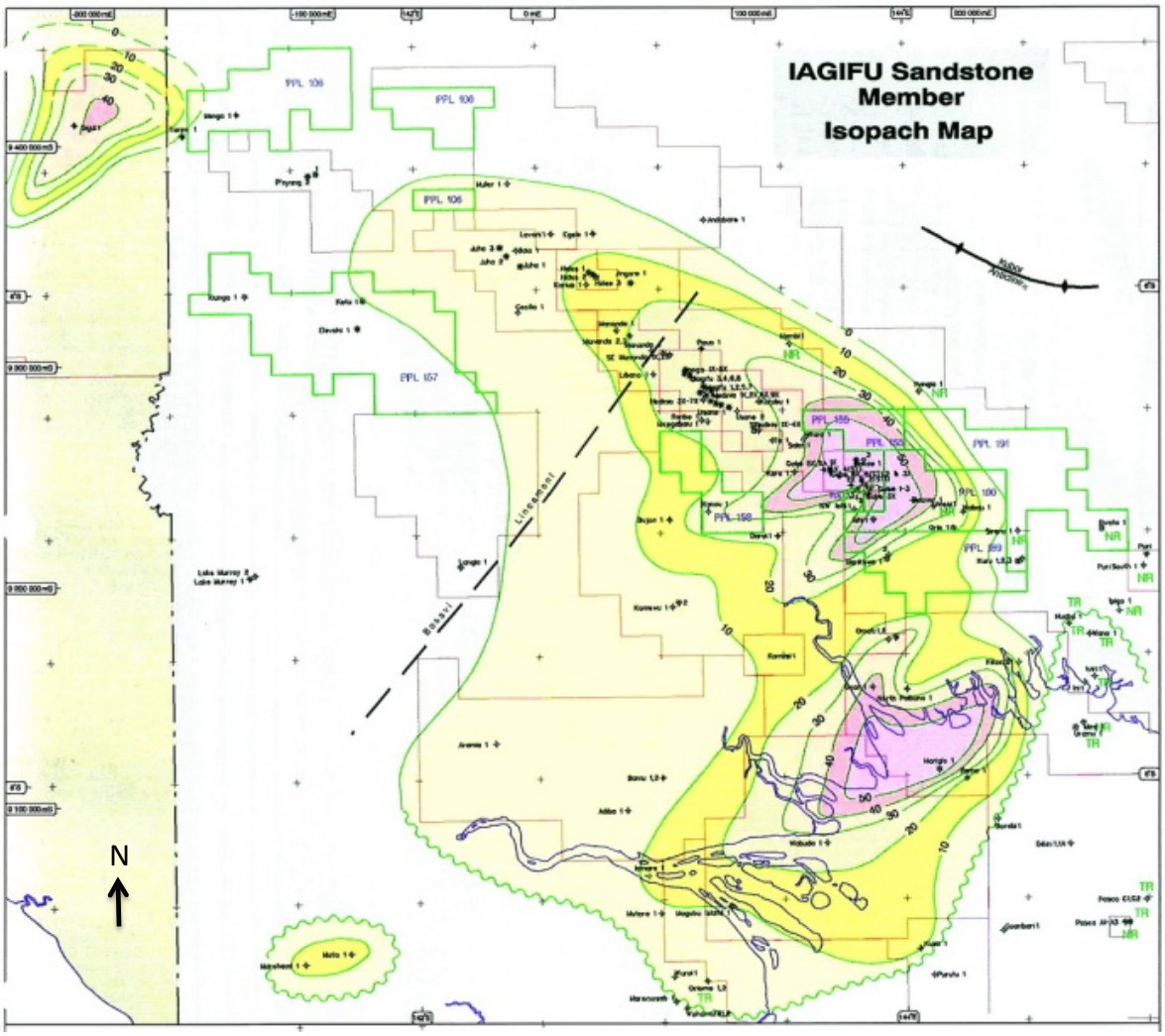

Figure 2.15: Iagifu Sandstone Distribution and Thickness in the Papuan Basin

Iagifu Sandstone distribution shown in yellow and pink shading and green contour lines (10m contour interval). (Santos, 2008)

Chapter 3: Hydrogeology/Hydrodynamics

3.1 General Introduction

Hydrodynamic flow is defined as the lateral movement of water through an aquifer, whereas in a hydrostatic environment, there is no horizontal component to the movement of the water (Dahlberg, 1995). Hydrodynamic flow of formation water is caused by lateral variations in pressure (potentiometric gradients) within a basin aquifer. Hydrodynamic flow can cause the OWCs and GWCs in a reservoir to be tilted (Dennis et al., 2000; Dahlberg, 1995) (Figure 3.1).

In a hydrodynamic environment, fluid movement occurs in response to differences in potential energy, with flow from regions of high to low energy (Dahlberg, 1995). Hydrodynamic flow direction can be identified using a potentiometric surface map that plots hydraulic potential (Hw) values for formation water at different points in a reservoir formation (see sections 4.4 and 4.5 for descriptions of Hw and potentiometric surface maps) (Figure 3.2).

Many examples of hydrodynamic flow have been described, and in most cases, are in basins where the flow of formation water is basin-ward driven by meteoric water recharge from neighbouring highland regions (eg. Persian Gulf oil fields - Zagros Fold Belt, and Rocky Mountain foreland basins of North America). The significant topographical relief and high rainfall in the Papuan Fold Belt favours such a basin-ward hydrodynamic mechanism (Cockroft et al., 1987). However, there are examples where the flow of formation water is outwards from the basin, because of dewatering, away from the over-pressured basin centre (eg. regions in the North Sea and Gulf of Mexico) (Dennis et al., 2000). Common effects of hydrodynamic flow include tilted OWCs, flushed structural or stratigraphic traps, and structurally offset hydrocarbon accumulations, as well as pools with no apparent trap (Cockroft et al., 1987).

Changes in OWC depth across reservoirs can be caused by factors other than hydrodynamic aquifer flow such as structural or stratigraphic barriers to flow within the reservoir (Muggeridge & Mahmode, 2012). Different OWCs and GWCs can be associated with reservoir compartmentalisation, which can occur in reservoirs that have undergone faulting. Significant faulting is characteristic of fold and thrust belts (Goffey et al., 2010).

It is often difficult to unambiguously identify whether compartmentalisation or a hydrodynamic aquifer is causing the different OWCs particularly if the lateral pressure gradients causing aquifer flow have changed in the recent geological past (Muggeridge & Mahmode, 2012). A characteristic of compartmentalisation is assumed to be different oil pressures in different parts of the reservoir, but this can also be evidence that the system has yet to reach equilibrium (Dennis et al., 2000). The existence of a lateral pressure gradient in the aquifer and no such gradient in the oil

leg is commonly assumed to indicate of a hydrodynamic aquifer behavior and good lateral communication. However, it is equally possible that pressures may have equilibrated through a low permeability baffle over geological time scales but would not equilibrate through such a baffle on production time scales (Dennis et al., 2000). Areal variations in reservoir permeability may also result in significant variations in tilt across a field (Muggeridge & Mahmode, 2012). It should be noted that hydrodynamic flow is extremely slow compared to production time scale water flow. Such flows are in the order of cm/year flow rates and potentially take several hundred thousand years to reach tilted equilibrium once flow starts or return to horizontal once flow stops (Dennis et al., 2000; Muggeridge & Mahmode, 2012).

The difficulty of differentiating hydrodynamic flow from compartmentalisation is shown when looking at various examples of potentiometric surface maps and trying to correctly interpret whether or not hydrodynamic flow or compartmentalisation is responsible for the observed potentiometric pattern (Figure 3.2). This situation is present in the Papuan Fold Belt where significant faulting has likely compartmentalised the reservoirs, but there is also good evidence for hydrodynamic aquifer behavior in several connected fields of the fold belt.

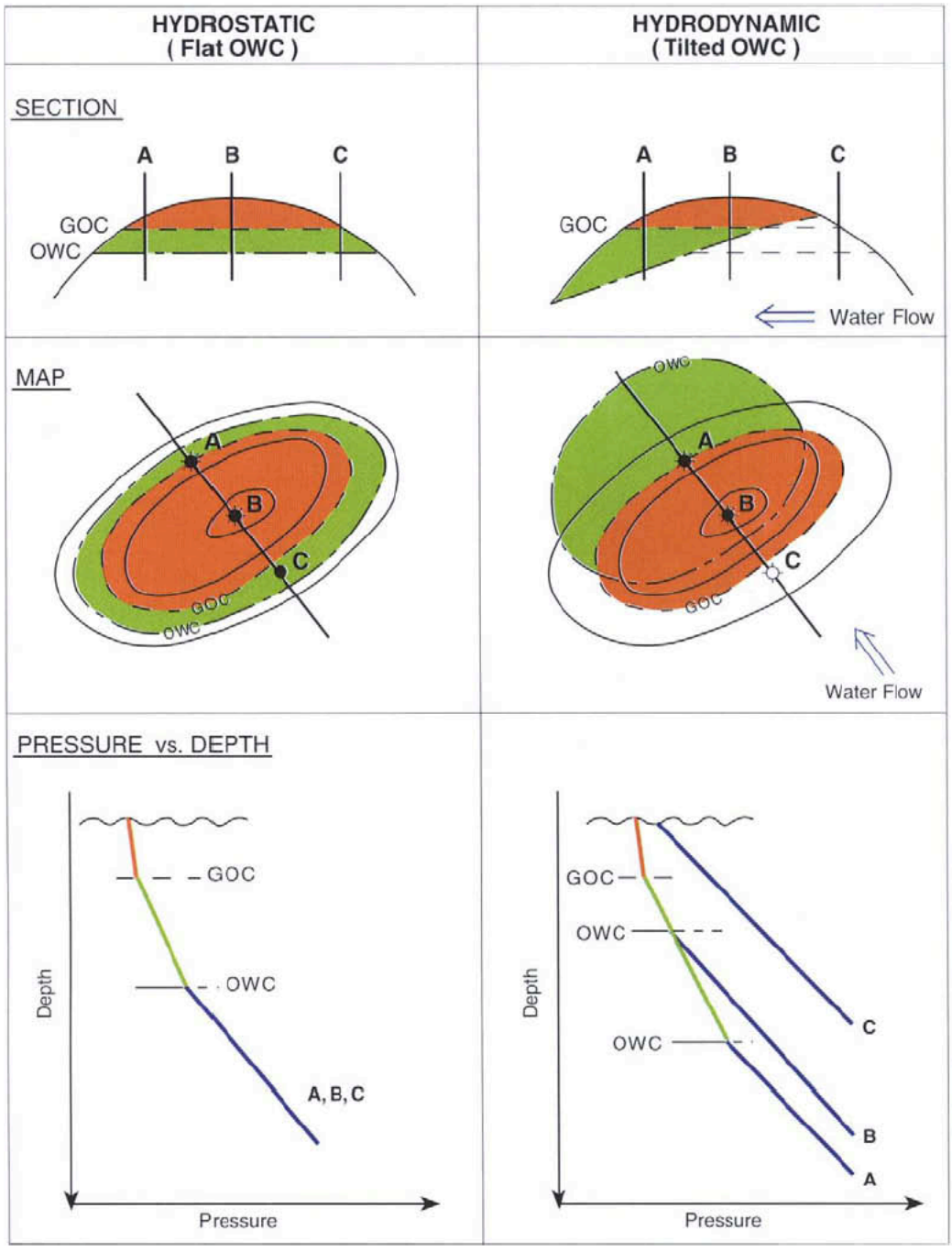

Figure 3.1: The Effect of Hydrodynamic Aquifer Behaviour on Oil and Gas Accumulations
In the hydrodynamic case the aquifer pressures vary across the field, whereas the oil and gas pressures remain constant. The oil-water contact (OWC) and gas-water contact (GWC) become tilted as a result. The GWC is less tilted than the OWC, due to the greater buoyancy of the gas. The gas-oil contact (GOC) remains flat because there is no movement of the underlying oil leg - the field is in hydrodynamic equilibrium. If the field was divided into static pressure cells, the oil pressures would also tend to differ between the wells (Dennis et al., 2000).

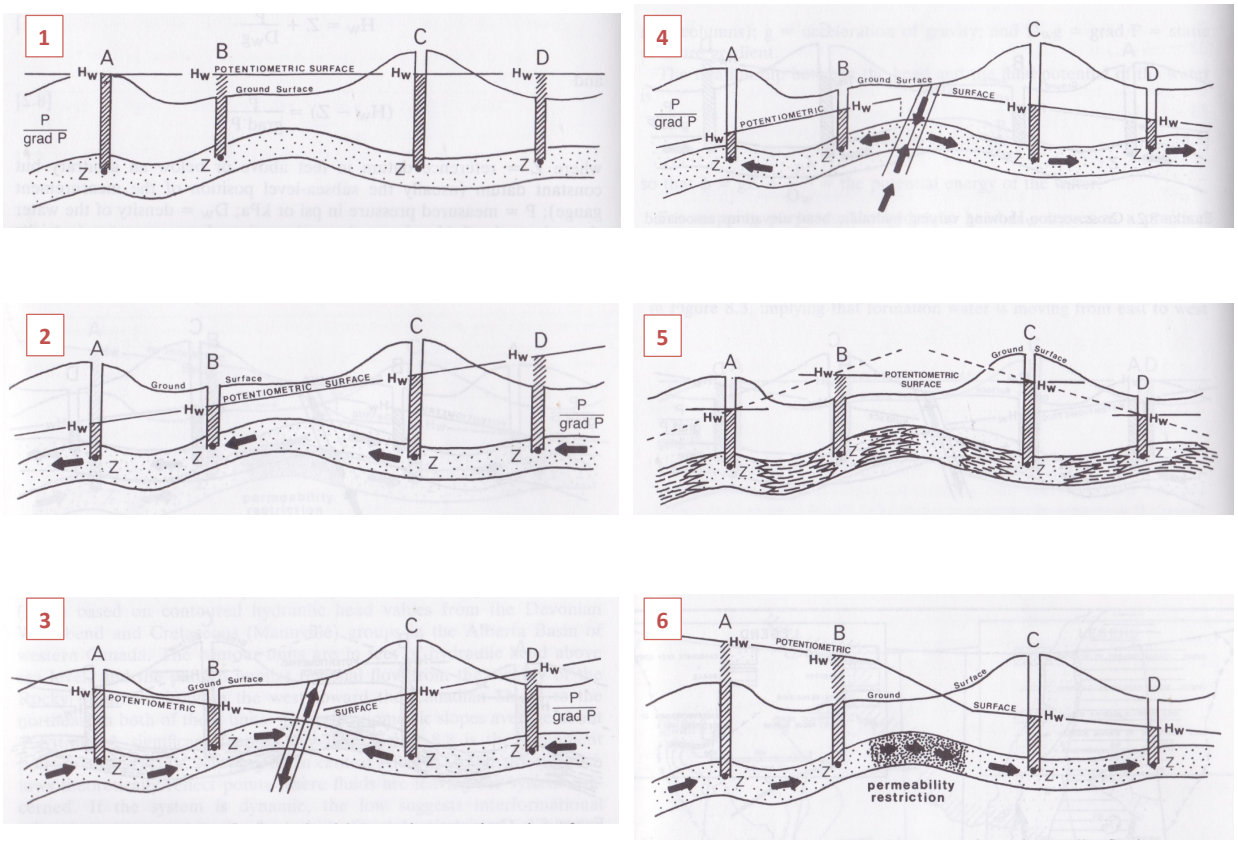

Figure 3.2: Examples of Subsurface Flow Patterns from Potentiometric Surface Mapping

(1) Cross section illustrating hydraulic potential (Hw) elevations and potentiometric surface based on four wells. Surface is horizontal so no flow inferred (hydrostatic situation).

(2) Cross section showing varying hydraulic potential elevations associated with four wells. Potentiometric surface slopes to the west, thus east to west water flow is inferred.

(3) Cross section reflecting a local low on the potentiometric surface. Converging water flow pattern is inferred. Water has to flow vertically either to formation above or formation below.

(4) Cross section illustrating local potentiometric high from which diverging water flow pattern is inferred.

(5) Cross section demonstrating a local potentiometric high from which diverging water flow pattern might be incorrectly inferred. Represents stratigraphically compartmentalised scenario but equally could be fault compartmentalised.

(6) Cross section illustrating a potentiometric step, reflecting water flow restriction due to a reduced permeability zone. Could also be due to fault disruption of the reservoir such that a restricted section of the reservoir is now in contact/juxtaposed across the fault.

Note - Hw = hydraulic potential, Z = depth of pressure measurement. (Dahlberg, 1995)

3.2 Papuan Basin Review

This section reviews the three previously published hydrogeology studies in the Papuan Basin (Eisenberg 1993, Eisenberg et al. 1994, Kotaka 1996) that form the framework for this study and which this study seeks to update and extend.

The Eisenberg (1993) and Eisenberg et al. (1994) papers identify and describe a hydrodynamic aquifer operating in the Toro reservoir in the Hedinia/Iagifu Fields of the Kutubu Complex (Figure 3.3). Eisenberg et al. (1994) have also proposed a more regional Toro aquifer system operating in the Papuan Fold Belt (Figure 3.4). Kotaka (1996) provides a more extensive regional study of formation fluid pressure and salinity for several of the aquifer units in the fold belt and foreland regions of the Papuan Basin (Figure 3.5).

Eisenberg (1993) has explained a trend of decreasing Hw values through the Hedinia/Iagifu Fields of the Kutubu Complex, from northwest to southeast, as generated by a hydrodynamic aquifer. This hydrodynamic behaviour has led to a dramatic change in the oil distribution in the Toro reservoir in the Kutubu Complex, with northwest to southeast water flow having swept the northwest side free of oil and produced a tilted OWC across the rest of the reservoir in these fields. The model then has water flowing into the Usano Field and exiting the fold belt at the southern end of the Usano Field into the foreland (Figures 3.3 and 3.4)

Neither Eisenberg (1993) nor Eisenberg et al. (1994) actually suggest a mechanism to explain how the formation water is exiting the fold belt at Usano. However, Grainge (1993) suggested that the under-pressured Toro reservoir is due to water exiting from the fold belt at Usano via hanging wall Toro juxtaposed against permeable Darai Limestone in the footwall of the field-bounding fault. This scenario is certainly more likely in the southeast of the fold belt where greater thin-skinned faulting of Toro is evident compared to the northwest of the fold belt that has thicker-skinned/basement-involved structures. However, this scenario is not unequivocally supported by the available cross sections through the southern region of the Usano Field (Figure 3.6). Kotaka (1996) also does not propose an exit mechanism from the fold belt at Usano, but point out that meteoric/fresh water is flowing into the foreland close to Iorogabaiu-1. Iorogabaiu-1 is immediately west in the foreland from the proposed exit point at Usano. Another possibility is that water exits via cross cutting faulting in the fold belt that permits connection with the Toro reservoir in the foreland of the basin and eventual discharge into the sea, rather than transfer to the Darai across the main frontal thrust of the fold belt as suggested by Grainge (1993).

Eisenberg et al. (1994) propose an extension to the hydrodynamic system they identified in Hedina/Iagifu-Usano Fields. They describe a more regional hydrodynamic Toro aquifer system

connecting fields northwest of Hedinia (Figure 3.5). However, evidence for this is not as convincing as that for the Kutubu Complex hydrodynamic system, as there are large distances between Hw data points and a general paucity of data to support this model. Eisenberg et al. (1994) have proposed regional northwest to southeast flow in the Toro Sandstone reservoir along approximately 115km of fold belt. From a potential recharge point at the Lavani Valley Toro outcrop, they postulate connection and continuous flow through highland fields including; Egele anticline, Angore, Hides, Mananda/South East Mananda, flowing into Agogo and then the Hedinia/Iagifu Fields, with discharge from the fold belt at Usano into the foreland. Eisenberg et al. (1994) postulate that the Juha Field could also be connected to this hydrodynamic Toro system.

A regional pressure-depth plot indicates that Egele, Angore, Hides, Mananda/South East Mananda could be in pressure communication and fed with meteoric water from Lavani Valley. There is a gradual and consistent decrease in Hw down through these fields into South East Mananda, consistent with a hydrodynamic system. However, there is a large discontinuity in this system with a large hydraulic potential drop across the structural junction, between the South East Mananda and Agogo Anticlines. It was suggested that this large drop in hydraulic potential and restriction in water flow could be caused by faulting and creation of a permeability barrier at this point in the Toro aquifer.

Kotaka (1996) also advocates the Eisenberg et al. (1994) hydrodynamic regional Toro aquifer model and has provided additional formation water pressure data and salinity data across the fold belt and foreland regions for Toro and several other reservoir units (Figure 3.6). Kotaka (1996) reports that the Toro aquifer generally becomes more saline and lower pressured towards the foreland, with significant step-changes in hydraulic potential between some regions perhaps due to recent tectonics causing faulting and subsequent baffles.

More recently Williams & Lund (2006) have put forward an alternative model for the non-uniform oil column seen in the Hedinia/Iagifu Fields that involves a fault-generated compartmentalisation mechanism rather than a hydrodynamic aquifer (Figures 3.7a-b). This model will have a significant impact on the recoverable gas and oil volumes and the field development planning (Muggeridge & Mahmode, 2012). The evidence for hydrodynamic flow is the regular systematic decrease of Hw across the Hedinia/Iagifu Fields, with water legs plotting on parallel but offset/stepped gradients in relation to each other. It is unlikely that fault compartmentalisation could produce such a geographically regular variation. The simplest explanation is that the Toro aquifer is flowing. In addition, the Toro gas and oil legs in Hedinia/Iagifu are part of one continuous reservoir (with single original gas and single original oil pressure gradients), which extends across both anticlines, which also argues against a fault compartmentalisation model.

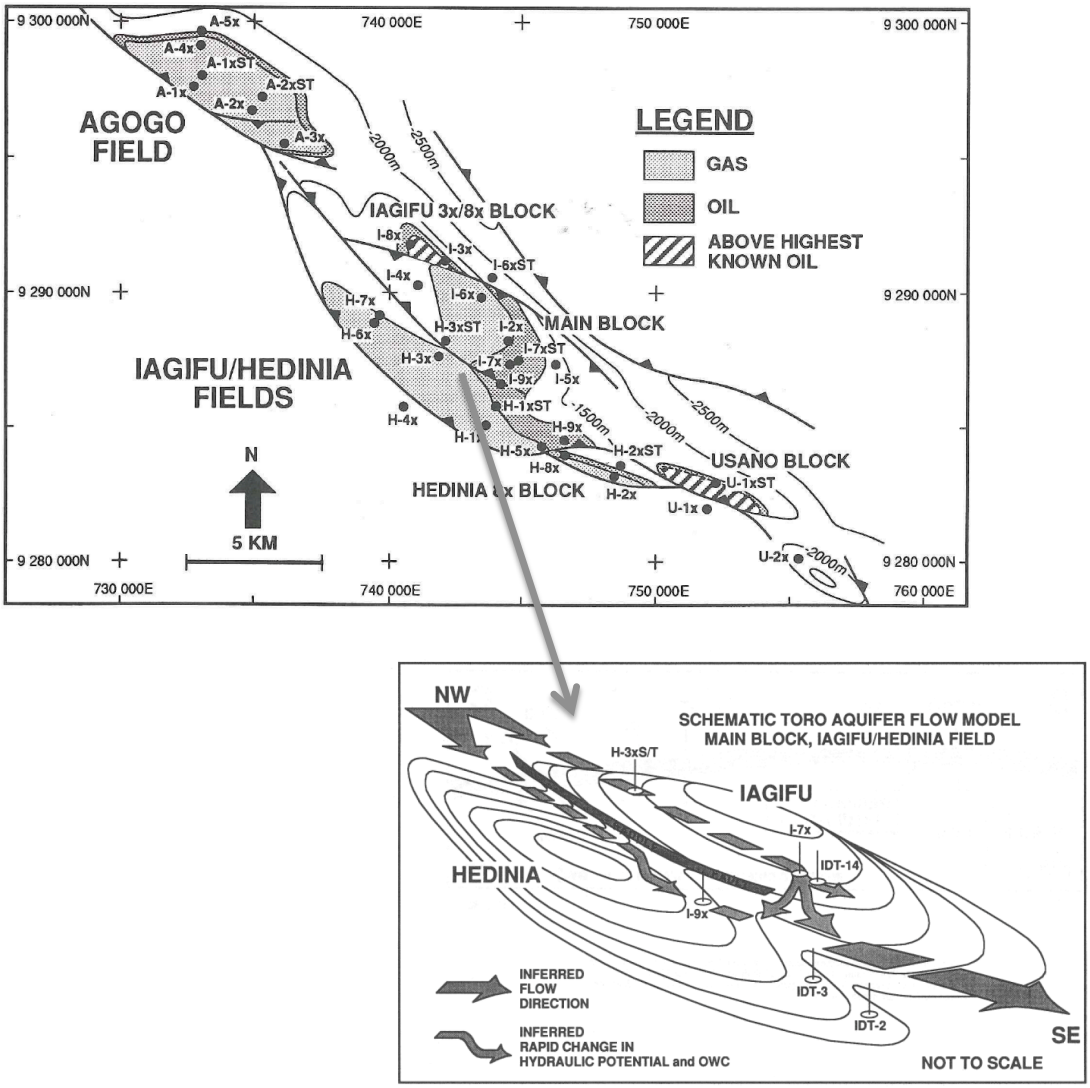

Figure 3.3: Hydrodynamic Toro Aquifer in the Kutubu Complex (Hedinia/Iagifu Fields)
Top panel - Hedinia/Iagifu area showing selected wells and top Toro structure contours (meters relative to sea level). Bottom panel depicts a perspective view across main section of Hedinia/Iagifu Fields. Toro structure, well penetrations and inferred flow paths are schematic (Eisenberg et al., 1994).

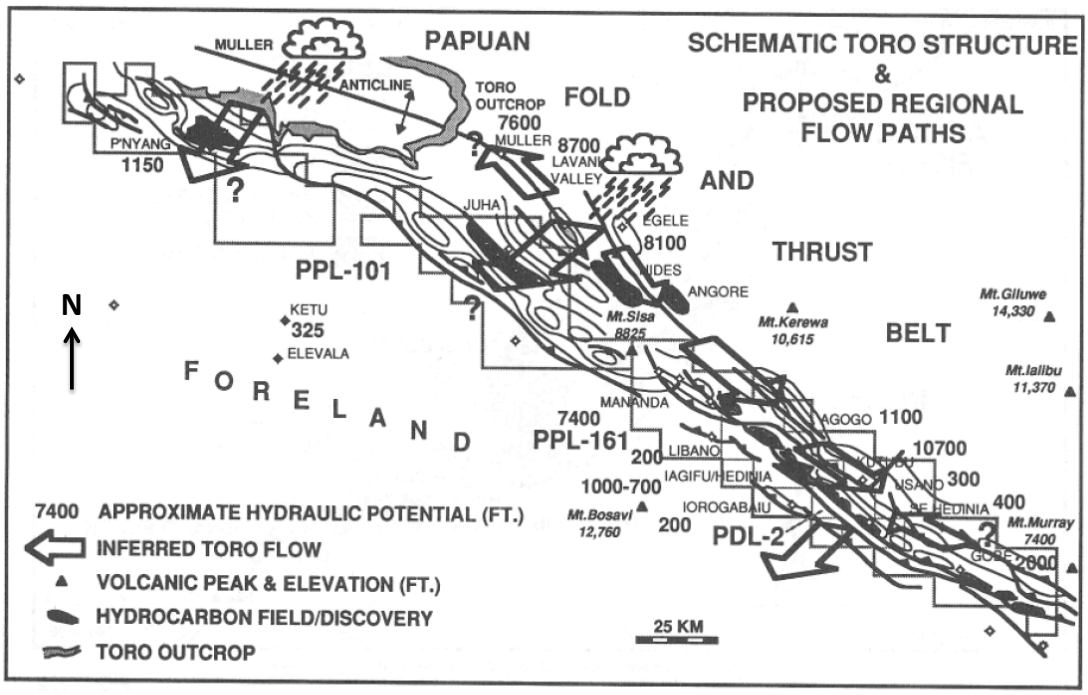

Figure 3.4: Proposed Regional Papuan Basin Toro Aquifer System
Schematic top Toro Sandstone structure map, hydraulic potential (Hw) and inferred flow paths (Eisenberg et al., 1994).

1

	name	hydraulic potential (m)	salinity ('000 ppm)	area	formation	system	hydrocarbon
1	Muller water	2200~2300	10~15	Muller ~ SE Mananda	Toro & Digimu	open	major gas
2	Water beneath main	1000~1300	26~30	Agogo ~ Hedinia	Hedinia & Iagifu	closed (semi-closed)	minor oil
3	Fold belt main	350->87	10~14	Fold belt main north Fold belt main south	Toro + Digimu + Iaigfu	open	major oil
4	Kutubu-1x water	3277	11	Kutubu-1x only	Toro	closed? open?	-
5	Gobe Toro water	655-663	10	Gobe Main ~ SE Gobe	Toro only	closed	-
6	Foreland margin water	25~170	16~26	Foreland margin	various	open	minor gas
7	Foreland centre water	-65~81	20~67	Foreland centre	various	open (semi-closed)	-

2

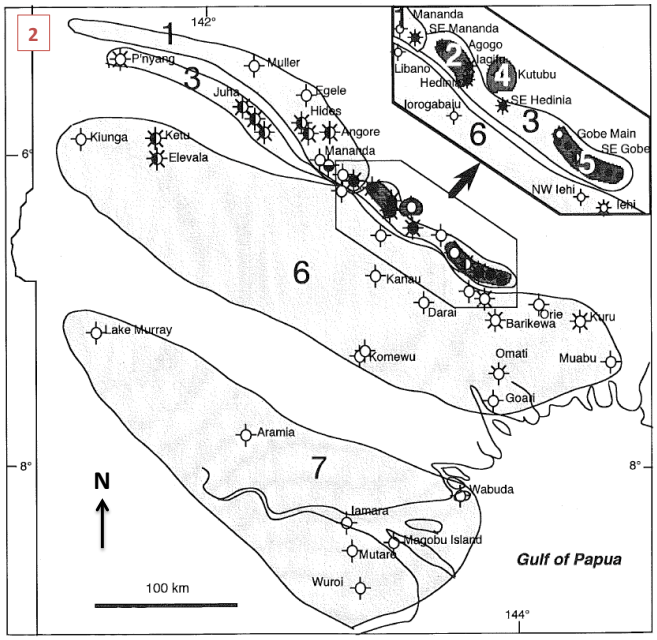

3

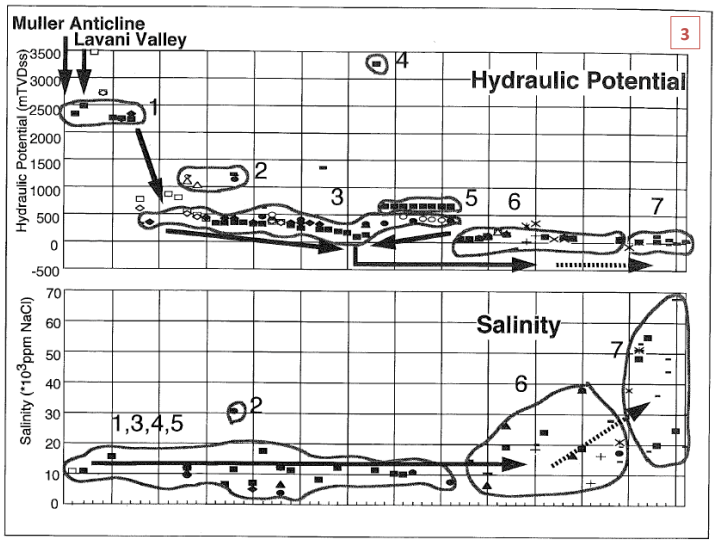

Figure 3.5: Kotaka (1996) Papuan Basin Formation Water Analysis

Panel 1 - Formation water groups and their characteristics. Panel 2 - Areal distribution of formation water groups. Panel 3 - Potential flow between formation water groups estimated from decrease in hydraulic potential and increase in salinity – wells lined up north to south going left to right across panel (Kotaka, 1996).

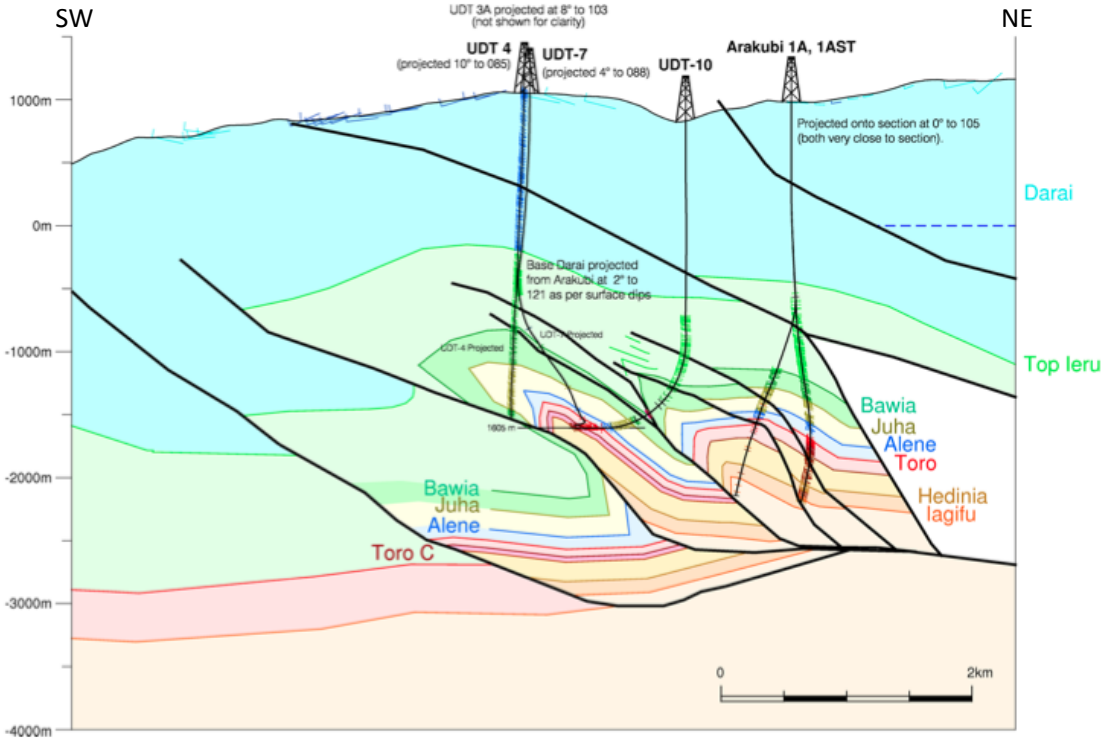

Figure 3.6: Cross Section Through Usano Field
(Buick et al., 2009).

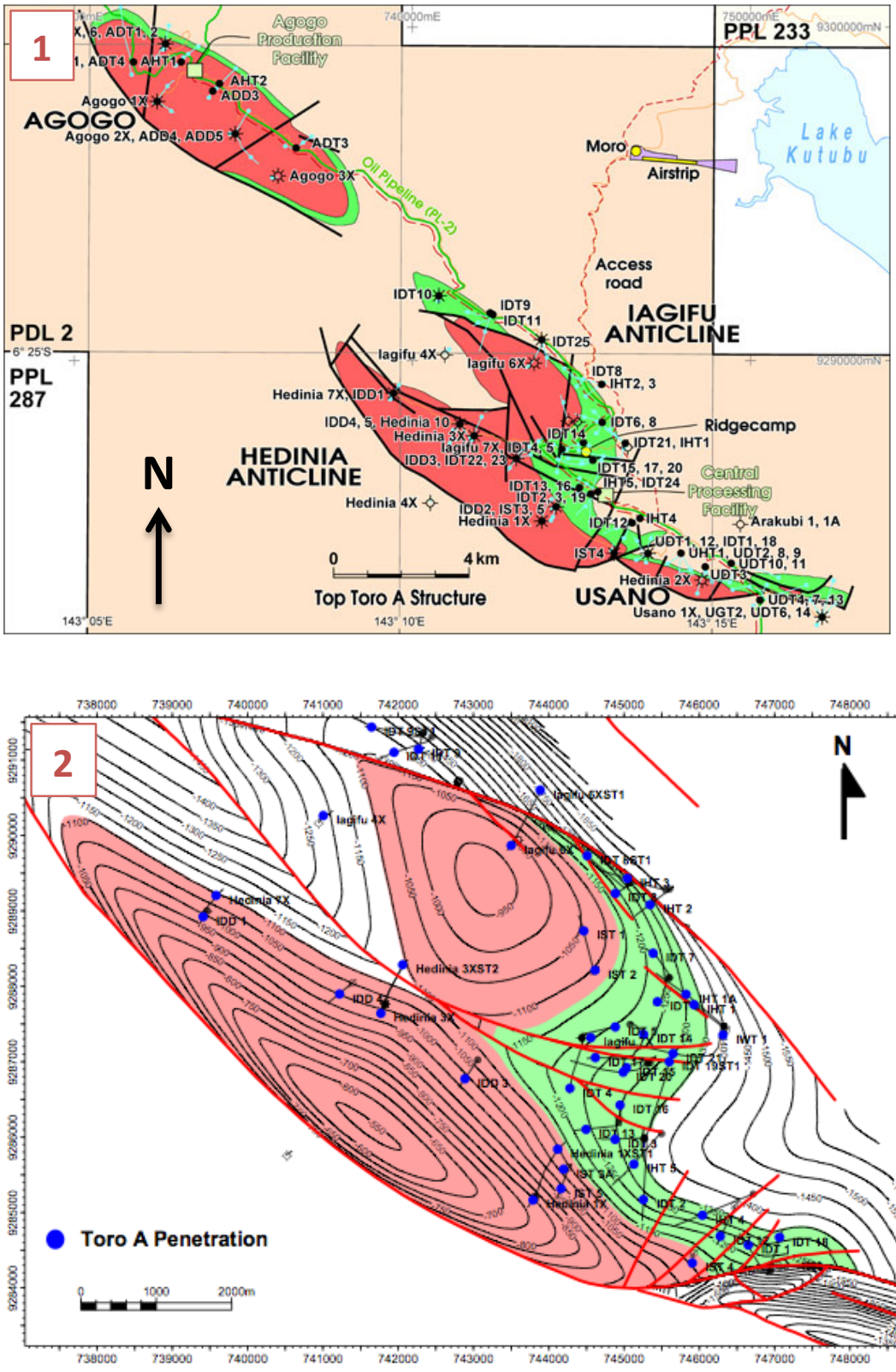

Figure 3.7a: Hedinia/Iagifu Fields Top Toro Structure Maps Showing Development of Models of Predicted Faults

Panel 1 - Map of Agogo-Hedinia/Iagifu-Usano Fields. Panel 2 - Pre-seismic fault model of Hedinia/Iagifu Fields. (Williams and Lund, 2006)

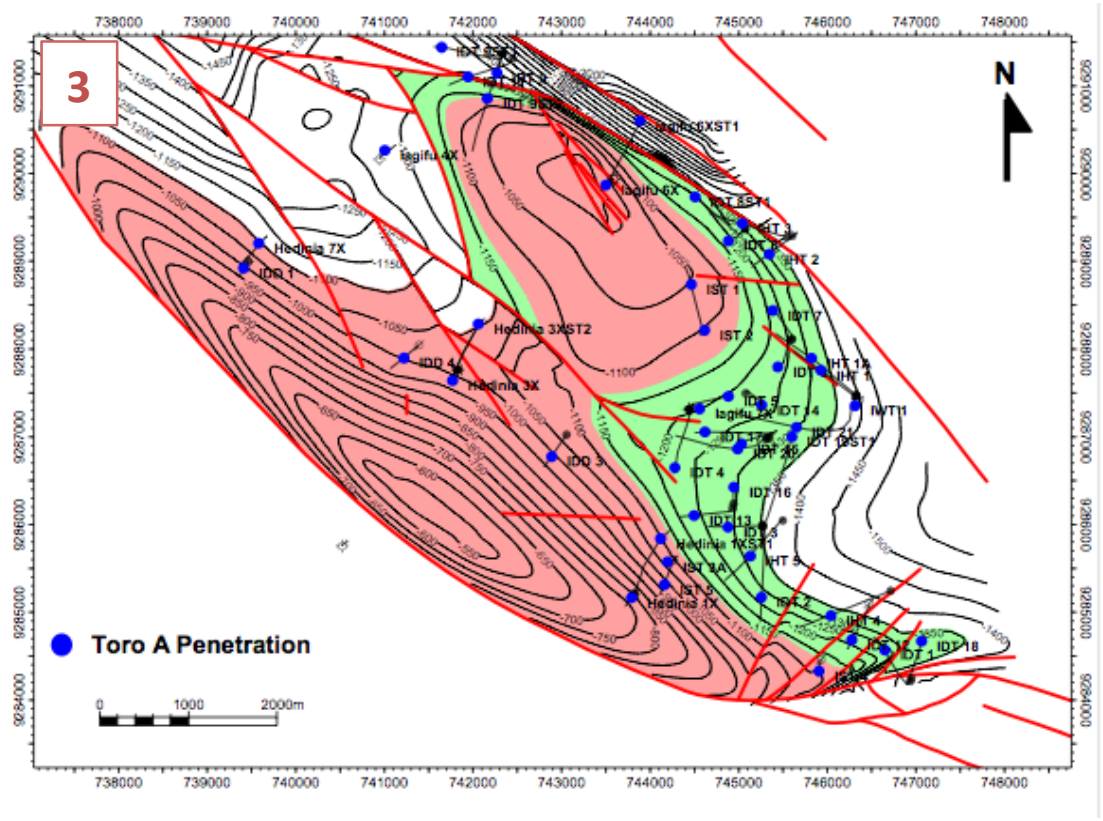

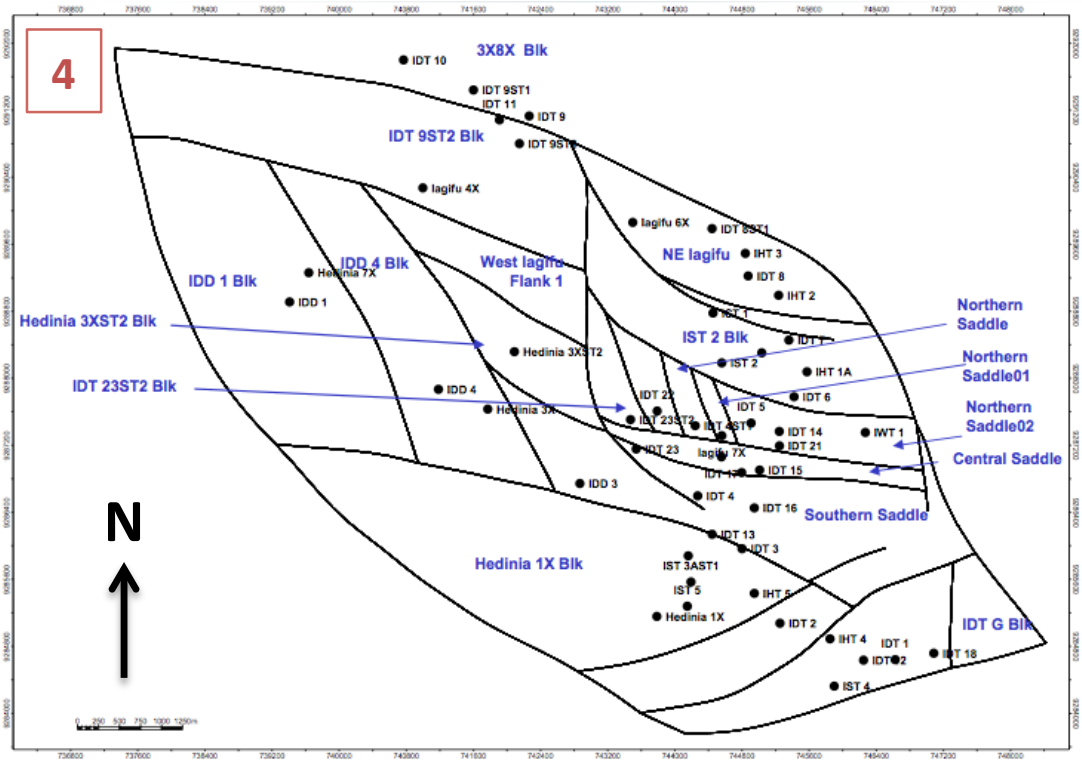

Figure 3.7b: Hedinia/Iagifu Fields Top Toro Structure Maps Showing Development of Models of Predicted Faults

Panel 3 – Post-seismic fault model. Panel 4 - Most recent proposed fault model for Hedinia/Iagifu Fields. (Williams and Lund, 2006)

Chapter 4: Methodology and Data Analysis

4.1 Data Set Construction

A regional well pressure data set was generated in Microsoft Excel for a total of 433 wells currently listed in the Santos database for the Papuan Basin. Two pre-existing well pressure data sets containing overlapping subsets of data from specific fields were combined and utilised to commence assembling the larger regional data set necessary for this study. Where there were discrepancies discovered, the data obtained from these two pre-existing data sets were checked against the original well completion reports (WCRs). Data for the remaining wells assessed in this study were obtained from WCRs available at the time of the project. All new and verified data were used to construct a final data matrix consisting of 6500 entries across 85 column identifiers (see section 4.4 for detailed data set analysis).

Formation pressure data were obtained from a variety of different types of down-hole pressure testing equipment including data from drill stem tests (DSTs), and data from wire-line pressure testers such as the Schlumberger repeat formation tester (RFT), Schlumberger modular formation dynamic tester (MDT/MFT), Halliburton reservoir description tool (RDT) and selective formation tester (SFT).

Entire sets of raw pressure data generated in the down-hole pressure tests were assembled into the data set. Pressure test data were screened using test operator comments and mobility values associated with the tests, which give an indication of the seal and pressure build up for each test. Poor quality and ambiguous data values were then omitted and only the most reliable pressure test data used to generate the pressure gradients, which were used to identify fluids present in the reservoir intervals and generate hydraulic potential (Hw) values for potentiometric surface mapping.

DSTs provide reasonable pressure data ideally based on initial shut in pressure (ISIP) (Dahlberg (1995). RFTs, and the similar wire-line tools from other companies, are able to obtain formation pressure measurements at numerous intervals up and down the hole in a single run (Eisenberg, 1993). Pressure tests in the Papuan Basin wells have been predominantly made using the Schlumberger RFT tool. The RFT uses two gauges for pressure measurement, the strain gauge and Hewlett Packard quartz gauge. Absolute pressure (psia) measurements from the Hewlett Packard quartz gauge were used in this study, as they are more accurate.

Salinity data were obtained from the Kotaka (1996) regional Papuan Basin study along with formation water reports covering Moran, Kutubu Complex and Gobe Fields (Chevron, 2000; Oil

Search, 2003). These data were integrated into the data set and, where discrepancies were identified, checked with the original WCRs. Additional salinity data was obtained from WCRs available at the time of the project. Where no formation water salinity values were measured, salinity values were calculated from formation water resistivity (Rw) values recorded in the WCRs. Rw calculated according to the relationship: $Rw_{RES} = Rw_{STD}\ [(T_{STD} + 6.77)/(T_{RES} + 6.77)]$ (deg F) (Dahlberg, 1995). The Rw_{RES} value was then converted to a NaCl concentration (ppm) using a resistivity of equivalent NaCl solutions chart. Temperature data for the formation interval being pressure tested were obtained from the WCRs.

4.2 Pressure-Depth Plots

Pressure-depth (P-D) plots were generated in Microsoft Excel and Tibco Spotfire. The P-D plots permitted generation of pressure gradients and identification of the fluid type within the reservoir, as the pressure gradient slope is directly related to the specific gravity of the fluid, and thus fluid type in the formation interval being tested. Specific gravity (SG) of a fluid is the density of the fluid compared to density of fresh water (Dahlberg, 1995).

Pressure (psia) was plotted against depth of reservoir interval [in total vertical depth meters subsea (TVDmSS)]. Pressure gradients were calculated by regression analysis of the data sets on the plots. Slopes of pressure gradient lines on the P-D plots were then converted from m/psi to psi/ft for presentation of the pressure gradient data in the tables for this study.

Pressure gradients were calculated for each reservoir interval in each well and fluids present in the reservoir formations identified. See Figure A.1 (in Appendix) for examples of Toro Formation P-D plots generated to calculate fluid pressure gradients used in this study. Fluid type was also confirmed from WCRs.

Examples of SG and corresponding hydrostatic pressure gradient values for various formation fluids were based on those outlined by Dahlberg (1995). Brine (SG range: 1.07-1.15) which corresponds to 0.46-0.50 psi/ft pressure gradient range, salty water (SG range: 1.02-1.06) which corresponds to 0.44-0.45 psi/ft pressure gradient range, fresh water (SG 1.0) which corresponds to a 0.433 pressure gradient, oil (SG range: 0.6-0.85) which corresponds to 0.25-0.37 psi/ft pressure gradient range, condensate (SG range: 0.45-0.6) which corresponds to 0.17-0.25 psi/ft pressure gradient range and gas (SG range: 0.12-0.47) which corresponds to 0.05-0.2 psi/ft. pressure gradient range.

The intersection of gradients of different fluid types can be used to define a fluid contact [gas-oil (GOC), oil-water (OWC) and gas-water GWC)] (Cockroft et al. 1987; Dahlberg, 1995) (Figure 4.1). The relative position on a P-D plot of a pressure gradient for an individual well formation interval with respect to other well pressure gradients gives an indication of reservoir continuity both between wells and within a reservoir section (Cockroft et al. 1987; Eisenberg, 1993) (Figure 4.2). Changes (decrease or increase) in the water pressure gradient can indicate hydrodynamic flow either up-dip or down-dip respectively (Cockroft et al., 1987) (Figure 4.3).

4.3 Hydraulic Potential Calculations

Hydraulic potential (Hw) is a simple indication of the potential energy of an aquifer at a given point, and is generally expressed as an elevation relative to a standard reference surface, generally sea level (Esienberg, 1993). Hw values were calculated using three methods in this study: (1) using a generic 0.435 psi/ft water pressure gradient value, (2) calculated using individual water pressure gradients values, (3) calculated using the 0.435 psi/ft water pressure gradient but also using input from formation fluid salinity and temperature values. Eisenberg (1993), Eisenberg et al. (1994) and Kotaka (1996) used a generalised water pressure gradient of 0.435 psi/ft for the entire basin when calculating Hw values. Dahlberg (1995) recommended this approach, as predominantly fresh water is present in the reservoir intervals being tested.

Hw values were generated from the pressure and depth data and the calculated pressure gradients using the equation: $Hw = z + P/\Delta P$ (Dahlberg, 1995). [Where, Hw = hydraulic potential, z= depth of the pressure expressed as an elevation relative to sea level, P is the formation pressure, and ΔP is the pressure gradient in the water leg]. The pressure value used in each case was the uppermost reliable pressure measurement for each reservoir interval. The exception to this practice was where lowest known gas (LKG) values were calculated. In these cases the lowermost reliable pressure measurement for the reservoir interval was utilized.

In the first method the water pressure gradient used was the constant 0.435 psi/ft. In the second method, individual water gradients have been calculated and substituted in each case for the 0.435 psi/ft water pressure gradient value in the equation above. This method was assessed to test whether there was significant variation in water densities/gradients within the basin reservoirs that may have been overlooked in the Eisenberg (1993), Eisenberg et al. (1994) and Kotaka (1996) studies, which may produce different results to the first method applied.

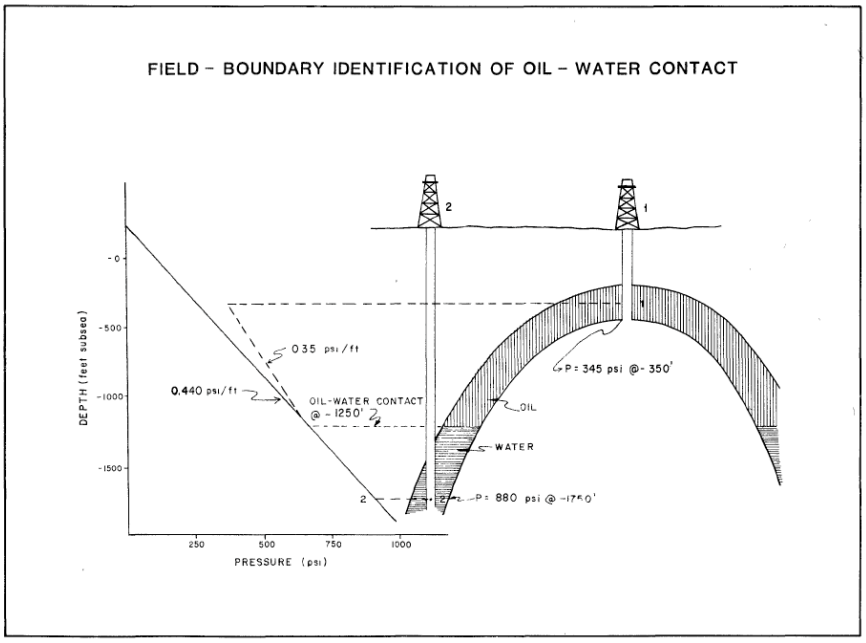

Figure 4.1: Determination of Fluid Contact Points

Where the calculated oil and water pressure gradients intersect is the oil water contact (OWC). This method is dependent on the accuracy of the pressure measurements (Cockroft et al., 1987).

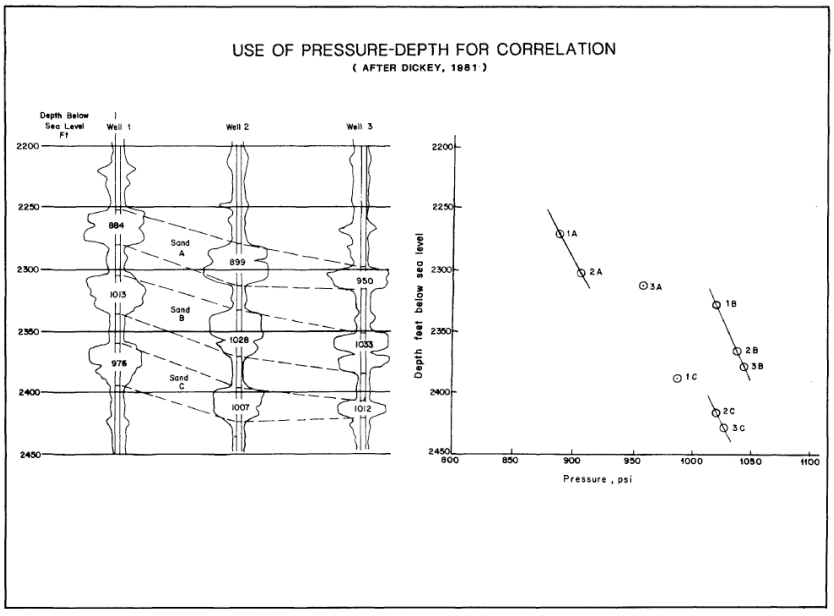

Figure 4.2: Use of P-D Plot Pressure Gradients to Indicate Reservoir Continuity

In this example reservoir B is fully connected, whereas 3A would appear not to be connected to 1A and 2A. Likewise 1C does not appear to be connected to 2C and 3C (Cockroft et al., 1987).

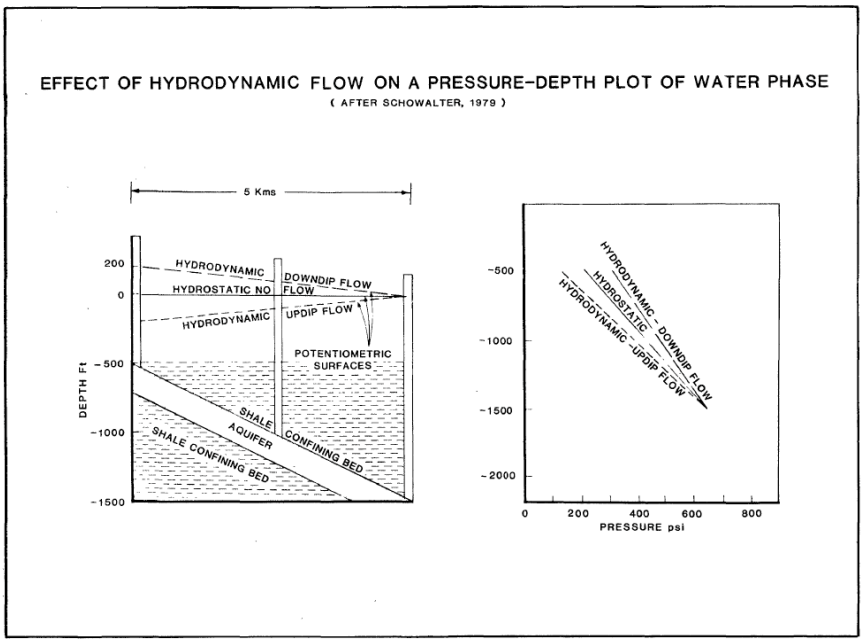

Figure 4.3: Effect of Hydrodynamic Flow on a Water Pressure Gradient on a P-D Plot
If hydrodynamic flow is occurring the pressure gradient will differ from hydrostatic (Cockroft et al., 1987).

In the third method undertaken, salinity and temperature values were used along with the constant water pressure gradient of 0.435 psi/ft, to calculate reservoir water pressure gradients for the formation interval fluid being tested (Langston, 2013; McCain, 1990). Salinity and temperature of the formation fluid have a strong bearing on fluid density and have not been taken into account in the first two methods (Cockroft et al. 1987). For the third method, water pressure gradients for standard (STD) and reservoir (RES) conditions were calculated by inputting values for P = pressure (psia), T = temperature (deg F) and B = % weight salt in brine (eg. Salinity of 10,000 ppm = 1%) into the following formulas:

(1) Brine density (STD) $= 62.368 + 0.4386 \times B + 0.001601 \times B^2$ (lb/ft^3)
(2a) $dVwp = -(3.589 \times 10^{-7} + 1.953 \times 10^{-9} \times T) \times P - (2.253 \times 10^{-10} + 1.728 \times 10^{-13} \times T) \times P^2$
(2b) $dVwt = -0.01 + 1.334 \times 10^{-4} \times T + 5.507 \times 10^{-7} \times T^2$
(3) Brine FVF = (1 + dVwp) x (1 + dVwt)
(4) Brine density (RES) = brine density (STD) /Brine FVF (lb/ft^3)
(5) Where SG = brine density/62.368
(6) Water pressure gradient (STD) = specific gravity (SG) x 0.435 (psi/ft)

Therefore brine density (RES)/62.368 = SG under reservoir conditions and multiplying by 0.435 generates the water pressure gradient under reservoir conditions. Water pressure gradient (RES) values have been used in this study to generate Hw values.

4.4 Data Set Analysis

A Total of 433 wells in the Papuan Basin were examined in this study (Table A.1). The well locations are shown on a set of 11 maps (1 master map, 6 sub-regional maps and 4 field-scale maps) (Maps A.1 - A.11) (see tables and maps in Appendix).

On assembly of the data set it was found that 151 wells had pressure data for the Toro and Imburu Formation reservoir units. From this total of 151 wells, 136 wells recorded data for Toro, 37 wells for Digimu, 21 wells for Hedinia and 33 wells for Iagifu Sandstone reservoir units. There were 155 Toro fluid pressure sample points (46 gas, 31 oil and 78 water), 39 Digimu fluid pressure sample points (5 gas, 17 oil and 17 water), 22 Hedinia fluid pressure sample points (2 gas, 5 oil and 15 water) and 45 Iagifu fluid sample points (7 gas, 1 oil and 25 water) (Table A.1).

Pressure data were not available from the remaining 282 wells in the Santos database for a variety of reasons: Group 1 - 102 wells with WCR unavailable, Group 2 - 95 wells with no or poor down-hole pressure test data, Group 3 - 58 wells outside Toro palaeo-deposition range and Group 4 - 27 wells where the Toro interval was expected but not intersected.

However, within the group of 102 wells with unavailable WCRs, there are 17 wells that are either actually still being planned, currently being drilled, or have been drilled too recently for WCR/pressure data to have been released for these wells. Within the group of 95 wells with no or poor pressure data, 21 of these wells actually have had pressure tests done and data exists but was unavailable at the time if this study.

It should be noted that 219 wells (178 fold belt and 41 foreland) have been drilled in the Papuan Basin since the Kotaka (1996) regional study (ie. actually post 1994 wells - see Table A.1 for listing) and could potentially add to the interpretation of regional aquifer dynamics. However, of these 219 wells, only 56 have provided new pressure information for the four reservoir intervals (60 Toro, 11 Digimu, 7 Hedinia and 15 Iagifu Formation sample values). Furthermore, of the 60 Toro fluid pressure values (12 gas, 12 oil and 36 water), 20 of these (10 water) are from post-production partially depleted wells and have been excluded from the analysis so as to derive an accurate potentiometric map. The Moran Field has been developed since the Kotaka (1996) study, with 40 wells having been drilled since 1994. However, from these 40 wells it has only been possible to obtain 11 Toro (7 water and 4 oil) and 11 Digimu (4 water, and 7 oil) pressure values for analysis in this study.

4.4.1 Toro Data Set Analysis

A total of 78 wells with reliable Toro water data were identified, comprising 60 wells from the fold belt and 18 from the foreland region of the basin (Table A.2). Wells were also identified as either pre-production wells (66) or post-production wells (12), so as to be able to help differentiate localised field depletion, which could then be taken into account when modelling Toro aquifer water flow. Post-production wells were excluded from potentiometric surface mapping for this study. Gas and oil Toro reservoir well data have also been assembled in Tables A.3 and A.4 respectively. Lowest known gas (LKG) and lowest known oil (LKO) values were used to help constrain preliminary potentiometric surface maps.

Underschultz et al. (2005) suggest that initially with the potentiometric surface mapping, only data from zones of formation water are used to characterize the hydraulic head distribution, but these can then be supplemented by pre-production hydrocarbon pressure data extrapolated to known free-water-level elevations. For this study an additional 7 wells have had an extrapolated gas-water contact (EGWC) value calculated by extending the gas pressure gradient to the intersection point with a relevant nearby water pressure gradient. These data were considered important to aid construction of the regional Toro potentiometric surface map where direct water pressure data were lacking [Hides-4, Angore-1, Tarim-1, Pnyang-1X, Elevala-1, Puk Puk-1 and Langia-1 - See Figure A.2 (in Appendix) and Table A.3]. Toro Hw data have been calculated according to the three methods detailed in section 4.3 and are listed in Tables A.2 - A.4.

A set of wells east and northeast of the central fold belt region (Andabare-1, Bakari-1, Nembi-1, Pangia-1, -1A, -1B, Trapia-1, Tumuli-1, 1ST, Wara-1), along with Karius-1 near the Hides field, and Baia-1 and Cecilia-1 near the Juha Field, failed to intersect Toro as expected and instead encountered Darai Formation thrust-repeats in the footwall. These wells would have been very useful (in conjunction with Korka-1 north of Angore Field - data not released yet) in better defining the Toro aquifer (and the palaeo shoreface/toro lateral extent) (see Map A.3).

4.4.2 Digimu, Hedinia and Iagifu Data Set Analysis

Formation fluid pressure data and Hw values for Digimu, Hedinia and Iagifu reservoir units are listed in Tables A.5 - A.7, Tables A.8 - A.10 and Tables A.11 - A.13 respectively.

4.4.3 Hw Calculation Method Comparison

Three methods were used to calculate Hw data sets in this study (see section 4.3). Comparison of the Toro Hw data (see Table A.2) showed that there was a very good correspondence between

Hw data generated by methods 1 and 3. However, there were some significant variations seen between method 2 data and the values generated by methods 1 and 3. These differences corresponded to instances (predominantly in the fold belt) of anomalously high or low water pressure gradient values in method 2 data. This may be indicative of an accurate pressure gradient measurement that legitimately varies from those measurements around it, but could also be because of inaccuracies in the pressure measurement and the quality and number of pressure test values used to generate the pressure gradient. Method 2 utilises calculated individual water pressure gradients for each well, whereas methods 1 and 3 share a common use of the constant 0.435 psi/ft water pressure gradient value (method 3 also uses salinity and temperature data). Similar patterns of correspondence between the Hw data sets generated by the three methods were seen for Digimu, Hedinia and Iagifu reservoirs (Tables A.5, A.8 and A.11).

In general for most of the data generated by method 2 there was a good correspondence between method 1 and 2 data values. This can be seen visually by comparing Hw-well plots of the method 1 and 2 data (Figures 4.4 and 4.5). These results suggest that for a relatively fresh water aquifer system a generalised regional water gradient value can be used with reasonable confidence (Eisenberg et al. 1994). Therefore because of the similarity between the Hw values generated by the three methods, regional Toro (and Digimu, Hedina and Iagifu) potentiometric surface maps were generated using only the Hw set of values produced by method 1 with the generic Papuan Basin constant 0.435 psi/ft water pressure gradient.

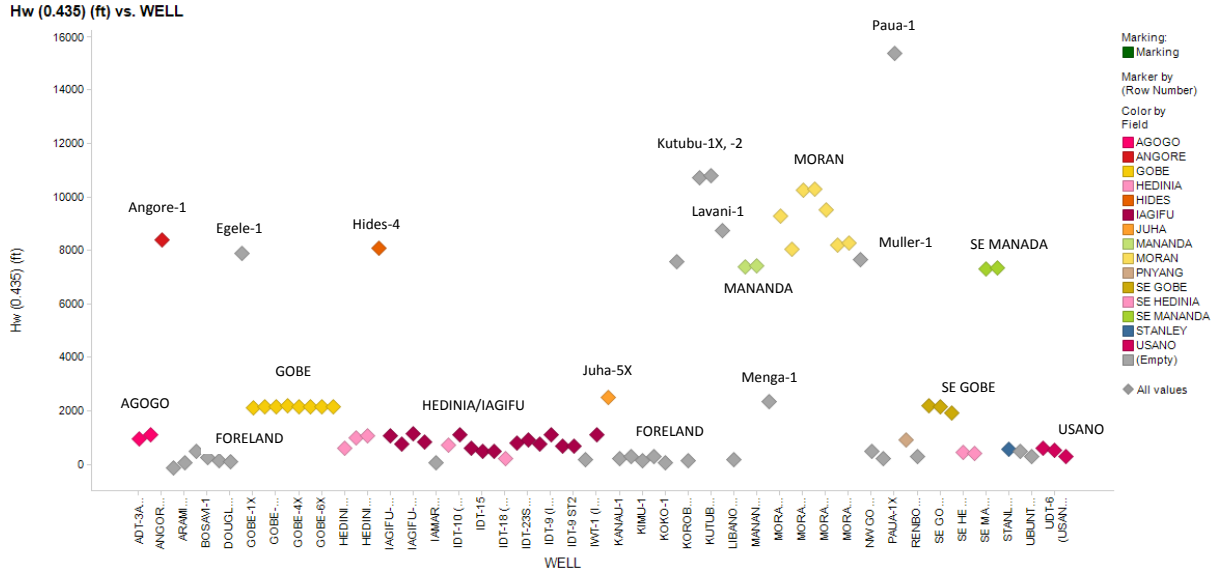

Figure 4.4: Hydraulic Potential (Hw - 0.435) - Well Plot

Hw data generated using constant 0.435 psi/ft water pressure gradient (Hw calculation method 1). Hw data listed in Table A.2.

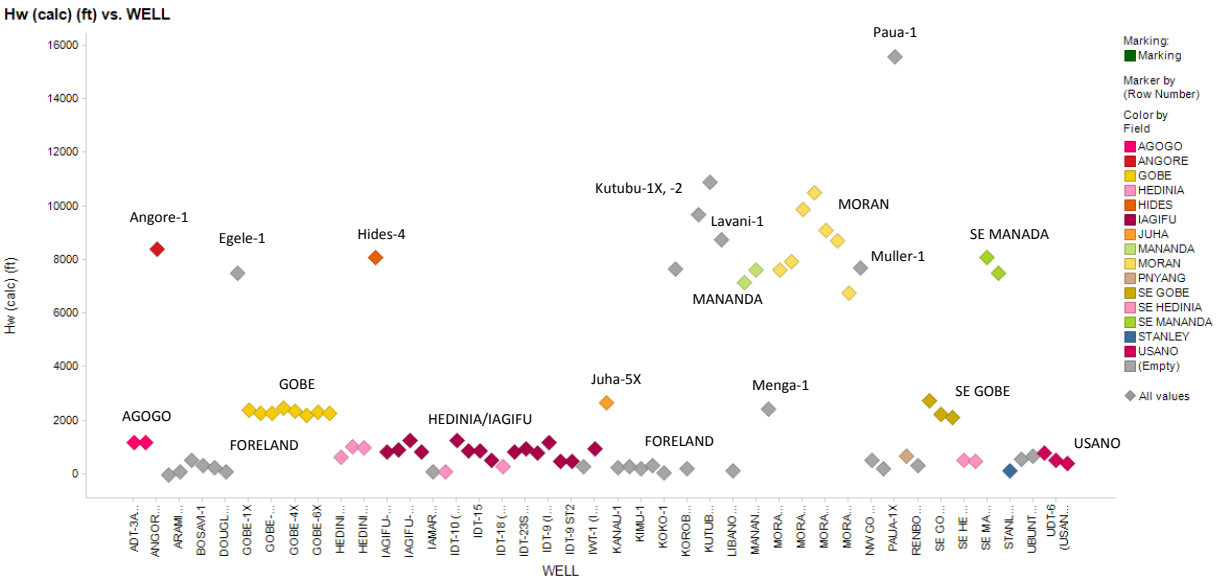

Figure 4.5: Hydraulic Potential (Hw - Calc) - Well Plot

Hw data generated using individually calculated water pressure gradients (Hw calculation method 2). Hw data listed in Table A.2.

4.5 Potentiometric Surface Map Construction

A potentiometric surface is a calculated surface that reflects variation in fluid/hydraulic potential (Hw) within an aquifer. The elevation of the surface at any point on it reflects the height to which a column of water would rise above a reference datum (have used sea level in this study) if not confined (Dalhberg, 1995). In instances where the Hw is calculated at an elevation above topography, the given well can be termed artesian. Where Hw is calculated at an elevation in the subsurface, the well can be termed sub-artesian. Water flow in a confined aquifer moves from high to low potentiometric values, perpendicular to potentiometric surface contours. Contours that are widely spaced indicate relatively better permeability, whilst those closely spaced represent areas of poorer permeability, which could also be a baffle or barrier to flow (Dahlberg, 1995).

An extra level of complexity is added to the potentiometric map when faults are added to the system. When a fault has a lower permeability than the aquifer it crosscuts, the flow direction will tend to be parallel to the plane of the fault (Hw contours will plot perpendicular to the fault suggesting it is sealing) (Figure 4.6). Whereas, Hw contours forming a closed high or low against a fault, can indicate that formation water is either flowing from the fault zone into the aquifer or flowing from the aquifer into the fault zone respectively. These scenarios suggest the fault is acting as a conduit for formation water flowing between vertically separated aquifers (Underschultz et al., 2005) (Figure 4.6). Where Hw contours are parallel or sub-parallel to the fault plane this suggests flow is able to cross the fault and it is not sealing, although the fault may be providing a baffle/restriction to flow, depending on the spacing of the contours.

Petrosys mapping software was used to construct potentiometric surface maps for the Toro, Digimu, Hedinia and Iagifu Sandstone reservoirs. Hw values were plotted onto the maps with combined layers including; regional faults, formation depth, surface topography and geology outcrop layers for key surfaces to create regional Papuan Basin potentiometric surface maps for each reservoir.

A regional fault set, PNG satellite image and topographic maps for the Papuan Basin were provided by Santos. A 1:250000 scale surface geology map for PNG was used to locate Toro and Imburu Formation outcropping in the fold belt region of the basin (D'Addario et al., 1976).

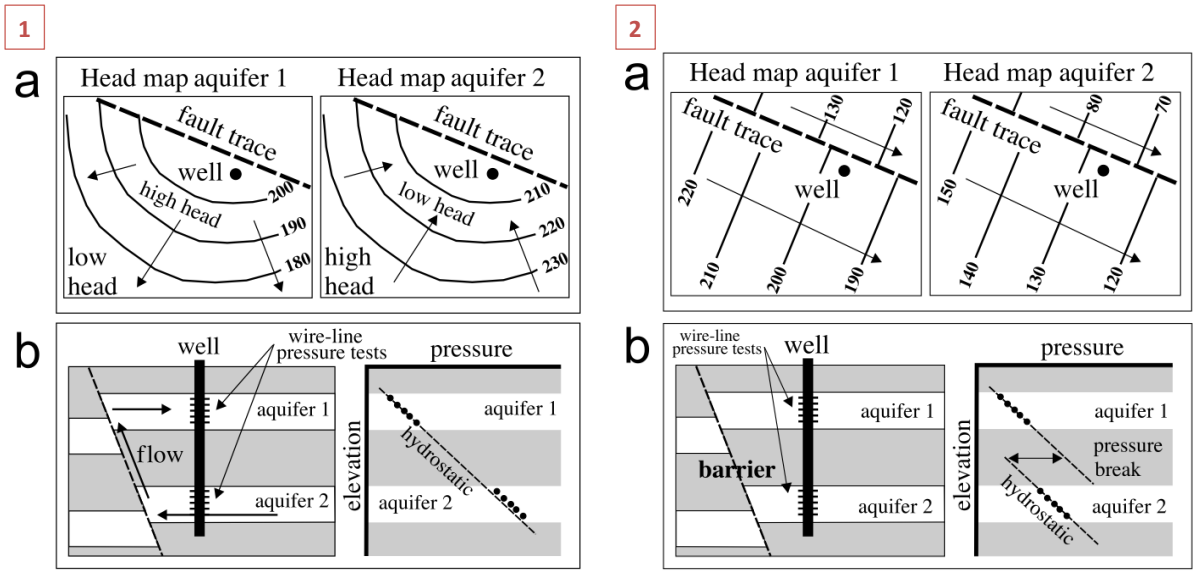

Figure 4.6: Schematic Fault Hydrodynamics

Panel 1 - An example of two aquifers in vertical connection with each other as the fault separating them is non-sealing/acting as a conduit. In this case there is up-fault flow. Panel 2 - The fault is sealing/acting as a barrier with a clear pressure offset between the two aquifers (Underschultz et al., 2005).

Chapter 5: Results and Interpretations

5.1 Regional Toro Pressure-Depth Analysis and Potentiometric Surface Maps

A regional Toro reservoir pressure-depth (P-D) plot was generated to help identify Toro aquifer connectivity versus discrete aquifer cells based on differences in water pressure gradients (Figure 5.1). Foreland and fold belt pressure regimes are clearly obvious from this plot. Within the fold belt there are four trends that stand out. There are the Kutubu Complex (Agogo-Hedinia/Iagifu-Usano), Gobe/South East Gobe, highlands (Muller-1, Lavani-1, Egele-1, Hides, Mananda/South East Mananda), and the hinterland region with highly pressurised compartments (Angore-1, Moran Field, Paua and Kutubu Anticlines). Those fields or wells that lie on similar pressure gradient trends may be connected in terms of a Toro aquifer system.

Regional Toro potentiometric surface maps were generated with Toro Hw data listed in Tables A.2 (Hw values from Toro pre-production wells) and A.3 (EGWC Hw values). Initially, a pair of preliminary Toro potentiometric surface maps were generated; map 1 was unconstrained by faults and map 2 was fault constrained. (Figures 5.2 and 5.3). These maps were both generated using a 20km diameter-limiting circle, extending from each well Hw value for mapping. They give a good representation of well distribution and regions where the map may be highly speculative versus those areas where there is increased confidence.

A third regional Toro potentiometric surface map was then generated, using a zero edge Toro polygon, as this represents the best estimate of actual areal extent of Toro aquifer, and the regional fault set to constrain the mapping (Figure 5.4a). Three overlapping map panes were assembled to visualise the potentiometric surface map in detail across the entire fold belt (Figures 5.4b-d). A fourth map pane was generated to visualise the foreland region, changing the colour contour scale to accentuate differences across the foreland sections of the basin (Figure 5.4e).

5.1.1 Fold belt

There is a trend of northwest to southeast decreasing Hw values from Lavani-1 to the southern boundary of South East Mananda Field (Figure 5.4c). This trend suggests the possibility of Toro aquifer water flow from Lavani-1 in the Lavani Valley, to Hides, to Mananda/South East Mananda (LV-H-M/SEM). Hw data also suggests southeast to northwest flow possible from Lavani Valley to Muller-1. Lavani Valley Toro outcrop represents the potentiometric high for the region and the likely recharge location for the Toro aquifer. Alternatively Muller-1 and Lavani-1

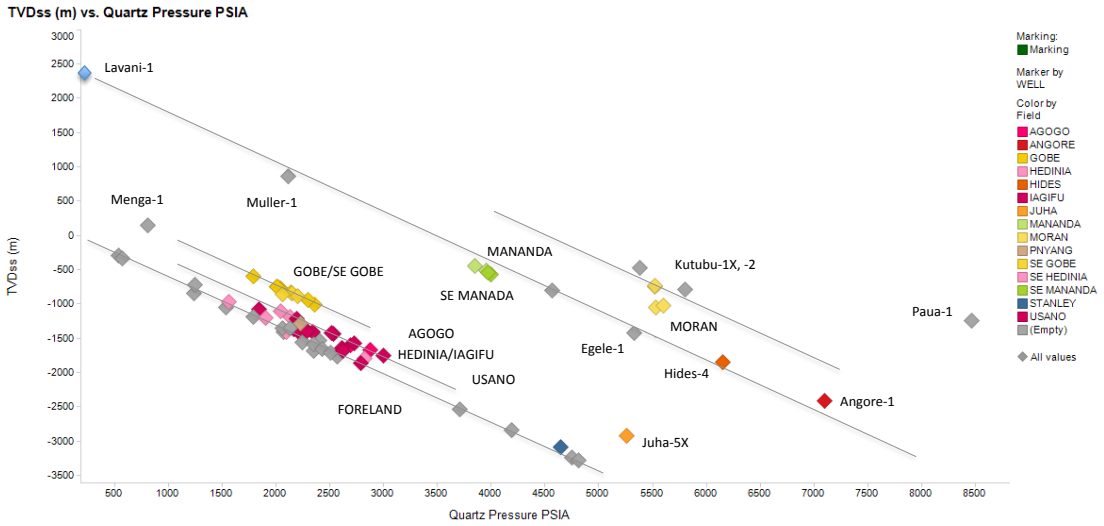

Figure 5.1: Regional Toro Aquifer Water Pressure Gradient Plot

P-D plot [x-axis: Pressure (psia) vs y-axis: Depth (total vertical depth meters sub sea (TVDmSS)]. Pressure gradient trends highlighted - Foreland and Foldebelt [including: Kutubu Complex (Agogo-Hedinia/Iagifu-Usano), Gobe/SE Gobe, Highlands (Lavani-1, Muller-1, Egele-1 and Hides-1), Hinterland (Angore-1, Moran wells, Kutubu-1X, -2 and Paua-1)]. The Toro water wells that have been plotted are listed in Tables A.2 and A.3 (66 pre-production Toro water wells, along with Hides-4 and Angore-1 extrapolated gas water contact values).

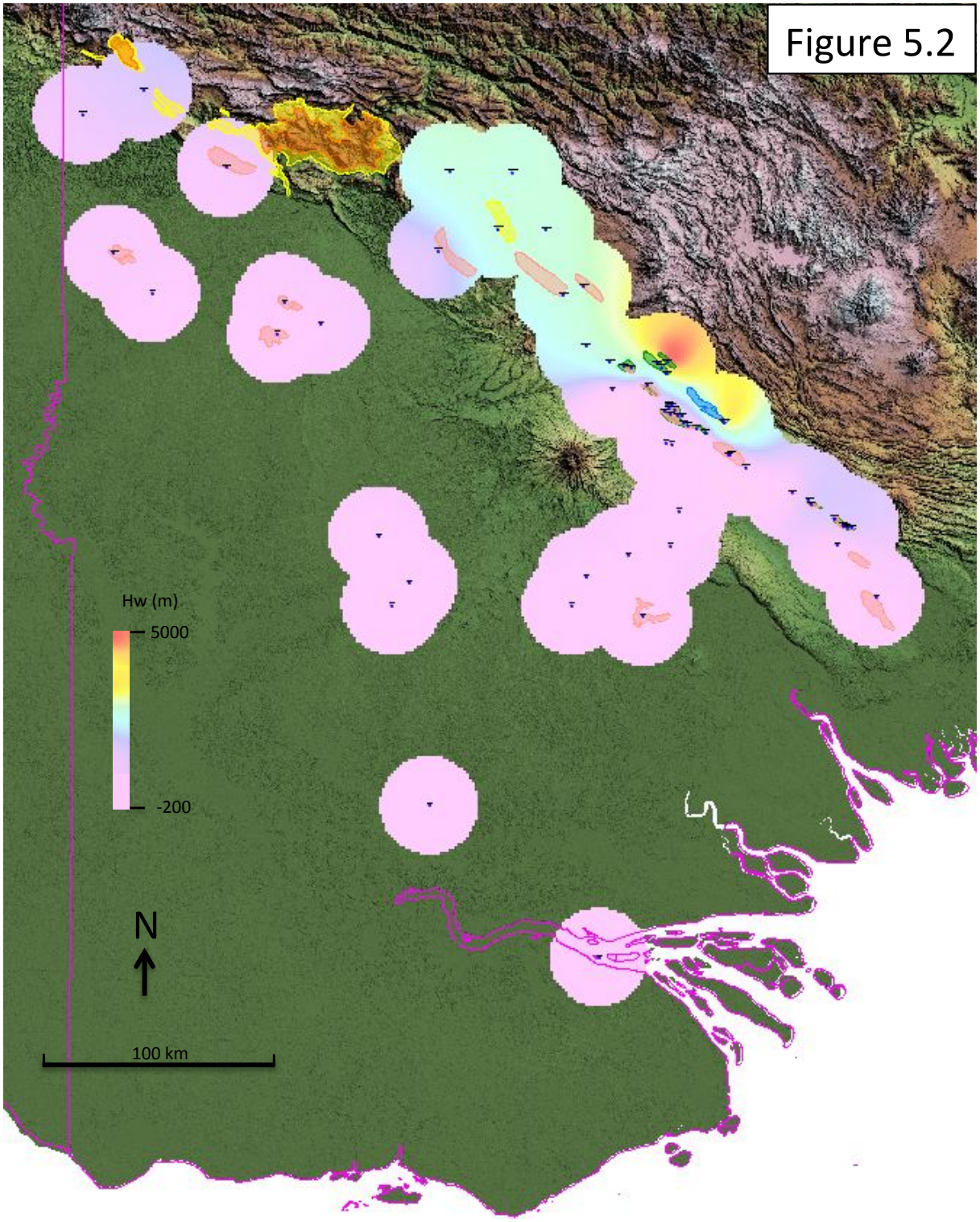

Figure 5.2: Regional Toro Potentiometric Map 1

Map generated using 20km diameter-limiting circle extending from each well Hw value.
Oil and gas field outlines shown in green and pink respectively. Lake Kutubu outline shown in blue east of Kutubu Complex. Toro outcrop (yellow) and Imburu Formation outcrop (orange) are shown in the northwest of the fold belt (see Map A.2 to orientate Muller Anticline and Lavani Valley areas).

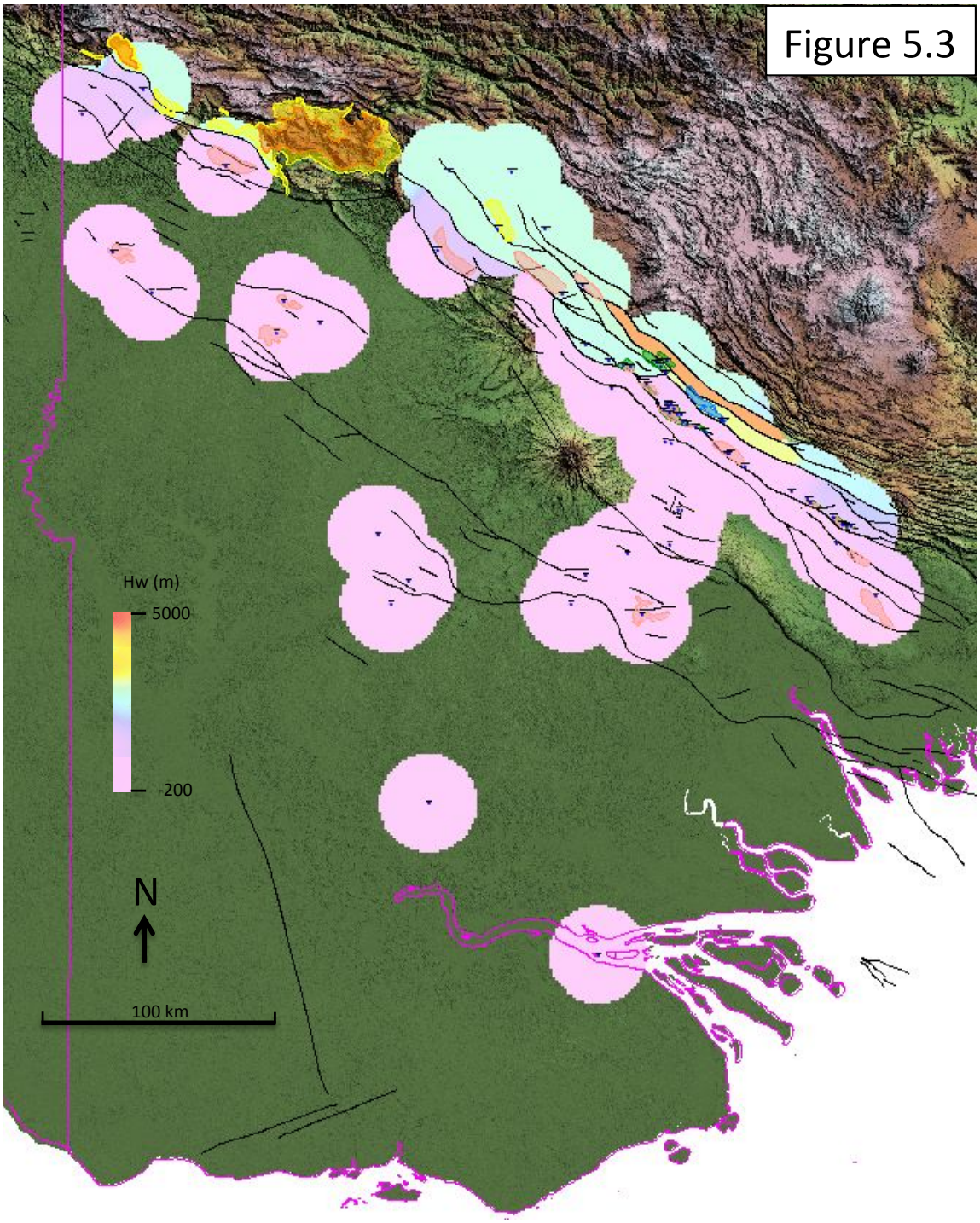

Figure 5.3: Regional Toro Potentiometric Map 2

Map generated using 20km diameter-limiting circle extending from each well Hw value, but also using regional fault set to constrain mapping. Begin to see northwest to southeast thrust fault control of Toro aquifer and compartmentalisation of aquifer in the hinterland. Oil and gas field outlines shown in green and pink respectively. Lake Kutubu outline shown in blue east of Kutubu Complex. Toro outcrop (yellow) and Imburu Formation outcrop (orange) are shown in the northwest of the fold belt (see Map A.2 to orientate Muller Anticline and Lavani Valley areas).

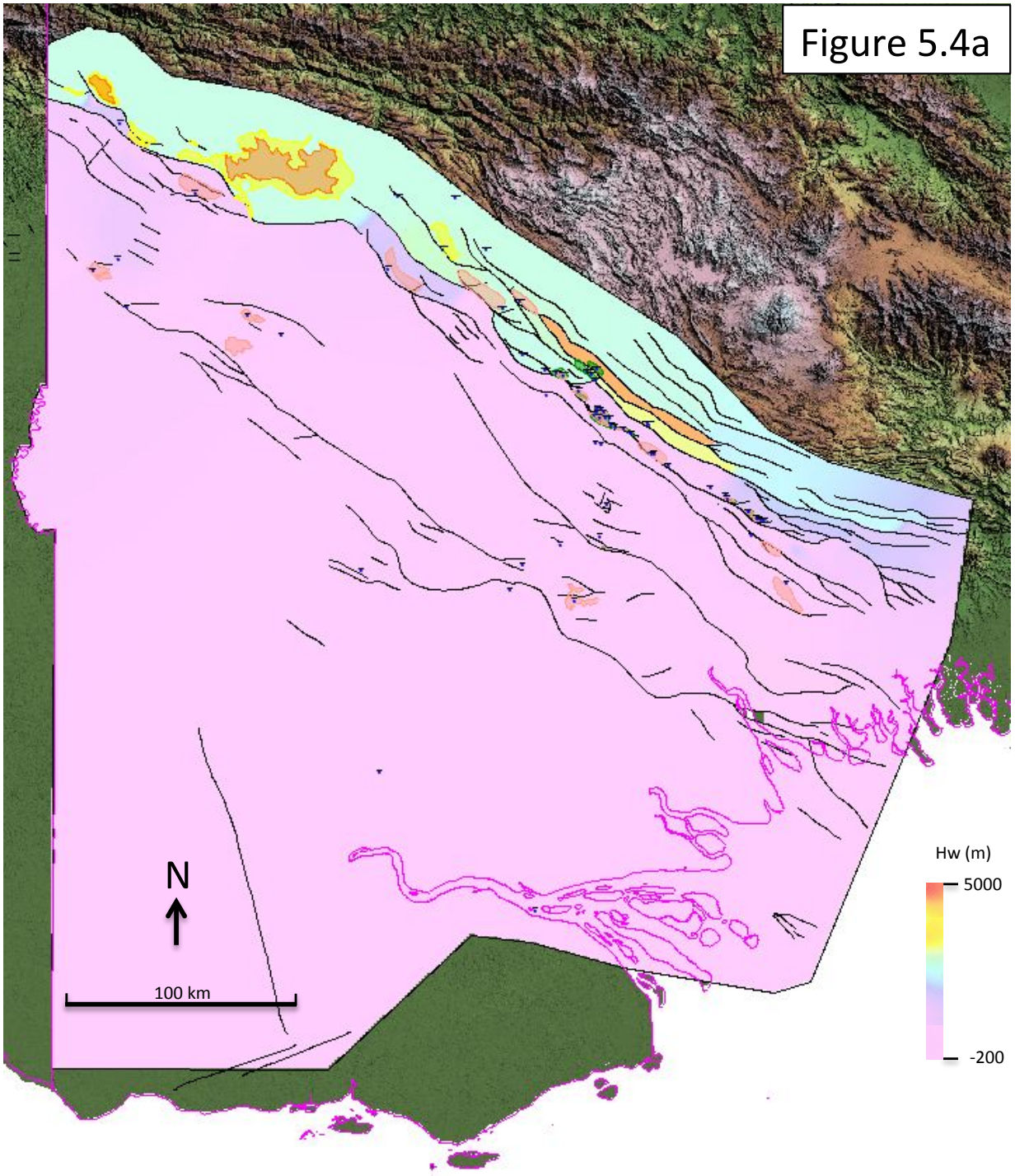

Figure 5.4a: Regional Toro Potentiometric Map 3

Fault constrained, top Toro formation structure map- and zero edge Toro polygon-limited. Considerable lateral extension/modelling of the Toro potentiometric surface produced in this map compared to maps 1 and 2. Oil and gas field outlines shown in green and pink respectively. Toro outcrop (yellow) and Imburu Formation outcrop (orange) are shown in the northwest of the fold belt (see Map A.2 to orientate Muller Anticline and Lavani Valley areas).

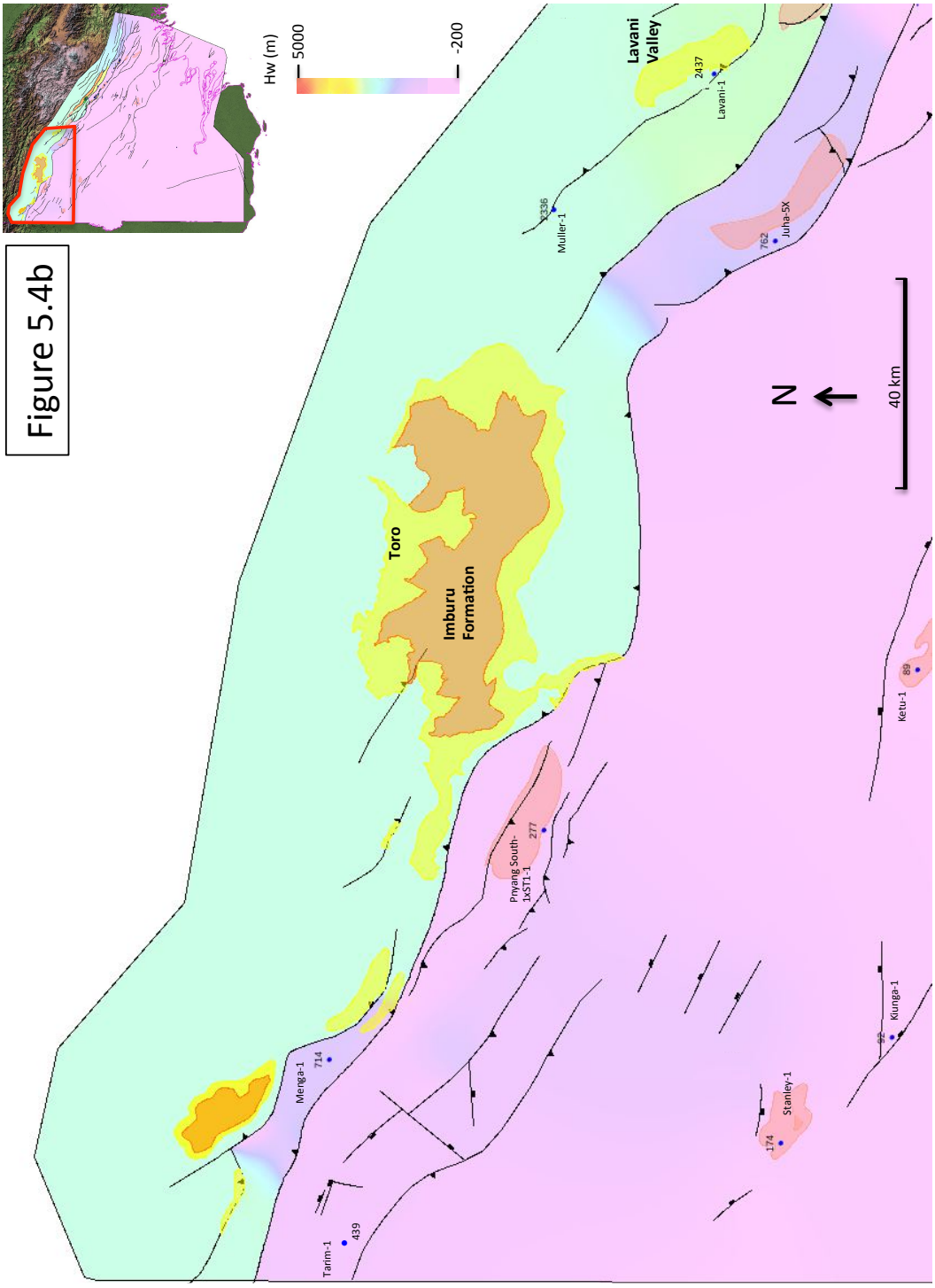

Figure 5.4b-d: Fold Belt Region of the Regional Toro Potentiometric Map 3

Assembled as three overlapping map panes to cover the fold belt region in sufficient detail for analysis. In each figure an inset shows the area covered compared to the master map (Figure 5.4a).
All wells contributing Hw values to the potentiometric surface are labelled with Hw value (m)
Oil and gas fields labeled and outlines shown in green and pink respectively. Toro outcrop (yellow) and Imburu Formation outcrop (orange) are labeled and shown in the northwest of the fold belt.

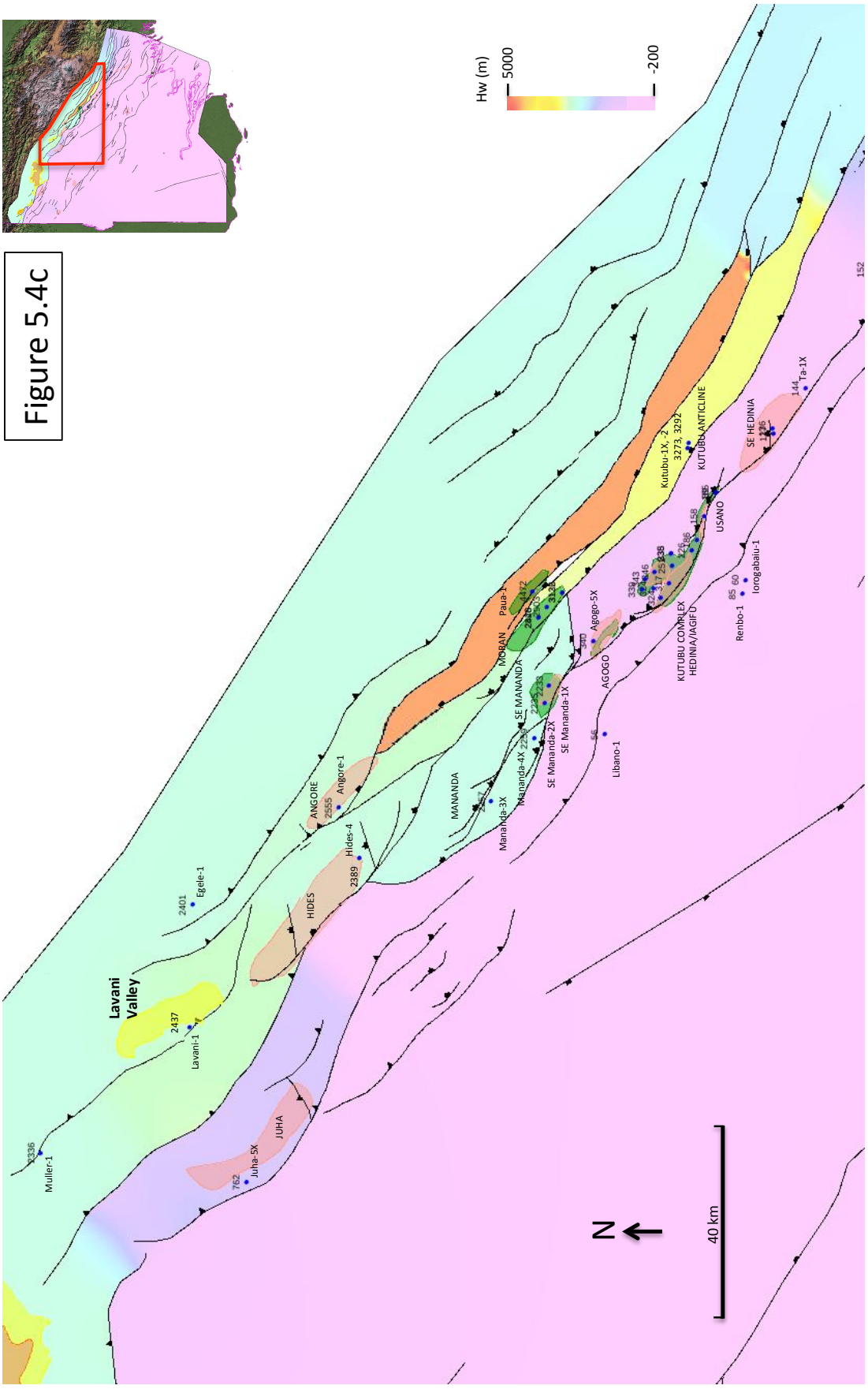
Hw (m)
5000
-200
Lavani Valley
Muller-1
Egele-1
Lavani-1
Juha-5X
JUHA
HIDES
Hides-4
ANGORE
Angore-1
MANANDA
Mananda-3X
Mananda-4X
SE MANANDA
SE Mananda-2X
SE Mananda-1X
MORAN
Paua-1
AGOGO
Agogo-5X
Libano-1
KUTUBU COMPLEX
HEDINIA/IAGIFU
Renbo-1
Ionogabalu-1
USANO
KUTUBU ANTICLINE
Kututu-1X, -2
SE HEDINIA
Ta-1X
N
40 km

Figure 5.4c

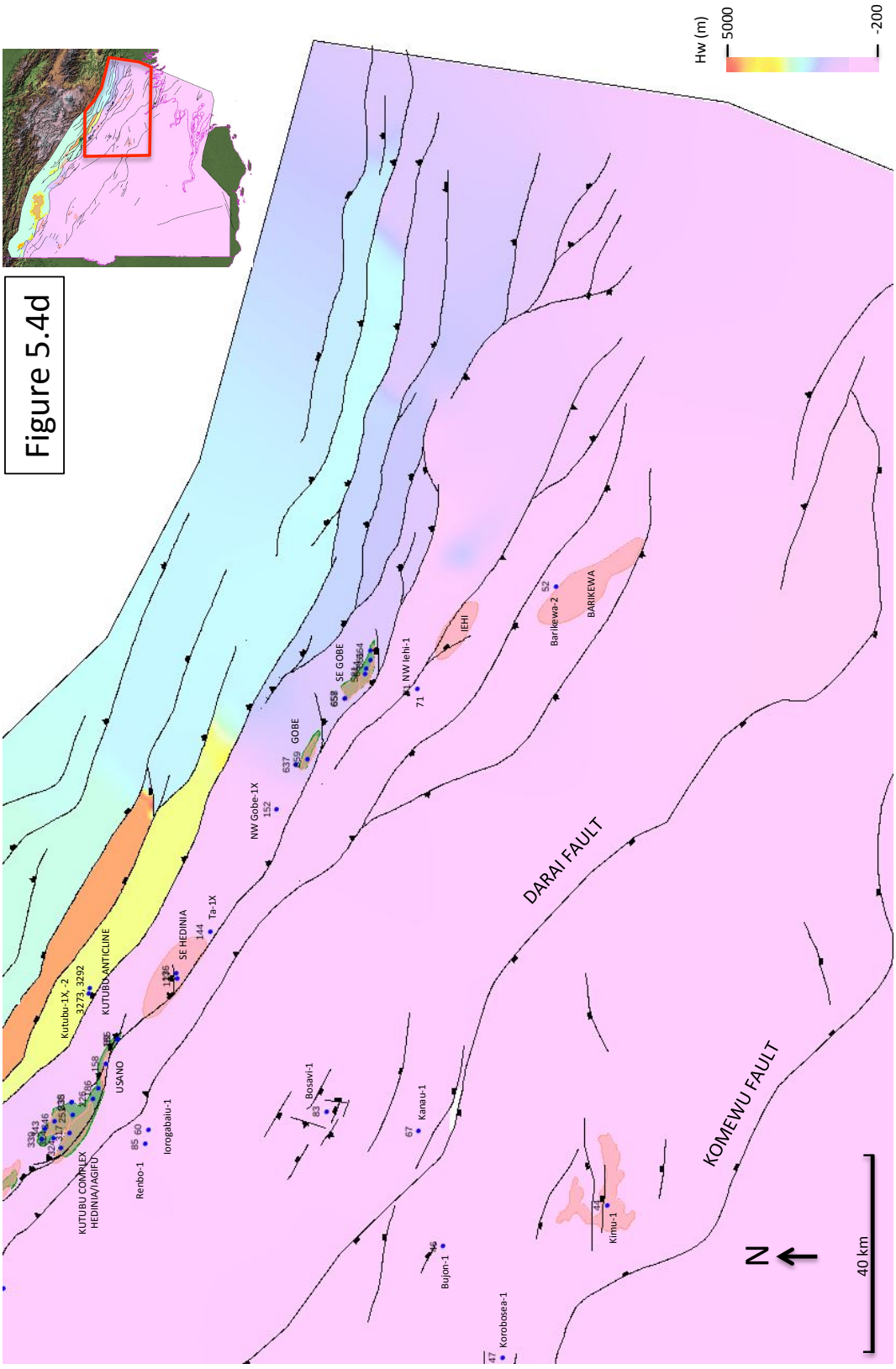
Figure 5.4d
Hw (m)
5000
-200
DARAI FAULT
KOMEWU FAULT
KUTUBU COMPLEX
HEDINIA/IAGIFU
KUTUBU ANTICLINE
USANO
SE HEDINIA
GOBE
SE GOBE
IEHI
BARIKEWA
Kutubu-1X, -2
Ta-1X
NW Gobe-1X
NW Iehi-1
Barikewa-2
Bosavi-1
Kanau-1
Renbo-1
Iorogabaiu-1
Bujon-1
Kimu-1
Korobosea-1
N
40 km

\\\\\\\\

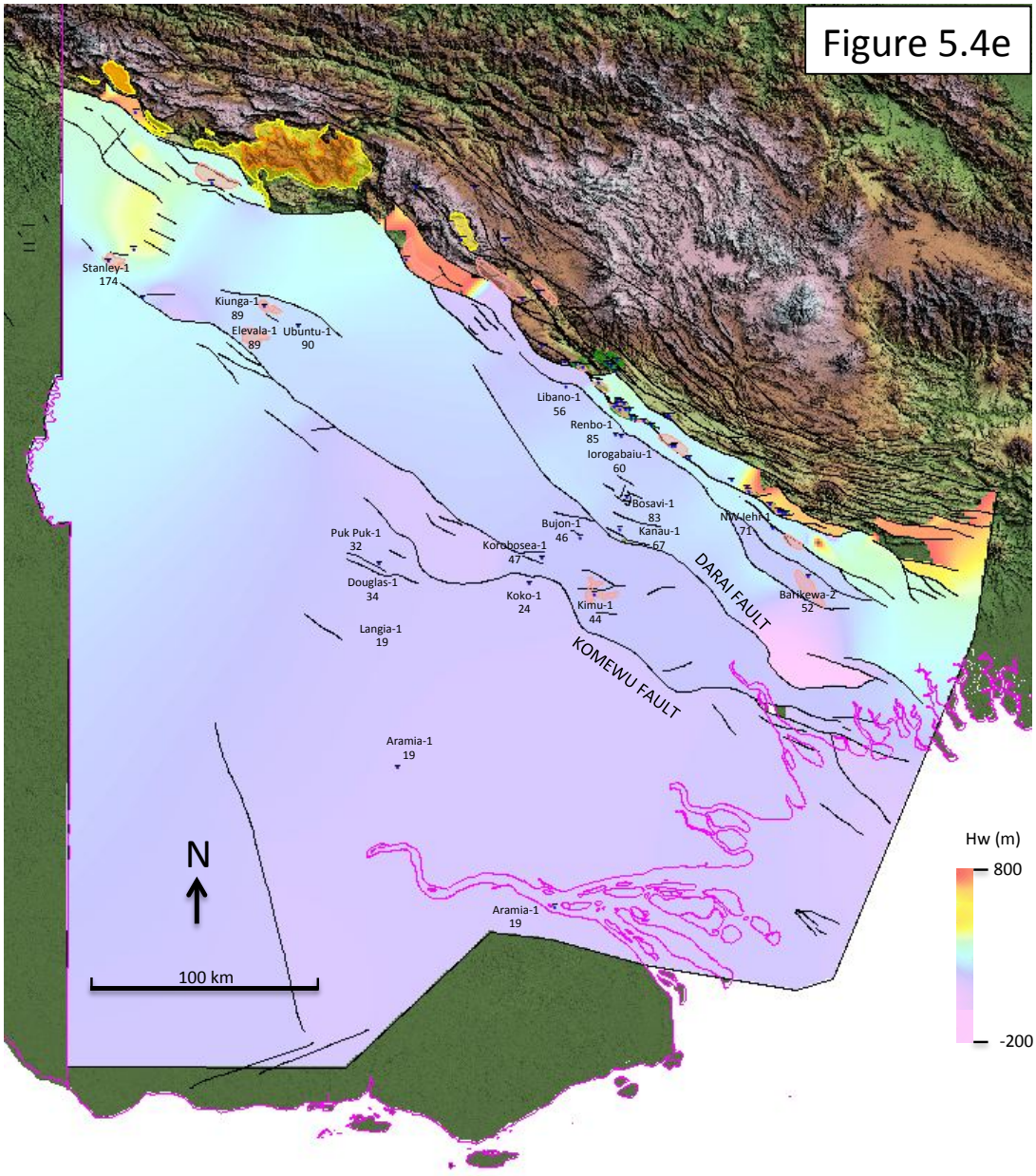

Figure 5.4e: Foreland Region of the Regional Toro Potentiometric Map 3

Colour scale adjusted to highlight lower Hw values in foreland and smaller differences in Hw between wells. All wells contributing Hw values to the potentiometric surface are labelled with Hw value (m). Gas field outlines shown in pink.

may not be connected and represent separate compartments. Likewise, Lavani Valley, Hides, Mananda/South East Mananda may also be separate compartments. Egele-1 may be connected to LV-H-M/SEM system but it is separated by northwest-southeast trending thrust faults that are sealing in other places in fold belt. It is likely that Angore, Moran and Paua Fields as well as the Kutubu Anticline are separate compartments as they too are all in the thrust sheet to the east of LV-H-M/SEM system (see Maps A.2 - A.3 and Figure 5.4c).

There is a significant Hw step between the South East Mananda and Agogo Fields in the central region of the fold belt (Figures 5.4c-d). Hw values then consistently decrease again from Agogo into Hedinia/Iagifu and finally through to Usano in a northwest to southeast direction (Figures 5.4.c-d).

Hw values in the South East Hedinia Field decrease consistently from the southeast to northwest to Usano This trend is consistent with Toro aquifer flow in the South East Hedinia Field exiting from the fold belt at the southern end of Usano (Figure 5.4d and see section 5.3.5 for more detailed results and analysis). Hw values were relatively invariant across the Gobe/South East Gobe Fields in the south of the central fold belt region, but were slightly higher than the values seen for the Kutubu Complex and the South East Hedinia Field. These data suggest a higher pressured hydrostatic Toro reservoir compartment is present in these fields.

5.1.2 Foreland

Several overall Hw trends are obvious in the foreland region of the basin (Figure 5.4e). There appears to be a general flow trend from the northwest to the southeast of the basin towards the sea. The Stanley Field in the northwest represents a potentiometric high for the foreland with consistently decreasing Hw values moving southeast from Stanley. In addition the fold belt flank regions adjacent to the Kutubu Complex and as far southeast as the Gobe/South East Gobe Fields have slightly higher Hw values than the areas southwest and more distal to the fold belt in the foreland. These data suggest flow from the potentiometric highs to the lows, northwest to southeast, in the foreland from the Stanley field (and likely the fold belt to the northwest of the Stanley Field). These data also suggest water flow from the fold belt into the foreland from adjacent the Kutubu Complex region and perhaps other regions along the fold belt, such as from Libano-1 west of the South East Mananda Field. The Komewu Fault appears to be acting as a barrier to Toro aquifer flow moving southwest, as there is a noticeable Hw step across the Komewu Fault (Figure 5.4e).

5.2 Regional Digimu, Hedinia and Iagifu Pressure-Depth Analysis and Potentiometric Surface Maps

P-D plots for the Digimu, Hedinia and Iagifu reservoir units are shown in Figures 5.5, 5.6 and 5.7 respectively. There were much less data available for all three of these reservoir units compared to the Toro reservoir, however like the Toro reservoir there were clear foreland versus fold belt pressure gradient trends for all three reservoir units.

Potentiometric maps for the Digimu, Hedinia and Iagifu reservoir units are shown in Figures 5.8, 5.9 and 5.10 respectively. As with the Toro potentiometric surface maps, only pre-production Hw data were used for the mapping (Hw data utilised in mapping is listed in Tables A.5, A.8 and A.11). Much less data were available for all three of these reservoirs compared to the Toro reservoir, consequently these maps are more restricted than the Toro potentiometric maps.

5.3 Sub-Regional/Field Scale Toro, Digimu, Hedinia and Iagifu Aquifer Analysis

5.3.1 Highlands/Hinterland

A Toro P-D plot was generated to help identify Toro aquifer connectivity versus discrete aquifer cells based on differences in water pressure gradients in the highlands/hinterland regions of the fold belt (Figure 5.11). There are clearly a set of wells with very similar pressure gradients (Lavani-1, Muller-1, Egele-1, Mananda/South East Mananda wells (Mananda-3X, 4X and SE Mananda-1X, -2X) as well as the extrapolated gas water contact (EGWC) values generated for Hides-4 and Angore-1. These slightly offset pressure gradients can suggest connectivity and water flow but can also mean these fields and the faulted anticline structures that contain them actually form separate aquifer compartments. It is worth noting that the Hides-1, -2, -3, -4 gas pressure data all plot on a single pressure gradient, suggesting well pressure connectivity across the Hides Anticline (see Figure A.2). Actual GWC(s) will need to be determined from planned wells in the Hides Field before it is possible to really begin to look at whether there is a hydrodynamic Toro aquifer operating through Hides potentially linking Lavani Valley Toro outcrop and Mananda/South East Mananda Fields.

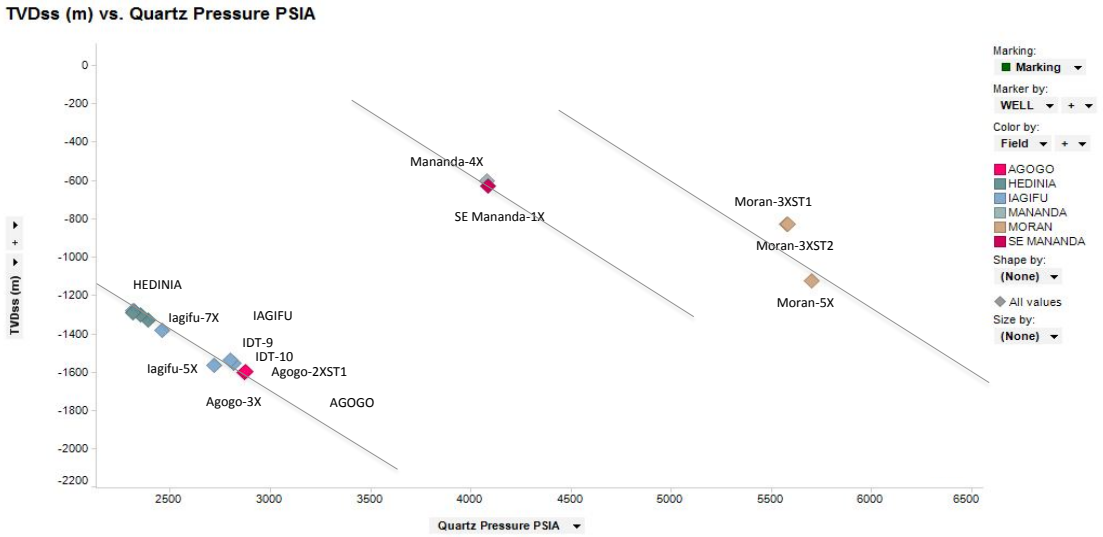

Figure 5.5: Regional Digimu Aquifer Water Pressure Gradient Plot

P-D plot [x-axis: Pressure (psia) vs y-axis: Depth (total vertical depth meters sub sea (TVDmSS)].

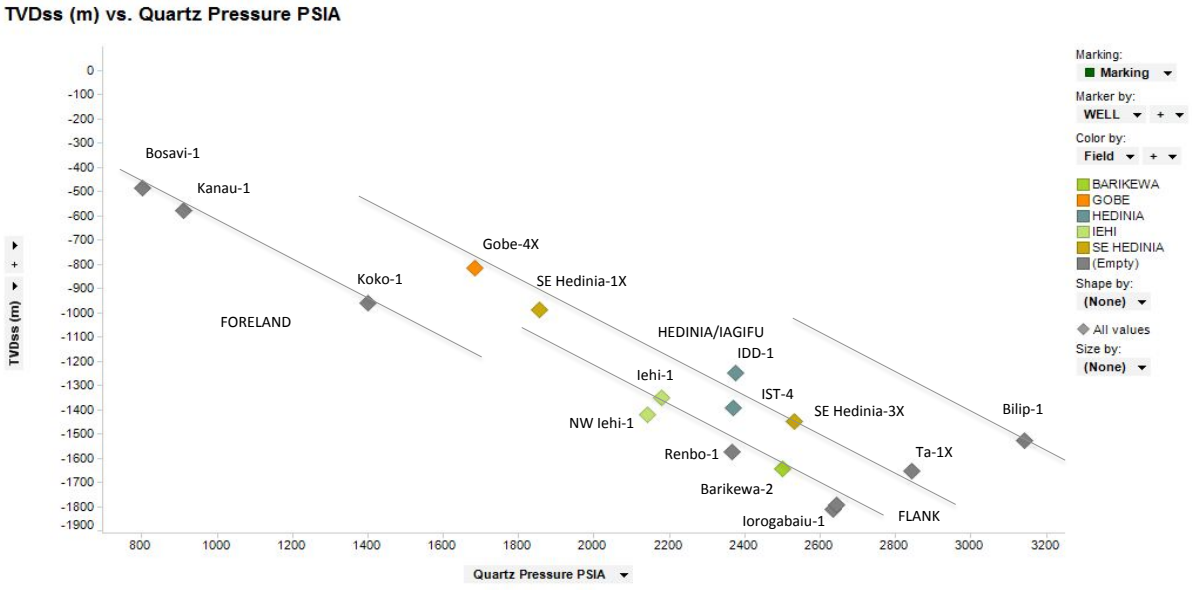

Figure 5.6: Regional Hedinia Aquifer Water Pressure Gradient Plot

P-D plot [x-axis: Pressure (psia) vs y-axis: Depth (total vertical depth meters sub sea (TVDmSS)].

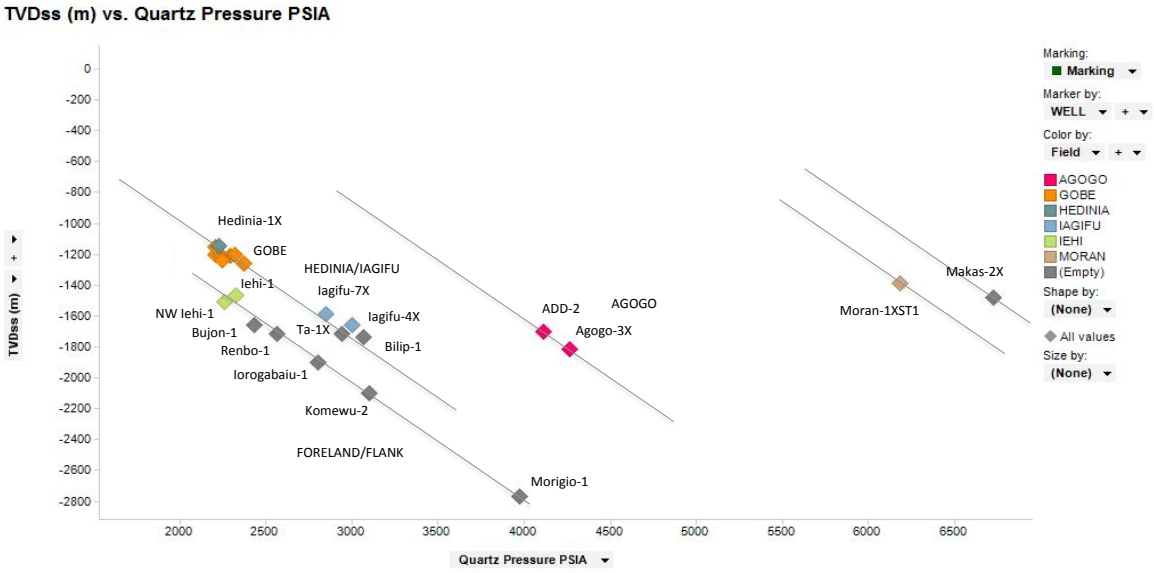

Figure 5.7: Regional Iagifu Aquifer Water Pressure Gradient Plot

P-D plot [x-axis: Pressure (psia) vs y-axis: Depth (total vertical depth meters sub sea (TVDmSS)].

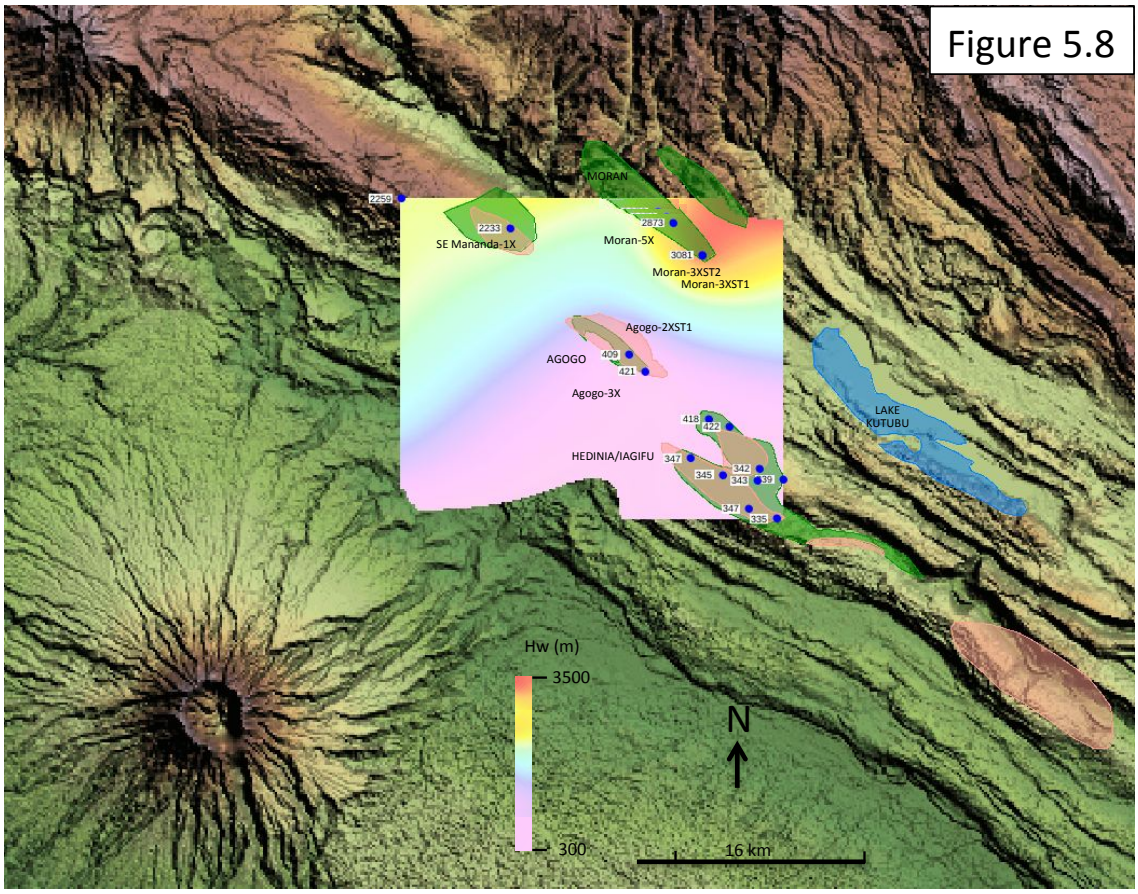

Figure 5.8: Regional Digimu Potentiometric Map

All wells contributing Hw values to the potentiometric surface are labelled with Hw value (m). Oil and gas fields labeled and outlines shown in green and pink respectively. Lake Kutubu labeled and outline shown in blue east of Kutubu Complex

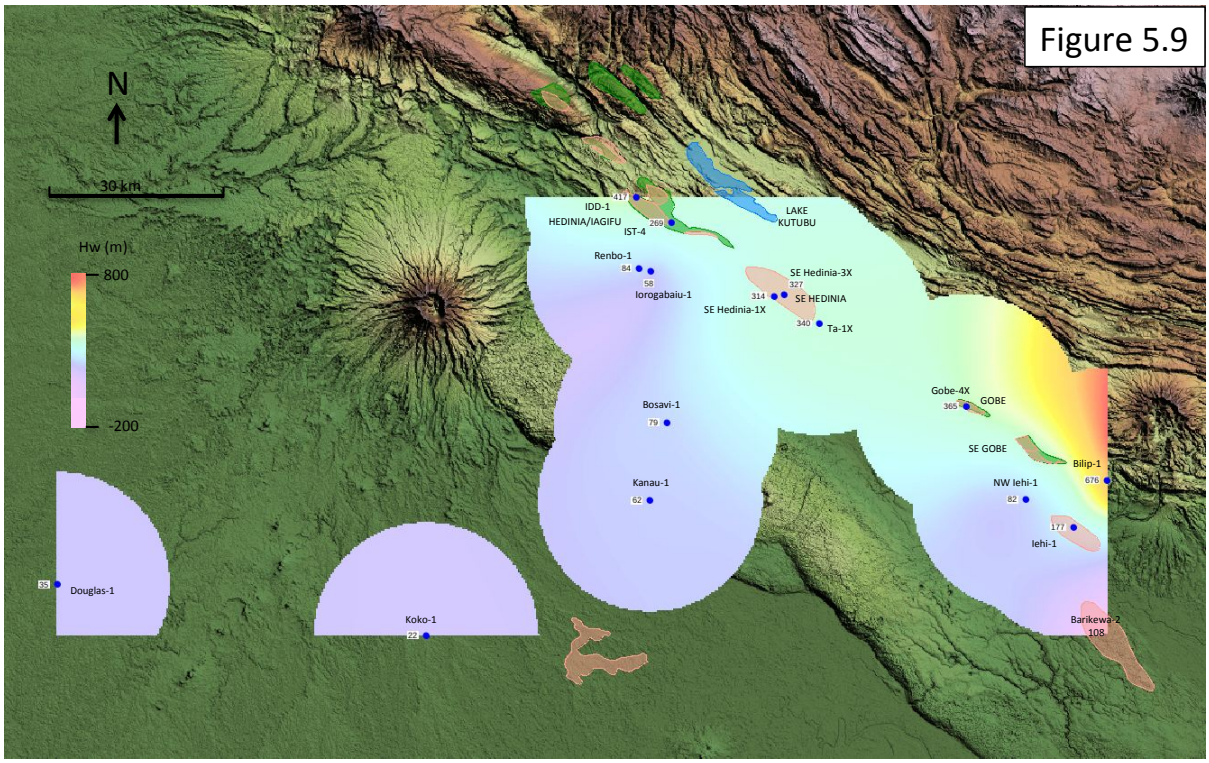

Figure 5.9: Regional Hedinia Potentiometric Map

All wells contributing Hw values to the potentiometric surface are labelled with Hw value (m). Oil and gas fields labeled and outlines shown in green and pink respectively. Lake Kutubu labeled and outline shown in blue east of Kutubu Complex

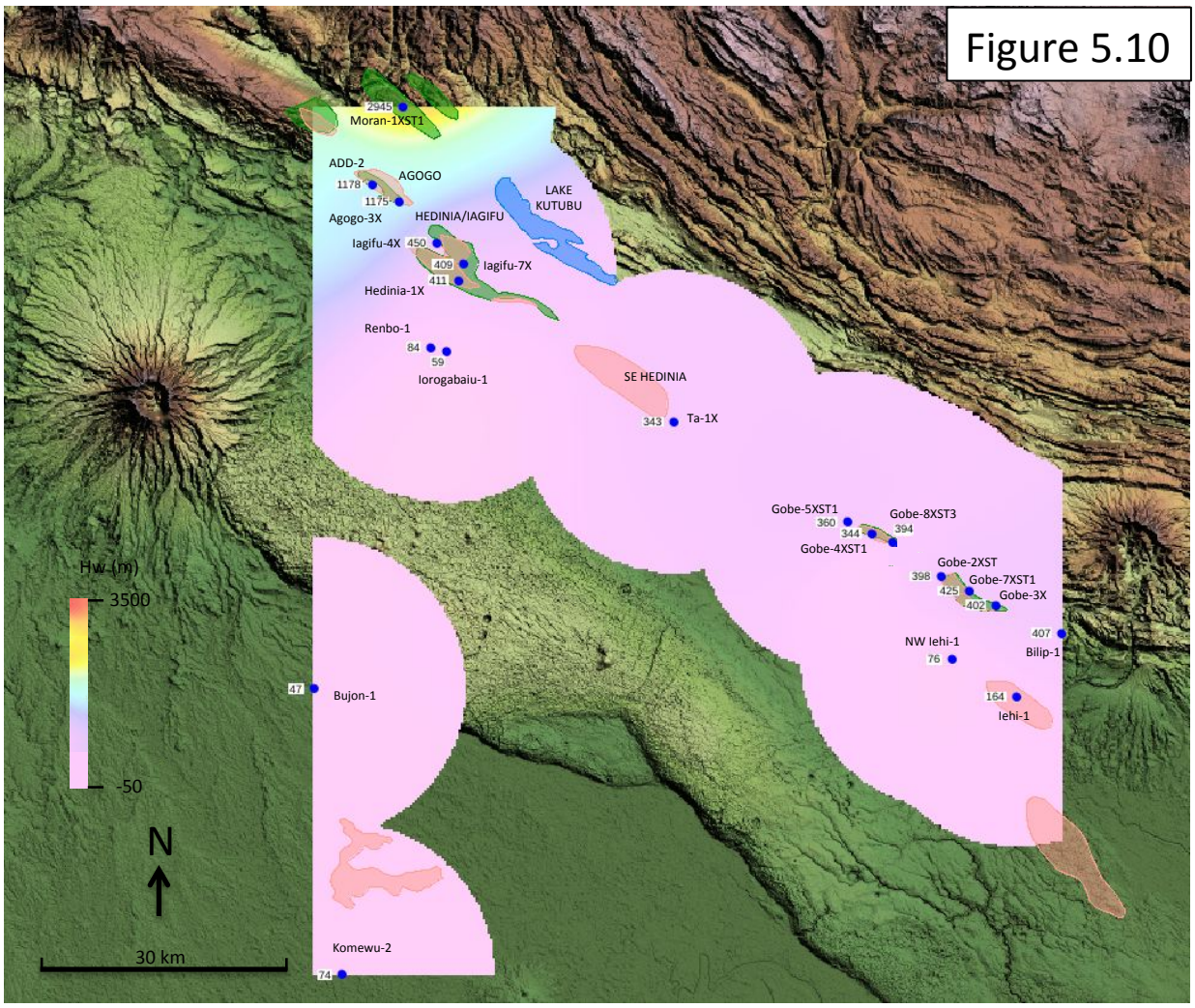

Figure 5.10: Regional Iagifu Potentiometric Map

All wells contributing Hw values to the potentiometric surface are labelled with Hw value (m). Oil and gas fields labeled and outlines shown in green and pink respectively. Lake Kutubu labeled and outline shown in blue east of Kutubu Complex

5.3.2 Mananda/South East Mananda

There were only four wells available to analyse the Toro aquifer trend across the Mananda and South East Mananda Fields. Pressure gradients (Figure 5.12) and Hw values (Figure 5.4c) were consistent with a hydrodynamic aquifer operating, flowing northwest to southeast with an Hw step (likely fault generated) between Mananda and South East Mananda. However, because of the limited number of Hw data points available, these data could also be interpreted as indicating a compartmentalised system between Mananda and South East Mananda. There were only oil pressure data for South East Mananda-1X, and 2X wells (no oil pressure data for Mananda) so it was not possible to investigate whether there is a single oil leg across Mananda Anticline, which would provide evidence for connectivity between the fields and potentially a hydrodynamic Toro aquifer. So with the limited data available, it is not possible to differentiate between either potential water flow between the fields or compartmentalisation in this instance.

5.3.3 Moran

The Moran Field has been developed since the Kotaka (1996) study (see section 4.4). Oil and gas have been produced from Toro and Digimu Sandstone reservoirs in the Moran Field since 1998 (Buick et al., 2009). The field is structurally complex, with an abundance of faulting, which appears to compartmentalise the field (see Figure 2.10). A significant amount of the faulting is likely a result of the Bosavi Lineament cross cutting through the field.

Toro and Digimu reservoir pressure gradient data (Figures 5.1 and 5.5) and Hw data (Figures 5.4c and 5.8) suggest significant compartmentalisation has occurred in the Moran Field. There appears to be no consistent trend in Hw values across the field and the water and oil pressure gradients are all offset in relation to each other (data not shown). All the Moran Field compartments are highly pressured, putting them in the same pressure regime in the fold belt as the Angore and Paua Fields and Kutubu Anticline, all of which are located in the thrust sheet east of the highlands region (Lavani Valley, Hides, Mananda/South East Mananda).

5.3.4 Kutubu Complex

The P-D plot of the Toro reservoir water, oil and gas pressure gradients shows that the water gradients were offset across the Agogo-Hedinia/Iagifu-Usano Fields, while there were single oil and gas gradients for each field (Figure 5.13). This is good evidence for a hydrodynamic aquifer operating in the Toro reservoir. There are sufficient data points to establish a convincing consistent decreasing trend of Hw values northwest to southeast through the fields (Figure 5.14).

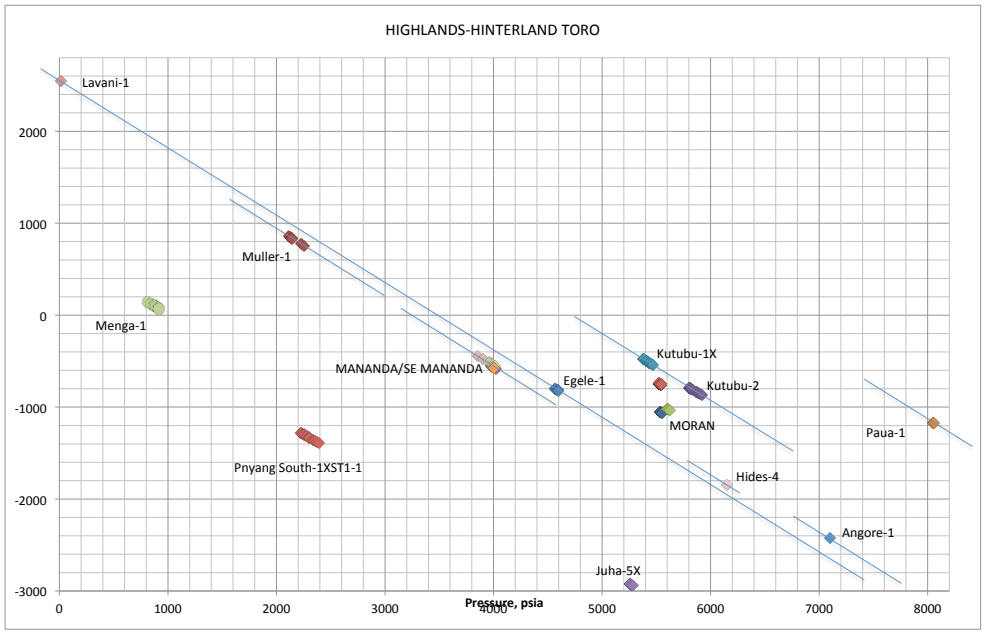

Figure 5.11: Highlands/Hinterland Toro Aquifer Water Pressure Gradient Plot
P-D plot [x-axis: Pressure (psia) vs y-axis: Depth (total vertical depth meters sub sea (TVDmSS)].

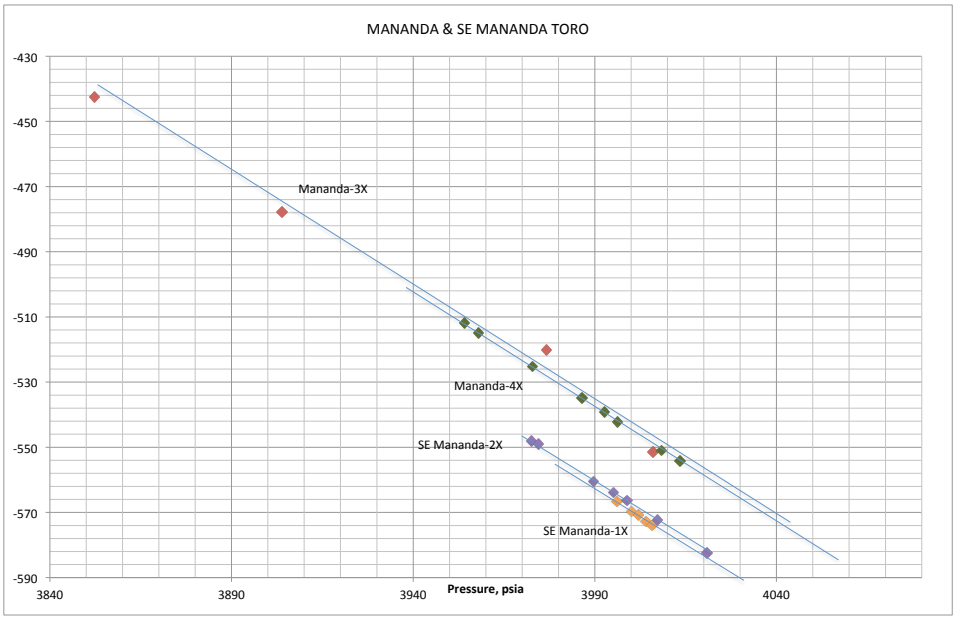

Figure 5.12: Mananda/South East Mananda Toro Aquifer Water Pressure Gradient Plot
P-D plot [x-axis: Pressure (psia) vs y-axis: Depth (total vertical depth meters sub sea (TVDmSS)].

In the Digimu reservoir, however, there does not appear to be a hydrodynamic aquifer operating in the Hedinia/Iagifu Fields (Figure 5.15). There appear to be separate Hw compartments for the main block and 3X/8X block of the Kutubu Complex. Each of these blocks displays a relatively invariant set of Hw values across the block. In addition the Digimu reservoir would appear to be compartmentalised in the Agogo Field (Figure 5.16). This is supported by the identification of multiple water and oil gradients in the Digimu reservoir in Agogo. Note this is very different to Toro reservoir behavior in Agogo, which has single oil and single gas gradients (Figure 5.13).

Hw data for the Hedinia and Iagifu reservoirs in the Kutubu Complex were limited but suggest for both reservoirs a northwest to southeast trend of decreasing Hw values within the Hedinia/Iagifu Fields. A significant Hw step was detected between Agogo and Hedinia/Iagifu Fields for the Iagifu reservoir (see Figure 5.10). This step is reflected in the shift of position of the Agogo Iagifu reservoir values on the P-D plot away from the Hedinia/Iagifu pressure regime they are been associated with for the Toro and Digimu reservoirs (see Figure 5.7).

5.3.5 South East Hedinia

Eisenberg et al. (1994) and Kotaka (1996) describe hydrodynamic aquifer behavior in the Toro reservoir in the South East Hedinia Field. Hw Data obtained in this study was consistent with a hydrodynamic aquifer operating (see section 5.1), but it should be noted that this interpretation was based on only three data points (Figure 5.17). Flow is in a southeast to northwest direction through South East Hedinia Field, in the opposite direction to the Toro reservoir aquifer flow from the Kutubu Complex. [Note - Hw value for North West Gobe-1, which is southeast of South East Hedinia Field, is also consistent with a flow direction from southeast to northwest and could extend the lateral extent of the hydrodynamic Toro reservoir in South East Hedinia a further 20 km southeast in the fold belt (Figure 5.4d)]. Water flow is potentially exiting the South East Hedinia structure and fold belt out into foreland flank via the same route water exits Usano from the Kutubu Complex to the north. Water flow in the South East Hedinia Field appears to be flowing down-dip as water pressure gradients are decreased compared to a hydrostatic situation (see Figure 4.3). [Ta-1X: -1350 TVDmSS; Hw 144m; pressure gradient (psi/ft); 0.428. SE Hedinia-3X: -1200 TVDmSS; Hw 136m; pressure gradient (psi/ft); 0.430. SE Hedinia-4X: -970 TVDmSS; Hw 122m; pressure gradient (psi/ft); 0.427.]

A similar southeast to northwest trend of decreasing Hw values is seen for the Hedinia reservoir in the South East Hedinia Field (Figure 5.9). Insufficient Hw data exist for the Iagifu reservoir in the South East Hedinia Field to analyse aquifer behavior.

5.3.6 Gobe/South East Gobe

The Toro reservoir is over-pressured compared to the Iagifu reservoir in the Gobe/South East Gobe Fields. The Toro reservoir appears to be behaving as a single hydrostatic connected compartment across the Gobe/South East Gobe Fields (Figure 5.18 and Table A.2). No oil or gas is present in the Toro reservoir in the Gobe/South East Gobe Fields. Whereas, oil and gas are present in the under-pressured Iagifu reservoir (Figure 5.19). There are multiple gas, oil and water pressure gradients present in the Gobe/South East Gobe Fields, which suggest that the Iagifu reservoir is compartmentalised.

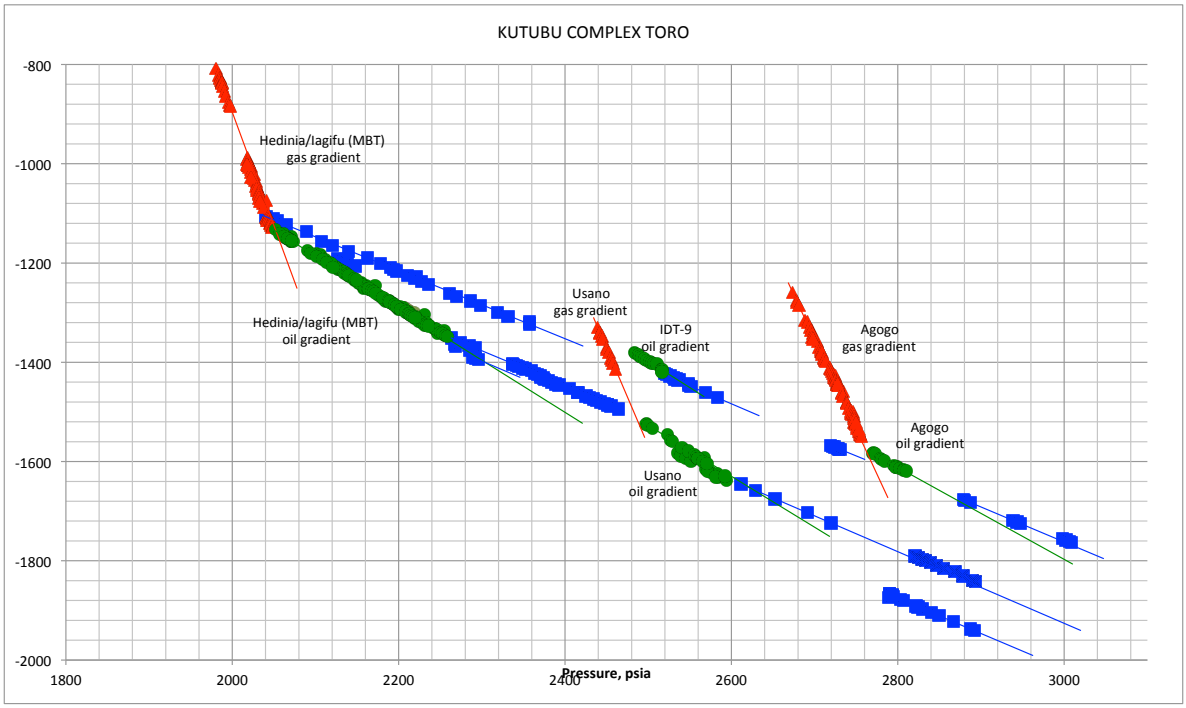

Figure 5.13: Kutubu Complex - Toro Reservoir P-D Plot

Single oil and gas gradients for the Main Block Toro (MBT) reservoir in the Hedinia/Iagifu Fields, but multiple water pressure gradients. Likewise, single oil and gas gradients for the Agogo and Usano Fields, but multiple water pressure gradients. Only pre-production well data used to generate P-D plot. Note IDT-9 located in Iagifu 3X/8X block, which represents a separate compartment from the MBT of the Kutubu Complex (Hedinia/Iagifu Fields). Gas, oil and water pressure values displayed in red, green and blue respectively. P-D plot [x-axis: Pressure (psia) vs y-axis: Depth (total vertical depth meters sub sea (TVDmSS)].

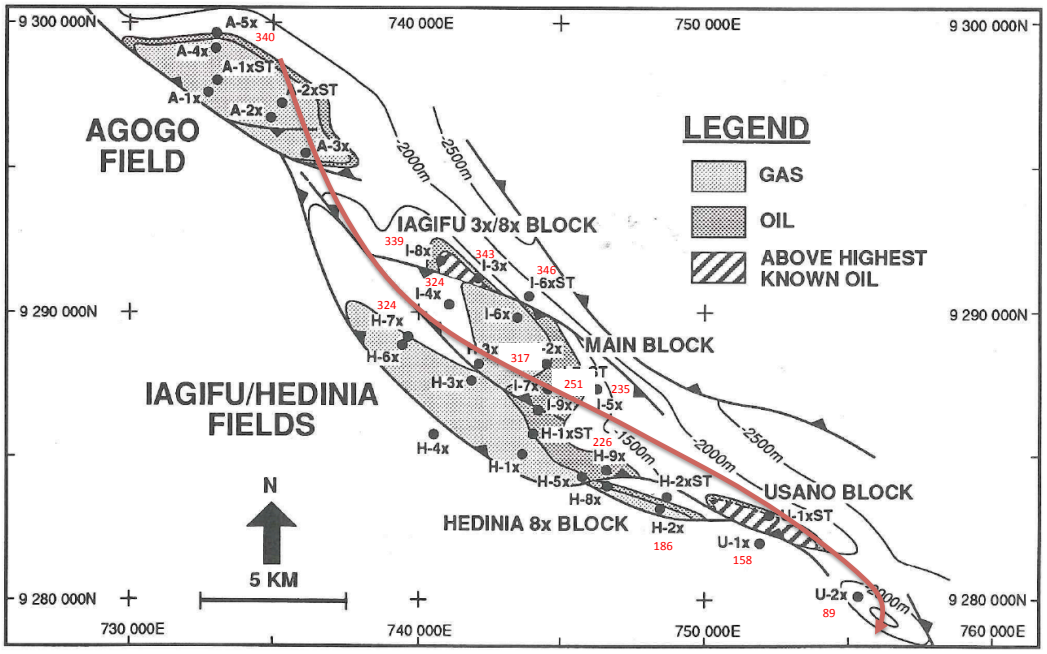

Figure 5.14: Potentiometric Surface Map for the Kutubu Complex – Toro Reservoir
Hw values (see Table A.2) plotted on Kutubu Complex map (red numbers) demonstrating consistent decrease in value in a northwest to southeast direction across Agogo-Hedinia/Iagifu-Usano Fields. Potential direction/path of water flow shown by red arrow (base map diagram modified from Eisenberg, 1993).

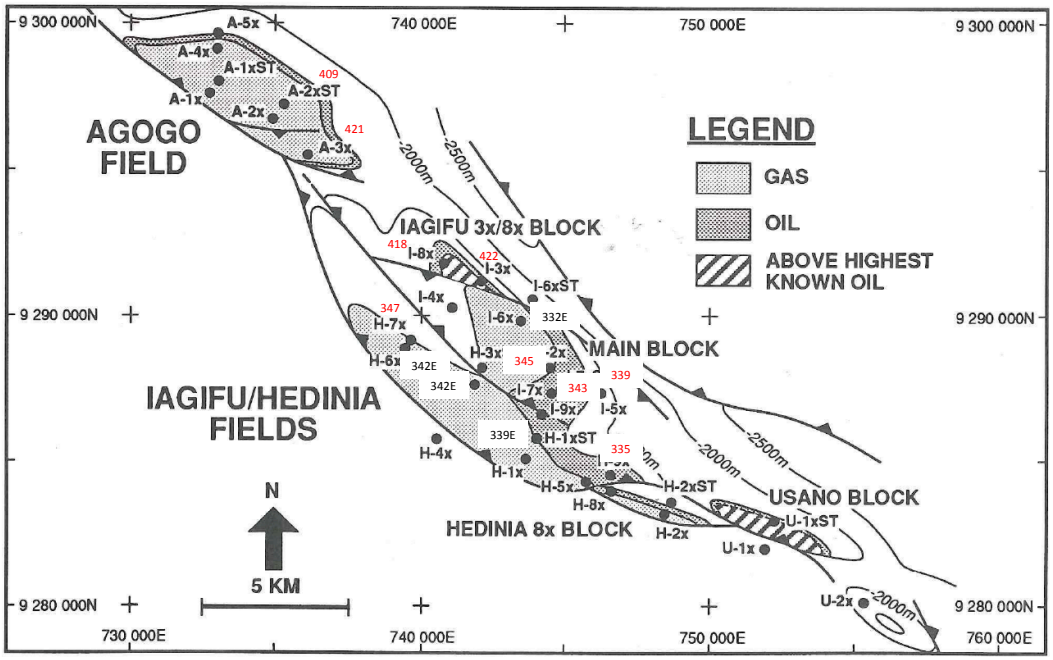

Figure 5.15: Potentiometric Surface Map for the Kutubu Complex - Digimu Reservoir
Digimu Hw values (see Table A.5) plotted on Kutubu Complex map (red numbers). Hw values generated by extrapolated OWC values displayed as black numbers with E suffix (base map diagram modified from Eisenberg, 1993).

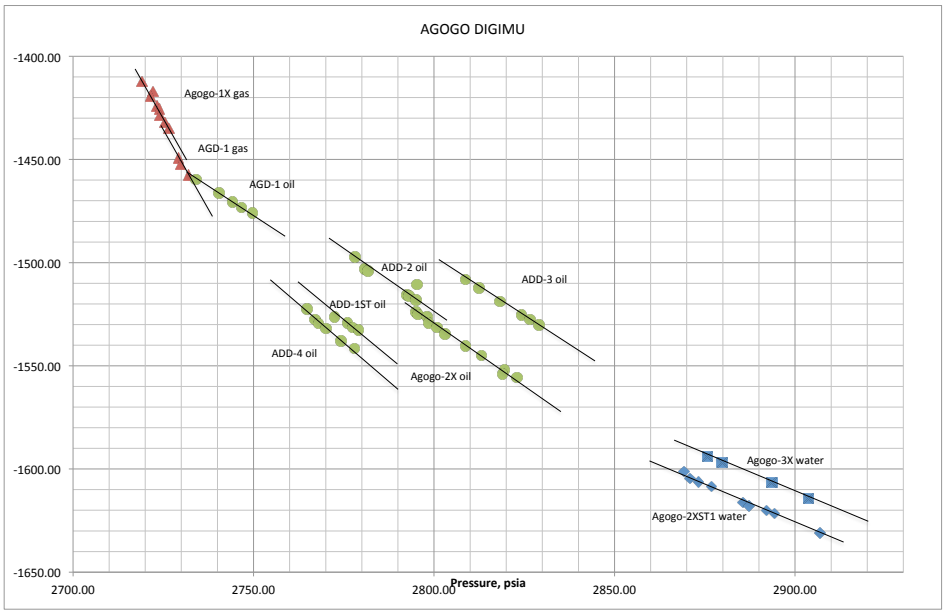

Figure 5.16: Agogo Field - Digimu Reservoir P-D Plot

Multiple gas, oil and water pressure gradients for the Digimu reservoir in the Agogo field. Gas, oil and water pressure values displayed in red, green and blue respectively. P-D plot [x-axis: Pressure (psia) vs y-axis: Depth (total vertical depth meters sub sea (TVDmSS)].

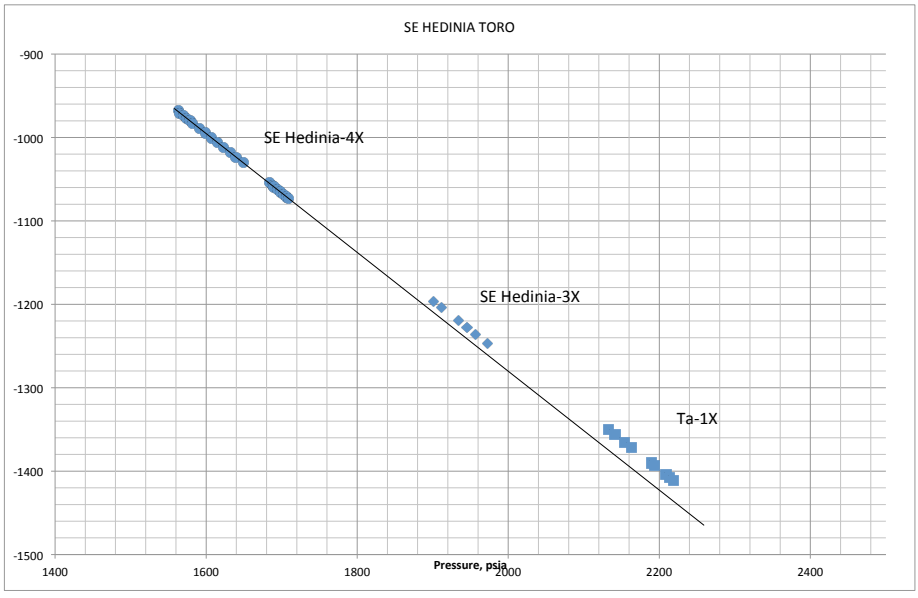

Figure 5.17: South East Hedinia Field - Toro Reservoir P-D Plot

Offset water pressure gradients for the Toro reservoir in the South East Hedinia Field. P-D plot [x-axis: Pressure (psia) vs y-axis: Depth (total vertical depth meters sub sea (TVDmSS

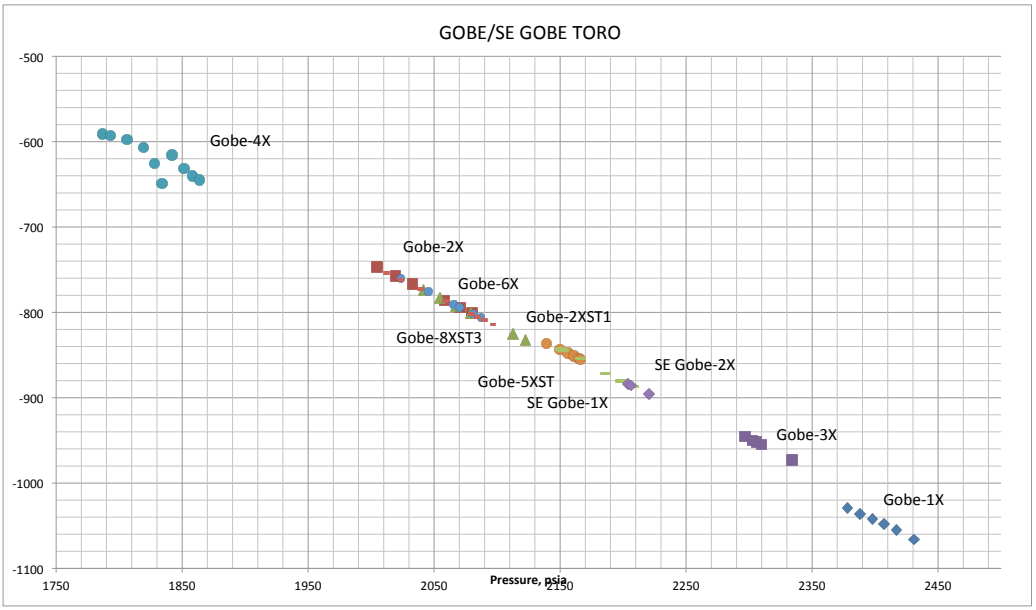

Figure 5.18: Gobe/South East Gobe Field - Toro Reservoir P-D Plot

P-D plot [x-axis: Pressure (psia) vs y-axis: Depth (total vertical depth meters sub sea (TVDmSS)].

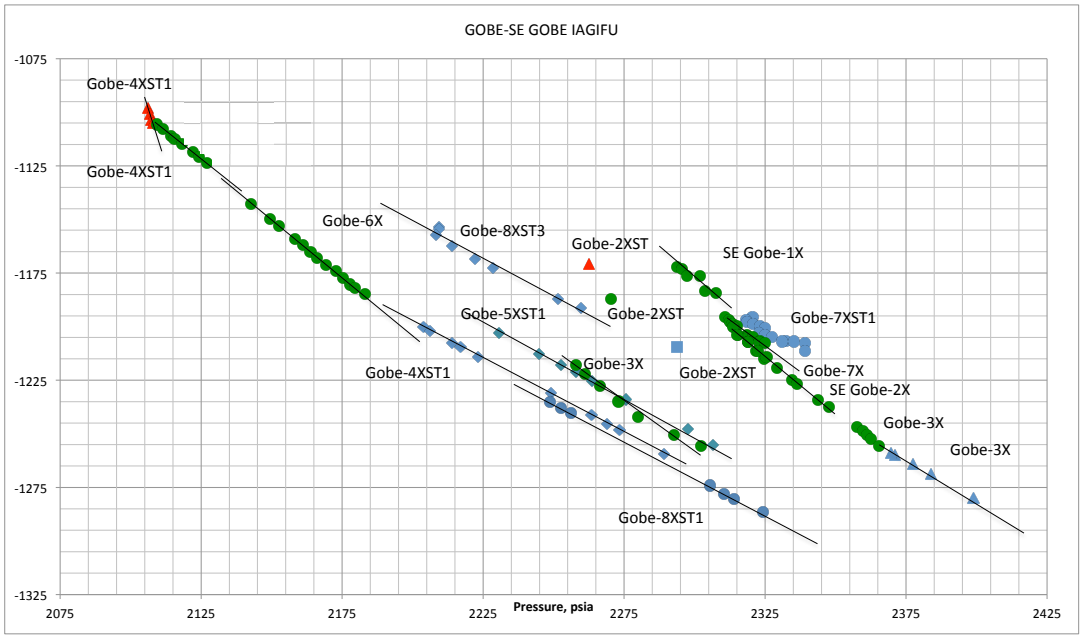

Figure 5.19: Gobe/South East Gobe Field - Iagifu Reservoir P-D Plot

P-D plot [x-axis: Pressure (psia) vs y-axis: Depth (total vertical depth meters sub sea (TVDmSS)]. Gas, oil and water values displayed in red, green and blue respectively.

Chapter 6: Final Discussion and Conclusions

6.1 Regional Toro Aquifer

Toro aquifer flow in the fold belt and foreland, while related, demonstrate different trends. As such, they are discussed separately below.

6.1.1 Fold Belt

The Toro potentiometric surface maps generated in this study are consistent with an extensive hydrodynamic Toro aquifer system existing in the Papuan Basin Fold Belt. The Toro aquifer likely flows northwest to southeast parallel to the fold belt, from the Lavani Valley Toro outcrop (likely recharge region) in the Highlands, through to the Kutubu Complex, potentially via Hides, (possibly Angore) and the Mananda/South East Mananda Fields (Figures 5.4b-5.4d). The evidence for Toro aquifer hydrodynamic flow is strongest through the Kutubu Complex of fields, with water flow, entering via Agogo and exiting the fold belt, at the southern end of the Usano Field into the foreland of the basin (figures 5.4c-e and 5.14). However, it should be noted that GWCs for Hides and Angore Fields are not yet available. These have been estimated in this study from Hides and Angore gas pressure gradient intersections with water pressure gradients identified from nearby wells (Lavani-1 and Egele-1). Therefore it is not currently possible to unequivocally identify a connected Toro aquifer system between Lavani Valley, (possibly Angore) and Hides. Nevertheless, the Lavani Valley-Hides-Mananda/South East Mananda system (LV-H-M/SEM) represents the most likely flow path for a Toro hydrodynamic aquifer model in the fold belt (Figure 6.1).

It is important to note that water flow out from the fold belt into the flank and foreland regions could be occurring elsewhere along the fold belt but a lack of wells to provide Hw values does not allow this possibility to be tested (Figures 5.4b-e). For instance, a structural cross section of the Mananda Anticline shows juxtaposition of the Toro Sandstone with the Darai Formation across the main thrust front, which could be a conduit for water flow out of the Toro reservoir in the fold belt into the foreland (Figure 6.2). Additional cross sections from other fields along the fold belt show juxtaposition with the Ieru Formation. Therefore, it is less likely in these regions for water to flow and discharge across the fault front through the regional seal into the foreland [see Figures 2.9c (5) and (6) and Figure 6.3]. Kotaka (1996) has suggested that fresh water is flowing into the foreland close to Libano-1 and Iorogabaiu-1 (Figure 5.4c). Iorogabaiu-1 is immediately west in the foreland from the proposed exit point at Usano. Libano-1 is immediately west of the junction between Agogo and South East Mananda Fields, which suggests another potential exit point for Toro water flow from the fold belt.

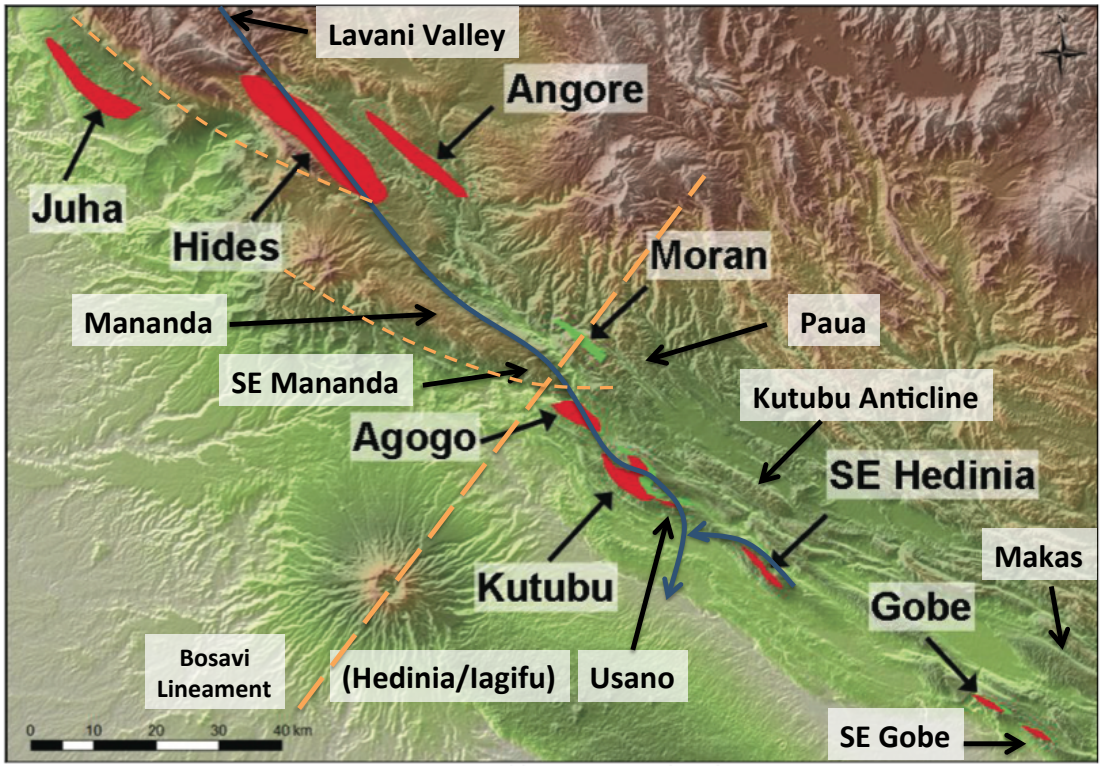

Figure 6.1: Regional Toro Hydrodynamic Aquifer Model

Possible water flow path in Toro Aquifer displayed in dark blue. A potential recharge region for the Toro aquifer exists at Lavani Valley where Toro outcrop is located. Flow path consists of northwest to southeast flow parallel to major folds and thrusts in fold belt through Lavani Valley-Hides-Mananda/South East Mananda-Kutubu Complex. Toro aquifer flow may also occur in a southeast to northwest direction through the South East Hedinia Field. Both Toro aquifer flow paths may exit the fold belt at the southern end of Usano Field. Faulting associated with the Bosavi Lineament cross cutting the fold belt may be the cause of the large hydraulic (Hw) step/baffle observed between South East Mananda and Agogo Fields. En-echelon faults that potentially allow connection between Juha and either Mananda and/or Agogo are shown (base map modified from Berryman and Braisted, 2010).

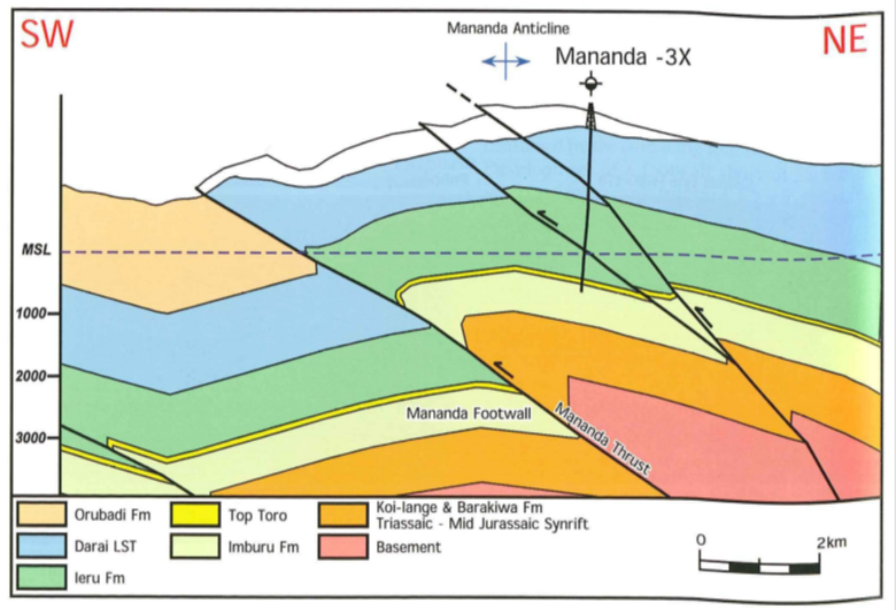

Figure 6.2: Cross section through Mananda Anticline
(Cole et al., 2000)

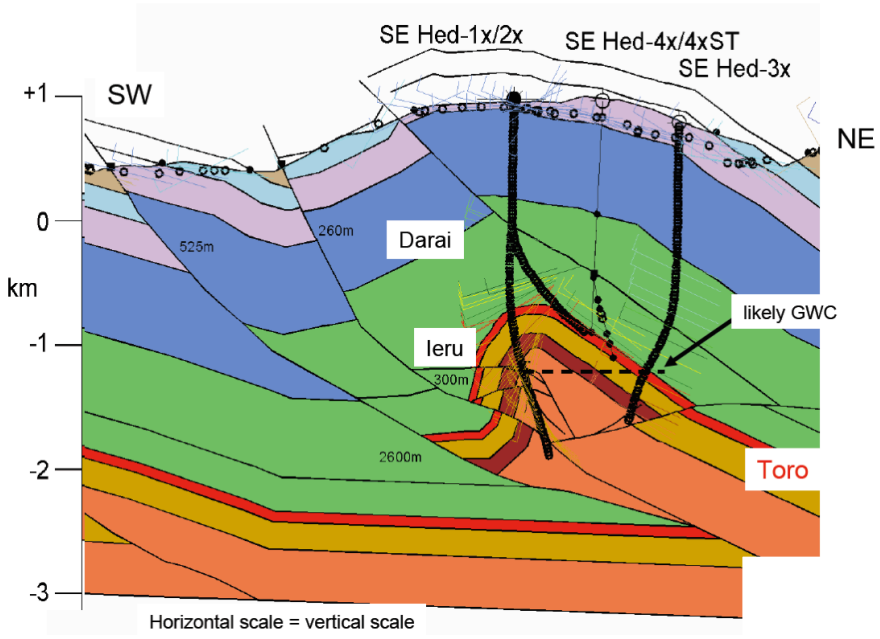

Figure 6.3: Cross section through South East Hedinia Anticline
(Santos, 2008)

In addition to the system described above for the Lavani Valley-Hides-Mananda/SE Mananda-Kutubu Complex (LV-H-M/SEM-KC) there is reasonable evidence for another region of Toro hydrodynamic aquifer, which also appears to exit the fold belt at the southern end of Usano. This system involves southeast to northwest water flow within the South East Hedinia Field (note - opposite direction of water flow to the LV-H-M/SEM-KC system) (Figures 5.4c-d and 6.1). It is unclear what recharge area may be driving this flow as there is no nearby Toro outcrop. Alternatively, South East Hedina may represent a recently opened compartment that is now draining into the foreland.

Within the fold belt, there is little evidence for substantial flow and interconnectivity between aquifer cells perpendicular to the fold belt structural grain (ie in a northeast-southwest direction). The northwest-southeast trending fold belt thrust faults appear to behave predominantly as sealing faults. They are perpendicular to the current stress field operating in region and more likely to be squeezed shut. Cross cutting faults running northeast-southwest through the fold belt, are potentially more likely to be non-sealing as they are parallel to the compressive stress field and are more likely to be forced open. This general trend is seen in other fold and thrust belt regions, for instance, the Rocky Mountains, where thrusts typically act as hydraulic barriers separating the aquifer between thrust sheets (Underschultz et al., 2005). This separation is characterised by large differences in Hw and often water chemistry between the thrust sheets. However, there can be significant vertical hydraulic communication with discharge and recharge of the aquifer seen, particularly at lateral ramps and locations where there are steeply dipping high-angle structures cross cutting the main structural grain. The Bosavi Lineament may represent such a feature in the Papuan Fold Belt, providing a discharge point at South East Mananda from the fold belt, via Libano-1, into the foreland. It may also be a baffle to northwest-southeast water flow into Agogo (see below).

Within the Papuan Fold Belt there is evidence for several isolated, highly pressured, Toro aquifer compartments (eg Kutubu and Paua Anticlines, as well as the Angore and Moran Fields) (see Figures 5.4c-d and 6.1). The presence of these isolated highly pressured compartments is also characteristic of other fold and thrust belt systems (Hennig et al. 2002; Underschulz et al. 2005). These compartments are high-pressure relics of deeper sections of the fold belt uplifted to higher elevations, as compression of the fold belt takes place. Eventually erosion exposes the reservoir, allowing aquifer recharge to occur, which appears to be what has occurred at Lavani Valley and further to the northwest in the case of the Muller Anticline.

The Muller Anticline northwest of Lavani Valley likely serves as another significant recharge area for the regional Toro aquifer system. The Juha Field, located southwest of the main thrust front

on the flank of the fold belt (see Figures 5.4b-c), has a lower pressure regime and Hw compared to the LV-H-M/SEM system. The Pnyang Field, located northwest of Juha and also on the flank southwest of the main thrust front of the fold belt (see Figure 5.4b) has a lower pressure regime and Hw compared to Juha and appears to be another separate system. Both the Juha and Pnyang Fields may be fed from the Muller Anticline, but via separate, more convoluted, Toro aquifer paths than the LV-H-M/SEM system. Alternatively the Juha and Pnyang Fields may be fed from additional Toro outcrop regions further northwest in the fold belt but southwest of the main thrust front of the fold belt in West Papua. A possible Hw baffle point exists northwest of Juha similar to the Hw baffle between South East Mananda and Agogo (Figures 5.4b-c). This baffle northwest of Juha may represent the point at which water flows from the Muller Anticline into the Juha Field dropping the Hw across this barrier from highland values down to the reduced Hw values seen at Juha. But realistically there are just not enough well Hw data values to be able to identify aquifer flow paths with any degree of confidence in these areas.

6.1.2 Foreland

Flow in the Toro reservoir in the foreland is even more difficult to constrain, as there is much less change in Hw and there are fewer Hw data points to model the Toro aquifer behaviour. There appears to be a general flow direction northwest to southeast in the foreland to the sea (Figure 5.4e and see section 5.1.2 for additional interpretation of foreland Toro aquifer behaviour). The Komewu Fault potentially provides a barrier to the foreland flow in the Toro aquifer system. Salinity data (Table A.2) is consistent with the flow direction determined from the Hw data. Lower salinity/fresh formation water samples were found in the fold belt, moderate salinity waters in the flank regions of the fold belt and increasing saline waters further out into the foreland towards the sea. The salinity data suggest that there is not a strong aquifer operating in the foreland as the saline formation waters originally present have not been completely displaced by the fresh meteoric waters likely entering the fold belt in the highlands.

6.2 Regional/Sub-Regional Digimu, Hedinia and Iagifu Aquifers

Like the Toro reservoir, the Hedinia and Iagifu reservoirs show clear foreland and fold belt pressure regime trends (Figures 5.1, 5.5-7). The Digimu reservoir has restricted distribution and is confined to the fold belt and perhaps the flank of the fold belt (see Figure 2.13). Within the fold belt all three reservoirs exhibit central fold belt pressure regime trends as well as highland and hinterland compartmentalisation pressure regime trends.

A significant point of difference for the Digimu reservoir, compared to the Toro reservoir, is its apparent hydrostatic and compartmentalised nature in both the Agogo Field and the

Hedinia/Iagifu Fields (see section 5.3.4 for more detailed interpretation). Conversely, the available Hw data for both the Hedina and Iagifu reservoirs (Figures 5.9 and 5.10) suggest northwest to southeast hydrodynamic flow could be occurring through the Hedinia/Iagifu Fields. An exit point for flow from the fold belt for both reservoirs appears to be present at Usano out into the foreland flank via Iorogabaiu-1X. The Iagifu reservoir also has a significant drop in Hw between the Agogo and Hedinia/Iagifu Fields that was not seen with the Toro (or Digimu) reservoirs. This may represent a barrier caused by fault juxtaposition of Iagifu Sandstone units with shalier intervals of the Imburu Formation, affecting only the Iagifu reservoir aquifer connectivity but not Toro (or Digimu). Finally, Hw data suggests that for the Hedinia reservoir, southeast to northwest water flow is occurring through the South East Hedinia Field. There were insufficient data available to accurately interpret the Hedinia and Iagifu aquifer behaviours in the foreland of the Papuan Basin. However, the limited data suggest similar Hw trends to that seen for the Toro aquifer, with slightly higher Hw values occurring on the flank of the fold belt with decreasing Hw values out into the foreland (see Figures 5.9 and 5.10).

The location(s) of potential recharge areas for the Digimu, Hedinia and Iagifu reservoirs are uncertain. Imburu Formation outcrop is present in the Muller Anticline region. But Digimu and Hedinia Sandstones have limited distributions, which do not extend to the Muller Anticline (see Figures 2.13 and 2.14). Iagifu Sandstone is present in the Muller Anticline region (see Figure 2.15). Imburu Formation extends throughout the fold belt, but this can represent shales and mudstones that make up the bulk of the Imburu Formation. So if there is a lack of outcropping Digimu, Hedinia and Iagifu Sandstones, there is a reduced possibility of meteoric water feeding a hydrodynamic aquifer in each case, unless one or more of the these reservoirs has fault juxta-positioned communication with the Toro reservoir in the fold belt. However, it was beyond the scope of this study to begin to identify these possible fault connections between the Toro and the Digimu, Hedinia and Iagifu reservoirs.

6.3 Sub-Regional/Field Scale Toro Aquifer

6.3.1 Highlands/Hinterland

The very closely aligned water gradients and progressively decreasing Hw values between the Lavani Valley, Egele Anticline, Hides, Angore, and Mananda/South East Mananda Fields (see Figures 5.4b-d and Figure 5.11), suggest the existence of a hydrodynamic Toro aquifer connected in some configuration between these regions. However, the amount of data that is being used to establish this connected hydrodynamic aquifer system is insufficient to unequivocally prove its existence. The observed trend of progressively decreasing values may be occurring just by chance and what actually may be present is just a faulted/compartmentalised set of aquifer cells with

little or no communication. For instance it would seem more likely that Angore Field and Egele Anticline represent separate aquifer cells, as they are in the parallel thrust/fold system directly northeast of the fold belt section containing Lavani Valley, Hides and Mananda/South East Mananda Fields (see Figures 5.4c and 6.1, and Maps A.2 - A.3). The variable Hw values for the Toro and Digimu reservoirs (see Tables A.2 and A.5) and pressure regimes (see Figures 5.1 and 5.5) within the Moran Field in the hinterland suggest a complex compartmentalised system likely operates in this field, independent of the other fields. Separate highly pressured aquifer compartments in the Paua and Kutubu Anticlines suggest they represent closed systems, as it is uncertain where a suitably high Hw recharge area could be operating for these structures. These structures also exist in the parallel thrust/fold system directly northeast of the fold belt section containing the Hides and Mananda Fields (see Figures 5.4c and 6.1, and Maps A.2 - A.3).

6.3.2 Mananda/South East Mananda and Kutubu Complex

Eisenberg (1993) and Eisenberg et al. (1994) provide good evidence for a hydrodynamic Toro aquifer system operating in the Kutubu Complex (Agogo-Hedinia/Iagifu-Usano) Fields. Data generated in this study were also consistent with a hydrodynamic Toro aquifer operating in the Kutubu Complex, with a common gas gradient, common oil gradient, but variable water gradients, along with Hw values consistently decreasing northwest to southeast through this group of fields (Figures 5.13 and 5.14). In this case, there are sufficient data for the decreasing Hw trend through the Kutubu Complex to be treated with more confidence. Connection of this likely hydrodynamic system with the structures to the northwest (Lavani Valley-Hides-Mananda/South East Mananda) has been proposed to occur between the South East Mananda and Agogo Fields. However, a large step in Hw exists between South East Mananda and Agogo. This may represent a long existing barrier in the Toro aquifer system between these two fields, or is possibly the result of recent tectonic activity, which may have reactivated faults and disrupted connectivity of the aquifer between South East Mananda-Agogo (Eisenberg, 1993; Eisenberg et al., 1994; McPhail, 2013).

A major structural feature, the Bosavi Lineament (see Figures 2.1b, 2.7 and 6.1), incorporating basement-involved faulting and affecting Toro reservoir continuity in the Moran Field (see Figures 2.10), cross cuts the fold belt between South East Mananda and Agogo. This feature may be affecting the connectivity between South East Mananda and Agogo by causing a fault generated restriction/barrier to Toro Aquifer flow. Alternatively (or in addition to the faulting), the differential palaeo deposition of Toro and Iagifu Formation sandstones in the region between the South East Mananda and Agogo Fields may have generated a lithological barrier to aquifer flow (Varney and Bradshaw, 1993; Hirst and Price, 1996). Palaeo delta depocentres at either end of the Kutubu Complex (Figure 2.6b) have been postulated to exist (Varney and Bradshaw, 1993;

Hirst and Price, 1996). These potentially could have resulted in shaley intervals being deposited in areas surrounding lobes of the delta, rather than clean wave reworked sands of the shoreline, which may considerably reduce the permeability of the reservoir and reduce aquifer flow.

The connection to South East Mananda, as part of a more regional hydrodynamic system is by no means unequivocal, with no data points across the junction between the two fields to more closely examine the potential linkage (similarly large steps in Hw in other areas of the fold belt have been used to justify compartmentalisation/isolation of aquifer cells). Several plausible alternative scenarios for this connection actually exist, none of which are excluded by the data obtained and are discussed below.

The Toro aquifer, seen to be operating from Agogo through the Hedinia/Iagifu Fields, into Usano, may be being fed from Toro aquifer flow from Juha, southwest of the main thrust front of the fold belt in the flank region. Hw in the Juha Field is closer to that seen in the Kutubu Complex than the highlands Hw operating in the Mananda/South East Mananda Fields. However, there are a lack of wells to test this proposal (Nomad-1 and Cecilia-1 did not intersect Toro) and there is currently no evidence for flow northwest to southeast through the Juha Field to support this pathway (see Map A.2) In addition Juha has poorer porosity and permeability compared to other central fold belt fields, so it is less likely to be an efficient conduit for water flow. However, large-scale en-echelon faults are present between the Juha Field and the Mananda Anticline and Agogo Field, potentially creating flow paths for aquifer connection (Figure 6.1).

Alternatively, the source of regional flow into the Kutubu Complex of fields could be the result of flow from other nearby higher pressured compartments. For example the highly over-pressured Kutubu-1X well suggests pressure is available to drive water flow from this compartment (Kutubu Anticline) into the Kutubu Complex (Eisenberg et al., 1994) (Figure 6.1). However, a connection mechanism must be modelled between the Kutubu Anticline and the Hedina/Iagifu Fields, perpendicular to fold belt.

It is also possible that the Agogo-Hedinia/Iagifu system is just draining without any involvement from other nearby compartmentalised systems, particularly as the Hedinia/Iagifu Toro reservoir is under-pressured and is likely draining via Usano. Eisenberg et al. (1994) comment on the weak nature of the Toro hydrodynamic aquifer and the lack of aquifer support in the Toro reservoir in the Hedinia/Iagifu Fields. An alternative reason for lack of aquifer support is siderite cementation at the OWC documented in several wells, potentially providing a seal between the oil and water legs. The Hedinia/Iagifu Fields also do not respond to water injection, which suggests compartmentalisation is in operation rather than a hydrodynamic aquifer (Williams and

Lund, 2006). However, modelling shows that if there is an open system draining at Usano then, even with continual injection of water into the system, pressure support will not occur (Eisenberg et al., 1994).

Eisenberg et al. (1994) report the biodegradation of the oil from South East Mananda. However, no such biodegradation of oil is seen in Agogo-Hedinia/Iagifu. The biodegradation suggests recent meteoric flow, which has been fed from Lavani Valley down as far as South East Mananda, but has not yet reached Agogo across the proposed Hw baffle. An alternative way to explain the biodegradation differentiation is that the water in the Agogo-Hedinia/Iagifu system is sourced from elsewhere and there is no connection to South East Mananda. The formation water in Agogo-Hedinia/Iagifu is fresh (would expect to be saline as sediments from marine source), but there is aqueous inclusion analysis evidence (Krieger et al., 1996; Lisk et al., 1993) that shows that pre-Pleistocene invasion of the Toro reservoir in the basin with meteoric water occurred before fold belt generation.

So, in conclusion, there are a number of alternatives that could be feeding the Kutubu Complex hydrodynamic aquifer. Perhaps a targeted water chemistry study could help identify the source of the water entering the Kutubu Complex and better constrain the Toro aquifer in this region of the central fold belt (Glynn and Plummer, 2005; Sundaram et al., 2009: Abdou et al., 2011).

6.3.3 Hydrodynamic Trapping

It was beyond the scope of this study, but once detailed potentiometric contours are mapped, regions of potential for hydrodynamic trapping of hydrocarbons can begin to be identified (Dahlberg, 1995; Cockcroft et al. 1987 describe extensive methodology to identify such regions/structures). For instance, if a hydrodynamic aquifer is operating in the Hides Field it will have an effect on the GWC, but the tilt will be much less than if it was an OWC [according to the equation described by Dennis et al. (2000) 4 x less tilt with gas compared to oil]. This could still cause a significant change in distribution and potentially the volume of gas in a large field such as Hides. It has been noted that if there is a strong down-dip flow this will significantly increase sealing/trapping capacity of the reservoir unit, allowing more gas to be trapped than would otherwise be expected (Cockroft et al., 1987). Many examples of this phenomenon have been reported in, for example, the Central and Eastern Alberta gas and oil fields (Cockroft et al., 1987). It is also possible for up-dip flow to increase hydrocarbon trapping, but in this case, it needs to be against a fault or lithological barrier. When the planned wells are drilled in the Hides Anticline, the necessary GWC values will become available to do this analysis. It may also be worth looking at Mananda/South East Mananda and South East Hedinia to see if hydrodynamic trapping is in play in these fields. Another region of interest in the fold belt is intersected by

Arakubi-1, which has a negative Hw value (located slightly east of the Iagifu Field at the southern end of the Kutubu Complex - see Map A.9). This region could represent a stagnation zone (Person et al., 2012; Cockroft et al., 1987). Stagnation zones can occur where there are two opposing flows meeting at a low Hw point. In this case flow from the Kutubu Complex in one direction and flow from South East Hedinia in the other. However, Arakubi-1 is a post-production well, so could just be sampling a depleted reservoir compartment at this location. Although, it is significantly more depleted than any of the other wells in close proximity in the Kutubu Complex, and as such may still represent a good place to look for hydrodynamic trapping of hydrocarbons.

6.4 Conclusions

The main accomplishment of this study has been the assembly/generation of a comprehensive up to date well formation fluid pressure, temperature and salinity data set for the Papuan Basin. This study has further extended the previous regional Toro aquifer studies (Eisenberg, 1993; Eisenberg et al., 1994; Kotaka, 1996) with up to date potentiometric maps for the Toro, Digimu, Hedinia and Iagifu Sandstone reservoirs in the Papuan Basin. However, there is now a need to generate potentiometric surface elevation maps for Toro, Digimu, Hedinia and Iagifu in combination with superimposed top Toro, Digimu, Hedinia and Iagifu formation maps respectively, to enable determination of potential hydrodynamic trapping locations in the fold belt and foreland regions of the basin for each of these reservoir units.

This study has clearly identified limitations to the discrimination of hydrodynamic versus compartmentalised aquifer systems in the fold belt and foreland regions. The principal limitations being, insufficient well data (outside of the Kutubu Complex) and relatively poor delineation of faults and stratigraphic barriers to aquifer flow. However, it is envisaged that formation water chemistry analyses could be used to determine connectivity of reservoirs in the fold belt in order to help identify hydrodynamic versus compartmentalised systems and better characterize aquifer behavior in the Toro, Digimu, Hedinia and Iagifu Sandstone reservoirs.

References

Abdou, M., Carnegie, A., Mathews, S.G., McCarthy, K., O'Keefe, M., Raghuraman, B., Wei, W. and Xian, C. 2011. Finding Value in Formation Water. Schlumberger Oilfield Review. 23(1), 24-35.

Ahmed, M., Volk, H., Allan, T. and Holland, D. 2012. Origin of oils in the Eastern Papuan Basin. Papua New Guinea. Organic Geochemistry. 53, 137-152.

Berryman, A.J. and Braisted, D.M. 2010. Development of the Gas Rsource Assessment for the Papua New Guinea PNG LNG Project. Society of Petroleum Engineers, SPE Asia Pacific Oil & Gas Conference, Brisbane, Australia. SPE135816.

Bradey, K., Hill, K., Lund, D., Williams, N., Kivior, T. and Wilson, N. 2008. Kutubu oil field, Papua New Guinea - a 350 MMbbl fold belt classic. PESA Eastern Australasian Basins Symposium III. 239-245.

Bradshaw, M. 1993. Australian Petroleum Systems. PESA Journal. July, 43-53.

Buchanan, P.G. and Warburton, J. 1996. The Influence of Pre-existing Basin Architecture in the Development of the Papuan Fold and Thrust Belt: Implications for Petroleum Prospectivity. Petroleum Exploration and Development in Papua New Guinea, Proceedings of the Third PNG Petroleum Convention, Port Moresby. 89-109.

Buick, G., McPhail, A., Ryan, L., Bainbrigge, P., Burgoyne, M., Lammerink, W., Little, A. and Theophilos, A. 2009. Santos PNG LNG Project Pre-Initial Determination Technical Report (unpublished).

Chevron 2000. Water analysis report (unpublished).

Cockroft, P.J, Edwards, G.A., Phoa, R.S.K. and Reid, H.W. 1987. Applications of Pressure Analysis and Hydrodynamics to Petroleum Exploration in Indonesia. Proceedings Indonesian petroleum Association 16th Annual Convention. IPA87-22/07.

Cole, J.P., Parish, M. and Schmidt, D. 2000. Sub-Thrust Plays in the Papuan Fold Belt: The Next Generation of Exploration Targets. Petroleum Exploration and Development in Papua New Guinea, Proceedings of the Fourth PNG Petroleum Convention, Port Moresby. 87-99.

Craig, M.S and Warvakai, K. 2009. Structure of an active foreland fold and thrust belt, Papua New Guinea. Australian Journal of Earth Sciences. 56, 719–738.

D'Addario, G. W., Dow, D.D. and Swoboda, R. (compilers) 1976, Geology of PNG, 1:250000 scale map. Bureau of Mineral Resources, Canberra. [PNG Geology Map - Geology of Papua New Guinea, 1972, Bureau of Mineral Resources, Geology and Geophysics, Department of National Development].

Dahlberg, E.C. 1995. Applied hydrodynamics in petroleum exploration. New York: Springer-Verlag. 295p.

Daniels, M.C. 1993. Formation Presure Measurements and their use in Oil Exploration in the Kutubu project, papua New Guinea. Petroleum Exploration and Development in Papua New Guinea, Proceedings of the Second PNG Petroleum Convention, Port Moresby. 579-588.

Dennis, H., Baillie, J., Holt, T. and Wessel-Berg, D. 2000. Hydrodynamic activity and tilted oil water contacts in the North Sea: Improving the Exploration Process by Learning from the Past. Norwegian Petroleum Society Special Publication 9, 171-185, Amsterdam: Elsevier Science.

Eisenberg, L.I. 1993. Hydrodynamic Character of the Toro Sandstone, lagifu-Hedinia Area, Southern Highlands, Papua New Guinea. Petroleum Exploration and Development in Papua New Guinea, Proceedings of the Second PNG Petroleum Convention, Port Moresby. 447-458.

Eisenberg, L.I., Langston, M.V. and Fitzmorris R.E.1994. Reservoir Management in a Hydrodynamic Environment, lagifu-Hedinia Area, Southern Highlands, Papua New Guinea. Society of Petroleum Engineers, SPE Asia Pacific Oil & Gas Conference, Melbourne, Australia. SPE28750.

Glynn, P.D. and Plummer, L.N. 2005. Geochemistry and the understanding of ground-water systems. Hydrogeology Journal. 13, 263-287.

Goffey, G.P., Craig, J., Needham, T. and Scott, R. 2010. Fold and thrust belts: overlooked provinces or justifiably avoided? Geological Society, London, Special Publications, 348, 1-6.

Grainge, A. 1993. Recent developments in prospect mapping in the hides/Karius area of the Papuan Fold Belt. Petroleum Exploration and Development in Papua New Guinea, Proceedings of the Second PNG Petroleum Convention, Port Moresby. 527-537.

Hennig, A., Yassir, N., Addis, M.A. and Warrington, A. 2002. Pore-Pressure Estimation in an Active Thrust Region and Its Impact on Exploration and Drilling. In Huffman, A.R. and Bowers, G.L eds., Pressure regimes in sedimentary basins and their prediction. The American Association of Petroleum Geologists (AAPG) Memoir. 76, 89-105.

Hill, K. C. 1991. Structure of the Papuan Fold Belt, Papua New Guinea. The American Association of Petroleum Geologists (AAPG) Bulletin. 75, 857-872.

Hill, K.C, Forewood, J., Rodda, C., Smyth, C. and Whitmore, G. 1993. Structural Styles and Hydrocarbon prospectivity around the Northern Muller Anticline, PNG. Petroleum Exploration and Development in Papua New Guinea, Proceedings of the Second PNG Petroleum Convention, Port Moresby. 325-334.

Hill, K.C., Norvick, M.S., Keetly, J.T. and Adams, A. 2000. Structural and Stratigraphic Shelf-Edge Hydrocarbon Plays in the Papuan Fold Belt. Petroleum Exploration and Development in Papua New Guinea, Proceedings of the Fourth PNG Petroleum Convention, Port Moresby. 67-84.

Hill, K. C., Keetley, J.T., Kendrick, R.D. and Sutriyono, E. 2004. Structure and hydrocarbon potential of the New Guinea Fold Belt, in McClay, K.R. ed., Thrust tectonics and hydrocarbon systems: AAPG Memoir 82, 494–514.

Hill, K.C., Bradey, K., Iwanec, J., Wilson, N. and Lucas, K. 2008. Structural Exploration in the Papua New Guinea Fold Belt. PESA Third Eastern Australasian Basins Symposium, Sydney. 225-238.

Hirst, J.P. and Price, C.A. 1996. Sequence stratigraphy and sandstone geometry of the Toro and Imburu formations, within the Papuan fold belt and foreland. Petroleum Exploration and Development in Papua New Guinea, Proceedings of the Third PNG Petroleum Convention, Port Moresby. 279-299.

Home, P.C, Dalton, D.G. and Brannan, J. 1990. Geological Evolution of the Western Papuan Basin. Petroleum Exploration and Development in Papua New Guinea, Proceedings of the First PNG Petroleum Convention, Port Moresby. 107-117.

Hulse, J.C. and Harris, G.I. 2000. The Darai Plateau Play: Foreland Basin Potential. Petroleum Exploration and Development in Papua New Guinea, Proceedings of the Fourth PNG Petroleum Convention, Port Moresby. 169-185.

Johnstone, D.C. and Emmett, J.K. 2000. Petroleum Geology of the Hides Gas Field, Southern Highlands, Papua New Guinea. Petroleum Exploration and Development in Papua New Guinea, Proceedings of the Fourth PNG Petroleum Convention, Port Moresby. 319-335.

Kotaka, T. 1996. Formation water systems in the Papuan Basin, Papua New Guinea. Petroleum Exploration and Development in Papua New Guinea, Proceedings of the Third PNG Petroleum Convention, Port Moresby. 391-405.

Krieger, F.W., Eadington, P.J. and Eisenberg, L.I. 1996. Rw, reserves and timing of oil charge in the Papuan Fold Belt. Petroleum Exploration and Development in Papua New Guinea, Proceedings of the Third PNG Petroleum Convention, Port Moresby. 407-416.

Kveton, K., Garcia, H., Lee, D. and Quam, S. 1998. Iterative structural modelling and 2D seismic imaging in the Papua New Guinea Highlands. SEG Expanded abstract.

Langston, S. 2013. Personal communication. Santos.

Lisk, M., Hamilton, J., Eadington, P. and Kotaka, T. 1993. Hydrocarbon and pore water migration history in relation to diagenesis in the Toro and Iaifu sandstones, SE Gobe-2. Petroleum Exploration and Development in Papua New Guinea, Proceedings of the Second PNG Petroleum Convention, Port Moresby. 477-488.

Madu, S. 1996. Correlation sections of the late Jurassic to early Cretaceous succession in the Papuan Fold Belt, Papuan Basin: sequence stratigraphic framework concepts and implications for exploration and exploitation. Petroleum Exploration and Development in Papua New Guinea, Proceedings of the Third PNG Petroleum Convention, Port Moresby. 259-277.

McCain, W. D. 1990. The Properties of Petroleum Fluids, second edition - PennWell Publishing Company, Tulsa, Oklamhoma.

McConachie, B., Lanzilli, E., Kendrick, D. and Burge, C. 2000. Extensions of the Papuan Basin Foreland Geology into Eastern Irian Jaya (West Papua) and the New Guiea Fold Belt in Papua New Guinea. Petroleum Exploration and Development in Papua New Guinea, Proceedings of the Fourth PNG Petroleum Convention, Port Moresby. 219-237.

McPhail, A. 2013. Personal communication. Santos.

Muggeridge, A. and Mahmode, H. 2012. Hydrodynamic aquifer or reservoir compartmentalization? The American Association of Petroleum Geologists (AAPG) Bulletin 96, 315-336.

Oil Search 2003. Water analysis report (unpublished).

Person, M., Butler, D., Gable, C.W., Villamil, T. Wavrek, D. and Schelling, D. 2012.Hydrodynamic stagnation zones: A new play concept for the Llanos Basin, Colombia. The American Association of Petroleum Geologists (AAPG) Bulletin 96, 23-41.

PNG CMP 2012. PNG Chamber of Mines ands Petroleum Report: Petroleum in PNG. http://pngchamberminpet.com.pg/petroleum-in-png/

Powley, D.E. 1990. Pressures and Hydrogeology in Petroleum Basins. Earth Science Reviews. 29, 215-226.

Santos 2008. PNG Group Santos. PNG Regional Overview (unpublished).

Santos 2013. PNG Group Santos. Papuan Basin Overview (unpublished).

Starcher, M. 2013. Personal communication. Santos.

Struckmeyer, H.I.M., Yeung, M. and Bradshaw, M.T. 1990. Mesozoic Palaeogeography of the northern margin of the Australian plate and its implications for hydrocarbon exploration. Petroleum Exploration and Development in Papua New Guinea, Proceedings of the First PNG Petroleum Convention, Port Moresby. 137-152.

Sundaram, B., Feitz, A.J., de Caritat, P., Plazinska, A., Brodie, R.S., Coram, J. and Tim Ransley, T. 2009. Groundwater Sampling and Analysis - A Field Guide. Geoscience Australia. Record 2009/27 68901.

Underschultz, J. R., C. J. Otto, and R. Bartlett, 2005, Formation fluids in faulted aquifers: Examples from the foothills of Western Canada and the North West Shelf of Australia, in P. Boult and J. Kaldi, eds., Evaluating fault and cap rock seals: AAPG Hedberg Series, no. 2, 247–260.

Van Ufford, A.Q and Cloos, M. 2005. Cenozoic Tectonics of New Guinea. The American Association of Petroleum Geologists (AAPG) Bulletin, 89, 119–140.

Varney, T.D and Brayshaw, A.C. 1993. A Revised Sequence Stratigraphic and Depositional Model for the Toro and Imburu Formations, with implications for Reservoir Distribution and Prediction. Petroleum Exploration and Development in Papua New Guinea, Proceedings of the Second PNG Petroleum Convention, Port Moresby. 139-154.

Williams, N. and Lund, D. 2006. Kutubu: A Rethink. Society of Petroleum Engineers, SPE Asia Pacific Oil & Gas Conference and Exhibition held in Adelaide, Australia. SPE101123.

Appendix

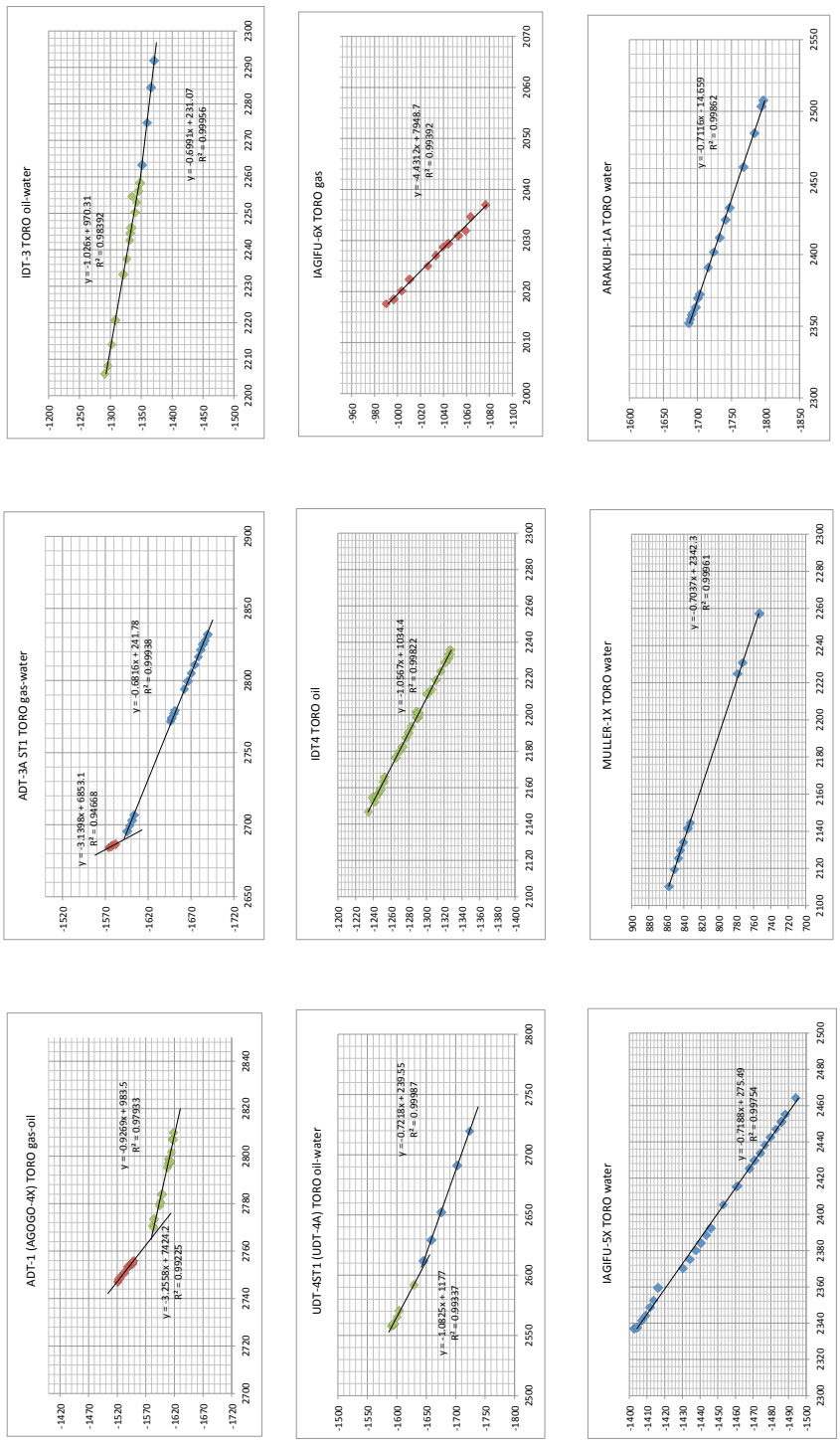

Figure A.1: Examples of P-D Plots Used to Generate Toro Fluid Pressure Gradients
P-D plot [x-axis: Pressure (psia) vs y-axis: Depth (total vertical depth meters sub sea (TVDmSS)].
Data used for the calculations/plotting are part of the regional data set assembled for this study - data not shown. Pressure gradients were calculated by regression analysis of the data sets on the plots and used to identify the fluids present in the reservoir formations being tested. Intersection points between fluid gradients represent fluid contact points.

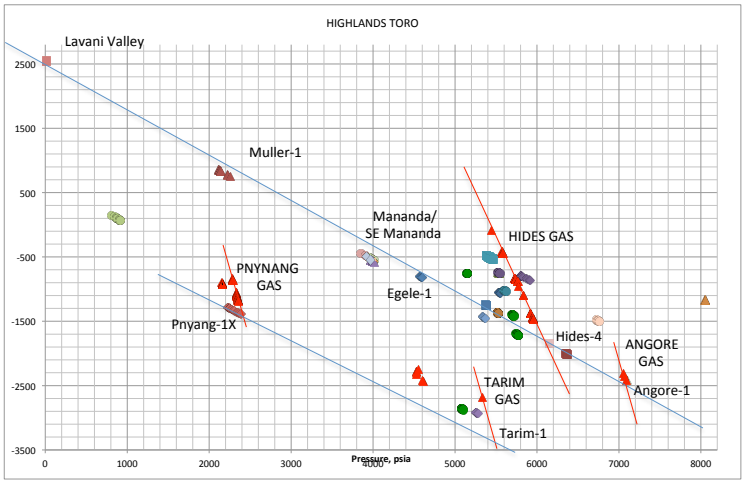

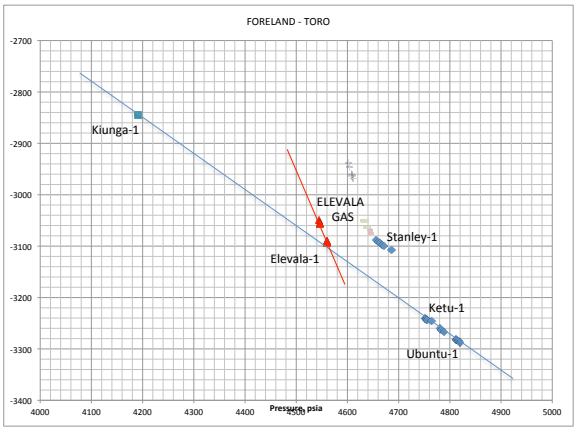

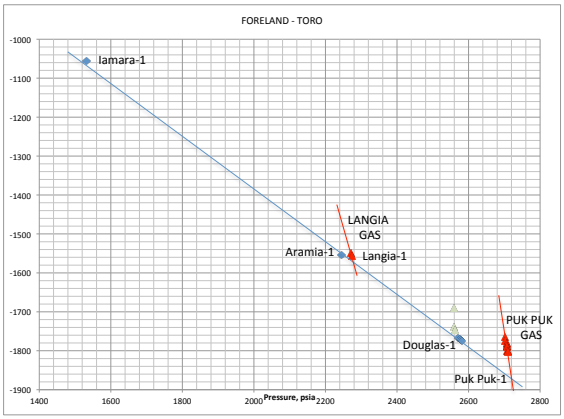

Figure A.2: Extrapolated Gas Water Contacts (EGWCs) for Selected Toro Wells

EGWCs for Hides-4, Angore-1, Tarim-1, Pnyang-1X, Elevala-1, Puk Puk-1 and Langia-1 were calculated by determining intersection point between calculated gas pressure gradient for the well and nearby calculated water pressure gradient. P-D plot [x-axis: Pressure (psia) vs y-axis: Depth (total vertical depth meters sub sea (TVDmSS)]. Data used for the calculations/plotting are part of the regional data set assembled for this study - data not shown.

Tables A.1 - A.13: Papuan Basin Well Data Sets

Table A.1 - Total Papuan Basin wells examined in this study
Wells arranged in alphabetical order within fold belt and foreland sections. Listing of wells then within fields, followed by those wells not assigned to a field. Fluid(s) present in each reservoir interval are listed under Toro, Digimu, Hedinia and Iagifu reservoir headings (G = gas, O = oil and W = water). Those wells excluded from the study and the reason why are also listed. (1) No well completion report (WCR) available. (2) No/poor pressure test. (3) Outside palaeo-deposition distribution for Toro. (4) Toro expected - but not intersected.

Tables A.2 - A.13: Contain well pressure and hydraulic potential (Hw) data for the Toro, Digimu, Hedinia and Iagifu reservoirs.

Table A.2 - Toro Wells (Water)
Lists Toro wells that have water pressure data. Wells arranged in alphabetical order within fold belt and foreland sections. Listing of wells then within fields, followed by those wells not assigned to a field. Pressure (psia) and depth (TVDmSS) values are listed. Hw data calculated by 3 methods: Method 1 - Hw (0.435), Method 2 - Hw (calc) and Method 3 - Hw (ST). See section 4.3 for detailed description of Hw calculation methods. Pressure gradients calculated for methods 2 and 3 are listed in the column preceding the relevant Hw column. Hydrocarbon-water contacts (HC-WCs) are identified. Pre- and post-production wells are identified. Salinity and temperature data are listed where obtained/calculated.

Table A.3 – Toro Wells (Gas)
Lists Toro wells that have gas pressure data. Similar arrangement, column headers and data listed as for Table A.2. Additional information though has been included; Extrapolated gas water contact (EGWC) values for several wells have been calculated (see Figure A.2) and these are listed along with the derived Hw (0.435) values. Lowest known gas (LKG) points identified.

Table A.4 - Toro Wells (Oil)
Lists Toro wells that have oil pressure data. Similar arrangement, column headers and data listed as for Table A.2

Table A.5 - Digimu Wells (Water)

Table A.6 - Digimu Wells (Gas)

Table A.7 - Digimu Wells (Oil)

Table A.8 - Hedinia Wells (Water)

Table A.9 - Hedinia Wells (Gas)

Table A.10 - Hedinia Wells (Oil)

Table A.11 - Iagifu Wells (Water)

Table A.12 - Iagifu Wells (Gas)

Table A.13 - Iagifu Wells (Oil)

Table A.1 Total Papuan Basin Wells

Foldbelt

WELL	FIELD	EASTING	NORTHING	Excluded	Toro	Digimu	Hedinia	Iagifu	>1994
ADD-1	AGOGO	731736	9298901	2					
ADD-1ST1	AGOGO	731736	9298901		G	O			
ADD-2	AGOGO	732460	9297776		G	O	O	W	
ADD-3	AGOGO	734125	9298071		G	O			
ADD-4	AGOGO	734768	9296799		G	O			
ADD-5	AGOGO	734860	9296946	1					*
ADT-1	AGOGO	733290	9299460		G O				
ADT-2	AGOGO	732730	9299461				O		
ADT-3	AGOGO	736576	9296369	2					*
ADT-3A ST1	AGOGO	736576	9296369		G W				*
ADT-3BST2	AGOGO	736576	9296369	2					*
AGD-1	AGOGO	732466	9297770		G	G O			
AGOGO-1X	AGOGO	732460	9297776		G	G	O	O	
AGOGO-2X	AGOGO	734769	9296800		G	O			
AGOGO-2XST1	AGOGO	734769	9296800		G	W			
AGOGO-3X	AGOGO	736030	9295544		G	W	O	W	
AGOGO-5X	AGOGO	732730	9299461		W				
AHT-1	AGOGO	733124	9298947	2					
AH1-ST3	AGOGO	733124	9298947	2					
AHT-2	AGOGO	734299	9298202	2					
AH2-ST1	AGOGO	734299	9298202	2					
ANGORE-1A	ANGORE	706958	9338814		G				
ANGORE-1AX	ANGORE	708587	9339152	1					
ANGORE1-AXST	ANGORE	708587	9339152	1					
ANGORE-1X	ANGORE	708584	9339164	4					
ANGORE-1XST	ANGORE	708584	9339164	4					
ANGORE-A1	ANGORE	706958	9338814	1					
ANGORE-B1	ANGORE	708878	9337269	1					
GOBE GAP-1	GOBE	797013	9253444	2					
GOBE GAP-2	GOBE	797104	9253806	2					
GOBE MAIN-1	GOBE	800324	9251881	2					*
GOBE MAIN-1ST1	GOBE	800324	9251881	2					*
GOBE MAIN 1ST2	GOBE	800324	9251881	2					*
GOBE MAIN 2	GOBE	800324	9251904	2					*
GOBE MAIN 2ST1	GOBE	800324	9251904	2					*
GOBE MAIN 3	GOBE	798060	9252995	2					*
GOBE MAIN 3ST1	GOBE	798060	9252995	2					*
GOBE MAIN 4	GOBE	798081	9252997	2					*
GOBE MAIN 4ST1	GOBE	798081	9252997	2					*
GOBE MAIN 4ST2	GOBE	798081	9252997	2					*
GOBE MAIN 4ST3	GOBE	798081	9252997	2					*
GOBE MAIN 5	GOBE	800706	9250858	2					*
GOBE_MAIN-5ST1	GOBE	800706	9250858					G O W	*
GOBE MAIN 5ST2	GOBE	800706	9250858	2					*
GOBE MAIN 5ST3	GOBE	800706	9250858	2					*
GOBE_MAIN-7	GOBE	800706	9250858					G O W	*
GOBE-1X	GOBE	797199	9253732		W				
GOBE-1XST1	GOBE	797200	9253731	2					
GOBE-2X	GOBE	807157	9246413		W				
GOBE-2XST	GOBE	807157	9246413		W			G O W	

WELL	FIELD	EASTING	NORTHING	Excluded	Toro	Digimu	Hedinia	Iagifu	>1994
GOBE-3X	GOBE	814359	9242603		W			O W	
GOBE-4X	GOBE	798027	9252045		W		W	G	
GOBE-4XST1	GOBE	798027	9252045					G O W	
GOBE-5AX	GOBE	794829	9253507	4					*
GOBE-5AXST1	GOBE	794829	9253507	1					*
GOBE-5X	GOBE	794829	9253507	4					*
GOBE-5XST1	GOBE	794829	9253507		W			W	*
GOBE-6X	GOBE	801799	9250363		W			O	*
GOBE-6XST1	GOBE	801799	9250363	2					*
GOBE-6XST2	GOBE	801799	9250363	2					*
GOBE-7X	GOBE	810826	9244502					O	*
GOBE-7XST1	GOBE	810826	9244502					O W	*
GOBE-7XST2	GOBE	810826	9244502	2					*
GOBE-7XST3	GOBE	810826	9244502	2					*
GOBE-8X	GOBE	801805	9250362	2					*
GOBE-8XST1	GOBE	801805	9250362					W	*
GOBE-8XST2	GOBE	801805	9250362	2					*
GOBE-8XST3	GOBE	801805	9250362		W			W	*
NW GOBE-1X	GOBE	790504	9256629		W				*
HEDINIA-1X	HEDINIA	743822	9285209		G	G		W	
HEDINIA-1XST	HEDINIA	743822	9285209		O	W			
HEDINIA-2X	HEDINIA	743719	9285271		G				
HEDINIA-2XST	HEDINIA	748557	9283444		W				
HEDINIA-2XST3	HEDINIA	747408	9285255	1					
HEDINIA-3X	HEDINIA	741826	9287764		G	O			
HEDINIA-3XST	HEDINIA	741826	9287764		G W	W			
HEDINIA-4X	HEDINIA	740526	9285753	4					
HEDINIA-7X	HEDINIA	739460	9288994		W	W			
IDD-1 (HEDINIA-6X)	HEDINIA	739617	9288998		G	O	W		
IDD-2	HEDINIA	744261	9285588			O			
IDD-3	HEDINIA	743553	9287131		G	O			
IDD-4	HEDINIA	741391	9288054	2					
IDD-5	HEDINIA	741401	9288055	1					*
IDT-1 (HEDINIA-9X)	HEDINIA	746952	9284245		O W				
IDT-18 (IWT 2)	HEDINIA	746938	9284214		O W				*
IST-3A	HEDINIA	744259	9285593	2					
IST-3AST1	HEDINIA	854956	9285004	2					*
IST4 (HEDINIA-5X)	HEDINIA	745907	9284459		G O	W	W		
UDT-1 (HEDINIA-8X)	HEDINIA	745958	9284246		O				
HIDES B1	HIDES	696974	9338321	2					*
HIDES B2	HIDES	696969	9338309	2					*
HIDES C1	HIDES	694434	9339985	2					*
HIDES C2	HIDES	694438	9339992	2					*
HIDES-D1	HIDES	693128	9342030	1					*
HIDES-D2	HIDES	693128	9342030	1					*
HIDES-G1	HIDES	686462	9346603	1					*
HIDES-G2	HIDES	686461	9346603	1					*
HIDES-PWD1	HIDES	700400	9336660	1					*
HIDES-1	HIDES	689727	9344121		G				
HIDES-2	HIDES	691636	9342137		G				

Table A.1 Total Papuan Basin Wells

Foldbelt

WELL	FIELD	EASTING	NORTHING	Excluded	Toro	Digimu	Hedinia	Iagifu	>1994
HIDES-3D (ST)	HIDES	693128	9342030	1					
HIDES-3	HIDES	693128	9342030		G				
HIDES-4	HIDES	699120	9335604		G				*
IAGIFU-1X	IAGIFU	744874	9288172	4					
IAGIFU-4X	IAGIFU	740946	9290162		W			W	
IAGIFU-5X	IAGIFU	746360	9287414		W	W			
IAGIFU-6X	IAGIFU	743598	9289936		G	G		G	
IAGIFU-6XST	IAGIFU	743598	9289936		W				
IAGIFU-6XST2	IAGIFU	743598	9289936	2					
IAGIFU-6XST3	IAGIFU	743598	9289936	2					
IAGIFU-7X	IAGIFU	744442	9287314		O W	W		W	
IAGIFU-7XST2	IAGIFU	744442	9287314		O				
IDT-10 (IAGIFU-8X)	IAGIFU	740781	9291938		W	W			
IDT-11	IAGIFU	742449	9291311		O				
IDT-12	IAGIFU	746475	9285101		O				
IDT-13	IAGIFU	744930	9286186		O				*
IDT-14	IAGIFU	745078	9287494		O W				*
IDT-15	IAGIFU	745318	9286986		W				*
IDT-16	IAGIFU	744938	9286201		W				*
IDT-17	IAGIFU	745311	9286974		O				*
IDT-19	IAGIFU	745259	9285962	2					*
IDT-19ST1	IAGIFU	745259	9285962		O W				*
IDT-2	IAGIFU	745267	9285989	2					
IDT-2ST2	IAGIFU	742334	9291364	1					*
IDT-20	IAGIFU	745470	9286983	2					*
IDT-21	IAGIFU	746330	9287470	2					*
IDT-22	IAGIFU	743080	9287050		G O				*
IDT-23	IAGIFU	743080	9287037		G				*
IDT-23ST1	IAGIFU	743080	9287037	2					*
IDT-23ST2	IAGIFU	743080	9287037	2					*
IDT-24	IAGIFU	745636	9286224	1					*
IDT-3	IAGIFU	745267	9285989		O W				
IDT-4 (IAGIFU-9X)	IAGIFU	744436	9287317		O				
IDT-5 (IAGIFU-7XST)	IAGIFU	744442	9287314		O				
IDT-6	IAGIFU	745598	9288113	2					
IDT-7	IAGIFU	745603	9288113	2					
IDT-7ST1	IAGIFU	745603	9288113	2					*
IDT-8	IAGIFU	745071	9289368		O				
IDT-8ST1	IAGIFU	745071	9289368	2					*
IDT-9 (IAGIFU-3X)	IAGIFU	742333	9291364		O W	W			
IDT-9 ST1	IAGIFU	742334	9291364		W				*
IDT-9 ST2	IAGIFU	742333	9291364		W				*
IHT-1	IAGIFU	746326	9287473	4					*
IHT-1A	IAGIFU	746326	9287473	2					*
IHT-2	IAGIFU	745604	9289290	2					*
IHT-3	IAGIFU	745560	9289261	2					*
IHT-4	IAGIFU	746715	9285245	2					*
IHT-5	IAGIFU	745498	9286045	2					*
IST-1	IAGIFU	744620	9288211		G O				
IST-2 (IAGIFU-2X)	IAGIFU	744617	9288211		O	W			

WELL	FIELD	EASTING	NORTHING	Excluded	Toro	Digimu	Hedinia	Iagifu	>1994
IWT-1 (IAGIFU-5XST1)	IAGIFU	746360	9287414		W				
JUHA-1X	JUHA	658948	9347274		G				
JUHA-2X	JUHA	652565	9353065		G				
JUHA-3X	JUHA	649558	9355863	2					
JUHA-3XST1	JUHA	649558	9355863		G				
JUHA-4X	JUHA	656897	9354626	2					*
JUHA-4XST1	JUHA	656897	9354626	2					*
JUHA-5X	JUHA	648929	9353150		W				*
MANANDA-1X	MANANDA	701995	9317698	1					
MANANDA-2X	MANANDA	708048	9315246	1					
MANANDA-3X	MANANDA	707953	9315242		W				
MANANDA-4X	MANANDA	717707	9308533		W	W			
MANANDA-5X	MANANDA	708498	9313633	1					*
MANANDA-6X	MANANDA	712865	9310833	1					*
MORAN-10	MORAN	735358	9309484	2					*
MORAN-10ST1	MORAN	735358	9309484	2					*
MORAN-11	MORAN	736488	9307948	1					*
MORAN-11ST1	MORAN	736488	9307948	1					*
MORAN-12	MORAN	731645	9311414	4					*
MORAN-12A	MORAN	731656	9311406	2					*
MORAN-13	MORAN	731667	9311398		O	O			*
MORAN-14A	MORAN	731721	9311867	1					*
MORAN-1X	MORAN	736469	9307951	4					*
MORAN-1X ST1	MORAN	736469	9307951		W	G O		W	*
MORAN-1X ST2	MORAN	736469	9307951			O			*
MORAN-1X ST3	MORAN	736469	9307951	2					*
MORAN-1X ST4	MORAN	736469	9307951	2					*
MORAN-2X	MORAN	736473	9307955	2					*
MORAN-2X ST1	MORAN	736473	9307955		W	W			*
MORAN-2X ST2	MORAN	736473	9307955		O	O			*
MORAN-3X	MORAN	740334	9304267	2					*
MORAN-3X ST1	MORAN	740334	9304267		W	W			*
MORAN-3X ST2	MORAN	740334	9304267		W	W			*
MORAN-4X	MORAN	733136	9309953		O	O			*
MORAN-5X	MORAN	738127	9306696		W	W			*
MORAN-5X ST1	MORAN	738127	9306696	2					*
MORAN-5X ST2	MORAN	738127	9306696	2					*
MORAN-6X ST1	MORAN	733731	9309963	2					*
MORAN-6X ST2	MORAN	733731	9309963		O	O			*
MORAN-7X	MORAN	738130	9306715						*
MORAN-7XST1	MORAN	738130	9306715		W	O			*
MORAN-8X	MORAN	735304	9309403		W				*
MORAN-9	MORAN	733664	9309950	2					*
MORAN-9ST1	MORAN	733664	9309950	2					*
MORAN-9ST2	MORAN	733664	9309950	2					*
MORAN-9ST3	MORAN	733664	9309950	2					*
MORAN-9ST4	MORAN	733664	9309950	2					*
NW MORAN-1X	MORAN	730212	9312196	1					*
NW MORAN-1X ST1	MORAN	730212	9312196	1					*
NW MORAN-1X ST2	MORAN	730212	9312196	1					*

Table A.1 Total Papuan Basin Wells
Foldbelt

WELL	FIELD	EASTING	NORTHING	Excluded	Toro	Digimu	Hedinia	Iagifu	>1994
NW MORAN-1X ST3	MORAN	730212	9312196	1					*
NW MORAN-1X ST4	MORAN	730212	9312196	1					*
NW MORAN-1X ST5	MORAN	730212	9312196	1					*
SE MORAN-1X	MORAN	741772	9302993	1					*
PNYANG-1X	PNYANG	566622	9390050		G				
PNYANG-2X	PNYANG	563045	9389201		G				
PNYANG-2XST1	PNYANG	563045	9389201	1					
PNYANG-2XST2	PNYANG	563045	9389201	1					
PNYANG-2X-ST3	PNYANG	563045	9389201		G				
PNYANG_SOUTH-1X	PNYANG	564216	9386363		G				*
PNYANG_SOUTH-1XST1	PNYANG	564216	9386363		W				*
SE GOBE-1X	SE GOBE	811635	9243159		W			O	
SE GOBE-1ST1	SE GOBE	811635	9243159	1					*
SE GOBE-10	SE GOBE	812842	9242628	1					*
SE GOBE-10 ST1	SE GOBE	812806	9242683	1					*
SE GOBE-11	SE GOBE	816114	9241003	1					*
SE GOBE-12	SE GOBE	814419	9241797	1					*
SE GOBE-13	SE GOBE	814408	9241805	1					*
SE GOBE-13 ST1	SE GOBE	814408	9241805	1					*
SE GOBE-14	SE GOBE	816135	9240983	1					*
SE GOBE-1C	SE GOBE	811757	9243321	1					
SE GOBE-2X	SE GOBE	812832	9242648		W			O	
SE GOBE-2C	SE GOBE	812957	9242808	1					
SE GOBE-3X	SE GOBE	810744	9243374		W			O	
SE GOBE-3C	SE GOBE	810820	9243582	1					
SE GOBE-4	SE GOBE	810828	9244477	1					*
SE GOBE-5	SE GOBE	814330	9242615	1					*
SE GOBE-5 ST1	SE GOBE	814330	9242615	1					*
SE GOBE-6	SE GOBE	814339	9242582	1					*
SE GOBE-6 ST1	SE GOBE	814339	9242582	1					*
SE GOBE-7	SE GOBE	811659	9243137	1					*
SE GOBE-8	SE GOBE	811616	9243128	1					*
SE GOBE-9	SE GOBE	811584	9243144	1					*
SE GOBE-9 ST1	SE GOBE	811584	9243144	1					*
SE HEDINIA-1X	SE HEDINIA	763974	9271500		G		O W		
SE HEDINIA-1XST1	SE HEDINIA	763974	9271500	2					
SE HEDINIA-2X	SE HEDINIA	763974	9271500	2					
SE HEDINIA-3X	SE HEDINIA	765855	9271807		W		W		
SE HEDINIA-4X	SE HEDINIA	765037	9271650		W				
SE HEDINIA-4ST1	SE HEDINIA	765037	9271650	2					
SE MANANDA-1X	SE MANANDA	725903	9306278		O W	W			
SE MANANDA-2X	SE MANANDA	723110	9306982		O W				*
SE MANADA-3X	SE MANANDA	724775	9306949	1					*
SE MANADA-4X	SE MANANDA	717707	9308534	1					*
UDT-10	USANO	749631	9284158	1					*
UDT-11	USANO	749643	9284156	1					*
UDT-12	USANO	747056	9284355	1					*
UDT-2	USANO	747947	9284192		O				
UDT-3	USANO	748675	9283871	1					*
UDT-3A	USANO	748677	9283825	1					*

WELL	FIELD	EASTING	NORTHING	Excluded	Toro	Digimu	Hedinia	Iagifu	>1994
UDT-3AST1	USANO	748677	9283825	1					*
UDT-4	USANO	755775	9280554	4					
UDT-4 ST1 (UDT-4A)	USANO	755775	9280554		O W				
UDT-6 (USANO-IX/ST)	USANO	752121	9282306		W				
UDT-7	USANO	750316	9282810	2					*
UDT-7ST1	USANO	750316	9282810		O				*
UDT-8	USANO	748050	9284347	1					*
UDT-9	USANO	748057	9284337	1					*
UGT-2	USANO	752116	9282301	1					*
UGT-2A	USANO	752116	9282301	1					*
UHT-1	USANO	747947	9284193	1					*
USANO-2X	USANO	755775	9280554		W				
ANDABARE-1		741676	9367535	4					
ARAKUBI-1A		749597	9284839		W				*
ARAKUBI-1AST		749597	9284839	1					*
BAIA-1		656833	9354507	4					
BAKARI-1				4					*
BEAVER-1		834674	9238810	3					*
BEAVER-1ST1		834674	9238810	3					*
BEAVER-1ST2		834674	9238810	3					*
BEAVER-1ST3		834674	9238810	3					*
BILIP-1		822988	9238942				W	G O W	*
COBRA-1		829767	9239800	1					*
EGELE-1X		691968	9361394		W				
KARIUS-1		689142	9338604	4					*
KERABI DDH1		890034	9251587	2					*
KORKA-1		678690	9384392	1					*
KUTUBU-1X		763527	9284711		W				
KUTUBU-2		762681	9284900		W				*
LAVANI-1		672844	9361815		W				
MAKAS-1X		809956	9257875	2					*
MAKAS-2X		811432	9257920					W	*
MENGA-1		531235	9417321		W				*
MULLER-1X		653389	9384864		W				
NEMBI-1		779956	9310783	4					
NW PAUA-1		736348	9313413	1					*
PANGIA-1		838221	9288479	4					
PANGIA-1A		838221	9288479	4					
PANGIA-1B		838221	9288479	4					
PAUA-1X		740503	9308843		W				*
SAUNDERS-1		816153	9240983	2					*
TA-1X		771981	9266677		W		W	W	*
TARIM-1		506778	9407689		G				
TUMULI-1		636610	9412414	2					*
TUMULI-1ST1		636610	9412414	2					*

Table A.1 Total Papuan Basin Wells

Foreland

WELL	FIELD	EASTING	NORTHING	Excluded	Toro	Digimu	Hedinia	Iagifu	>1994
BARIKEWA-1	BARIKEWA	822950	9212786		G		G		
BARIKEWA-2	BARIKEWA	823902	9214726		W		W		
ELEVALA-1	ELEVALA	584746	9320000		G				
ELEVALA-2	ELEVALA	582169	9320311		G				*
ELEVALA-2ST1	ELEVALA	582169	9320311	2					*
IEHI-1	IEHI	816998	9230624				W	W	
NW IEHI-1	IEHI	808494	9235530		W		W	W	
KETU-1	KETU	587313	9332566	2					
KETU-1ST	KETU	587313	9332566		W				
KETU-2	KETU	595318	9328652	1					*
KIMU-1	KIMU	730892	9207081		W				*
STANLEY-1	STANLEY	519240	9352306		G W				*
STANLEY-2	STANLEY	520200	9350721		G				*
STANLEY-4	STANLEY	521021	9350417		G				*
ADIBA-1		704255	9100395	2					*
AIEMA-1		646525	9226986	1					*
ANAMA-1		841866	9116809	4					*
ANCHOR CAY-1		835907	8954865	3					
ANESI-1		844428	9236418	4					
ANTELOPE-1		957213	9209041	3					*
ANTELOPE-2		958391	9205842	3					*
ARAMIA-1		645313	9131562		W				
AWAPA-1		697404	9121793	1					*
BAMU-1		761283	9121585	1					
BAMU-2		736897	9164556	1					
BAMU-3		647681	9125196	1					
BAMU-4		693169	9170927	1					
BAMU-B4		720563	9115339	1					
BORABI-1		871925	9094482	3					
BOSAVI-1		745032	9249170		W		W		*
BUJON-1		724756	9231625		W			W	*
BWATA-1		921040	9225710	3					
CECILIA-1		657540	9326452	4					
DARAI-1		773567	9223892	4					
DIBIRI-1		904600	9082527	3					
DIBIRI-1A		904557	9082597	3					
DOUGLAS-1		637118	9220456		G W		W		*
DUA DUA-1ST1		821980	9068322	2					*
ELK-1		957670	9213131	3					*
ELK-2		956948	9217807	3					*
ELK-4		957435	9212927	3					*
FLINDERS-1		945539	9042411	3					*
GOARI-1		815819	9154931	2					
GOARIBARI-1		873566	9043739	3					
HAGANA-1		955153	9048051	3					*
HOHORO-1		983703	9127265	3					
HOHORO-2		983726	9129165	3					
IAMARA-1		713459	9070827		W				
INI-1		912188	9155710	2					
INI-1ST1		912188	9155710	1					

WELL	FIELD	EASTING	NORTHING	Excluded	Toro	Digimu	Hedinia	Iagifu	>1994
INI-1ST2		912188	9155710	1					
IOROGABAIU-1		742254	9275951		W		W	W	
IPIGO-1		928348	9187978	3					
IVIRI-1		916693	9158287	3					
KAMUSI-1		767735	9169659	1					*
KANAU-1		742051	9235352		W		W		
KAPUL-1		770708	9177064	1					*
KARA-1X		781431	9252989	4					
KARIAVA-1		996183	9178082	3					
KIKORI-1		882240	9165220	3					
KIUNGA-1		534365	9336299		W				
KOKO-1		702401	9211481		W		W		*
KOMEWU-1		725772	9192418	2					
KOMEWU-2		728510	9194127					W	
KOROBOSEA-1		708030	9222787		W				*
KURU-1		883858	9211662	3					
KURU-1A		883858	9211662	3					
KURU-2		882870	9211299	3					
KURU-3		883859	9211785	3					
KUSA-1		835744	9036081	3					
LAKE MURRAY-1		535087	9207689	1					
LAKE MURRAY-2		537369	9209085	1					
LANGIA-1		630254	9211600		G				
LIBANO-1X		718343	9297670		W				
LIBANO-1XST		718343	9297670	1					
MAGOBU ISLAND-1		750470	9056386	2					
MAREMOSAB-1		724872	9013735	1					
MATA-1		578303	9037701	2					
MIRA-1		910941	9136042	3					
MOOSE-1		962872	9228319	3					*
MOOSE-2		964975	9224899	3					*
MOOSE-2ST1		964975	9224899	3					*
MOREHEAD-1		557885	9033163	1					
MORIGIO-1		845458	9117033					W	
MUABU-1		905258	9182448	3					
MUTARE-1		718850	9053838	2					
NOMAD-1		680732	9325291	2					*
NORTH PAIBUNA-1		831326	9153756	1					
OMATI-1		826582	9177234	4					
OMATI-2		823158	9176365	4					
ORIE-1		853254	9226270	2					
ORIOMO-1		738431	9023041	1					
ORIOMO-2		738310	9022878	1					
ORIOMO-5		738310	9022878	1					
ORIOMO-6		738310	9022878	1					
ORIOMO-7		738310	9022878	1					
OROKOLO-1		985157	9104948	3					
PANAKAWA-1		736151	9150117	1					*
PANDORA-1X		938217	8980269	3					
PANDORA-B1		941144	8987274	3					

Table A.1 Total Papuan Basin Wells

Foreland

WELL	FIELD	EASTING	NORTHING	Excluded	Toro	Digimu	Hedinia	Iagifu	>1994
PASCA-A1		928928	9046359	3					
PASCA-A2		931092	9046461	3					
PASCA-A3		929478	9046043	3					
PASCA-C1		937852	9056803	3					
PASCA-C2		939042	9056715	3					
PUK PUK-1		625362	9239161		G		G		*
PUK PUK-2		624760	9240921	1					*
PURARI-1-9		967361	9150612	3					
PURI-1A		941932	9212546	3					
PURI-1B		941932	9212546	3					
PURI-1		939724	9208198	3					
PURI SOUTH-1		939724	9208198	3					
PURUTU-1		842206	9024243	3					
RAMA-1		858106	9113043	3					
RARAKO CREEK-1		987239	9153584	3					
RENBO-1X		740154	9276447		W		W	W	*
SIPHON		530211	9357500	1					*
SIRERU-1		882573	9224777	4					
STERLING MUSTANG-1		986132	9229688	3					*
TRAPIA-1ST1		722861	9337558	1					*
TRICERATOPS-1		921671	9229177	3					*
TRICERATOPS-2		917469	9227104	3					*
TURAMA-1		794239	9197275	2					*
UBUNTU-1		602059	9323733		G W				*
UPOIA-1		995363	9140030	3					
URAMU-1		907608	9135267	3					
URAMU-1A		907572	9135323	3					
WABAU-1		858403	9234195	3					
WABUDA-1		794247	9084700	3					
WANA-1		914588	9177693	3					
WARA-1		787569	9268460	4					
WASUMA-1		819753	9247517	1					*
WEIMANG-1		640468	9227983	1					*
WOHOMUL-1		729591	9010636	1					
WOHOMUL-2		729591	9010636	1					
WONIA-1		738310	9022878	1					
WONIA-2		738310	9022878	1					
WUROI-1		724262	9025047	2					

Table A.2 Toro Wells Water Foldbelt

WELL	FIELD	EASTING	NORTHING	SPUD DATE	TEST TYPE	TVDss (m)	Quartz Pressure PSIA	Hw (0.435) (m)	pressure gradient (psi/ft)	Hw (calc) (m)	HC-W Contact	Pre vs Post Production	WATER SALINITY (ppm)	TEMP (F)	gradient (HR-ST) (psi/ft)	Hw (S-T) (m)
ADT-3A ST1	AGOGO	736576	9296369	24/08/96	RFT	-1595.76	2695.36	293	0.422	351	GWC	Post	12000	165	0.427	328
AGOGO-5X	AGOGO	732730	9299461	11/03/90	RFT	-1677.03	2879.20	340	0.432	355		Pre	12500	152	0.429	369
GOBE-1X	GOBE	797199	9253732	6/07/88	RFT	-1029.00	2378.00	637	0.442	609		Pre	10200	130	0.431	653
GOBE-2X	GOBE	807157	9246413	12/05/92	RFT	-746.94	2004.50	658	0.425	692		Pre	10030	110	0.433	664
GOBE-2XST	GOBE	807157	9246413	16/06/92	RFT	-774.03	2041.60	657	0.425	690		Pre				
GOBE-3X	GOBE	814359	9242603	29/11/92	RFT	-945.62	2296.90	664	0.414	747		Pre				
GOBE-4X	GOBE	798027	9252045	6/11/93	RFT	-592.85	1786.87	659	0.419	708		Pre				
GOBE-5XST1	GOBE	794829	9253507	9/06/94	RFT	-836.31	2139.33	663	0.435	663		Pre				
GOBE-6X	GOBE	801799	9250363	18/07/94	RFT	-760.48	2023.66	657	0.422	701		Pre				
GOBE-8XST3	GOBE	801805	9250362	4/09/94	RFT	-753.74	2010.31	655	0.426	686		Pre				
NW GOBE-1X	GOBE	790504	9256629	31/07/99	RFT	-720.38	1245.54	152	0.436	151			16300			
HEDINIA-2XST	HEDINIA	748557	9283444	21/11/88	RFT	-1790.60	2820.82	186	0.435	184		Pre	12000			
HEDINIA-3XST	HEDINIA	741826	9287764	26/12/88	RFT	-1116.79	2046.16	317	0.413	393	GWC	Pre	11200	118	0.432	327
HEDINIA-7X	HEDINIA	739460	9288994	29/03/89	RFT	-1105.70	2040.69	324	0.446	290		Pre	7000	128	0.430	341
IDT-1 (HEDINIA-9X)	HEDINIA	746952	9284245	27/12/89	RFT	-1363.08	2267.40	226	0.498	24	OWC	Pre	7150	142	0.428	252
IDT-18 (IWT 2)	HEDINIA	746938	9284214	14/03/94	RFT	-1345.71	1972.70	37	0.400	158	OWC	Post	6400	155	0.426	66
IAGIFU-4X	IAGIFU	740946	9290162	27/12/86	RFT	-1212.95	2193.80	324	0.458	248		Pre	17500	127	0.433	331
IAGIFU-5X	IAGIFU	746360	9287414	3/10/87	RFT	-1402.69	2337.00	235	0.425	275		Pre	8200	138	0.429	258
IAGIFU-6XST	IAGIFU	743598	9289936	19/08/88	RFT	-1754.90	2998.12	346	0.428	380		Pre				
IAGIFU-7X	IAGIFU	744442	9287314	18/05/89	RFT	-1294.70	2206.50	251	0.437	243	OWC	Pre	12400	134	0.431	266
IDT-10 (IAGIFU-8X)	IAGIFU	740781	9291938	22/07/89	RFT	-1436.81	2534.80	339	0.425	383		Pre	6000	148	0.426	377
IDT-14	IAGIFU	745078	9287494	8/04/94	RFT	-1329.87	2166.46	188	0.415	262	OWC	Post	9640			
IDT-15	IAGIFU	745318	9286986	19/02/95	RFT	-1368.92	2163.55	147	0.404	265		post				
IDT-16	IAGIFU	744938	9286201	17/01/95	RFT	-1395.53	2203	148	0.433	155		Post				
IDT-19ST1	IAGIFU	745259	9285962	6/10/97	RFT	-1329.86	2007.00	243	0.435	243	OWC	Post	11780	139	0.43	93
IDT-3	IAGIFU	745267	9285989	5/01/92	RFT	-1350.90	2263.20	235	0.436	231	OWC	Post				
IDT-9 (IAGIFU-3X)	IAGIFU	742333	9291364	9/07/86	RFT	-1422.69	2519.60	343	0.433	351	OWC	Pre	12400	141	0.433	351
IDT-9 ST1	IAGIFU	742334	9291364	17/09/97	RFT	-1389.47	2289.02	214	0.456	142		Post				
IDT-9 ST2	IAGIFU	742333	9291364	13/06/04	RFT	-1082.66	1841.00	207	0.457	145		Post				
IWT-1 (IAGIFU-5XST1)	IAGIFU	746360	9287414	3/10/87	RFT	-1575.24	2730.30	338	0.447	288		Pre	9800	130	0.431	356
JUHA-5X	JUHA	648929	9353150	23/12/06	RFT	-2922.3	5258.65	762	0.430	805			20000	237	0.423	867
MANANDA-3X	MANANDA	707953	9315242	30/04/85	DST	-442.50	3852.33	2257	0.448	2180			15600			
MANANDA-4X	MANANDA	717707	9308533	23/03/90	RFT	-511.85	3954.10	2259	0.426	2317			14200			
MORAN-1X ST1	MORAN	736469	9307951	25/07/96	RFT	-1049.37	5531.31	2826	0.501	2314		Pre				
MORAN-2X ST1	MORAN	736473	9307955	4/05/97	RFT	-2000.40	6349.00	2448	0.439	2412		Pre				
MORAN-3X ST1	MORAN	740334	9304267	9/08/97	RFT	-744.10	5522.96	3126	0.449	3006		Pre	15000	115	0.437	3108
MORAN-3X ST2	MORAN	740334	9304267	26/09/97	RFT	-735.26	5519.80	3132	0.428	3195		Pre	15000	110	0.438	3106
MORAN-5X	MORAN	738127	9306696	22/04/98	RFT	-1018.90	5597.13	2903	0.450	2769		Pre				
MORAN-7XST1	MORAN	738130	9306715	3/12/05	RFT	-1378.60	5533.37	2499	0.419	2651		Post				
MORAN-8X	MORAN	735304	9309403	7/06/02	RFT	-1245.73	5376	2521	0.496	2060		Post				
PNYANG_SOUTH-1XST1	PNYANG	564216	9386363	19/03/12	RFT	-1282.35	2225.12	277	0.457	202						
SE GOBE-1X	SE GOBE	811635	9243159	16/02/91	RFT	-842.47	2150.36	664	0.392	830						
SE GOBE-2X	SE GOBE	812832	9242648	4/10/91	RFT	-883.67	2203.84	661	0.430	680						
SE GOBE-3X	SE GOBE	810744	9243374	23/03/92	RFT	-863.60	2061.60	581	0.418	641						
SE HEDINIA-3X	SE HEDINIA	765855	9271807	2/04/89	RFT	-1196.80	1901.50	136	0.430	150			15000	131	0.432	145
SE HEDINIA-4X	SE HEDINIA	765037	9271650	4/08/90	RFT	-968.04	1563.00	127	0.428	145						

Table 4.2 Toro Wells Water Foldbelt

WELL	FIELD	EASTING	NORTHING	SPUD DATE	TEST TYPE	TVDss (m)	Quartz Pressure PSIA	Hw (0.435) (m)	pressure gradient (psi/ft)	Hw (calc) (m)	HC-W Contact	Pre vs Post Production	WATER SALINITY (ppm)	TEMP (F)	gradient (HR-ST) (psi/ft)	Hw (S-T) (m)
SE MANANDA-1X	SE MANANDA	725903	9306278	14/01/91	RFT	-566.70	3996.10	2233	0.403	2456	OWC		11000			
SE MANANDA-2X	SE MANANDA	723110	9306982	22/01/94	RFT	-548.03	3972.50	2235	0.428	2280	OWC					
UDT-4 ST1 (UDT-4A)	USANO	755775	9280554	27/01/92	RFT	-1645.20	2611.60	185	0.422	240	OWC	Pre				
UDT-6 (USANO-IX/ST)	USANO	752121	9282306	14/11/89	DST	-1679.40	2622.50	158	0.435	158		Pre				
USANO-2X	USANO	755775	9280554	14/11/90	RFT	-1866.08	2789.80	89	0.429	114		Pre	14700	102	0.435	89
ARAKUBI-1A		749597	9284839	30/08/07	RFT	-1687.45	2352.20	-39	0.428	-14		Post	18000	158	0.430	-20
EGELE-1X		691968	9361394	10/05/90	RFT	-797.10	4564.15	2401	0.452	2284			10800			
KUTUBU-1X		763527	9284711	8/02/88	RFT	-795.60	5806.00	3273	0.472	2954			11400			
KUTUBU-2		762681	9284900	13/03/07	RFT	-477.33	5379.40	3292	0.432	3315			10000	101	0.437	3275
LAVANI-1		672844	9361815	21/05/82		2546.91	14.70	2437	0.435	2437						
MENGA-1		531235	9417321	4/11/94	RFT	146.00	810.35	714	0.415	741						
MULLER-1X		653389	9384864	3/05/91	RFT	857.30	2110.32	2336	0.433	2342			11200	148	0.429	2357
PAUA-1X		740503	9308843	9/09/95	RFT	-1167.87	8049.65	4473	0.450	4279						
TA-1X		771981	9266677	17/12/94	RFT	-1350.08	2132.79	144	0.428	168						
Foreland																
BARIKEWA-2	BARIKEWA	823902	9214726	8/12/81	DST	-1528.80	2256.00	52	0.435	52			19000			
NW IEHI-1	IEHI	808494	9235530	25/03/94	RFT	-1182.10	1788.90	71	0.440	58						
KETU-1ST	KETU	587313	9332566	19/11/90	RFT	-3240.56	4752.10	89	0.436	83						
KIMU-1	KIMU	730892	9207081	21/11/98	RFT	-1655.90	2425.60	44	0.431	61						
STANLEY-1	STANLEY	519240	9352306	18/01/99	RFT	-3082.32	4647.87	174	0.454	205	GWC					
ARAMIA-1		645313	9131562	12/04/55	DST	-1553.60	2245.00	19	0.435	19			48000	160	0.438	9
BOSAVI-1		745032	9249170	22/01/03	MFT	-292.50	536.00	83	0.422	94						
BUJON-1		724756	9231625	23/01/94	RFT	-1404.00	2070.00	46	0.427	72						
DOUGLAS-1		637118	9220456	4/04/06	RFT	-1767.20	2571.10	34	0.439	20	GWC					
IAMARA-1		713459	9070827	29/10/62	DST	-1054.9	1532.00	19	0.435	19			19850			
IOROGABAIU-1		742254	9275951	4/06/89	RFT	-1588.00	2352.40	60	0.431	77			14000	155	0.429	83
KANAU-1		742051	9235352	21/05/75	DST	-331.80	569.50	67	0.435	67			6300	109	0.431	71
KIUNGA-1		534365	9336299	10/03/80	DST	-2844.50	4191.00	92	0.435	92			23900	263	0.418	212
KOKO-1		702401	9211481	9/02/99	RFT	-842.40	1236.80	24	0.440	13						
KOROBOSEA-1		708030	9222787	22/10/07	RFT	-1709.60	2506.9	47	0.431	63						
LIBANO-1X		718343	9297670	25/04/90	RFT	-2541.97	3707.30	56	0.440	28						
RENBO-1X		740154	9276447	12/12/95	RFT	-1356.15	2057.09	85	0.432	96						
UBUNTU-1		602059	9323733	13/12/10	RFT	-3281.70	4811.60	90	0.422	150	GWC					

Table A.3 Toro Wells Gas Foldbelt

WELL	FIELD	EASTING	NORTHING	SPUD DATE	TEST TYPE	TVDss (m)	Quartz Pressure PSIA	Hw (0.435) (m)	pressure gradient (psi/ft)	Last Known Gas (LKG)	Quartz Pressure PSIA	EGWC (m)	Hw (0.435) (m)	Pre vs Post Production	WATER SALINITY (ppm)	TEMP (F)
ADD-1ST1	AGOGO	731736	9298901	14/09/93	RFT	-1394.78	2683.20	485	0.103					Post		
ADD-2	AGOGO	732460	9297776	16/05/89	RFT	-1334.46	2695.99	555	0.104					Pre		
ADD-3	AGOGO	734125	9298071	5/08/92	RFT	-1365.9	2733.91	550	0.097					Pre		158
ADD-4	AGOGO	734768	9296799	31/12/92	RFT	-1377.7	2706.90	519	0.103					Pre		
ADT-1 (AGOGO-4X)	AGOGO	733290	9299460	3/02/90	RFT	-1521.06	2747.09	404	0.094					Pre		
ADT-3A ST1	AGOGO	736576	9296369	24/08/96	RFT	-1574.18	2683.88	306	0.097					Post		
AGD-1	AGOGO	732466	9297770	3/09/92	RFT	-1352.68	2699.43	539	0.104					Pre		
AGOGO-1X	AGOGO	732460	9297776	10/03/89	RFT	-1259.17	2673.38	614	0.084					Pre	11900	127
AGOGO-2X	AGOGO	734769	9296800	16/07/89	RFT	-1373.03	2706.70	524	0.083					Pre		
AGOGO-2XST1	AGOGO	734769	9296800	15/08/89	RFT	-1441.53	2726.24	469	0.095					Pre		
AGOGO-3X	AGOGO	736030	9295544	26/11/89	RFT	-1411.73	2718.58	493	0.088					Pre		
ANGORE-1A	ANGORE	706958	9338814	10/08/89	DST	-2414.60	7094.70	2557	0.118	LKG	7100	-2420	2555			
HEDINIA-1X	HEDINIA	743822	9285209	21/01/88	RFT	-808.33	1980.42	579	0.067					Pre		117
HEDINIA-2X	HEDINIA	743719	9285271	19/09/88	RFT	-1329.54	2439.30	380	0.078					Pre		
HEDINIA-3X	HEDINIA	741826	9287764	24/10/88	RFT	-993.28	2019.73	422	0.065					Pre	12000	119
HEDINIA-3XST	HEDINIA	741826	9287764	26/12/88	RFT	-1107.83	2040.03	322	0.094					Pre		
IDD-1 (HEDINIA-6X)	HEDINIA	739617	9288998	10/02/89	RFT	-999.10	2020.04	416	0.064					Pre		
IDD-3	HEDINIA	743553	9287131	25/05/92	RFT	-1002.00	2017.60	412	0.103					Pre		
IST4 (HEDINIA-5X)	HEDINIA	745907	9284459	22/11/88	RFT	-1104.90	2043.85	327	0.068					Pre		
HIDES-1	HIDES	689727	9344121	3/06/87	RFT	-450.58	5585.10	3463	0.102	LKG						
HIDES-2	HIDES	691636	9342137	21/04/90	DST	-92.12	5447.80	3725		LKG						
HIDES-3	HIDES	693128	9342030	9/02/93	RFT	-1103	5834	2985	0.053	LKG						
HIDES-4	HIDES	699120	9335604	26/12/97	RFT	-1472.3	5957.20	2702	0.114	LKG	6050	-1850	2389			
IAGIFU-6X	IAGIFU	743598	9289936	2/07/88	RFT	-990.28	2017.60	423	0.069					Pre		
IDT-22	IAGIFU	743080	9287050	18/01/05	RFT	-1136.58	1855.97	164	0.053					Post		131
IDT-23	IAGIFU	743080	9287037	12/03/05	RFT	-1144.00	1862.52	161	0.077					Post		139
IST-1	IAGIFU	744620	9288211	18/04/82	RFT	-1058.00	2031.12	365	0.075					Pre		
JUHA-1X	JUHA	658948	9347274	23/10/82	DST	-2309.80	4833.00	1077		LKG						
JUHA-2X	JUHA	652565	9353065	13/10/83	DST	-2324.60	4532.00	852		LKG						
JUHA-3XST1	JUHA	649558	9355863	6/05/85	DST	-2466.80	4905.00	971		LKG						
PNYANG-1X	PNYANG	566622	9390050	3/08/90	RFT	-949.00	2309.16	669	0.065	LKG	2400	-1400	282			
PNYANG-2X	PNYANG	563045	9389201	9/05/91	RFT	-1183.00	2352.86	466	0.070	LKG						
PNYANG-2X-ST3	PNYANG	563045	9389201	18/10/91	DST	-1314.00	2379.00	353		LKG						
PNYANG_SOUTH-1X	PNYANG	564216	9386363	29/01/12	RFT	-931.71	2163.05	584	0.059	LKG						
SE HEDINIA-1X	SE HEDINIA	763974	9271500	20/04/87	RFT	-746.62	1521.40	319	0.045							111
TARIM-1		506778	9407689	17/04/90	DST	-2688.30	5320	1039		LKG	5450	-3380	439			
Foreland																
BARIKEWA-1	BARIKEWA	822950	9212786	11/08/56	DST	-1531.60	2404.70	153								
ELEVALA-1	ELEVALA	584746	9320000	11/12/89	RFT	-3049.00	4543.80	135	0.157	LKG	4565	-3110	89			
ELEVALA-2	ELEVALA	582169	9320311	14/11/11	RFT	-3093	4560	102	0.118							
STANLEY-1	STANLEY	519240	9352306	18/01/99	RFT	-3067.83	4640.69	184	0.088							259
STANLEY-2	STANLEY	520200	9350721	5/12/10	RFT	-2938.00	4602.30	287	0.085							
STANLEY-4	STANLEY	521021	9350417	29/03/11	RFT	-3049.10	4632.50	197	0.112							
DOUGLAS-1		637118	9220456	4/04/06	RFT	-1738.50	2558.70	54	0.036							
LANGIA-1		630254	9211600	1/04/91	RFT	-1557.50	2273.10	35		LKG	2275	-1575	19			
PUK PUK-1		625362	9239161	13/05/08	RFT	-1803.00	2710.40	96	0.072	LKG	2715	-1870	32			
UBUNTU-1		602059	9323733	13/12/10	RFT	-3185.50	4651.60	74	0.149							

Table A.4 Toro Wells Oil Foldbelt

WELL	FIELD	EASTING	NORTHING	SPUD DATE	TEST TYPE	TVDss (m)	Quartz Pressure PSIA	Hw (0.435) (m)	pressure gradient (psi/ft)	HC Contact	Pre vs Post Production	WATER SALINITY (ppm)	TEMP (F)
ADT-1 (AGOGO-4X)	AGOGO	733290	9299460	3/02/90	RFT	-1582.06	2770.73	359	0.329	GOC	Pre		
HEDINIA-1XST	HEDINIA	743822	9285209	30/03/88	DST	-1166.16	2084.00	294			Pre		
IDT-1 (HEDINIA-9X)	HEDINIA	746952	9284245	27/12/89	RFT	-1252.13	2157.60	260	0.328		Pre		
IDT-18 (IWT 2)	HEDINIA	746938	9284214	14/03/94	RFT	-1325.90	1947.94	39	0.285		Post		
IST4 (HEDINIA-5X)	HEDINIA	745907	9284459	22/11/88	RFT	-1141.48	2056.83	300	0.290	GOC	Pre		
UDT-1 (HEDINIA-8X)	HEDINIA	745958	9284246	2/11/89	RFT	-1582.83	2535.20	194	0.324		Pre		
IAGIFU-7X	IAGIFU	744442	9287314	18/05/89	RFT	-1201.52	2118.21	283	0.284		Pre		
IAGIFU-7XST2	IAGIFU	744442	9287314	18/05/89	RFT	-1208.96	2123.8	279	0.298		Pre		124
IDT-11	IAGIFU	742449	9291311	22/11/92	RFT	-1325.18	2159.97	188	0.243		Pre		
IDT-12	IAGIFU	746475	9285101	14/11/92	RFT	-1221.79	2086.62	240	0.294		Pre		
IDT-13	IAGIFU	744930	9286186	1/02/94	RFT	-1328.99	2179.26	244			Post		
IDT-14	IAGIFU	745078	9287494	8/04/94	RFT	-1303.38	2141.08	197	0.299		Post		
IDT-17	IAGIFU	745311	9286974	13/06/96	RFT	-1333.66	2224.85	246			Post		
IDT-19ST1	IAGIFU	745259	9285962	6/10/97	RFT	-1309.44	1987.70	83	0.290		Post		
IDT-22	IAGIFU	743080	9287050	18/01/05	RFT	-1206.07	1845.71	87	0.298	GOC	Post		142
IDT-3	IAGIFU	745267	9285989	5/01/92	RFT	-1290.80	2206.00	255	0.297		Pre		
IDT-4 (IAGIFU-9X)	IAGIFU	744436	9287317	2/10/89	RFT	-1234.44	2146.60	270	0.289		Pre		
IDT-5 (IAGIFU-7XST)	IAGIFU	744442	9287314	11/08/89	RFT	-1212.30	2127.00	278	0.286		Pre		
IDT-8	IAGIFU	745071	9289368	2/09/91	RFT	-1182.30	2101.30	290	0.279		Pre		
IDT-9 (IAGIFU-3X)	IAGIFU	742333	9291364	9/07/86	RFT	-1380.00	2483.30	360	0.286		Pre		
IST-1	IAGIFU	744620	9288211	18/04/82	RFT	-1132.00	2051.53	306	0.398	GOC	Pre		
IST-2 (IAGIFU-2X)	IAGIFU	744617	9288211	8/12/85	RFT	-1148.21	2064.14	298	0.286		Pre		
MORAN-13	MORAN	731667	9311398	28/07/06	RFT	-2852.80	5081.26	708	0.203		Post		162
MORAN-2X ST2	MORAN	736473	9307955	17/06/97	RFT	-750.70	5142.89	2853	0.290		Pre		
MORAN-4X	MORAN	733136	9309953	19/11/97	RFT	-1394.60	5694.30	2595	0.297		Pre		
MORAN-6X ST2	MORAN	733731	9309963	17/08/01	RFT	-1690.66	5744.50	2335	0.272		Post		
SE MANANDA-1X	SE MANANDA	725903	9306278	14/01/91	RFT	-536.20	3960.43	2239	0.340				
SE MANANDA-2X	SE MANANDA	723110	9306982	22/01/94	RFT	-493.81	3916.50	2250	0.315				
UDT-2	USANO	747947	9284192	7/03/92	RFT	-1523.68	2497.55	226	0.297		Pre		
UDT-4 ST1 (UDT-4A)	USANO	755775	9280554	27/01/92	RFT	-1591.00	2557.80	201	0.282		Pre		
UDT-7ST1	USANO	750316	9282810	5/11/06	RDT	-1588.50	2309.70	30	0.252		Post		154

Table A.5 Digimu Wells Water Foldbelt

WELL	FIELD	EASTING	NORTHING	SPUD DATE	TEST TYPE	TVDss (m)	Quartz Pressure PSIA	Hw (0.435) (m)	pressure gradient (psi/ft)	Hw (calc) (m)	HC-W Contact	Pre vs Post Production	WATER SALINITY (ppm)	TEMP (F)	gradient (HR-ST) (psi/ft)	Hw (S-T) (m)
AGOGO-2XST1	AGOGO	734769	9296800	15/08/89	RFT	-1601.23	2869.20	409	0.399	588		Pre	6100	166	0.425	457
AGOGO-3X	AGOGO	736030	9295544	26/11/89	RFT	-1593.85	2875.80	421	0.420	493		Pre	8300	164	0.426	464
HEDINIA-1XST	HEDINIA	743822	9285209	30/03/88	DST	-1327.71	2390.00	347	0.435	347		Pre				
HEDINIA-3XST	HEDINIA	741826	9287764	26/12/88	RFT	-1280.71	2319.54	345	0.477	202		Pre	3300	127	0.429	367
HEDINIA-7X	HEDINIA	739460	9288994	29/03/89	RFT	-1299.40	2349.10	347	0.442	320		Pre	4600	133	0.429	370
IAGIFU-5X	IAGIFU	746360	9287414	3/10/87	RFT	-1566.37	2718.70	339	0.428	370		Pre				
IAGIFU-7X	IAGIFU	744442	9287314	18/05/89	RFT	-1379.22	2458.40	343	0.441	320		Pre	4400	139	0.428	372
IDT-10 (IAGIFU-8X)	IAGIFU	740781	9291938	22/07/89	RFT	-1554.47	2814.70	418	0.435	418		Pre	5500	153	0.427	455
IDT-9 (IAGIFU-3X)	IAGIFU	742333	9291364	9/07/86	RFT	-1539.15	2799.20	422	0.409	546		Pre	7500	144	0.429	450
IST-2 (IAGIFU-2X)	IAGIFU	744617	9288211	8/12/85	RFT	-1279.70	2313.95	342	0.440	325		Pre				
IST4 (HEDINIA-5X)	HEDINIA	745907	9284459	22/11/88	RFT	-1288.08	2315.79	335	0.435	335		Pre	5700	143	0.428	361
MANANDA-4X	MANANDA	717707	9308533	23/03/90	RFT	-599.90	4080.50	2259	0.435	2259		Pre	11400			
MORAN-2X ST1	MORAN	736473	9307955	4/05/97	RFT	-2090.30	6370.60	2374	0.440	2324		Pre				
MORAN-3X ST1	MORAN	740334	9304267	9/08/97	RFT	-828.57	5574.22	3077	0.427	3149		Pre	15000	116	0.437	3059
MORAN-3X ST2	MORAN	740334	9304267	26/09/97	RFT	-828.06	5579.50	3081	0.450	2951		Pre				
MORAN-5X	MORAN	738127	9306696	22/04/98	RFT	-1120.40	5698.50	2873	0.437	2851		Pre				
SE MANANDA-1X	SE MANANDA	725903	9306278	14/01/91	RFT	-628.20	4083.04	2233	0.496	1882			5300			

Table A.6 Digimu Wells Gas
Foldbelt

WELL	FIELD	EASTING	NORTHING	SPUD DATE	TEST TYPE	TVDss (m)	Quartz Pressure PSIA	Hw (0.435) (m)	pressure gradient (psi/ft)	Last Known Gas (LKG)	Quartz Pressure PSIA	EGWC (m)	Hw (0.435) (m)	Pre vs Post Production	WATER SALINITY (ppm)	TEMP (F)
AGD-1	AGOGO	732466	9297770	3/09/92	RFT	-1449.23	2729.26	463	0.0453					Pre		
AGOGO-1X	AGOGO	732460	9297776	10/03/89	RFT	-1412.17	2719.09	493	0.0947					Pre		
HEDINIA-1X	HEDINIA	743822	9285209	21/01/88	RFT	-963.41	2014.83	448	0.0623		2040	-1090	339	Pre		
IAGIFU-6X	IAGIFU	743598	9289936	2/07/88	RFT	-1152.74	2197.90	387	0.0938		2215	-1220	332	Pre		
MORAN-1X ST1	MORAN	736469	9307951	25/07/96	RFT	-1177.98	5520.00	2690	0.1743	LKG				Pre		

Table A.7 Digimu Wells Oil
Foldbelt

WELL	FIELD	EASTING	NORTHING	SPUD DATE	TEST TYPE	TVDss (m)	Quartz Pressure PSIA	Hw (0.435) (m)	pressure gradient (psi/ft)	HC Contact	Pre vs Post Production	WATER SALINITY (ppm)	TEMP (F)
ADD-1ST1	AGOGO	731736	9298901	14/09/93	RFT	-1526.24	2772.41	416	0.3076029		Post		
ADD-2	AGOGO	732460	9297776	16/05/89	RFT	-1497.29	2778.11	449	0.3122989		Pre		
ADD-3	AGOGO	734125	9298071	5/08/92	RFT	-1508.2	2808.73	460	0.2796364		Pre		162
ADD-4	AGOGO	734768	9296799	31/12/92	RFT	-1522.5	2764.74	415	0.2177169		Pre		
AGD-1	AGOGO	732466	9297770	3/09/92	RFT	-1457.46	2731.96	457	0.0452634	GOC	Pre		
AGOGO-2X	AGOGO	734769	9296800	16/07/89	RFT	-1523.93	2795.00	435	0.2638993		Pre		
HEDINIA-3X	HEDINIA	741826	9287764	24/10/88	RFT	-1156.78	2158.09	355	0.2898751		Pre		
IDD-1 (HEDINIA-6X)	HEDINIA	739617	9288998	10/02/89	RFT	-1150.00	2147.50	355	0.3026849		Pre		
IDD-2	HEDINIA	744261	9285588	4/04/92	RFT	-1132.97	2132.12	361	0.2665533		Pre		
IDD-3	HEDINIA	743553	9287131	25/05/92	RFT	-1133.40	2134.70	362	0.3666591		Pre	7286	134
MORAN-13	MORAN	731667	9311398	28/07/06	RFT	-2967.90	5180.33	662	0.2571315		Post		165
MORAN-1X ST1	MORAN	736469	9307951	25/07/96	RFT	-1177.46	5526.26	2695	0.2623321	GOC	Pre		
MORAN-1X ST2	MORAN	736469	9307951	6/10/96	RFT	-1247.23	5584.88	2666	0.2564177		Pre		
MORAN-2X ST2	MORAN	736473	9307955	17/06/97	RFT	-832.00	5257.52	2852	0.2389868		Pre		
MORAN-4X	MORAN	733136	9309953	19/11/97	RFT	-1483.20	5778.80	2566	0.2425622		Pre		
MORAN-6X ST2	MORAN	733731	9309963	17/08/01	RFT	-1852.23	4221.10	1105	0.302055		Post		
MORAN-7XST1	MORAN	738130	9306715	3/12/05	RFT	-1446.00	4584.06	1766	0.2913715		Post		

Table A.8 Hedinia Wells Water
Foldbelt

WELL	FIELD	EASTING	NORTHING	SPUD DATE	TEST TYPE	TVDss (m)	Quartz Pressure PSIA	Hw (0.435) (m)	pressure gradient (psi/ft)	Hw (calc) (m)	HC-W Contact	Pre vs Post Production	WATER SALINITY (ppm)	TEMP (F)	gradient (HR-ST) (psi/ft)	Hw (S-T) (m)
GOBE-4X	GOBE	798027	9252045	6/11/93	RFT	-814.28	1682.57	365	0.432	372		Pre				
IDD-1 (HEDINIA-6X)	HEDINIA	739617	9288998	10/02/89	RFT	-1248.90	2377.00	417	0.466	305		Pre				
IST4 (HEDINIA-5X)	HEDINIA	745907	9284459	22/11/88	RFT	-1390.50	2368.02	269	0.417	341		Pre				
SE HEDINIA-1X	SE HEDINIA	763974	9271500	20/04/87	DST	-986.46	1856.00	314	0.435	314	OWC					
SE HEDINIA-3X	SE HEDINIA	765855	9271807	2/04/89	RFT	-1447.19	2532.20	327	0.480	161			15000	147	0.430	348
BILIP-1		822988	9238942	17/10/02	RFT	-1526	3142.1	676	0.506	367						
TA-1X		771981	9266677	17/12/94	RFT	-1651.16	2842.17	340	0.430	365						
Foreland																
BARIKEWA-2	BARIKEWA	823902	9214726	8/12/81	DST	-1644.00	2500.00	108	0.435	108			26000			
IEHI-1	IEHI	816998	9230624	22/06/60	DST	-1350.00	2178.70	177	0.435	177			6600	118	0.431	191
NW IEHI-1	IEHI	808494	9235530	25/03/94	RFT	-1418.10	2141.13	82	0.439	67						
BOSAVI-1		745032	9249170	22/01/03	MFT	-483.00	802.10	79	0.428	88				141		
DOUGLAS-1		637118	9220456	4/04/06	RFT	-1811.20	2634.80	35	0.432	49						
IOROGABAIU-1		742254	9275951	4/06/89	RFT	-1793.00	2642.30	58	0.411	165						
KANAU-1		742051	9235352	21/05/75	DST	-576.20	911.20	62	0.435	62			16200	117	0.433	65
KOKO-1		702401	9211481	9/02/99	RFT	-959.60	1401.40	22	0.431	31						
RENBO-1X		740154	9276447	12/12/95	RFT	-1573.93	2366.76	84	0.435	84						

Table A.9 Hedinia Wells Gas
Foreland

WELL	FIELD	EASTING	NORTHING	SPUD DATE	TEST TYPE	TVDss (m)	Quartz Pressure PSIA	Hw (0.435) (m)	pressure gradient (psi/ft)	Las Known Gas (LKG)	Pre vs Post Production	WATER SALINITY (ppm)	TEMP (F)
BARIKEWA-1	BARIKEWA	822950	9212786	11/08/56	DST	-1700.50	2669.70	170		LKG			
PUK PUK-1		625362	9239161	13/05/08	RFT	-1859.00	2779.20	88	0.05845	LKG			

Table A.10 Hedina Wells Oil
Foldbelt

WELL	FIELD	EASTING	NORTHING	SPUD DATE	TEST TYPE	TVDss (m)	Quartz Pressure PSIA	Hw (0.435) (m)	pressure gradient (psi/ft)	HC-W Contact	Pre vs Post Production	WATER SALINITY (ppm)	TEMP (F)
ADD-2	AGOGO	732460	9297776	16/05/89	RFT	-1600.55	3757.67	1032	0.306		Pre		
ADT-2	AGOGO	732730	9299461	14/10/92	RFT	-1857.46	4063.80	990	0.278		Pre		
AGOGO-1X	AGOGO	732460	9297776	10/03/89	RFT	-1511.17	3703.35	1084	0.263		Pre		
AGOGO-3X	AGOGO	736030	9295544	26/11/89	RFT	-1710.35	3829.45	973	0.260		Pre		
SE HEDINIA-1X	SE HEDINIA	763974	9271500	20/04/87	DST	-944.40	1855.00	355	0.353				

Table A.11 Iagifu Wells Water Foldbelt

WELL	FIELD	EASTING	NORTHING	SPUD DATE	TEST TYPE	TVDss (m)	Quartz Pressure PSIA	Hw (0.435) (m)	pressure gradient (psi/ft)	Hw (calc) (m)	HC-W Contact	Pre vs Post Production	WATER SALINITY (ppm)	TEMP (F)	gradient (HR-ST) (psi/ft)	Hw (S-T) (m)
ADD-2	AGOGO	732460	9297776	16/05/89	RFT	-1702.15	4110.00	1178	0.412	1335		Pre				
AGOGO-3X	AGOGO	736030	9295544	26/11/89	RFT	-1811.33	4261.70	1175	0.427	1227		Pre				
GOBE MAIN-5ST1	GOBE	800706	9250858	3/10/01	RFT	-1201.21	1884.8	119	0.424	155	OWC	Post				
GOBE MAIN-7	GOBE	801794	9250352	24/08/06	RDT	-1178.63	1755.83	52	0.417	105	OWC	Post				
GOBE-2XST	GOBE	807157	9246413	16/06/92	RFT	-1209.56	2293.90	398	0.435	398	OWC	Pre	10700	120	0.432	409
GOBE-3X	GOBE	814359	9242603	29/11/92	RFT	-1259.78	2371.00	402	0.422	454	OWC	Pre	7500	136	0.429	425
GOBE-4XST1	GOBE	798027	9252045	8/11/93	RFT	-1200.24	2203.88	344	0.443	316	OWC	Pre				
GOBE-5XST1	GOBE	794829	9253507	9/06/94	RFT	-1202.83	2230.82	360	0.448	317		Pre				
GOBE-7XST1	GOBE	810826	9244502	12/10/99	RFT	-1200.78	2320.53	425	0.427	454	OWC	Post				
GOBE-8XST1	GOBE	801805	9250362	4/09/94	RFT	-1235.05	2248.68	341	0.444	310		Pre				
GOBE-8XST3	GOBE	801805	9250362	4/09/94	RFT	-1153.55	2209.28	394	0.429	417		Pre				
HEDINIA-1X	HEDINIA	743822	9285209	21/01/88	RFT	-1148.85	2226.67	411	0.424	452		Pre				
IAGIFU-4X	IAGIFU	740946	9290162	27/12/86	RFT	-1654.61	3002.90	450	0.424	502		Pre	9700	140	0.430	474
IAGIFU-7X	IAGIFU	744442	9287314	18/05/89	RFT	-1586.03	2847.05	409	0.450	343		Pre				
MORAN-1X ST1	MORAN	736469	9307951	25/07/96	RFT	-1388.04	6184.04	2945	0.484	2508		Pre				
BILIP-1		822988	9238942	17/10/02	RFT	-1739	3063.7	407	0.430	432	OWC					
MAKAS-2X		811432	9257920	10/01/97	MDT	-1482.02	6727.58	3232	0.438	3195						
TA-1X		771981	9266677	17/12/94	RFT	-1715.72	2938.21	343	0.410	468						
Foreland																
IEHI-1	IEHI	816998	9230624	22/06/60	DST	-1463.72	2322.70	164	0.435	164			10500	124	0.431	179
NW IEHI-1	IEHI	808494	9235530	25/03/94	RFT	-1508.60	2261.90	76	0.442	52						
BUJON-1		724756	9231625	23/01/94	RFT	-1657.50	2433.00	47	0.406	167						
IOROGABAIU-1		742254	9275951	4/06/89	RFT	-1903.00	2800.00	59	0.437	51						
KOMEWU-2		728510	9194127	30/11/57	DST	-2097.00	3098.00	74	0.435	74			17200			
MORIGIO-1		845458	9117033	11/05/89	RFT	-2767.68	3972.10	16	0.416	145						
RENBO-1X		740154	9276447	12/12/95	RFT	-1713.77	2565.22	84	0.430	104						

Table A.12 Iagifu Wells Gas
Foldbelt

WELL	FIELD	EASTING	NORTHING	SPUD DATE	TEST TYPE	TVDss (m)	Quartz Pressure PSIA	Hw (0.435) (m)	pressure gradient (psi/ft)	Last Known Gas (LKG)	Quartz Pressure PSIA	EGWC (m)	Hw (0.435) (m)	Pre vs Post Production	WATER SALINITY (ppm)	TEMP (F)
GOBE MAIN-5ST1	GOBE	800706	9250858	3/10/01	RFT	-1103.66	2124.2	385	0.2189367					Post		
GOBE MAIN-7	GOBE	801794	9250352	24/08/06	RDT	-1112.67	1691.25	72						Post		123
GOBE-2XST	GOBE	807157	9246413	16/06/92	RFT	-1170.76	2262.50	415						Pre		
GOBE-4X	GOBE	798027	9252045	6/11/93	RFT	-937.25	2071.65	514	0.0665496					Pre		
GOBE-4XST1	GOBE	798027	9252045	8/11/93	RFT	-1097.86	2106.20	378	0.0760469					Pre		
IAGIFU-6X	IAGIFU	743598	9289936	2/07/88	RFT	-1365.14	2655.60	496	0.1288484		2680	-1430	448	Pre		
BILIP-1		822988	9238942	17/10/02	RFT	-1711	3038.2	418	0.1168054							

Table A.13 Iagifu Wells Oil
Foldbelt

WELL	FIELD	EASTING	NORTHING	SPUD DATE	TEST TYPE	TVDss (m)	Quartz Pressure PSIA	Hw (0.435) (m)	pressure gradient (psi/ft)	HC-W Contact	Pre vs Post Production	WATER SALINITY (ppm)	TEMP (F)
AGOGO-1X	AGOGO	732460	9297776	10/03/89	RFT	-1625.67	4007.13	1182	0.253		Pre		
GOBE MAIN-5ST1	GOBE	800706	9250858	3/10/01	RFT	-1160.93	1850	135	0.310	GOC	Post		
GOBE MAIN-7	GOBE	801794	9250352	24/08/06	RDT	-1166.36	1742.29	54		GOC	Post		134
GOBE-2XST	GOBE	807157	9246413	16/06/92	RFT	-1187.24	2270.40	404		GOC	Pre		
GOBE-3X	GOBE	814359	9242603	29/11/92	RFT	-1247.01	2357.60	405	0.273		Pre		
GOBE-4XST1	GOBE	798027	9252045	8/11/93	RFT	-1105.72	2109.46	372	0.301	GOC	Pre		
GOBE-6X	GOBE	801799	9250363	18/07/94	RFT	-1142.57	2142.70	359	0.288		Pre		
GOBE-7X	GOBE	810826	9244502	18/10/95	RFT	-1195.34	2310.83	424	0.345		Pre		
GOBE-7XST1	GOBE	810826	9244502	12/10/99	RFT	-1195.33	2310.83	424	0.273		Pre		
SE GOBE-1X	SE GOBE	811635	9243159	16/02/91	RFT	-1172.20	2293.79	435	0.346				
SE GOBE-2X	SE GOBE	812832	9242648	4/10/91	RFT	-1200.35	2313.95	421	0.280				
SE GOBE-3X	SE GOBE	810744	9243374	23/03/92	RFT	-1218.10	2257.84	364	0.356				

Maps A.1 - A.11: Regional Papuan Basin Map Set Displaying Well Locations

Map A.1: Regional Papuan Basin master map. Satellite image layer overlain on Papuan Basin map to enable visualisation of fold belt and foreland features. Toro (yellow) and Imburu Formation (orange) are shown in shaded areas in the northwest of the fold belt. Map is shown for orientation purposes for the sub-regional maps and to show the well distribution in the basin. Map details: Scale 1:1000000. AGD66/AMG zone 54. Transverse Mercator. Australian National Spheroid spheroid (Santos, 2013).

Maps A.2 - A.7: Represent 6 sub-regional Papuan Basin maps covering entire map region shown in Map A.1. In each Map an inset shows the area covered compared to the master map. These maps allow all of the wells outside of the Moran, Agogo, Hedinia/Iagifu. Gobe/South East Gobe Fields to be identified (Santos, 2013).

Maps A.8 - A.11: Represent 4 additional sub-regional/field scale maps covering regions unable to be adequately displayed in the sub-regional scale maps above. In each Map an inset shows the area covered compared to the master map.

Map A.8: Moran, Mananda/South East Mananda and Agogo Fields (Santos, 2013)

Map A.9: Agogo, Hedinia/Iagifu and Usano Fields (Oil Search, 2013)

Map A.10: Hedinia/Iagifu Fields (additional wells not listed on Map A.9) (Williams and Lund, 2006)

Map A.11: Gobe/South East Gobe Fields (Oil Search, 2013)

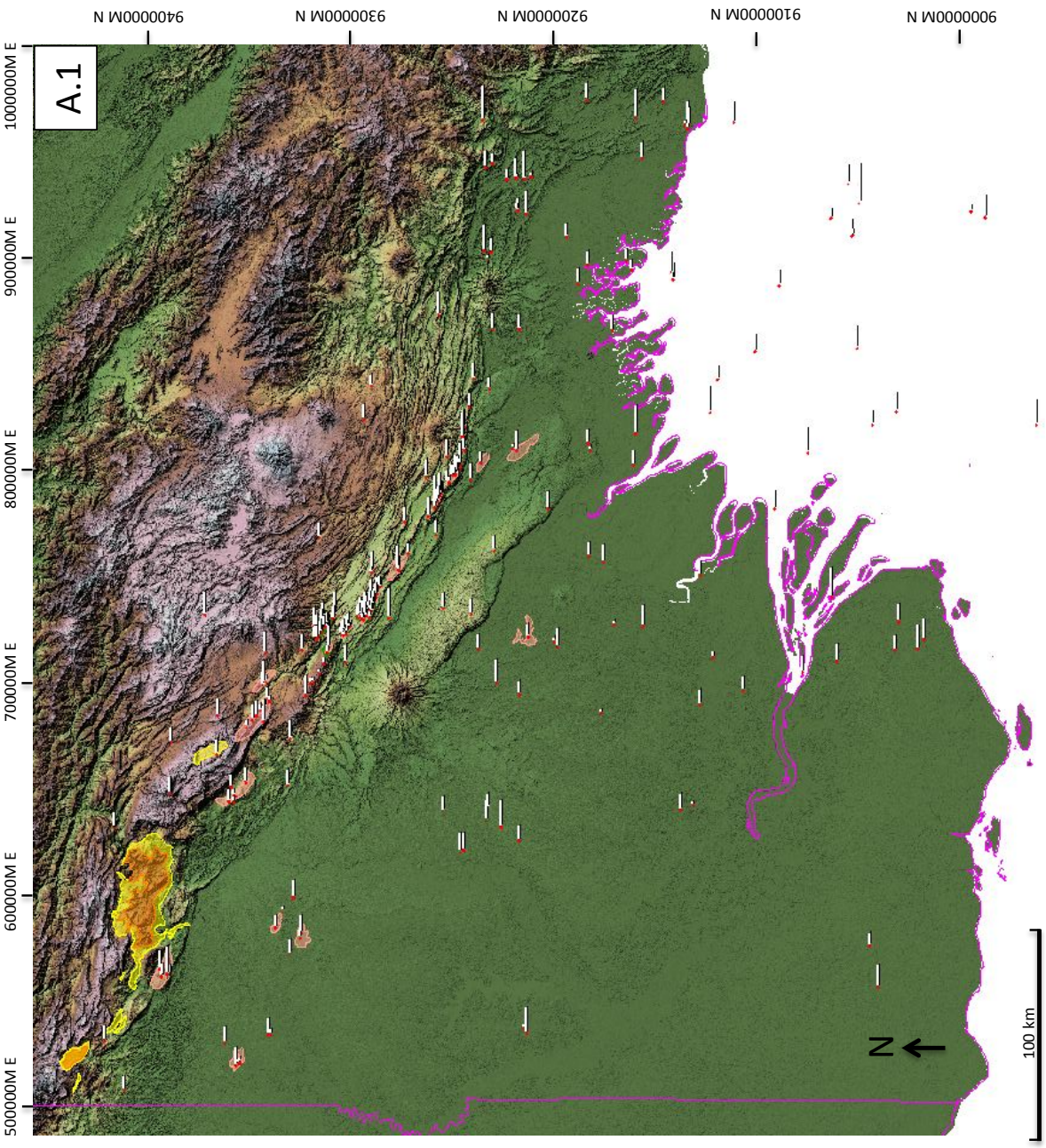
A.1
940000M N
930000M N
920000M N
910000M N
900000M N
1000000M E
900000M E
800000M E
700000M E
600000M E
500000M E
N
100 km

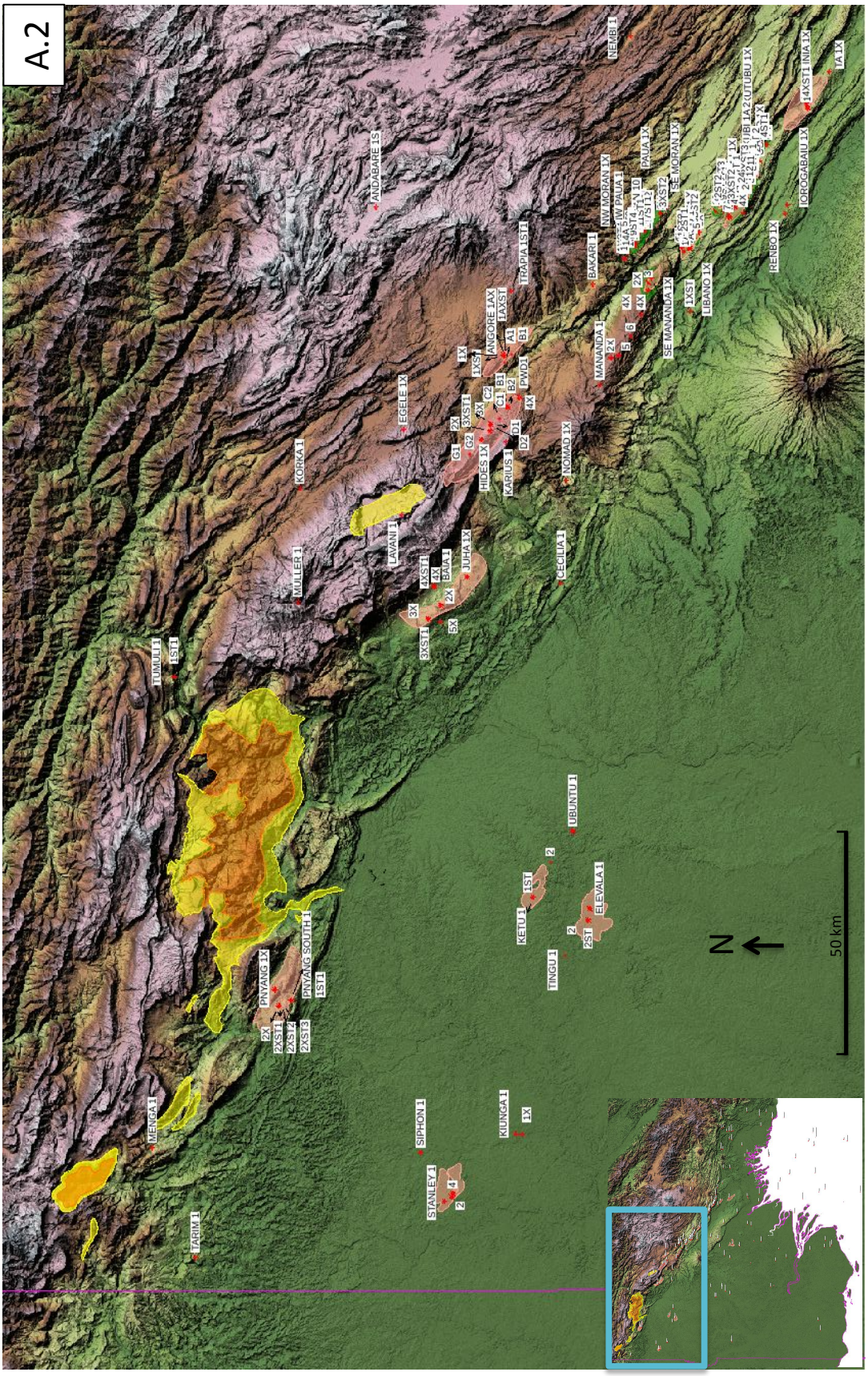
A.2
ANDABARE 1S
NEMBI 1
1A 1X
1XST1 UNA 1X
OROGABAIU 1X
PAUA 1X
SE MORAN 1X
NW MORAN 1X
BAKARI 1
TRAPIA 1ST1
LIBANO 1X
RENGO 1X
SE MANANDA 1X
MANANDA 1
EGELE 1X
KORKA 1
MULLER 1
LAVANI 1
JUHA 1X
BALA 1
HIDES 1X
KARIUS 1
ANGORE 1AX
NOMAD 1X
CECILIA 1
PWDI 1
TUMUL 1
1ST1
MENGA 1
TARIM 1
PNYANG 1X
PNYANG SOUTH 1
1ST1
2X
2XST1
2XST2
2XST3
SIPHON 1
STANLEY 1
KIUNGA 1
1X
KETU 1
1ST
TINGU 1
ELEVALA 1
2ST
UBUNTU 1
N
50 km

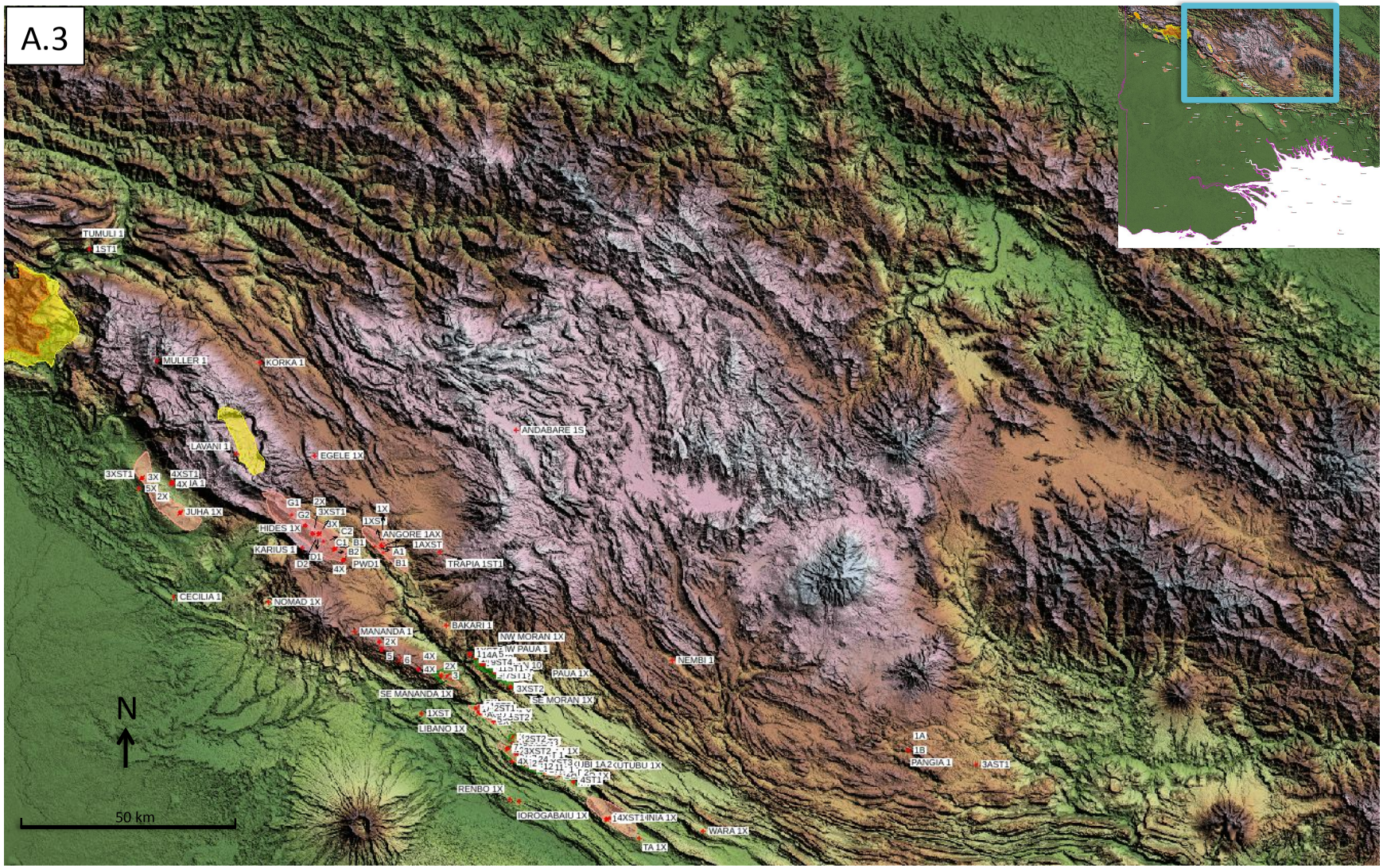
A.3
TUMULI 1
1ST1
MULLER 1
KORKA 1
ANDABARE 1S
LAVANI 1
EGELE 1X
3XST1
3X
4XST1
4X IA 1
5X
2X
JUHA 1X
G1
2X
G2
3XST1
1X
1XST
HIDES 1X
4X
C2
ANGORE 1AX
C1
B1
KARIUS 1
B2
1AXST
A1
D1
D2
PWD1
B1
TRAPIA 1ST1
4X
CECILIA 1
NOMAD 1X
BAKARI 1
MANANDA 1
NW MORAN 1X
2X
W PAUA 1
NEMBI 1
5
6
4X
2X
4X
3
PAUA 1X
3XST2
SE MANANDA 1X
SE MORAN 1X
1XST
LIBANO 1X
1A
1B
PANGIA 1
3AST1
UBI 1A2
UTUBU 1X
RENBO 1X
IOROGABAIU 1X
14XST1
INIA 1X
WARA 1X
TA 1X
N
50 km

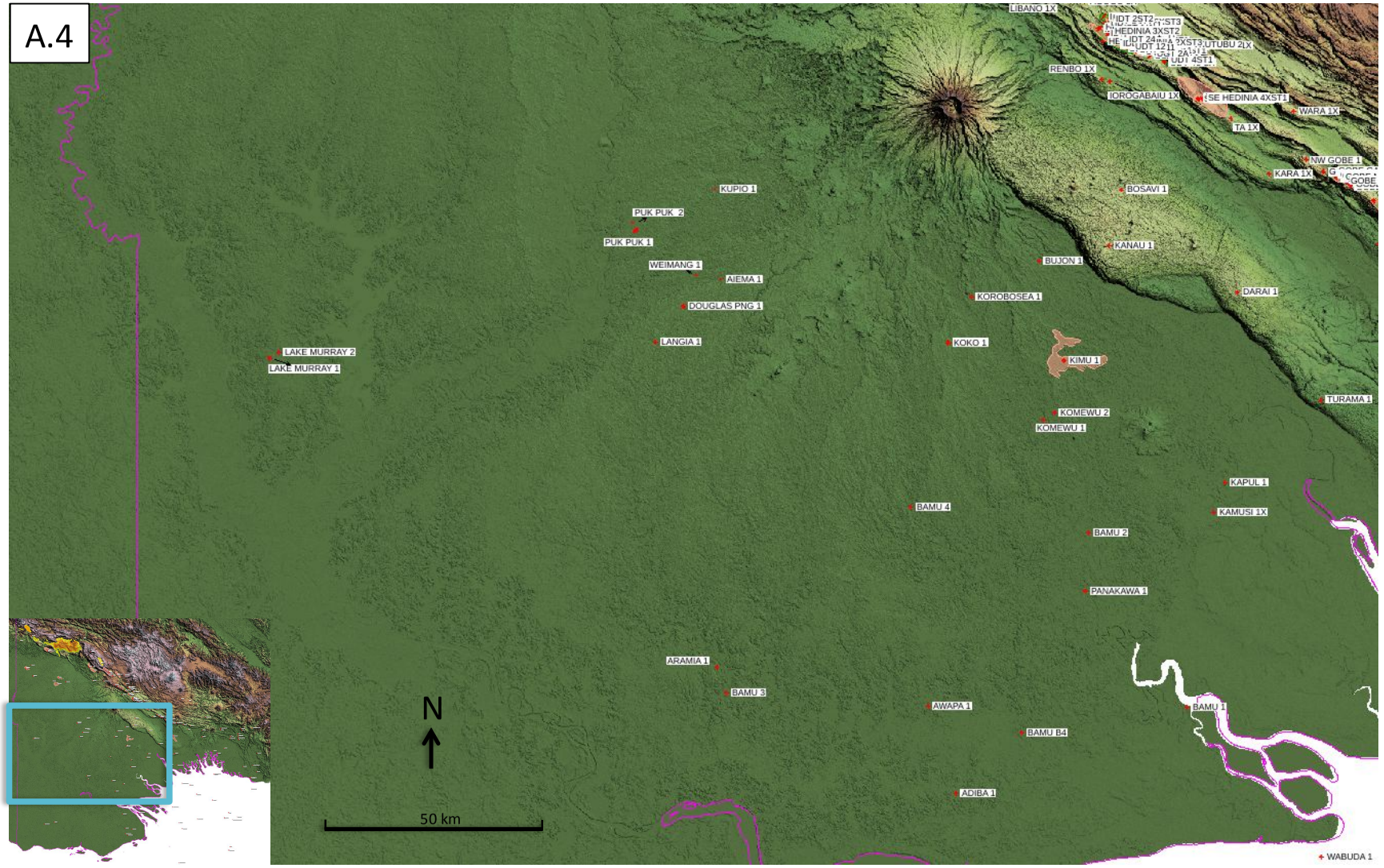
A.4
LIBANO 1X
IDT 2ST2
HEDINIA 3XST2
UTUBU 2IX
UDT 12 J1
UDI 4ST1
RENBO 1X
IOROGABAIU 1X
SE HEDINIA 4XST1
WARA 1X
TA 1X
NW GOBE 1
KARA 1X
KUPIO 1
BOSAVI 1
PUK PUK 2
PUK PUK 1
KANAU 1
BUJON 1
WEIMANG 1
AIEMA 1
KOROBOSEA 1
DARAI 1
DOUGLAS PNG 1
LANGIA 1
KOKO 1
LAKE MURRAY 2
LAKE MURRAY 1
KIMU 1
TURAMA 1
KOMEWU 2
KOMEWU 1
KAPUL 1
BAMU 4
KAMUSI 1X
BAMU 2
PANAKAWA 1
ARAMIA 1
BAMU 3
AWAPA 1
BAMU 1
BAMU B4
ADIBA 1
WABUDA 1
N
50 km

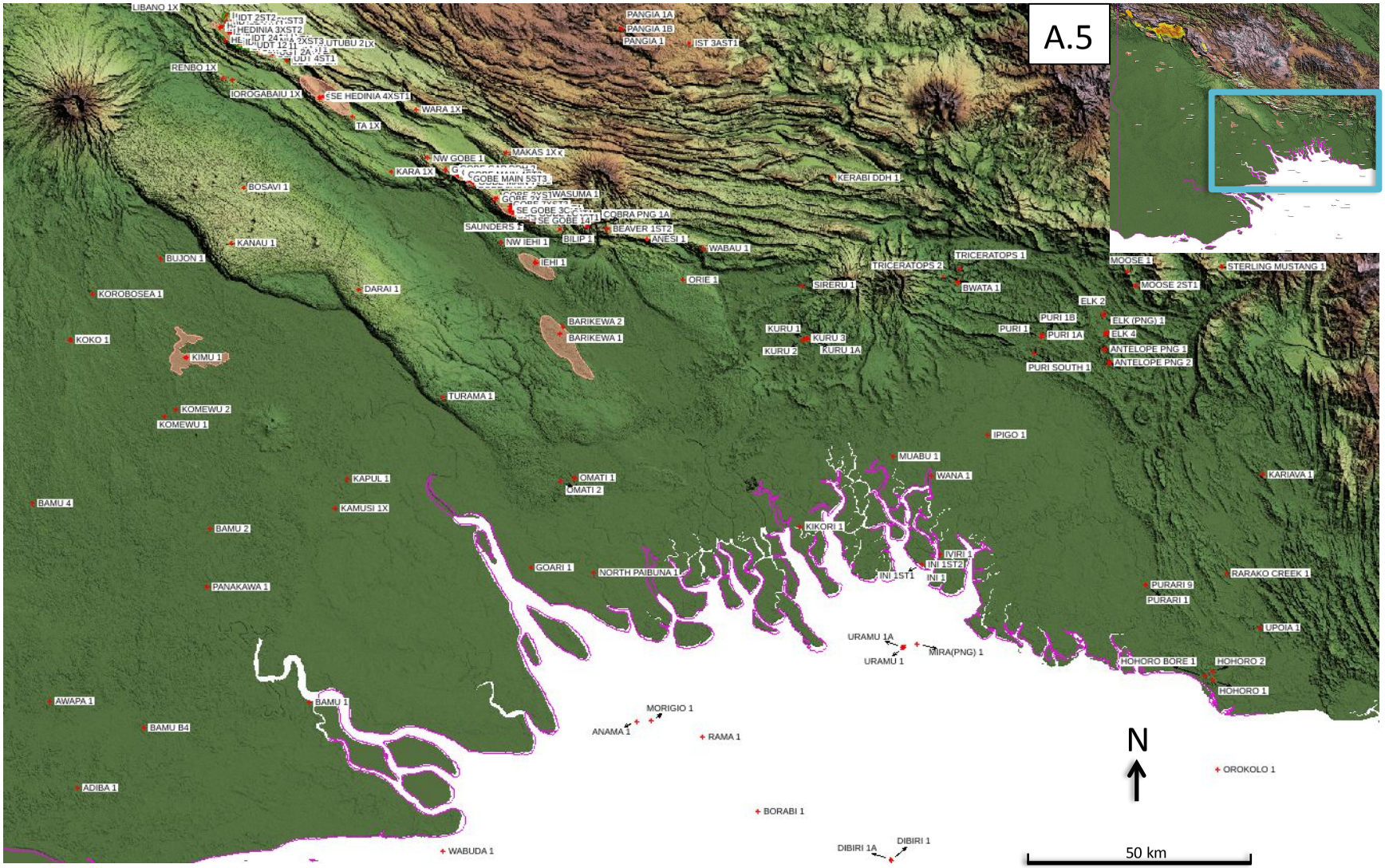
A.5
LIBANO 1X
IDT 2ST2
HEDINIA 3XST2
UTUBU 2X
UDI 4ST1
RENBO 1X
IOROGABAIU 1X
SE HEDINIA 4XST1
WARA 1X
TA 1X
NW GOBE 1
MAKAS 1X
KARA 1X
GOBE MAIN 5ST3
BOSAVI 1
WASUMA 1
SE GOBE 3
SE GOBE 1
COBRA PNG 1A
BEAVER 1ST2
SAUNDERS 1
BILIP 1
ANESI 1
NW IEHI 1
IEHI 1
WABAU 1
KANAU 1
BUJON 1
KOROBOSEA 1
DARAI 1
ORIE 1
KERABI DDH 1
TRICERATOPS 1
TRICERATOPS 2
SIRERU 1
BWATA 1
MOOSE 1
MOOSE 2ST1
STERLING MUSTANG 1
ELK 2
ELK (PNG) 1
ELK 4
PURI 1B
PURI 1
PURI 1A
ANTELOPE PNG 1
ANTELOPE PNG 2
PURI SOUTH 1
BARIKEWA 2
BARIKEWA 1
KURU 1
KURU 3
KURU 2
KURU 1A
KOKO 1
KIMU 1
TURAMA 1
KOMEWU 2
KOMEWU 1
PANGIA 1A
PANGIA 1B
PANGIA 1
IST 3ST1
IPIGO 1
MUABU 1
WANA 1
KARIAVA 1
OMATI 1
OMATI 2
KAPUL 1
KAMUSI 1X
BAMU 4
BAMU 2
KIKORI 1
IVIRI 1
INI 1ST2
INI 1ST1
INI 1
GOARI 1
NORTH PAIBUNA 1
RARAKO CREEK 1
PURARI 9
PURARI 1
PANAKAWA 1
UPOIA 1
URAMU 1A
URAMU 1
MIRA(PNG) 1
HOHORO BORE 1
HOHORO 2
HOHORO 1
AWAPA 1
BAMU 1
BAMU B4
MORIGIO 1
ANAMA 1
RAMA 1
OROKOLO 1
ADIBA 1
BORABI 1
WABUDA 1
DIBIRI 1A
DIBIRI 1
N
50 km

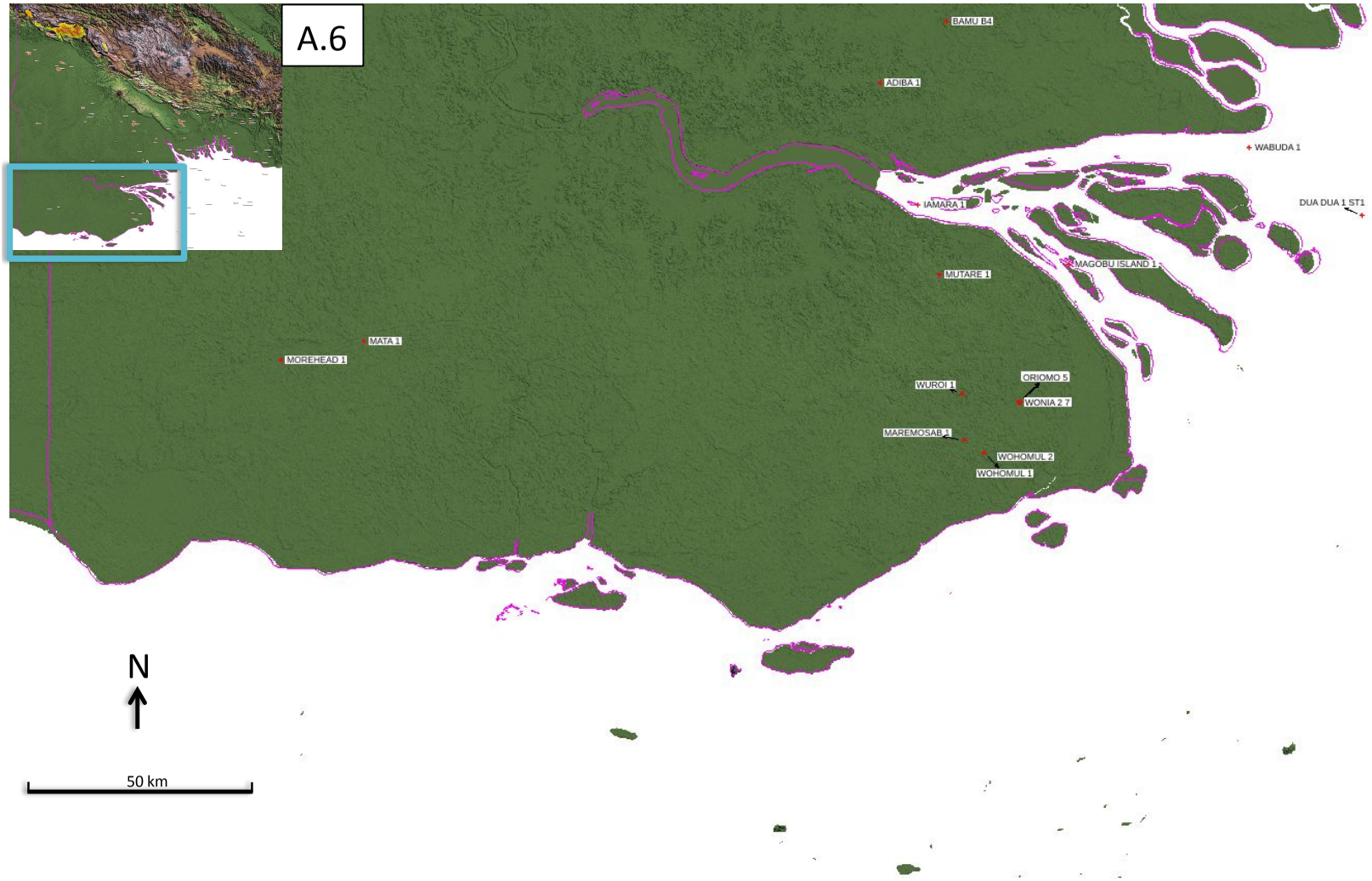
A.6
BAMU B4
ADIBA 1
WABUDA 1
IAMARA 1
DUA DUA 1 ST1
MAGOBU ISLAND 1
MUTARE 1
MATA 1
MOREHEAD 1
WUROI 1
ORIOMO 5
WONIA 2 7
MAREMOSAB 1
WOHOMUL 2
WOHOMUL 1
N
50 km


A.7
WABUDA 1
IAMARA 1
DUA DUA 1 ST1
MAGOBU ISLAND 1
MUTARE 1
KUSA 1
WUROI 1
ORIOMO 5
WONIA 2 7
PURUTU 1
MAREMOSAB 1
WOHOMUL 2
WOHOMUL 1
ANCHOR CAY 1
DIBIRI 1A
DIBIRI 1
PASCA C1
PASCA C2
PASCA A2
HAGANA 1
PASCA A1
GOARIBARI 1
PASCA A3
KIDUKIDU 1
FLINDERS PNG 1
PANDORA B1
PANDORA 1X
N
50 km

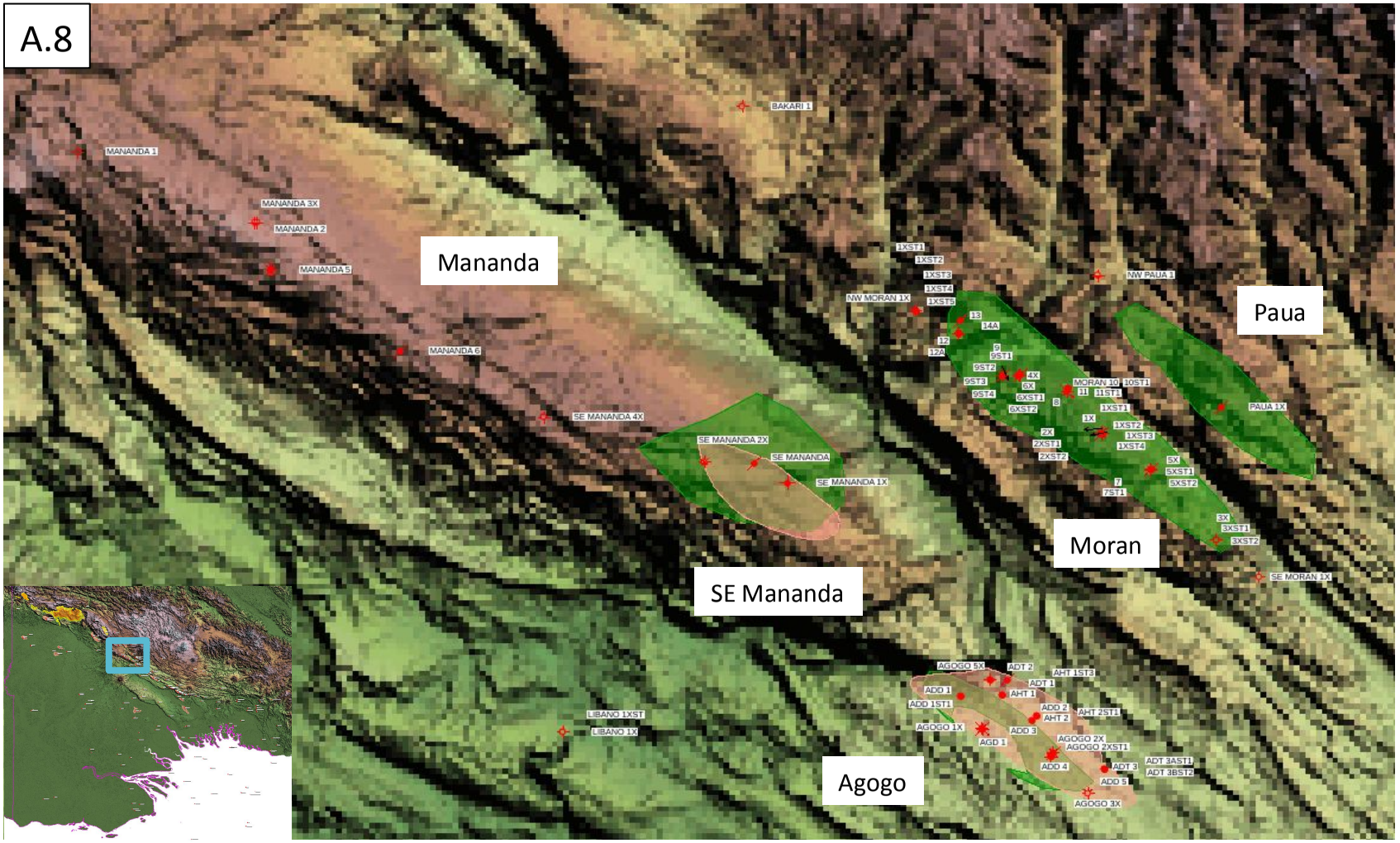
A.8
Mananda
Paua
Moran
SE Mananda
Agogo
BAKARI 1
MANANDA 1
MANANDA 3X
MANANDA 2
MANANDA 5
MANANDA 6
SE MANANDA 4X
SE MANANDA 2X
SE MANANDA
SE MANANDA 1X
NW MORAN 1X
NW PAUA 1
PAUA 1X
SE MORAN 1X
LIBANO 1XST
LIBANO 1X
AGOGO 5X
AGOGO 1X
AGOGO 2X
AGOGO 3X

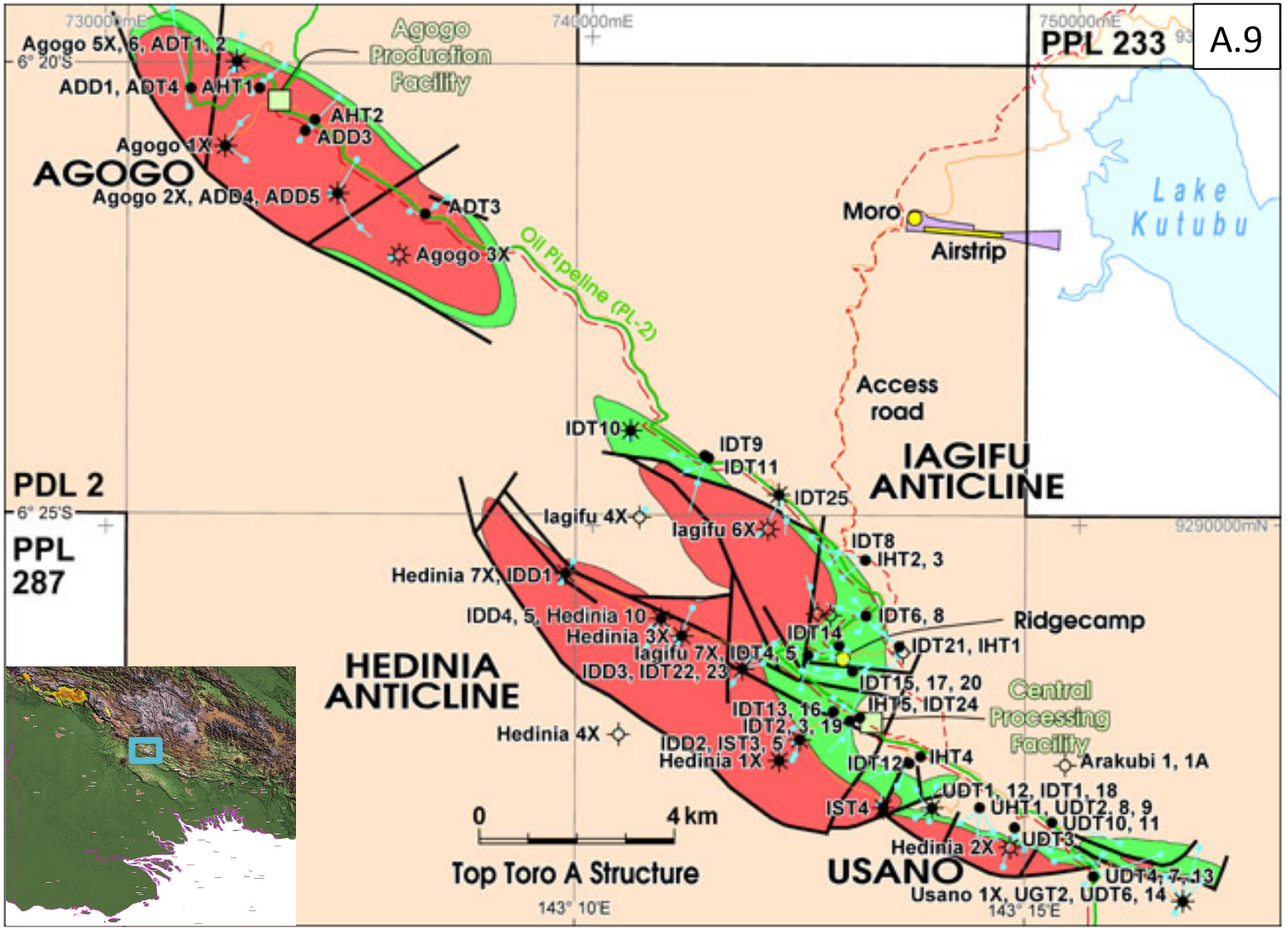
A.9
PPL 233
Agogo Production Facility
Agogo 5X, 6, ADT1, 2
ADD1, ADT4
AHT1
AHT2
ADD3
Agogo 1X
AGOGO
Agogo 2X, ADD4, ADD5
ADT3
Agogo 3X
Oil Pipeline (PL-2)
Moro
Airstrip
Lake Kutubu
Access road
IDT10
IDT9
IDT11
IAGIFU ANTICLINE
IDT25
PDL 2
PPL 287
Iagifu 4X
Iagifu 6X
IDT8
IHT2, 3
Hedinia 7X, IDD1
IDD4, 5, Hedinia 10
IDT6, 8
Ridgecamp
Hedinia 3X
IDT14
IDT21, IHT1
Iagifu 7X, IDT4, 5
IDD3, IDT22, 23
HEDINIA ANTICLINE
IDT15, 17, 20
Central Processing Facility
IHT5, IDT24
IDT13, 16
IDT2, 3, 19
Hedinia 4X
IDD2, IST3, 5
Hedinia 1X
IDT12
IHT4
Arakubi 1, 1A
UDT1, 12, IDT1, 18
IST4
UHT1, UDT2, 8, 9
UDT10, 11
Hedinia 2X
UDT3
UDT4, 7–13
USANO
Usano 1X, UGT2, UDT6, 14
0
4 km
Top Toro A Structure
143° 10'E
143° 15'E

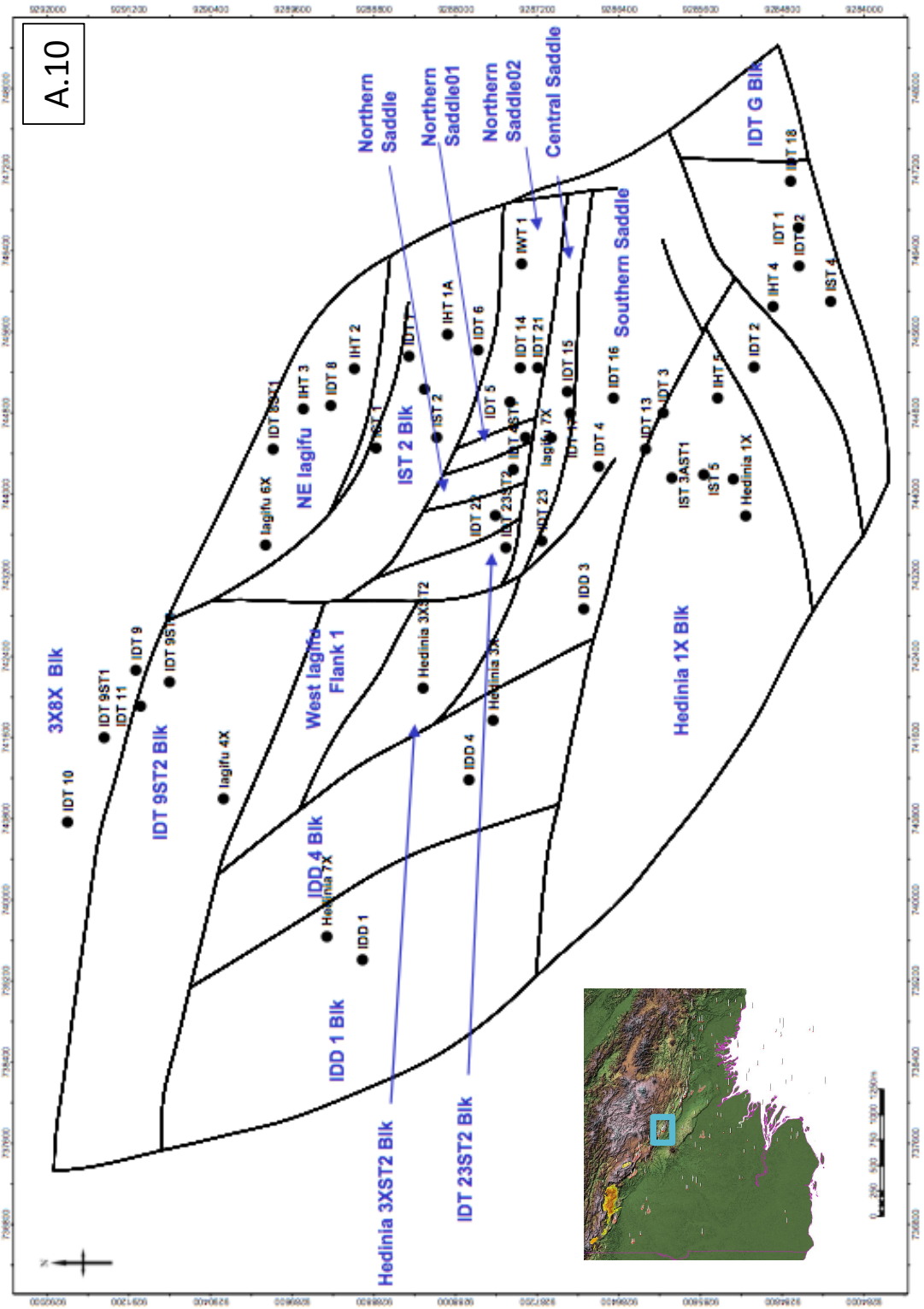
A.10
Northern Saddle
Northern Saddle01
Northern Saddle02
Central Saddle
Southern Saddle
IDT G Blk
3X8X Blk
IDT 9ST2 Blk
NE Iagifu
IST 2 Blk
West Iagifu Flank 1
IDD 4 Blk
IDD 1 Blk
Hedinia 1X Blk
Hedinia 3XST2 Blk
IDT 23ST2 Blk
IDT 10
IDT 9ST1
IDT 11
IDT 9
IDT 8ST1
IHT 3
IDT 8
IHT 2
IST 1
IDT 7
IHT 1A
IDT 6
IDT 5
IST 2
IDT 14
IDT 21
IWT 1
IDT 15
IDT 16
IDT 4
IDT 13
IDT 3
IST 3AST1
IST 5
IHT 5
Hedinia 1X
IDT 2
IHT 4
IDT 1
IDT 2
IST 4
IDT 18
Iagifu 6X
Iagifu 4X
Hedinia 7X
IDD 1
IDD 4
Hedinia 3XST2
Hedinia 3X
IDT 23ST2
IDT 23
IDT 24
IDD 3
Iagifu 7X

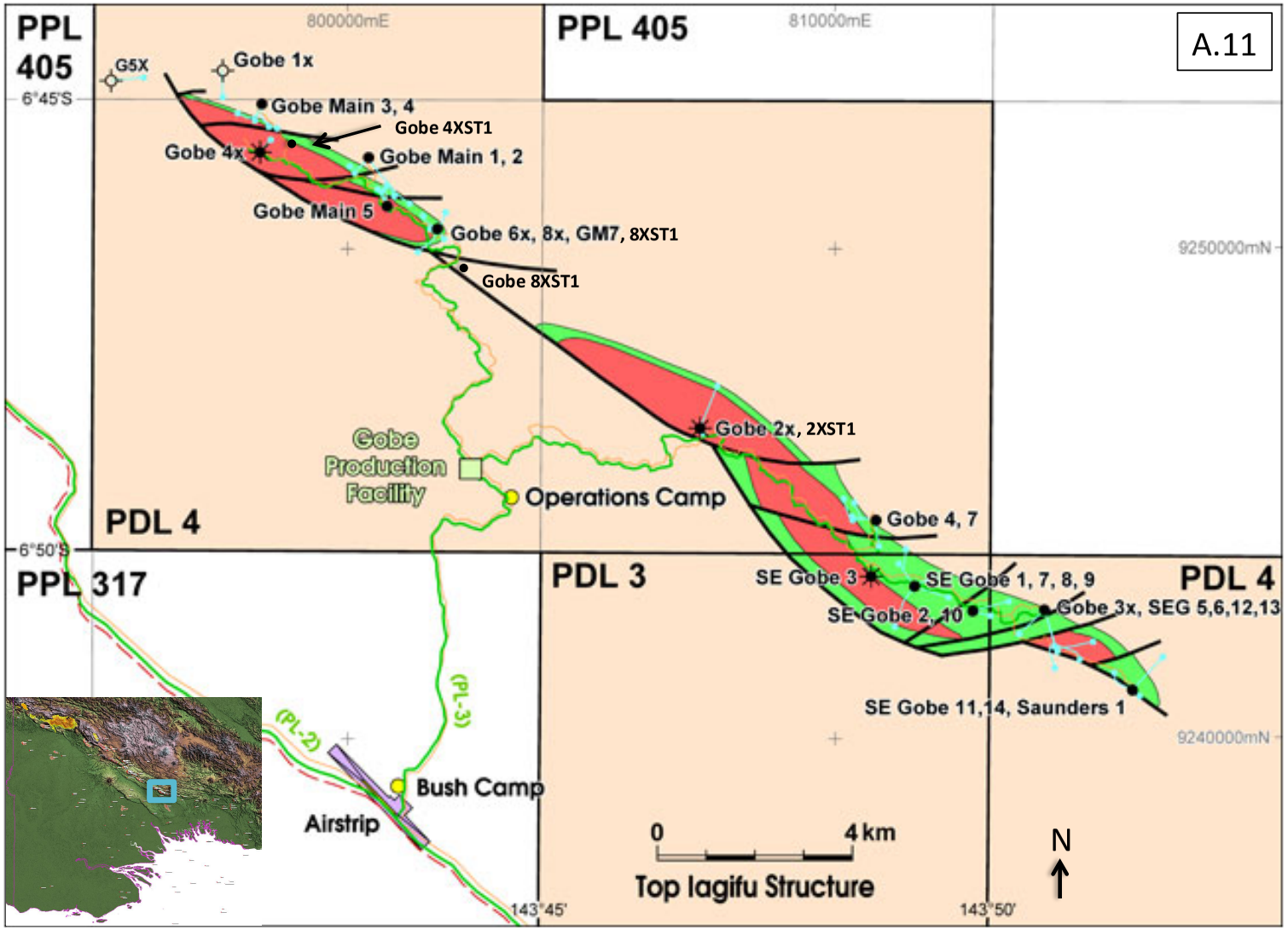
A.11
PPL 405
800000mE
PPL 405
810000mE
G5X
Gobe 1x
6°45'S
Gobe Main 3, 4
Gobe 4XST1
Gobe 4x
Gobe Main 1, 2
Gobe Main 5
Gobe 6x, 8x, GM7, 8XST1
9250000mN
Gobe 8XST1
Gobe 2x, 2XST1
Gobe Production Facility
Operations Camp
PDL 4
Gobe 4, 7
6°50'S
PPL 317
PDL 3
SE Gobe 3
SE Gobe 1, 7, 8, 9
PDL 4
SE Gobe 2, 10
Gobe 3x, SEG 5,6,12,13
SE Gobe 11,14, Saunders 1
9240000mN
(PL-3)
(PL-2)
Bush Camp
Airstrip
0
4 km
N
Top Iagifu Structure
143°45'
143°50'